Programa de Doctorado en Bioingeniería

TESIS DOCTORAL

Caracterización morfológica de la arquitectura radicular en plántulas de tomate y su regulación hormonal

---

Aurora Alaguero Cordovilla

Director: Prof. Dr. José Manuel Pérez Pérez

Universidad Miguel Hernández de Elche

Instituto de Bioingeniería

Elche, 2022

La presente Tesis Doctoral, titulada *"Caracterización morfológica de la arquitectura radicular en plántulas de tomate y su regulación hormonal"*, se presenta bajo la modalidad de **tesis por compendio** de las siguientes **publicaciones**:

- **Aurora Alaguero-Cordovilla**, Ana Belén Sánchez-García, Sergio Ibáñez, Alfonso Albacete, Antonio Cano, Manuel Acosta, José Manuel Pérez-Pérez (2021). An auxin-mediated regulatory framework for wound-induced adventitious root formation in tomato shoot explants. *Plant Cell and Environment* **44**, 1642-1662. doi: 10.1111/pce.14001.

- **Aurora Alaguero-Cordovilla**, Francisco Javier Gran-Gómez, Paula Jadczak, Mariem Mhimdi, Sergio Ibáñez, Cécile Bres, Daniel Just, Christophe Rothan, José Manuel Pérez-Pérez (2020). A quick protocol for the identification and characterization of early growth mutants in tomato. *Plant Science* **301**, 110673. doi: 10.1016/j.plantsci.2020.110673.

- **Aurora Alaguero-Cordovilla**, Francisco Javier Gran-Gómez, Sergio Tormos Moltó, José Manuel Pérez-Pérez (2018). Morphological characterization of root system architecture in diverse tomato genotypes during early growth. *International Journal of Molecular Sciences* **19**, 3888. doi: 10.3390/ijms19123888.

El Dr. D. José Manuel Pérez Pérez, director de la tesis doctoral titulada **"Caracterización morfológica de la arquitectura radicular en plántulas de tomate y su regulación hormonal"**

INFORMA:

Que Dña. Aurora Alaguero Cordovilla ha realizado bajo mi supervisión el trabajo titulado **"Caracterización morfológica de la arquitectura radicular en plántulas de tomate y su regulación hormonal"** conforme a los términos y condiciones definidos en su Plan de Investigación y de acuerdo al Código de Buenas Prácticas de la Universidad Miguel Hernández de Elche, cumpliendo los objetivos previstos de forma satisfactoria para su defensa pública como tesis doctoral.

Lo que firmo para los efectos oportunos, en Elche.

Director de la tesis

Prof. Dr. D. José Manuel Pérez Pérez

La Dra. Dña. Piedad de Aza Moya, Coordinadora del Programa de Doctorado en Bioingeniería de la Universidad Miguel Hernández de Elche

INFORMA:

Que Dña. Aurora Alaguero Cordovilla ha realizado bajo la supervisión de nuestro Programa de Doctorado el trabajo titulado **"Caracterización morfológica de la arquitectura radicular en plántulas de tomate y su regulación hormonal"** conforme a los términos y condiciones definidos en su Plan de Investigación y de acuerdo al Código de Buenas Prácticas de la Universidad Miguel Hernández de Elche, cumpliendo los objetivos previstos de forma satisfactoria para su defensa pública como tesis doctoral.

Lo que firmo para los efectos oportunos, en Elche

Profa. Dra. Dña. Piedad de Aza Moya

Coordinadora del Programa de Doctorado en Bioingeniería

El trabajo recogido en esta memoria ha sido realizado en el marco de los siguientes proyectos de investigación:

- Caracterización de nuevos reguladores de la formación de raíces adventicias: función de la demetilasa de histonas LSD1 en la regulación de la respuesta a las auxinas. Ref. RTI2018-096505-B-I00. Ministerio de Ciencia e Innovación. 2019-2021.
- Genómica comparada de la formación de raíces adventicias en tomate y clavel. Ref. BIO2015-64255-R. Ministerio de Economía, Industria y Competitividad. 2016-2018.

Lo que firmo para los efectos oportunos, en Elche

Investigador Principal

Prof. Dr. D. José Manuel Pérez Pérez

ÍNDICE DE CONTENIDOS

ÍNDICE DE FIGURAS

ÍNDICE DE TABLAS

RESUMEN GLOBAL

ABSTRACT

The root system is a key structure for the correct growth and development of plants, as it contributes to water and nutrient absorption. The roots display great plasticity in their development, which is influenced by the environmental conditions of the substrate. Many plants also have the ability to develop adventitious roots from non-root tissues. The cultivated tomato, *Solanum lycopersicum*, with a production that exceeds 180 million tons in 2019, is one of the most important horticultural species worldwide. It has a fleshy fruit, compound leaves and the ability to regenerate the root system thanks to the formation of adventitious roots in the stem, hence it is not surprising that it has become a model species for studying Solanaceae biology. Due to its small size and short life cycle, the Micro-Tom dwarf cultivar is one of the most widely used in laboratory studies.

In this doctoral thesis, a standardized protocol for the characterization of the early root system has been established and it has been applied to the study of a collection of 19 wild species, commercial cultivars and tomato mutants. We have analyzed a collection of 395 M_3 lines of tomato mutants obtained by mutagenesis with ethyl methanesulfonate in the cultivar Micro-Tom and we identified 659 individuals (belonging to 203 M_3 lines) whose early seedling and root phenotypes differed from those of their reference background. Using a combination of physiological and genetic approaches, we provided additional evidence about the relevance of auxin transport in regulating wound-induced adventitious root formation in young Micro-Tom explants. The regulation of basipetal auxin transport through the hypocotyl and the activation of local auxin biosynthesis in the region near the wound create an endogenous auxin gradient in the vascular region that promotes cell proliferation in the cambium and the initiation of the new root primordia. Our results provide a conceptual framework to initiate the genetic dissection of de novo organ formation in tomato.

RESUMEN GLOBAL

El sistema radicular es una estructura fundamental para el correcto crecimiento y desarrollo de las plantas, ya que contribuye a la absorción de agua y nutrientes. Las raíces muestran una gran plasticidad en su desarrollo, en función del entorno que las rodea. Muchas plantas presentan, además, la capacidad de desarrollar raíces adventicias, a partir de tejidos no radiculares. El tomate cultivado, *Solanum lycopersicum*, con una producción que superó los 180 millones de toneladas en 2019, es una de las especies hortícolas más importante a nivel mundial. Si a esto le sumamos que presenta un fruto carnoso, hojas compuestas y la capacidad de regenerar el sistema radicular gracias a la formación de raíces adventicias en el tallo, no es de extrañar que se haya convertido en modelo de estudio de la biología de las Solanáceas. Debido a su pequeño tamaño y su ciclo de vida corto, la variedad ornamental Micro-Tom es una de las más utilizadas en estudios de laboratorio.

En esta Tesis doctoral se ha establecido un protocolo estandarizado para la caracterización del sistema radicular temprano y se ha aplicado para el estudio de una colección de 19 especies silvestres, cultivares comerciales y mutantes de tomate. Hemos analizado una colección de 395 líneas M_3 de mutantes de tomate obtenidas mediante mutagénesis con metanosulfonato de etilo en el cultivar Micro-Tom e identificamos 659 individuos (pertenecientes a 203 líneas M_3) cuyos fenotipos tempranos de plántulas y raíces diferían de los de su parental de referencia. Utilizando una combinación de enfoques fisiológicos y genéticos, hemos proporcionado evidencias adicionales acerca de la relevancia del transporte de las auxinas en la regulación de la formación de las raíces adventicias inducidas por herida en explantos jóvenes de Micro-Tom. La regulación del transporte basípeto de auxinas a través del hipocótilo y la activación de la síntesis local de auxinas en la región próxima al corte generan un gradiente endógeno de auxinas en la región vascular que promueve la proliferación celular en el

cambium y la iniciación de los nuevos primordios radiculares. Nuestros resultados proporcionan un marco conceptual para iniciar la disección genética de la formación de órganos *de novo* en tomate.

INTRODUCCIÓN GENERAL Y OBJETIVOS

1. INTRODUCCIÓN GENERAL

1.1 Orígenes del tomate y taxonomía

El tomate (*Solanum lycopersicum*), es una planta herbácea, vascular, angiosperma, y dicotiledónea de la familia de las Solanáceas. Esta familia destaca principalmente por su interés agronómico ya que a ella pertenecen, además del tomate, especies tan importantes como la patata (*Solanum tuberosum*) o la berenjena (*Solanum melongena*), plantas medicinales como la belladona (*Atropa belladona*), y ornamentales como la petunia (*Petunia × hybrida*), entre otras (Knapp *et al*., 2004). Podemos encontrar especies del género *Solanum* tanto en regiones templadas como en regiones tropicales y en altitudes que oscilan entre el nivel del mar y los 3300 metros (Warnock, 1991). También se pueden encontrar en una gran diversidad de ecosistemas con diferentes condiciones edafológicas y climáticas, cuyos rangos de precipitaciones y temperaturas varían ampliamente. Todo ello explica la diversidad de variedades silvestres de esta familia de plantas (Peralta y Spooner, 2006; Nakazato, Warren y Moyle, 2010).

Gracias a los nuevos métodos de análisis basados en secuenciación y a las herramientas bioinformáticas disponibles, se han propuesto varias hipótesis acerca del proceso de la domesticación del tomate (Razifard *et al*., 2020; Blanca *et al*., 2021). El modelo más reciente (figura 1) está basado en un análisis detallado de haplotipos. Este modelo está de acuerdo con las teorías existentes previamente, y todos ellos coinciden en que el tomate cultivado deriva de *Solanum pimpinellifollium*, que se considera la especie ancestral silvestre (Peralta, Spooner y Knapp, 2008; Blanca *et al*., 2015; Blanca *et al*., 2021).

La hipótesis propuesta por Blanca y colaboradores en 2021 postula que, en una primera etapa, *S. pimpinellifollium* migró de Perú a México derivando en *S. lycopersicum* var. *cerasiforme*, seguramente por alguna adaptación rápida, por lo que no surgieron muchos haplotipos nuevos. Y fue

aquí, en Ecuador y Perú, donde tuvo lugar una semidomesticación del tomate.

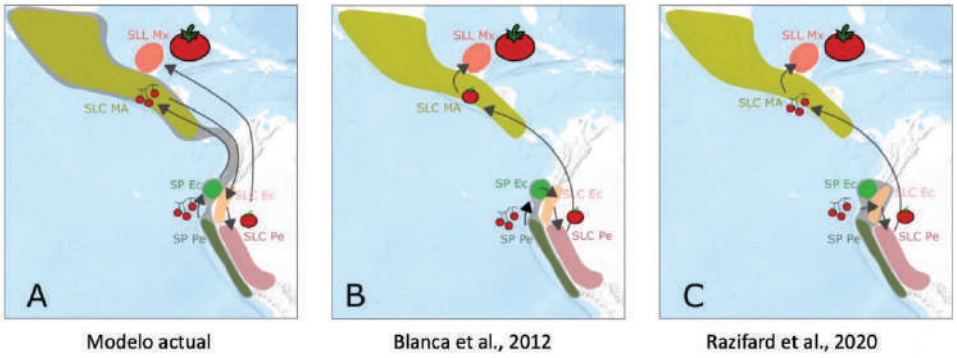

Figura 1. Hipótesis más plausible de la ruta de domesticación del tomate. Los rangos de población genética están representados por el color de las diferentes áreas geográficas. Las áreas mostradas en gris incluyen poblaciones que se supone que se han diversificado antes de cualquier alteración humana. Las flechas indican migraciones. Se representan tres tamaños de fruto: frutos pequeños (similares a los silvestres), formas semidomesticadas y frutos tipo *S. lycopersicum* var. *lycopersicum*. (A) Modelo propuesto por Blanca *et al*,. 2021 (B) Hipótesis propuesta por Blanca *et al*., 2012. (C) Hipótesis propuesta por Razifard *et al*., 2020. Tomado, con algunas modificaciones, de Blanca *et al*., 2021.

Fue entonces cuando volvió a migrar a Mesoamérica, donde finalmente se domesticó, transformándose en *S. lycopersicum* var. *lycopersicum*, que pudo entrar en contacto con los europeos a partir de 1512 con la llegada de Hernán Cortés a la ciudad azteca de Tenochtitlán, la actual Ciudad de México (Díez y Nuez, 2008). En 1753, Linneo realizaría la clasificación taxonómica actual del tomate en el género *Solanum* bajo el nombre específico de *S. lycopersicum*, publicado en su libro "*Species Plantarum*". La taxonomía aceptada actualmente para describir al tomate cultivado es la siguiente: Reino: Plantae; Subreino: Traqueobionta; Superdivisión: Spermatophyta; Clase: Magnoliopsida; Subclase: Asteridae;

Orden Solanales; Suborden: Solanineae; Familia: Solanaceae; Género: *Solanum*; Especie: *lycopersicum* (Foolad, 2007).

Junto con el tomate cultivado, se reconocen otras 12 especies de tomate. Estas 13 especies están englobadas en 4 grupos en la sección *Lycopersicon*: (I) grupo *Lycopersicon*, que engloba las especies *S. lycopersicum*, *S. pimpinellifollium*, *S. cheesmaniae* y *S. galapagense*; (II) grupo *Neolycopersicon*, con una única especie, *S. pennellii*; (III) grupo *Ericopersicon*, que engloba a las especies *S. habrochaites*, *S. huaylasense*, *S. corneliomulleri*, *S. peruvianum* y *S. chilense*; y (IV) el grupo Arcanum, que engloba las especies *S. arcanum*, *S. chmielewskii* y *S. neorickii* (Peralta, Spooner y Knapp, 2008).

1.2 Micro-Tom como sistema modelo en tomate cultivado

De manera reciente, el tomate se ha convertido en modelo de las Solanáceas para el estudio del desarrollo de los frutos carnosos (Karlova *et al*., 2014; Kim *et al*., 2018; Li *et al*., 2018), del desarrollo de las hojas compuestas (Shani *et al*., 2010) o de la asociación de las raíces con los microorganismos del suelo para la formación de micorrizas (Song *et al*., 2015). Además, desde 2012 se encuentra secuenciado completamente su genoma, lo que facilita el uso de técnicas moleculares de análisis (Sato *et al*., 2012; Rothan *et al*., 2016). Otras de las características clave en el desarrollo del tomate como planta modelo son el tamaño de su genoma, unas 950 Mb distribuidas en 12 cromosomas, y la existencia de mapas genéticos y físicos que ofrecen una vasta colección de marcadores moleculares (Suresh *et al*., 2014; Zhao *et al*., 2019). Además, se encuentra disponible una amplia gama de variedades de tomate, de mutantes monogénicos bien caracterizados, de líneas recombinantes consanguíneas y se han desarrollado numerosas herramientas de edición génica (Eshed y Zamir, 1995; Sato *et al*., 2012; Pérez-Martín *et al*., 2017; Martín-Pizarro y Posé, 2018; Rothan, Diouf y

Causse, 2019;). Por último, los avances más recientes en metabolómica del fruto del tomate han proporcionado información detallada sobre el metabolismo primario y secundario de esta especie y las vías involucradas en la biosíntesis de estos compuestos (Luo, 2015; Tieman *et al*., 2017; Zhu *et al*., 2018).

Sin embargo, existen dos problemas principales a la hora de utilizar el tomate en los laboratorios. En primer lugar, el tamaño de las variedades más conocidas, como M82 o Moneymaker, ambas de más de un metro de atura, obliga a disponer de grandes invernaderos para su cultivo. En segundo lugar, el ciclo de vida de estas plantas (de unos 4 meses hasta el cuajado de los primeros frutos) incrementa la duración de los experimentos considerablemente (Campos *et al*., 2010). Algunos autores han propuesto que la variedad de tomate ornamental Micro-Tom presenta características fenotípicas y fisiológicas idóneas para su cultivo en condiciones de laboratorio (Meissner *et al*., 1997).

Micro-Tom se obtuvo en 1989 en la Universidad de Florida mediante el cruzamiento de las variedades Florida Basket y Ohio 4013-3 (Scott y Harbaugh, 1989). Micro-Tom presenta un tamaño ultracompacto, de unos 15 cm de altura, y su ciclo de vida es de unas 12 semanas, por lo que supone una clara mejoría en cuanto al espacio y tiempo de cultivo en comparación con las variedades comerciales de tomate empleadas tradicionalmente (Campos *et al*., 2010). Los rasgos más característicos de Micro-Tom están determinados por, al menos, seis mutaciones diferentes: *dwarf* (*d*), *miniature* (*mnt*), *self-pruning* (*sp*), *uniform ripering* (*u*), *Stemphylium resistance* (*Sm*) e *Immunity to fusarium wilt* (*I*) (Martí *et al*., 2006). La presencia en Micro-Tom de entrenudos cortos y hojas rugosas y de color verde oscuro se debe a la presencia de una mutación recesiva de pérdida de función en el gen *DWARF* (*D*). Este gen codifica una proteína del citocromo P450 implicada en la biosíntesis de brasinosteroides, por lo que los mutantes *d* y, en consecuencia, la variedad Micro-Tom, presentan niveles reducidos

de brasinosteroides. Por otro lado, la mutación *mnt*, parece estar relacionada con la ruta de señalización de las giberelinas, sin que los niveles de éstas se vean afectados, contribuyendo también al pequeño tamaño de Micro-Tom (Martí *et al*., 2006). Esta variedad, al igual que muchas de las variedades de tomate cultivado, presenta crecimiento determinado, debido a una mutación en el gen *SELF-PRUNING* (*SP*). Este gen pertenece a la familia de genes *CETS* (*CENTRORADIALIS/TERMINAL FLOWER 1/SELF PRUNING*) que determinan el potencial crecimiento continuo del meristemo apical de la planta (Pnueli *et al*., 2001). La presencia de la mutación *u* hace que los frutos maduren de manera uniforme careciendo del "cuello verde" que caracteriza a la región apical de las especies silvestres de tomate (Powell *et al*., 2012). Las mutaciones *Sm* e *I*, confieren inmunidad a los hongos patógenos *Stemphylium solani* y *Fusarium oxysporum*, respectivamente (Meissner *et al*., 1997). Por último, cabe destacar que otras variedades de tomate utilizadas habitualmente en investigación también presentan múltiples mutaciones. En la tabla 1 se recogen los cultivares de tomate más utilizados en investigación y las mutaciones asociadas a cada cultivar.

Tabla 1. Comparación de las mutaciones que afectan a Micro-Tom y a otras variedades de tomate utilizadas en investigación.

Cultivar	Código TGRC	Mutaciones
Micro-Tom	LA3911	*d*; *ej-2*^{w}; *mnt*; *I*; *Sm*; *sp*; *u*
M82	LA3475	*I*; *obv*; *sp*; *u*; *Ve*
Moneymaker	LA2706	*ej-2*^{w}; *obv*$^{+}$; *sp*$^{+}$; *u*
Heinz 1706-BG	LA4345	*I*; *obv*; *sp*; *u*; *Ve*
UC-82	LA1706	*obv*; *sp*; *u*
Ailsa Craig	LA2828A	*ej-2*^{w}; *obv*$^{+}$; *sp*$^{+}$; *u*$^{+}$
Craigella	LA3247	*u*

ej-2^{w} (*enhancer of jointless-2*^{weak}), aumento de la subdivisión de la inflorescencia; *obv* (*obscuravenosa*): ausencia de cloroplastos en las células epidérmicas debajo de las venas; *Ve*: resistencia a *Verticillium*. Información obtenida del C.M. Rick Tomato Genetics Resource Centre (TGRC) en https://tgrc.ucdavis.edu/.

1.3 Mutantes en fondo Micro-Tom

Debido al potencial de Micro-Tom como sistema modelo, se han obtenido en los últimos años varias colecciones de mutantes mediante mutagénesis química (Saito *et al*., 2011) mediante la transformación genética con *Agrobacterium tumefaciens* (Sun *et al*., 2006) o por la obtención de líneas mutantes isogénicas mediante introgresión (Carvalho *et al*., 2011). Existen varias bases de datos donde se recogen éstas y otras colecciones de mutantes, que facilitan la identificación de los rasgos de interés (Saito *et al*., 2011). Una vez identificados estos rasgos, se pueden transferir fácilmente a variedades comerciales mediante cruzamiento (Mubarok *et al*., 2015). Además, los polimorfismos presentes en Micro-Tom respecto a otras variedades de tomate cultivado facilitan la identificación del gen o genes causantes de una mutación determinada en este fondo genético (Hirakawa *et al*., 2013).

Una de las colecciones que hemos utilizado para estudiar las mutaciones que pudieran afectar al sistema radicular es la de mutantes hormonales clásicos que habían sido introgresados en fondo Micro-Tom por el grupo del profesor Lázaro Peres en la Universidad de Sao Paulo en Brasil (Carvalho *et al*., 2011). En la tabla 2 se muestran algunas de las características de los mutantes utilizados en este trabajo.

Tabla 2. Mutantes hormonales. Colección de mutantes hormonales en fondo Micro-Tom.

Mutante	Efecto fenotípico de la mutación. Proteína que codifica el gen silvestre
anthocyanin absent	Deficiente en antocianinas. Afectado un gen implicado en el transporte de antocianina.
anthocyanin less	Bajos niveles de antocianinas. Mutación en la Flavonoide-3-hidroxilasa. Afectado en la biosíntesis de antocianinas.
bushy	Reducción de la expansión o división celular. No se ha identificado el gen silvestre.
diageotropica (dgt)	Defectos en el transporte polar de auxinas. Peptidil-prolil isomerasa de la familia de las ciclofilinas.
entire (*e*)	Respuesta constitutiva a auxinas. Correpresor de la respuesta a auxinas de la familia Aux/IAA.
flacca (flc)	Deficiente en ABA. Sulfurasa de un cofactor de molibdeno para la Aldehído oxidasa (AO).
lutescent	Deficiente en la regulación de clorofila y cloroplastos. Mutación de terminación prematura de la ruta de desarrollo de los cloroplastos.
Never ripe (Nr)	Baja sensibilidad a etileno. Receptor de etileno homólogo a ETR1 de *A. thaliana*.
notabilis (not)	Deficiente en ABA. 9-cis-epoxicarotenoide dioxigenasa (NCED) de la biosíntesis de ABA.
procera (pro)	Respuesta constitutiva a GA. Represor GAI de la familia DELLA.
sitiens (sit)	Deficiente en ácido abscísico (ABA). AO que participa en las etapas finales de la biosíntesis del ABA.

Información obtenida de (Carvalho *et al*., 2011) con algunas modificaciones.

Uno de los mutágenos químicos más empleados es el metanosulfonato de etilo o MSE, el cual alquila selectivamente las bases de guanina que, durante la replicación del ADN, se acoplan preferiblemente con una timina en vez de con la citosina, como sería normal. La mayoría de las mutaciones (70-99%) generadas por MSE consisten en la transición de G:C a A:T (Greene *et al*., 2003; Till *et al*., 2004; 2007). Se han observado diferentes densidades de mutación generadas por MSE. Por ejemplo, en cebada (*Hordeum vulgare*) se ha observado una mutación por cada Mb (Caldwell, Langridge y Powell, 2004) mientras que en el trigo harinero (*Triticum aestivum*) la tasa de mutación puede ser de hasta una por cada 25 Kb (Slade *et al*., 2005). Se han obtenido varias colecciones de mutantes de MSE en tomate (Meissner *et al*., 1997; Menda *et al*., 2004; Gady *et al*., 2009; Saito *et al*., 2009; Minoia *et al*., 2010; Garcia *et al*., 2016), habiéndose observado una densidad de mutación de hasta una por cada 125 Kb (Garcia *et al*., 2016).

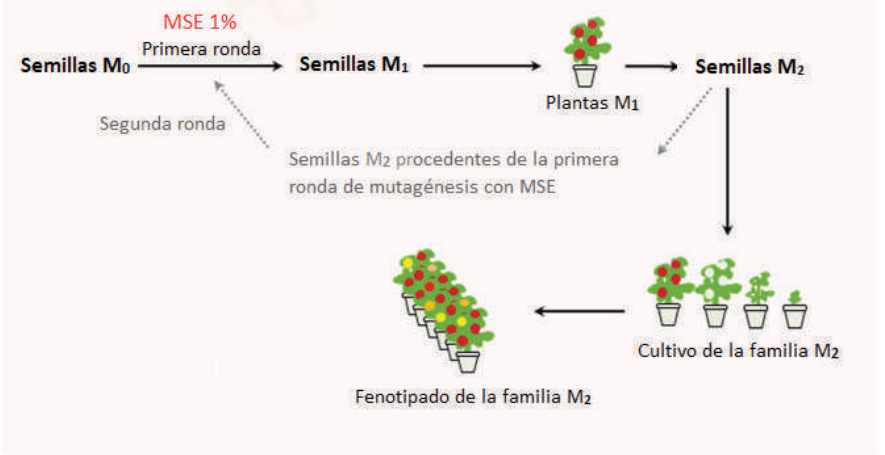

Figura 2. Mutagénesis con MSE y fenotipado de las semillas. Esquema detallado de las dos rondas de mutagénesis con MSE. Imagen tomada de (Garcia *et al*., 2016) con algunas modificaciones.

1.4 La importancia del sistema radicular

Las funciones principales de las raíces de las plantas son la absorción de agua y nutrientes y el anclaje de la planta a su entorno. Además, actúan como barrera selectiva frente a patógenos y modulan algunas respuestas a distintos tipos de estreses (Petricka, Winter y Benfey, 2012). Una de las principales características de las raíces es su gran plasticidad, lo que permite una gran adaptabilidad a las necesidades y limitaciones físicas que la planta encuentra en su entorno (Hodge *et al*., 2009; Herder *et al*., 2010; Lynch y Brown, 2012; Lavenus *et al*., 2013).

Por la enorme contribución del sistema radicular al rendimiento final de un cultivo, el estudio de la arquitectura radicular es un rasgo importante en los programas de mejora de cultivos en los últimos años (Lynch, 2007; Kell, 2011; Jung y McCouch, 2013). Por lo tanto, resulta de vital importancia la continua adquisición de conocimiento sobre la arquitectura radicular y los factores fisiológicos y genéticos que controlan su formación y desarrollo, así como conocer como éstos afectan a otros elementos de la planta como las hojas o los frutos.

Recientemente se han desarrollado nuevas tecnologías que nos han permitido comprender mejor la arquitectura de los sistemas radiculares complejos como, por ejemplo, la obtención de imágenes de raíces en 3D, los suelos transparentes o las cámaras de cultivo automatizadas, entre otros (Tötzke *et al*., 2019). A día de hoy se sabe que el sistema radicular está influenciado por la acción de diferentes hormonas, así como por su interacción entre ellas y con los factores ambientales presentes en el entorno de la planta. Todos estos factores actúan como un conjunto de reguladores que conducen a cambios en la expresión génica, transducción de señales y conversiones metabólicas (Liu, Rowe y Lindsey, 2014; Sengupta y Reddy, 2018).

Existen dos tipos de sistemas radiculares definidos por sus patrones de ramificación y origen de desarrollo: las raíces pivotantes y las raíces fibrosas. Las plantas gimnospermas y dicotiledóneas presentan una raíz pivotante central gruesa que puede o no desarrollar raíces secundarias, llamadas raíces laterales. La zanahoria (*Daucus carota*) sería un ejemplo extremo de este tipo radicular. Este tipo de raíz primaria es importante durante todo el ciclo de vida de la planta. Por otro lado, en las plantas monocotiledóneas, el sistema radicular deriva de una raíz principal pequeña que frena su desarrollo en las etapas tempranas. A partir de aquí, se desarrolla un nuevo sistema radicular, de raíces fibrosas que consiste en un sistema radicular adventicio, estas raíces tienen la particularidad de que se desarrollan de forma postembrionaria y nunca a partir de tejido radicular, si no que emergen a partir de brotes, tallos u hojas (Bellini, Pacurar y Perrone, 2014). En las plantas dicotiledóneas también podemos encontrar raíces adventicias, aunque en este caso su función natural es de apoyo al sistema radicular principal (Sorin *et al*., 2006).

1.4.1 Sistema radicular en tomate

En el tomate, como en el resto de las plantas dicotiledóneas, el sistema radicular presente es el pivotante (Bellini, Pacurar y Perrone, 2014) (figura 3A-B). La raíz principal se establece durante la embriogénesis, emerge con la germinación de la semilla (Scheres *et al*., 1994) y deriva del tejido meristemático formado embrionariamente que origina la hipófisis, cerca de la base del embrión globular temprano. Se produce una división asimétrica, que da lugar a una célula superior que eventualmente forma el centro quiescente y una célula inferior que da lugar a las células superiores de la columela. Numerosas células madre rodean al centro quiescente y, dependiendo de su posición, dan lugar a diferentes tipos de tejidos como la columela, el tejido vascular, el córtex o la endodermis (Dolan *et al*., 1993) (figura 3C).

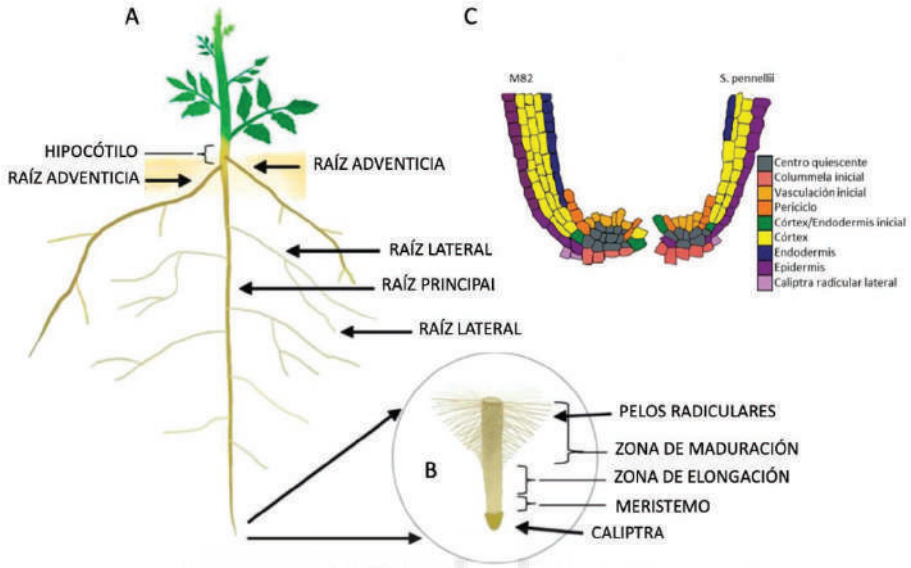

Figura 3. Estructura del sistema radicular de tomate. (A) Sistema de raíces pivotantes en una planta de tomate; raíz primaria embrionaria, raíces laterales y raíces adventicias en el hipocótilo de la planta. (B) Ápice radicular que muestra la caliptra, la zona meristemática, la zona de elongación y la zona de maduración con los pelos radiculares. (C) Esquema del ápice radicular en *S. lycopersicum* var. M82 a la izquierda y *S. pennellii* a la derecha. Imágenes tomadas de (Sharma *et al*., 2021) y (Ron *et al*., 2013) con algunas modificaciones.

En la raíz principal podemos observar diferentes zonas de desarrollo a lo largo de su eje longitudinal. En el meristemo apical de la raíz todas las células se originan a partir del centro quiescente y las células madre que lo rodean. Las células hijas se dividen en diferentes proporciones y velocidades para generar la zona de división en el meristemo de la raíz. Estas células salen del ciclo celular y se alargan generando la zona de elongación. A continuación, las células se diferencian y adquieren las características específicas del tejido. Esta zona se denomina zona de diferenciación o zona de maduración (figura 3B). La raíz principal comienza a elongar de forma

gravitrópica debido a las divisiones celulares del meristemo apical (Beemster y Baskin, 1998) y crece hasta convertirse en una raíz central gruesa que desarrollará raíces laterales.

El desarrollo de las raíces laterales se rige principalmente por la actividad de las auxinas y los máximos de respuesta a esta hormona (Lavenus *et al*., 2013; Du y Scheres, 2018; Motte, Vanneste y Beeckman, 2019). La formación de las raíces laterales comienza en el periciclo de la raíz principal con un patrón de formación dependiente de la disposición de los haces vasculares, y suelen iniciarse en las células del periciclo contiguas al xilema. Después de varias divisiones anticlinales y de la elongación celular, se produce un máximo de auxinas. Sin embargo, este máximo de auxinas no es regular, ya que se ha descrito la existencia de un patrón de oscilación (Moreno-Risueno *et al*., 2010).

1.4.2 Raíces adventicias

Las raíces postembrionarias que surgen de tejidos no radiculares como hipocótilos, tallos u hojas, se denominan raíces adventicias. Generalmente estas raíces se desarrollan en respuesta a condiciones ambientales adversas, en respuesta a un daño mecánico (figura 4) o durante el cultivo *in vitro* de tejidos vegetales (Bellini, Pacurar y Perrone, 2014; Druege *et al*., 2019; Gonin *et al*., 2019). Sin embargo, muchas especies de plantas pueden desarrollar de forma natural raíces adventicias para complementar las funciones del sistema radicular (Mhimdi y Pérez-Pérez, 2020).

La formación de raíces adventicias permite a las plantas enfrentarse a algunas tensiones ambientales (Ramirez-Carvajal y Davis, 2010). Esta cualidad de las plantas de poder formar un sistema radicular funcional a partir de tejidos no radiculares se ha convertido en un método eficaz para la propagación vegetativa de plantas, y ha sido y es ampliamente utilizada en la producción de especies hortícolas (Li *et al*., 2009; Steffens y Rasmussen, 2016).

El proceso de formación de las raíces adventicias sigue un programa de desarrollo estrictamente controlado, en el que están implicadas tres fases sucesivas (de Klerk, van der Krieken y de Jong, 1999). En primer lugar, durante la inducción se da la especificación y reprogramación celular. Las células diferenciadas adquieren nuevos programas de destino celular que conducen a la especificación de las células fundadoras de raíces adventicias. En segundo lugar, durante la iniciación, las células fundadoras de raíces adventicias experimentan sucesivas divisiones celulares que conducen a la formación de los primordios. La iniciación de las raíces adventicias puede ocurrir en varios tipos celulares, con distinta identidad anatómica y molecular, dependiendo tanto de la especie como de los estímulos ambientales involucrados, pero las raíces adventicias siempre se desarrollan a partir de células vecinas a los tejidos vasculares (Geiss, Gutierrez y Bellini, 2009; Lakehal y Bellini, 2019). Por último, en la fase de expresión, se observa el crecimiento del primordio radicular y se desarrollan las conexiones del sistema vascular (de Klerk, van der Krieken y de Jong, 1999). Independientemente del tipo celular del que surja la raíz adventicia, las fitohormonas en coordinación con los estímulos ambientales guían cada paso de la formación de los nuevos primordios. Por lo general, estas interacciones son complejas y proporcionan las señales espaciales y temporales necesarias para el desarrollo de la raíz adventicia (Lakehal y Bellini, 2019).

Los primeros pasos de la formación de las raíces adventicias, y la mayor parte de la organogénesis, incluyen la formación de un gradiente de la auxina ácido indol-3-acético (AIA) y su acumulación en tipos celulares específicos. Tanto la formación del gradiente como la acumulación de auxinas se producen a través de diferentes procesos que incluyen el transporte polar de auxinas y la biosíntesis, conjugación y degradación local de estas hormonas (Lakehal y Bellini, 2019). La principal fuente de auxinas en las plantas es el ápice de los brotes. En estas regiones, las auxinas se

sintetizan mediante dos vías: una vía dependiente de triptófano y otra independiente de triptófano (Mano y Nemoto, 2012).

Por otro lado, las plantas establecen un transporte polar de auxinas a través del tallo desde el ápice del brote hasta las raíces mediante el empleo de varios transportadores como LIKE-AUX1 (LAX), PIN FORMED (PIN) y ABCB (ATP-Binding Cassette transporters of the B subfamily) (Geisler, Bailly e Ivanchenko, 2016). Las proteínas LAX funcionan como transportadores de entrada de auxinas (Swarup, Péret y Geisler, 2012); las proteínas PIN, ampliamente estudiadas, facilitan el trasporte polar de auxinas célula a célula; y los miembros de la familia ABCB funcionan principalmente en la exportación de auxinas de los tejidos meristemáticos cuando existe una gran concentración de ésta y en el mantenimiento del flujo de auxinas a larga distancia, de modo que establecen una distribución diferencial de auxinas a través de varios tejidos (Geisler, Bailly e Ivanchenko, 2016). En *A. thaliana* se han descubierto ocho tipos de proteínas PIN diferentes; PIN1-4 y PIN7 son exportadores localizados en la membrana plasmática y su localización polar determina la dirección del flujo de auxinas; PIN5 y PIN8 se localizan en el retículo endoplásmico; y PIN6 se detecta tanto en el retículo endoplásmico como en la membrana plasmática, lo que sugiere posibles funciones en la regulación de la homeostasis intracelular de auxinas (Mravec *et al*., 2009; Anfang y Shani, 2021).

En los últimos años se han publicado numerosos estudios centrados en las bases moleculares del enraizamiento adventicio (Druege, Franken y Hajirezaei, 2016; Li, 2021) habiéndose identificado una gran cantidad de reguladores implicados directamente en la inducción e iniciación de la formación de las raíces adventicias (Lee *et al*., 2019; Shu *et al*., 2019; Xiao *et al*., 2020). Se ha demostrado que todos los genes que funcionan tanto en la percepción, el transporte y la homeostasis de las auxinas, así como en la división celular, la síntesis de la pared celular, la formación del meristemo de la raíz y el mantenimiento del centro quiescente modulan también la

formación de las raíces adventicias (Brinker *et al*., 2004; Sorin *et al*., 2006; Holmes, Djordjevic e Imin, 2010).

En lo que respecta a la señalización mediada por las auxinas, se han identificado tres grupos de genes directamente relacionados en el proceso de formación de las raíces adventicias. El primer grupo está compuesto por genes cuya función regula la síntesis y homeostasis de las auxinas, el segundo grupo de genes presenta funciones relacionadas con el transporte de las auxinas, y el último grupo está formado por genes de respuesta a auxinas (Li, 2021). Un ejemplo son los genes de la familia de genes *YUCCA* que codifican la flavina monooxigenasa que participa en la biosíntesis del AIA a partir de triptófano (Cheng, Dai y Zhao, 2006; Mashiguchi *et al*., 2011). La sobreexpresión de *YUCCA6* en *A. thaliana* causa fenotipos típicos de sobreproducción de auxinas, y produce un aumento de AIA libre para mantener los niveles locales de AIA en el meristemo apical de la raíz (della Rovere *et al*., 2013).

A pesar de que las auxinas juegan un papel central en la modulación de las raíces adventicias, existen otras fitohormonas que también modulan la formación y desarrollo de las raíces adventicias, bien a través de la ruta de las auxinas o bien de forma independiente a la ruta de las auxinas (Lavenus *et al*., 2013). En la figura 4B se muestra un resumen de la función de las diferentes hormonas en la formación de las raíces adventicias. Otras fitohormonas que se han estudiado y caracterizado ampliamente son las citoquininas. Estas moléculas son derivados de adenina y deben su nombre a su capacidad para promover la división celular o citocinesis. En los sistemas de organogénesis *de novo* inducidos por hormonas, el equilibrio entre auxinas y citoquininas es el factor principal de los mecanismos de reprogramación celular. Las altas concentraciones de citoquininas promueven la formación de brotes, pero inhiben la formación de raíces (Kareem *et al*., 2016).

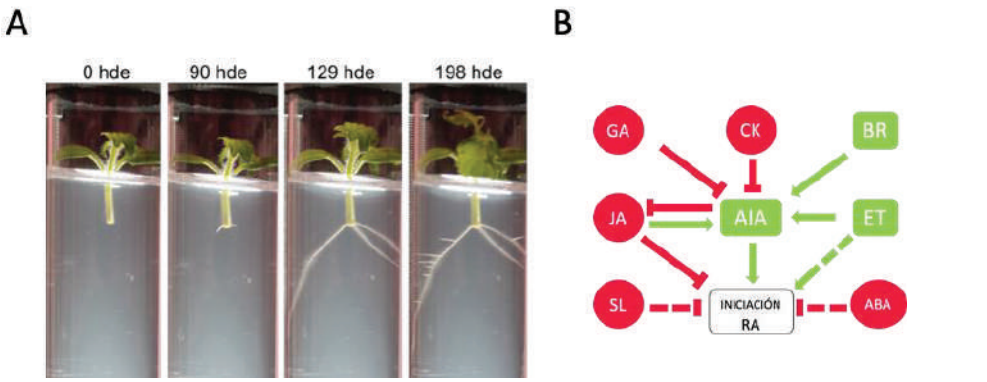

Figura 4. Formación de raíces adventicias de tomate. (A). Imágenes de la formación de raíces adventicias en una planta de tomate. hde: horas después de la escisión del sistema radicular principal. (B) Resumen de la intercomunicación hormonal durante la formación de raíces adventicias. RA: raíces adventicias, AIA: ácido indol acético, ET: etileno y BR: brasinoesteroides, CK: citoquininas, JA: ácido jasmónico, GA: giberelinas, SL: estrigolactonas, y ABA: ácido abscísico. Las líneas continuas y discontinuas incidan vínculos probados y posibles, respectivamente. Los colores verde y rojo indican reguladores positivos y negativos respectivamente. El panel B de la figura está tomado de (Lakehal y Bellini, 2019) con algunas modificaciones.

Por otro lado, el etileno es una fitohormona relacionada con el estrés que se induce rápidamente en respuesta a varios estímulos ambientales, y su biosíntesis está controlada por las auxinas y viceversa. En el caso de las raíces adventicias, las auxinas y el etileno actúan de forma sinérgica, por lo que el etileno promueve la formación de raíces adventicias (Negi *et al*., 2010); sin embargo, su modo de acción no está claro todavía. Encontrar pruebas directas sobre su función reguladora sería muy útil para dilucidad su modo de acción (Lakehal y Bellini, 2019). Las estrigolactonas, son fitohormonas derivadas de carotenoides que participan en la regulación de muchos programas de desarrollo, incluido el desarrollo de la arquitectura radicular (Waters *et al*., 2017). Sus funciones en el control de la formación

de las raíces adventicias no se comprenden claramente, pero estudios recientes han demostrado que participan de forma activa en este proceso. Aparentemente las estrigolactonas promueven la formación de raíces adventicias en arroz (Sun *et al*., 2015) Sin embargo, parecen inhibir la formación de estas raíces en tomate (Kohlen *et al*., 2012).

Por último, las funciones del ácido abscísico (ABA), las giberelinas y los brasinoesteroides en la formación de las raíces adventicias no están claras, a pesar de la existencia de indicios interesantes acerca de su participación en el proceso de formación de raíces adventicias. Por ejemplo, las giberelinas estimulan la formación de raíces adventicias en arroz a través de un mecanismo que requiere la presencia de etileno (Steffens y Rasmussen, 2016) en cambio se ha observado la inhibición de raíces adventicias en hipocótilos de *A. thaliana* (Mauriat *et al*., 2014). El ABA es una hormona relacionada con el estrés que inhibe la formación de raíces adventicias en plantas de arroz al interferir, posiblemente, con las vías de señalización del etileno y las giberelinas (Steffens y Rasmussen, 2016). De manera similar, se ha observado una inhibición de raíces adventicias en plantas de tomate probablemente a través de las vías de regulación de auxinas y etileno (McAdam, Brodribb y Ross, 2016). Se ha observado también que los brasinoesteroides estimulan la iniciación de las raíces adventicias en los hipocótilos de *A. thaliana* (Maharjan *et al*., 2014) Es posible que la señalización de los brasinoesteroides actúe de forma sinérgica con las auxinas promoviendo así la iniciación de las raíces adventicias (Gutierrez *et al*., 2012).

1.5 Objetivos

La formación y desarrollo del sistema radicular, y en especial de las raíces adventicias, es clave durante el ciclo vital de numerosas especies vegetales, por lo que conocer las bases genéticas y hormonales que regulan estos procesos en una especie de interés agronómico como es el tomate, resulta de gran interés tanto en el contexto de la ciencia básica como la aplicada.

En este contexto se enmarcan los trabajos científicos presentados en esta memoria y que constituyen mi Tesis Doctoral, encaminada a:

- Caracterizar el sistema radicular en diferentes genotipos del género *Solamun* durante el crecimiento temprano. Así como buscar nuevos reguladores del sistema radicular adventicio en una colección de mutantes hormonales en fondo Micro-Tom.
- Establecer un protocolo estandarizado para el estudio del sistema radicular en plántulas jóvenes de tomate que nos permita llevar a cabo una rápida clasificación y una búsqueda de regiones candidatas para las mutaciones observadas.
- Indagar en la función de las auxinas en la formación y desarrollo de las raíces adventicias con la finalidad de desarrollar un modelo detallado de la función y el transporte de esta hormona para dar lugar a este tipo radicular.

RESUMEN GLOBAL DE MATERIALES Y MÉTODOS

2. RESUMEN GLOBAL DE MATERIALES Y MÉTODOS

2.1 Caracterización morfológica del sistema radicular en el género *Solanum*

Para la realización de este trabajo hemos estudiado el sistema radicular en una colección de 19 entradas (*accessions*) del género *Solanum*: 9 de estirpes silvestres, 4 de variedades comerciales y 6 de mutantes de tomate en fondo Micro-Tom. Tanto las estirpes silvestres como las variedades comerciales se obtuvieron del C.M. Rick Tomato Genetics Resource Centre, mientras que el cultivar de tomate Micro-Tom y los mutantes estudiados en este mismo fondo genético fueron cedidos por el Dr. Lázaro Eustáquio Pereira Peres de la Escola Superior de Agricultura "Luiz de Queiroz", Universidade de São Paulo en Brasil.

Tras la esterilización superficial de las semillas con hipoclorito sódico, éstas se transfirieron a una cámara húmeda en las condiciones habituales de crecimiento del laboratorio y después de 4 días se pasaron a medio de cultivo las semillas germinadas con una radícula de longitud superior a 2 mm (véanse los materiales y métodos del primer artículo en las páginas 73-74). Tras 3 días en el medio de cultivo, se determinó la longitud de la raíz principal y se seccionó el ápice radicular para inducir el desarrollo de las raíces laterales. Tres días después de cortar el ápice de la raíz principal se estudiaron varios parámetros relacionados con la emergencia y formación de las raíces laterales como la densidad de raíces laterales, su longitud o su ángulo. A continuación, se indujo la formación de raíces adventicias mediante la eliminación completa del sistema radicular y se estudió el sistema radicular adventicio a los 6 y 12 días después del corte (que corresponden, respectivamente a los 12 y 18 días después de su transferencia a placas, según se describe en los materiales y métodos del primer artículo (páginas 73-74).

El procesamiento de las imágenes obtenidas, el análisis estadístico de los datos y su representación gráfica se llevó a cabo según los

procedimientos habituales utilizados en el laboratorio, y que se describen detalladamente en los materiales y métodos del primer artículo (páginas 73-74). Por último, se construyó un mapa de calor con los genotipos y parámetros estudiados, lo que permitió definir 8 ideotipos representativos de algunos de los sistemas radiculares estudiados (véase el apartado de materiales y métodos del primer artículo en la página 74).

2.2 Protocolo para la identificación y caracterización de mutantes radiculares de tomate

La colección de mutantes utilizada en este trabajo es una población de semillas M_3 procedentes de una colección de plantas M_2 generada con MSE en el Institut National de Recherche pour l´Agriculture, l´Alimentation et l´Environnement (INRAE), Bordeaux en el fondo genético Micro-Tom (Just *et al*., 2013; Garcia *et al*., 2016), cuyo fruto y parte aérea ya habían sido caracterizados fenotípicamente (Petit *et al*., 2014; Musseau *et al*., 2017), y que ha sido cedida por el Prof. Christophe Rothan. Con el fin de iniciar la disección genética del desarrollo radicular en tomate, hemos estudiado esta colección de mutantes durante el desarrollo temprano, centrándonos en el análisis del sistema radicular. Para ello, las semillas se esterilizaron y germinaron en cámara húmeda según los procedimientos habituales, y aquellas que presentaban una radícula de más de 4 mm a las 96 horas desde la esterilización, se transfirieron a un medio de cultivo adecuado para su crecimiento *in vitro*, según se indica en los materiales y métodos del segundo artículo (página 94).

Hemos establecido un vocabulario descriptivo y estandarizado para la anotación de los 12 rasgos fenotípicos analizados en las plántulas durante los 26 días posteriores a la siembra, como se indica en los materiales y métodos del segundo artículo (páginas 94-95).

Para la confirmación de los fenotipos mutantes observados en las líneas M_3 estudiadas, se traspasaron plantas con fenotipo silvestre a maceta

y se recogieron sus semillas para el estudio de las plántulas M_4 según el protocolo descrito en los materiales y métodos del segundo artículo (páginas 95-96).

Por último, de la línea P14A1, cuya mutación se confirmó en plantas M_4, se recogió el material vegetal de las plantas con fenotipo silvestre y mutante por separado, se extrajo su ADN y se utilizó para secuenciar su genoma completo en el Beijing Genomics Institute (BGI, China).

2.3 Estudio de la formación de raíces adventicias en tomate

Las semillas empleadas en este trabajo fueron cedidas por el C.M. Rick Tomato Genetics Resource Centre. En primer lugar, las semillas se esterilizaron y germinaron en cámara húmeda según los procedimientos habituales, y aquellas que presentaban una radícula de más de 4 mm a las 96 horas desde la esterilización, se transfirieron a un medio de cultivo adecuado para su crecimiento *in vitro*, según se indica en los materiales y métodos del tercer artículo (página 136), hasta que las plántulas de tomate se encontraron en el estadio 100-101 (cotiledones completamente expandidos y primera hoja con un tamaño aproximado de 0,5 cm) (Feller *et al*., 1995). En este momento procedió a seccionar la raíz principal desde la base del hipocótilo para favorecer la inducción de las raíces adventicias, según se indica en los materiales y métodos del tercer artículo (página 136).

Para los estudios macroscópicos de las raíces adventicias, se incubaron explantos de brotes o de hipocótilos durante 21 días en un medio de cultivo adecuado para su crecimiento *in vitro*. Además, dependiendo del experimento, este medio de cultivo podía estar suplementado con auxinas (ácido 1-naftalenacético, ANA), o inhibidores de auxinas (2-ácido naftoxiacético [2-NOA], ácido N-1 naptiltalámico [NPA]). Estos mismos inhibidores y auxinas también se aplicaron en otros experimentos en la parte superior de los explantos, bien en forma de gotas sobre las hojas y/o

cotiledones, o bien en forma de anillo de lanolina rodeando la parte superior del hipocótilo (véase el apartado de materiales y métodos del tercer artículo en las páginas 137-138). Para los estudios gravitrópicos se reorientaron los botes que contenían los explantos, colocándolos boca abajo, y se observó su efecto durante los 21 días siguientes a la reorientación. Para el estudio de la formación *de novo* de las raíces a partir de diferentes fragmentos de hipocótilo, éstos se cortaron en 2 o 3 fragmentos que se colocaron en el medio de cultivo control, y otros medios suplementados con ANA o con yucasina (véase el apartado de materiales y métodos del artículo 3 en las páginas 137-138). En todos estos casos, se monitorizó la emergencia y el desarrollo del sistema radicular durante 21 días. Pasado este tiempo, se anotaron parámetros como el día de emergencia de la primera raíz adventicia, la longitud total del sistema radicular adventicio y la longitud del hipocótilo al finalizar el experimento, entre otros (véase el apartado de materiales y métodos del tercer artículo en las páginas 137-138).

2.4 Análisis de microscopía

Con el fin de obtener una visión más completa de los mecanismos que actúan en la formación y desarrollo de las raíces adventicias y los tipos celulares implicados en este proceso, se llevaron a cabo una serie de estudios de microscopía para observar por una parte las células implicadas en los primeros estadios de formación de las raíces y por otra parte el mecanismo de acción de las auxinas que produce este cambio celular, así como la zona de acumulación de auxinas que estaría produciendo este cambio celular.

En el primer experimento se fijaron hipocótilos de diferentes puntos temporales y se realizaron secciones de 5 μm con ayuda de un micrótomo. Estas secciones se tiñeron posteriormente para su visualización en el microscopio óptico. En otro experimento, se realizaron secciones manuales de los hipocótilos y se clarificaron para su posterior tinción y visualización

en el microscopio láser confocal. Por último, para la inmunolocalización de auxinas, se cortaron manualmente secciones de la parte basal del hipocótilo las cuales se fijaron inmediatamente para, posteriormente, detectar la presencia en ellos de auxinas mediante el empleo de anticuerpos específicos. El diseño experimental detallado de estos estudios se encuentra descrito en el apartado de materiales y métodos del tercer artículo (páginas 138-139).

2.5 Análisis estadístico

Los parámetros estadísticos utilizados, como la media, la desviación estándar, máximos y mínimos, se calcularon utilizando el programa StatGraphics Centurion XV y el programa SPSS 21.0.0. Se identificaron y se descartaron los valores atípicos como se describe en Grubbs, 1969. Se llevaron a cabo test de ANOVA o test no paramétricos para estudiar la significación estadística de las diferencias entre muestras (p-valor < 0.05 a no ser que se indique lo contrario). La descripción detallada de los parámetros empleados para los análisis estadísticos en cada caso puede encontrarse en el apartado de materiales y métodos de los artículos adjuntos a este trabajo (páginas 74-97-142 respectivamente).

DISCUSIÓN

3. DISCUSIÓN

3.1 Caracterización morfológica del sistema radicular en *Solanum* spp.

Para estudiar la variación en la arquitectura del sistema radicular de tomate, hemos seleccionado nueve especies silvestres emparentadas y cuatro variedades comerciales de tomate cultivado (*S. lycopersicum*), junto con seis líneas mutantes en el fondo genético Micro-Tom (Carvalho *et al*., 2011). Hemos determinado el porcentaje de germinación cada 24 horas después de la imbibición de las semillas y hasta las 96 h, así como la longitud de la raíz principal a los tres días tras la germinación (véase la figura S1 del primer artículo en la página 79). Los mayores porcentajes de germinación, así como las germinaciones más tempranas se observaron en los cultivares comerciales de tomate, lo que podría deberse a una selección positiva de estos caracteres durante la domesticación del tomate o durante la mejora genética posterior (Bai y Lindhout, 2007; Abbo *et al*., 2014).

Micro-Tom y algunos mutantes estudiados en este fondo genético, como *lutescent* y *anthocyaninless*, presentaron una germinación similar a la observada en la especie *S. pimpinellifolium* en cuanto al tiempo de germinación. Algunas variedades comerciales estudiadas, como Moneymaker y Ailsa Craig, presentaron una tasa de crecimiento radicular significativamente mayor que Craigella en los tres primeros días, y similar a las especies silvestres como *S. chilense* o *S. huaylasense* (valor de $P < 0,01$). Por otra parte, entre los mutantes estudiados en fondo Micro-Tom, tanto *anthocyanin absent* como *bushy* mostraron una tasa de crecimiento radicular significativamente menor que su genotipo silvestre (véase la figura 1 del primer artículo en la página 66). Estas diferencias observadas en el crecimiento temprano de la raíz principal pueden deberse a dos factores principalmente: (i) el tiempo de germinación tras la imbibición, y (ii) la tasa de crecimiento de la raíz principal durante los tres días siguientes a la germinación. En el caso del mutante *bushy*, su menor tasa de crecimiento

radicular podría estar relacionada con las mutaciones recesivas que presenta y que le confieren una deficiencia en brasinoesteroides (Martí *et al*., 2006). Las similitudes observadas entre *S. pimpinellifolium* y las variedades comerciales podrían deberse a su proximidad taxonómica (Peralta *et al*., 2008). Algo similar podría ocurrir con las especies *S. chmielewskii* y *S. arcanum*, las cuales presentan la menor tasa de crecimiento de todas las especies silvestres estudiadas, pudiendo indicar una adaptación común a unas condiciones de suelo menos favorables.

Hemos llevado a cabo una caracterización de las raíces laterales de los genotipos estudiados tras la escisión del ápice radicular de la raíz principal (véase la tabla S1 del primer artículo en la página 88). El número de raíces laterales observadas a los tres días de la escisión del ápice radicular estaba positivamente relacionado con la longitud de la raíz principal, como ya se ha observado en otras especies (Loudet *et al*., 2005; Shi *et al*., 2013; Song *et al*., 2016). Cabe destacar *S. pimpinelifollium*, con un número de raíces laterales incluso mayor que el de las variedades comerciales (véase la figura 2A y 2B del primer artículo en la página 67). Esta característica puede resultar muy interesante para los programas de mejora vegetal, ya que las raíces laterales muestran tropismos de crecimiento en respuesta a factores como la gravedad, la luz y gradientes de humedad que contribuyen a la absorción de nutrientes del suelo, mejorando así el crecimiento y rendimiento de las plantas (Miyazawa *et al*., 2011). Los mutantes *anthocyanin absent, bushy*, *Never ripe* y *sitiens* mostraron un menor número de raíces laterales que su fondo genético Micro-Tom (véase la figura 3B y 3C del primer artículo en la página 69), lo que podría indicar un defecto en su especificación o en su iniciación. La distribución de las raíces laterales a lo largo de la raíz principal observada durante este estudio (véase la figura S4 del primer artículo en la página 82) no siempre seguía el mismo patrón (mayor número de raíces en la parte proximal y media y un menor número en la parte distal de la raíz principal). Algunos genotipos como *S. arcanum* o *S. cheesmaniae*

presentaron una mayor concentración de raíces laterales en la parte central de la raíz principal; mientras que en los mutantes *anthocyanin absent* y *sitiens*, la mayoría de las raíces laterales emergían de la parte proximal de la raíz principal (la más cercana al hipocótilo), observándose ninguna o casi ninguna raíz lateral en la zona distal de la raíz principal o zona apical (véanse las figuras 2C, 3D y S4 del primer artículo en las páginas 67, 69 y 82 respectivamente). Las variedades comerciales y *S. arcanum,* presentaron una menor distancia entre raíces laterales sucesivas. Por otro lado, las variedades comerciales y *S. peruvianum* presentaron una mayor longitud de las raíces laterales. Tanto una mayor densidad radicular como una mayor longitud de raíces laterales son características deseables en las plantas de cultivo (Miyazawa *et al*., 2011). No hemos encontrado diferencias significativas en la distancia entre raíces laterales consecutivas en el caso de los mutantes en fondo Micro-Tom comparados con su genotipo silvestre (valor de $P < 0,01$). Sin embargo, en *sitiens* observamos unas raíces laterales significativamente más cortas que las del resto de genotipos (véase la figura 3F del primer artículo en la página 69), característica esperada en este mutante por su incapacidad para transformar ABA-aldehído en ABA ácido abscísico (ABA) (Harrison *et al*., 2011), una hormona necesaria para mantener las células madre en el meristemo de la raíz (Zhang *et al*., 2010).

Uno de los mecanismos implicados en la mejora de la absorción de agua por parte de las raíces es el ángulo de las raíces laterales. En plantas monocotiledóneas se ha observado que un ángulo mayor de estas raíces secundarias con respecto al eje de la raíz principal favorece la captura de agua en condiciones de déficit hídrico (Kato *et al*., 2006; Manschadi *et al*., 2006). En el estudio que hemos llevado a cabo en plántulas de tomate hemos observado diferencias significativas en los ángulos de las raíces laterales entre genotipos, siendo *S. arcanum* y Moneymaker los que presentaron los ángulos más extremos con valores de $106,4 \pm 10,3°$ y $123,5 \pm 20,5°$ respectivamente (véase la figura S2 del primer artículo en la

página 80). Junto con Moneymaker y Ailsa Craig, las especies silvestres que presentaron mayores ángulos en sus raíces laterales fueron *S. galapaguense* y *S. cheesmaniae*, con valores de 119,0±15,2° y 116,4±14,3° respectivamente. Estas dos últimas son originarias de las islas Galápagos donde habitan en elevaciones costeras salobres (Darwin *et al*., 2003), lo que podría explicar su mayor grado de inclinación.

En nuestro sistema experimental, inducimos la formación de raíces adventicias mediante la escisión del sistema radicular completo a los seis días después de la germinación, y observamos la formación de raíces adventicias en la parte basal del hipocótilo a diferentes tiempos tras la escisión (véase el apartado de Materiales y métodos del primer artículo). Las especies *S. chilense* y *S. cheesmaniae* y el mutante *Never ripe* presentaron un retraso en la emergencia de la primera raíz adventicia con respecto al resto de especies silvestres y variedades comerciales (véase la figura S8 del primer artículo en la página 86).

En trabajos publicados previamente se ha observado que el etileno actúa reduciendo la longitud de la raíz principal, así como inhibiendo la iniciación y elongación de las raíces laterales (Negi, Ivanchenko y Muday 2008; Negi *et al*. 2010). La función reguladora del etileno sobre la formación de raíces adventicias la realiza mediante la modulación del transporte de auxinas (Kim, Lynch y Brown, 2008; Vidoz *et al*., 2010), lo que justifica el retraso en la iniciación de las raíces adventicias que observamos en el mutante *Never ripe*, deficiente en etileno.

El número de raíces adventicias a los seis y 12 días tras la inducción resultó muy variable entre los diferentes genotipos estudiados, presentando las variedades comerciales el mayor número de raíces adventicias (véase la figura 4C del primer artículo, página 71). Este incremento en el número de raíces adventicias de las variedades comerciales podría estar relacionado con el proceso de domesticación del tomate, ya que un aumento en el número de raíces adventicias supondría una mejora en el rendimiento

causado por una mejora en la absorción de agua y nutrientes (Soyk *et al*., 2017), por lo que esta característica se podría haber seleccionado de forma directa o indirecta durante la domesticación del tomate. Las tasas de crecimiento de las tres primeras raíces adventicias en cada genotipo no variaron, por lo que no observamos una competencia en cuanto a recursos entre las raíces de la misma planta. Sin embargo, al comparar diferentes genotipos entre sí se observan diferencias significativas en las tasas de crecimiento de las raíces adventicias, obteniéndose una tasa mayor en las variedades comerciales y una tasa menor en *S. peruvianum* y *S. chilense* (véase la figura 4D del primer artículo en la página 71). La longitud de las raíces adventicias a los seis días tras la inducción fue muy variable entre genotipos, siendo las de mayor longitud las de los cultivares comerciales junto con los mutantes *anthocyanin absent* y *sitiens*; mientras que las del mutante *Never ripe* fueron las más cortas de entre los mutantes en fondo Micro-Tom. Sin embargo, las longitudes de las raíces adventicias se igualaron a los 12 días, observándose diferencias menos marcadas en esta etapa (véase la figura S8 del primer artículo en la página 86). Los ángulos de crecimiento de las raíces adventicias, como en el caso de las laterales, fueron más extremos en *S. arcanum* (110,8±8,2°) y Moneymaker (131,4±24,1°) (véase la figura S8D del primer artículo en la página 86). No hemos encontrado diferencias significativas en ninguno de los parámetros de las raíces adventicias estudiados (el tiempo de iniciación, la longitud, la velocidad de crecimiento y el ángulo), comparando Micro-Tom con las variedades comerciales a excepción del número de raíces adventicias, que podría depender de la menor longitud del hipocótilo observada en Micro-Tom (véase la figura 4B y 4C del primer artículo en la página 71).

3.2 Protocolo para la identificación y caracterización de mutantes radiculares de tomate

Hemos establecido un protocolo de cultivo *in vitro* para el estudio del sistema radicular en líneas mutantes de tomate durante las etapas tempranas del desarrollo. Hemos estudiado 12 rasgos fenotípicos diferentes en cuatro etapas de crecimiento fenológico consecutivas. Para llevar a cabo este estudio hemos analizado una colección de 395 líneas M_3 de mutantes de tomate obtenidas mediante mutagénesis con MSE en el cultivar Micro-Tom (Just *et al*., 2013; Garcia *et al*., 2016;). De ellas, 95 líneas presentaron menos de ocho semillas germinadas y se descartaron para análisis posteriores. El estudio final se realizó con un total de 4543 semillas procedentes de las 300 líneas M_3 seleccionadas (véase el apartado de materiales y métodos del segundo artículo). De éstas, hemos anotado diferencias fenotípicas respecto a su fondo Micro-Tom en 946 plántulas procedentes de 252 líneas M_3.

Hemos encontrado 235 plántulas que presentaron un fenotipo de letalidad temprana, similar al que presentan los mutantes *embryo-defective* (*emb*) de *A. thaliana* (Meinke, 2020). Un 29% de las líneas estudiadas (87 líneas), presentaba algún individuo con este fenotipo mutante, en concordancia con su modo de herencia recesivo y con los resultados observados anteriormente para esta población (Garcia *et al*., 2016). En estudios realizados anteriormente en colecciones mutagenizadas de *A. thaliana* se ha observado que la frecuencia de individuos afectados en su embriogénesis puede variar entre el 5 y el 50% (Meinke, 2020). Únicamente hemos localizado una línea que presentaba este tipo de mutación de forma dominante, la línea P11H6. Hemos clasificado los mutantes de letalidad temprana en dos categorías dependiendo del estadio de desarrollo de las plántulas mutantes: (i) aquellas que no eran capaces de desarrollar su radícula y que detuvieron su crecimiento en el estadio 005 (Feller *et al*., 1995), y (ii) aquellas que tuvieron un mayor grado de desarrollo. Estas

últimas se agruparon en cuatro subcategorías dependiendo de la zona afectada por la mutación, definidas como Emb-1 hasta Emb-4 (véase la figura 2 del segundo artículo en la página 117). Veinticinco de las líneas estudiadas presentaban al menos dos individuos con defectos similares a los descritos en los mutantes *gurke* en *A. thaliana* (Mayer *et al*., 1991). En cuatro líneas se observaron individuos que recordaban al fenotipo de *monopteros* (Mayer *et al*., 1991), y en otras tres a los mutantes que recordaban a los *gnom* estudiados también previamente en *A. thaliana* (Mayer *et al*., 1991). Treinta y cuatro de las líneas estudiadas presentaban al menos dos de los fenotipos de letalidad temprana en la misma línea (véase la figura 2C del segundo artículo en la página 117). Hemos anotado 91 plántulas en 49 líneas mutantes con alguna alteración en sus tejidos aéreos en comparación con Micro-Tom, pudiendo distinguir las plántulas que sufrían un retraso en el desarrollo de aquellas que presentaban un fenotipo enano. En *A. thaliana* se conocen mutaciones en la ruta de los brasinoesteroides y de las giberelinas (Fridman y Savaldi-Goldstein, 2013; Barboza-Barquero *et al*., 2015) que causan una reducción de tamaño, tanto en la parte aérea como de la parte radicular. Hemos identificado también tres líneas M_3 en las que observamos plántulas albinas, y otras 20 líneas que presentaban algún individuo con tres cotiledones.

El estudio de la raíz principal se llevó a cabo tres días después de la siembra, y hemos observado diferencias significativas (valor de $p < 0,001$) en el crecimiento de este órgano respecto a su ancestro Micro-Tom en 465 plántulas de 160 líneas M_3. La mutación anotada como “raíz principal corta” fue la más frecuente, encontrándose en 427 plántulas de 145 líneas; tres de las cuales tenían una segregación dominante y una de ellas presentaba todas las plántulas con este fenotipo, la línea P11G10 (véanse la figura 3A del segundo artículo en la página 118). Diez líneas presentaron individuos con raíz principal más larga que el silvestre, y nueve plántulas en cuatro líneas presentaron alteraciones en la longitud de los pelos radiculares. Además,

observamos seis plántulas en tres líneas (P11G11, P12A4 y P13D11) con un crecimiento agravitrópico de la raíz principal (véanse la figura 3 del segundo artículo en las páginas 118), un rasgo fenotípico que podría no ser específico de una única mutación (Su *et al.*, 2017) puesto que depende directamente del gradiente intracelular de auxinas en la zona de elongación de la raíz (Abas *et al*., 2006; Rosquete *et al*., 2013). En el caso del mutante de tomate *diageotropica* afectado en el flujo polar de auxinas dentro de la raíz, se observa una respuesta gravitrópica reducida (Oh *et al*., 2006; Ivanchenko *et al*., 2015). El crecimiento de la raíz principal depende de la producción de células nuevas en el meristemo apical y de su expansión en la zona de elongación de la raíz (Petricka, Winter y Benfey, 2012), por lo que las plantas que presentan un fenotipo con una raíz principal significativamente más corta o más larga que la raíz de los individuos silvestres podría tener alguna mutación que afecte o bien a la formación de nuevas células en el meristemo radicular o a su expansión en la zona de elongación de la raíz. Por ejemplo, las mutaciones que afecten a la ruta hormonal de las auxinas podrían presentar este tipo de fenotipos (Meinke, 2013).

Llevamos a cabo el estudio de las raíces laterales al quinto día después de escindir el ápice de la raíz principal para promover la formación de raíces laterales (Moreno-Risueno *et al*., 2010; Du y Scheres, 2018;). Hemos anotado 141 plántulas pertenecientes a 43 líneas M_3 con alteración en el número de raíces laterales, de las cuales 32 líneas presentaron individuos con un número significativamente menor de raíces laterales que en Micro-Tom. De estas, 12 líneas presentaban algún individuo sin ninguna raíz lateral. Por el contrario, 34 plántulas de 11 líneas M_3 presentaron un número de raíces laterales significativamente mayor que en Micro-Tom (véase la figura 3D del segundo artículo en la página 118). Las raíces laterales son determinantes para incrementar la capacidad de exploración del sustrato y favorecer la absorción de agua y nutrientes (Atkinson *et al*., 2014; Banda *et al*., 2019). En el caso de las plántulas con mayor número de raíces laterales

que su ancestro, unos niveles anormalmente altos de flavonoides podrían derivar en este fenotipo, debido a la acumulación de auxinas en los lugares de formación de las raíces laterales (Maloney, DiNapoli y Muday, 2014). Por otro lado, en *A. thaliana* se han observado varios mutantes recesivos que presentaban raíces más largas y que revelaron una conexión interesante entre las rutas del ácido jasmónico y las auxinas (Khan y Stone, 2007; Zheng *et al*., 2016), lo que podría estar afectando a algunos de los mutantes observados en este trabajo. Por último, observamos líneas M_3 que presentaban plántulas afectadas tanto en la raíz principal como en el desarrollo de las raíces laterales. En 11 de estas líneas se encontraron individuos afectados o bien en la longitud de la raíz principal o bien afectados en el número de raíces laterales, por lo que su fenotipo mutante podría deberse a dos mutaciones independientes. Tres líneas M_3 presentaron plántulas donde se veía afectada tanto la longitud de la raíz principal como el número de raíces laterales. Las líneas P13C12 y P15A4 presentaron una longitud de raíz principal menor y un menor número de raíces laterales, y en la línea P16E10 observamos una longitud de raíz principal menor pero un mayor número de raíces laterales.

Para el estudio de las raíces adventicias se procedió a eliminar el sistema radicular completo a los ocho días tras la siembra. Hemos identificado 105 plántulas pertenecientes a 48 líneas M_3 con algún fenotipo mutante en su sistema radicular adventicio. 36 de estas líneas contenían algún individuo con un número significativamente menor de raíces adventicias que el silvestre, incluso plántulas que no presentaron ninguna raíz adventicia al finalizar el experimento. Vimos 24 plántulas en otras 11 líneas M_3 que presentaban un mayor número de raíces adventicias que el silvestre (véase la figura 4A y 4B del segundo artículo en la página 119). Más de la mitad de las líneas que presentaban individuos con fenotipo mutante en las raíces adventicias también presentaron individuos con fenotipos mutantes en otro tipo radicular (raíz principal, raíces laterales o ambas). La

mayoría presentaban fenotipo mutante en diferentes plántulas, por lo que las mutaciones que afectaban a las raíces adventicias y a otros tipos radiculares podrían ser independientes (véase la figura 4C del segundo artículo en las páginas 119). Además, hemos observado dos líneas (P13D11 y P14C12) que presentaban individuos afectados tanto en la longitud de la raíz principal (menor longitud) como en el número de raíces adventicias (menor número), indicando en este caso una mutación que podría estar afectando a ambos tipos radiculares. Tanto las raíces laterales como las adventicias son esenciales para aumentar el área de exploración de las plantas en el suelo (Atkinson *et al*., 2014; Banda *et al*., 2019), y las mutaciones que afectan a estos tipos radiculares podrían conferir a las plantas ventajas o desventajas evolutivas a la hora de absorber agua y nutrientes (Beeckman *et al*., 2002), lo que repercutiría además en el crecimiento total de la planta. En trabajos publicados previamente se ha observado que los mutantes de tomate afectados en la síntesis de flavonoides desarrollan un 50% menos de raíces laterales que el silvestre, mientras que unos niveles elevados de flavonol dieron lugar a plantas con un mayor número de raíces laterales (Maloney, DiNapoli y Muday, 2014). La regulación de estos compuestos podría afectar al desarrollo de las raíces laterales y adventicias, por lo que las líneas con fenotipos radiculares estudiadas en este trabajo podrían tener alterada la ruta de los flavonoides.

Con el fin de confirmar las mutaciones observadas en las líneas M_3, seleccionamos 14 líneas que presentaban alteraciones en la longitud de la raíz principal. De cada línea se trasplantaron y recogieron semillas de entre dos y cuatro individuos silvestres. Finalmente, se germinaron semillas pertenecientes a seis líneas M_3 obteniendo 18 familias M_4. Evaluamos la herencia recesiva del fenotipo “raíz principal corta” en 11 de las 18 familias, observando que seis líneas M_4 segregaron para dos mutaciones independientes que afectaban tanto a la raíz principal como al desarrollo temprano del embrión; y tres líneas M_4 derivadas de la línea M_3 P16F4

presentaron fenotipo de “raíz principal larga” (véase la tabla 2 del segundo artículo en las páginas 125-126). Otras cinco familias M_4 derivadas de dos líneas M_3 (P14D10 y P14D2) que presentaban un menor número de raíces laterales y adventicias se incluyeron en el estudio de confirmación y observamos que dos de las familias M_4 derivadas de la línea P14D2 presentaron individuos con un menor número de raíces adventicias.

3.3 Estudio de la formación de raíces adventicias en tomate

Para llevar a cabo el estudio detallado de la formación de raíces adventicias propuesto en este trabajo, hemos seleccionado el cultivar Micro-Tom, ya propuesto como sistema modelo en trabajos anteriores (Emmanuel y Levy, 2002). En primer lugar, se llevó a cabo un experimento para definir las condiciones de crecimiento de las plantas, con el que se determinó un ciclo de luz/oscuridad de 16h/8h, una concentración de sacarosa del 2% y un porcentaje de Gelrite de 0,25% p/v (véase la figura S1 del tercer artículo en la página 184). A continuación, realizamos un estudio de la zona de formación de las raíces adventicias en el hipocótilo mediante secciones transversales del mismo, y observamos cuatro haces vasculares compuestos por células del floema, varias capas de células del cambium y células del xilema en el interior del haz vascular. A los dos días tras el corte, comenzaron a dividirse de forma irregular pequeños grupos de células en el borde de los haces vasculares que podrían estar relacionados con la fase de la iniciación de las raíces adventicias (de Klerk, van der Krieken y de Jong, 1999). Estas células parecen tener su origen en el cambium más próximo al floema, y continúan dividiéndose hasta formar una raíz funcional que comienza a crecer a través del córtex, emergiendo finalmente a través de la epidermis (véanse las figuras 1A del tercer artículo en las páginas 173-174). En los hipocótilos de *A. thaliana*, las raíces adventicias se forman a partir de

las células del periciclo cercanas al xilema (Sukumar, Maloney y Muday, 2013). En otras especies como *S. dulcamara*, los primordios de las raíces adventicias están preformados en el tallo y emergen en respuesta a las inundaciones (Dawood *et al*., 2014). En cambio, en los hipocótilos jóvenes de Micro-Tom, las raíces adventicias se forman *de novo* después de la escisión del sistema radicular. Para investigar más a fondo el papel de las auxinas durante la formación de las raíces adventicias, en un trabajo reciente se han visualizado plantas de tomate transgénicas que expresan el gen *YELLOW FLUORESCENT PROTEIN* (*YFP*) bajo el control del promotor sintético DR5 sensible a auxina, *DR5pro:YFP,* y han localizado la expresión del marcador en un grupo de células del cambium durante la formación de raíces adventicias en los explantos de Micro-Tom (Guan *et al*., 2019), lo que concuerda con el lugar exacto donde hemos localizado la división celular que dará lugar posteriormente a la formación de las raíces adventicias.

Las auxinas, hormonas ampliamente estudiadas por sus múltiples implicaciones en el desarrollo de las plantas, juegan un papel fundamental en el origen y desarrollo de las raíces adventicias de diversas especies (Pacurar, Perrone y Bellini, 2014), incluido el cultivar Micro-Tom de tomate (Guan *et al*., 2019). Hemos detectado mediante inmunolocalización en el hipocótilo de tomate una zona de acumulación de auxinas próxima a las células del xilema (véase la figura 1E del tercer artículo en las páginas 173-174). Con el fin de determinar la relevancia de las auxinas endógenas en la formación de raíces adventicias, se estudió la formación de estas raíces en hipocótilos a los que se les eliminó la zona apical de la plántula seccionando por debajo de los cotiledones. Se observó un claro descenso en la capacidad de enraizamiento de los explantos de hipocótilo en comparación con los explantos que mantenían su parte apical intacta. La adicción a estos explantos de ANA provocó la proliferación de la región basal del hipocótilo (véanse las figuras 2A, 2B y 2C del tercer artículo en la página 175), por lo que la formación de raíces adventicias se vio retrasada, aunque el número

final de raíces adventicias fue mayor en las plántulas tratadas con ANA. Al aplicar esta hormona en la región apical de los hipocótilos, ésta se transporta de forma polar a la región basal (Hošek *et al*., 2012). La aportación de ANA a los hipocótilos sin parte apical produjo el rescate de la capacidad de enraizamiento de los explantos (véase la figura 2 del tercer artículo en la página 175).

El siguiente paso para la comprobación del transporte de auxinas desde la zona apical de la plántula consistió en inhibir el transporte activo aplicando 2-NOA y NPA (Laňková *et al*., 2010; Teale y Palme, 2018), compuestos que bloquean el transporte de auxinas. Al añadir NPA en el medio de cultivo se bloquea completamente la formación de raíces adventicias y se retrasa significativamente su aparición en el caso de 2-NOA, produciéndose en este caso un aumento de la proliferación celular en la base del hipocótilo (véase la figura 3A, 3B y 3C del tercer artículo en la página 176). La aplicación de estos inhibidores en la parte apical del hipocótilo, tanto en plántulas con o sin parte apical, produjo un retraso significativo en la formación de raíces adventicias, siendo de nuevo más extremo en el caso del ANA. En el mutante hormonal *diageotropica* (Oh *et al*., 2006; Ivanchenko *et al*., 2015), también observamos un retraso en la formación de raíces adventicias (véase la figura 3G del tercer artículo en la página 176). En el experimento en el que evaluamos el efecto de la gravedad en la formación de raíces adventicias, observamos que el transporte polar de auxinas a través del hipocótilo de la planta no se vio afectado por la gravedad, ya que las plántulas no presentaron diferencias ni en la emergencia, ni en la capacidad de enraizamiento, ni en la longitud de las raíces adventicias a los 14 días (véase la figura 4 del tercer artículo en la página 177). En otras especies como *A. thaliana*, la estimulación por gravedad produce una acumulación de auxinas que conduce a un crecimiento asimétrico y flexión de los órganos (Su *et al*., 2017), hecho que observamos en nuestras plántulas únicamente en los nuevos brotes en la parte apical. A los 21 días tras el

corte, se observa un incremento significativo de raíces adventicias en los explantos girados 180° que conservaban la parte apical. Este incremento podría deberse a la expansión hacia arriba de la zona de formación de las raíces adventicias (véase la figura 4E y 4F del tercer artículo en la página 177) debida a un flujo reducido de transporte de auxinas, probablemente a través de la repolarización de PIN3, como ocurre en *A. thaliana* (Rakusová *et al*., 2011; 2016).

En estudios previos con diferentes especies, se ha observado que la auxina producida en las hojas maduras se transporta hasta la zona basal del hipocótilo desencadenando la formación de raíces adventicias (Druege *et al*., 2019). En este trabajo hemos observado que tanto las hojas como los cotiledones de las plántulas de Micro-Tom actúan como fuente de auxinas necesaria para la formación de las raíces adventicias, ya que, aunque eliminemos una de las dos fuentes, no observamos diferencias en la emergencia de las raíces (véanse las figuras 5A y 5B del tercer artículo en la página 178). En cuanto al número de raíces, sí hemos observado diferencias significativas entre plántulas que solo mantenían los cotiledones y plántulas completas, observándose un mayor número de raíces en las plantas que únicamente mantenían los cotiledones (véase la figura 5C del tercer artículo en la página 178). Estos resultados sugieren que los cotiledones podrían ser una mayor fuente de auxinas para la formación de raíces adventicias, mientras que las hojas actuarían al mismo tiempo como fuente y sumidero al no estar completamente desarrolladas. Para confirmar esta hipótesis añadimos un inhibidor del transporte de auxinas en los cotiledones, el NPA, lo que redujo significativamente la capacidad de enraizamiento de las plántulas a los 14 días tras el corte, disminuyendo la cantidad de raíces adventicias a valores similares a los observados en los explantos de hipocótilo (véanse las figuras 5C y 5D del tercer artículo en la página 178). Finalmente, encontramos diferencias significativas en la región del hipocótilo en la que se formaron raíces adventicias en los distintos

explantos, siendo los que conservaban únicamente los cotiledones los que presentaron una zona más amplia de formación de raíces.

Hemos dividido el hipocótilo de tomate en tres fragmentos del mismo tamaño y hemos observado que el fragmento correspondiente a la parte basal del hipocótilo tiene una capacidad de respuesta más temprana que la parte intermedia, y esta a su vez más temprana que la parte apical del hipocótilo. Este mismo resultado lo obtuvimos cuando estudiamos la capacidad de enraizamiento de cada fragmento, observando más raíces en el fragmento correspondiente a la parte basal del hipocótilo, seguido del fragmento intermedio y por último el fragmento de la parte apical del hipocótilo a los 14 días de la escisión (véanse las figuras 6A, 6B, 6C y 6D del tercer artículo en la página 179). Las diferencias observadas podrían deberse a dos factores; por un lado, la diferencia en los niveles de auxina endógena en cada fragmento, y por otro lado la capacidad de respuesta a una misma concentración de auxina de cada uno de los explantos. Para estudiar este mecanismo, añadimos auxina exógena en el medio de cultivo de los explantos a la misma concentración, y observamos una mejoría significativa en los explantos de la parte apical del hipocótilo, que aumentaron su enraizamiento. Sin embargo, no observamos diferencias ni en el tiempo de emergencia de las raíces ni en el número de raíces formadas (véanse las figuras 6A, 6B, 6C y 6D del tercer artículo en la página 179). Las diferencias observadas en la longitud final de las raíces podrían deberse a la diferencia en el tiempo de emergencia de las raíces en cada fragmento.

Con el fin de estudiar la respuesta de fragmentos de hipocótilo de distintos tamaños con diferentes concentraciones de auxinas, dividimos el hipocótilo de Micro-Tom en dos fragmentos de diferentes tamaños (un tercio y tres tercios del hipocótilo completo). En unos casos el fragmento de mayor tamaño abarcaba las zonas apical y central del hipocótilo, y en otros casos el fragmento de mayor tamaño abarcaba las zonas central y basal del hipocótilo (véase la figura 6A del tercer artículo en la página 179). En los

fragmentos apicales observamos un retraso significativo en la emergencia de las raíces adventicias que era independiente del tamaño de los fragmentos, tanto si solo correspondían a un tercio del hipocótilo como si correspondían a dos tercios del hipocótilo (incluyendo la zona central del hipocótilo). Con la incorporación de auxina exógena observamos una mejoría significativa en cuanto al tiempo de emergencia de las raíces en los fragmentos apicales y en los apicales-mediales (véanse las figuras 7A y 7B del tercer artículo en la página 180). Además, observamos diferencias en la capacidad de enraizamiento entre los fragmentos de la parte basal y apical, pero no entre fragmentos de diferentes tamaños pertenecientes a la misma zona del hipocótilo, tampoco al añadir auxinas de forma exógena. Observamos diferencias significativas (valor de $p < 0,01$) en la formación de callo en la parte basal de los explantos a los que se les añadió auxina exógena en todos los fragmentos basales, y únicamente en el fragmento apical de mayor tamaño (véanse las figuras 7C y 7D del tercer artículo en la página 180). Estos resultados apoyarían la hipótesis de que existe un gradiente de respuesta a auxinas preestablecido en el hipocótilo de Micro-Tom, siendo mayor en la parte basal y menor en la parte apical del hipocótilo.

Para obtener información adicional del papel de la respuesta a las auxinas endógenas, hemos estudiado el mutante *entire*, que contiene una mutación de perdida de función en el represor IAA9 que provoca una reducción en los niveles de este correpresor de la familia Aux/IAA en este mutante (Zhang *et al*., 2007). Para ello hemos utilizado un mutante *entire* en fondo Micro-Tom que presenta hojas simples en vez de compuestas, pero un desarrollo normal de sus raíces laterales (Zhang *et al*., 2007). No hemos observado diferencias significativas ni en la emergencia de las raíces adventicias ni en la longitud final de las raíces entre *entire* y su genotipo silvestre. Sin embargo, sí se observaron diferencias significativas en el número de raíces adventicias, siendo mayor en el caso del mutante, lo que podría explicarse por la capacidad de *entire* de formar raíces en una zona

más extensa del hipocótilo, posiblemente debido a una reducción del umbral de respuesta a auxinas (véanse las figuras 8A, 8B, 8C, 8D y 8E del tercer artículo en la página 181). Al realizar cortes transversales de la zona basal del hipocótilo de *entire*, observamos un mayor número de capas de células del cambium desde 24 h tras el corte, lo que podría explicar junto con otros factores la mayor capacidad de enraizamiento observada en este mutante.

Con la finalidad de observar si el gradiente de respuesta a auxinas también se mantiene en el tallo de las plantas de tomate, realizamos fragmentos del tallo de plántulas de Micro-Tom y estudiamos tres regiones; hipocótilo, nudo y ápice (véase la figura 9C y 9D del tercer artículo en las páginas 182-183). Comprobamos que la mayoría de los fragmentos correspondientes a la parte apical de la plántula no fueron capaces de generar raíces adventicias. Aquellos que sí lo hicieron, presentaban un gran retraso con respecto al nudo intermedio, en el que observamos los mismos problemas si lo comparábamos con el hipocótilo (véase la figura 9C del tercer artículo en las páginas 182-183). La capacidad de enraizamiento del entrenudo fue significativamente menor que la del hipocótilo, y los fragmentos que no consiguieron formar raíces presentaron un callo en su zona basal (véanse las figuras 9D, 9F y 9G del tercer artículo en las páginas 182-183). Estos resultados confirmaron la existencia de un gradiente de respuesta a auxinas a lo largo del eje apical-basal de la planta que modula la formación de raíces adventicias.

Algunas de las variedades comerciales estudiadas en este trabajo presentaron diferencias en la región de formación de las raíces adventicias con respecto a Micro-Tom, como fue el caso de Moneymaker o Heinz 1706-BG, donde observamos diferencias significativas en parámetros como la capacidad de enraizamiento o el número de raíces adventicias. Sin embargo, otras variedades comerciales también utilizadas en el ámbito de la investigación, como es UC-82, no presentó diferencias estadísticamente

significativas en estos parámetros cuando la comparábamos con Micro-Tom. Comprobamos que la región de formación de raíces en el hipocótilo es similar entre Micro-Tom y cultivares como Moneymaker o Heinz 1706-BG, mientras que UC-82 presentó una región de enraizamiento significativamente menor. Las diferencias observadas en el número de raíces adventicias formadas en el caso de Micro-Tom podrían deberse a la diferencia de tamaño existente entre los diferentes hipocótilos (véase la figura S3 del tercer artículo en la página 186).

CONCLUSIONES

4. CONCLUSIONES Y PROYECCIÓN FUTURA

4.1 Conclusiones

- Hemos establecido un protocolo efectivo para explorar la arquitectura del sistema radicular de diferentes genotipos de tomate en estadios tempranos de crecimiento. Se han estudiado nueve entradas de tomates silvestres, cuatro de cultivares comerciales y seis de mutantes en fondo Micro-Tom.

- Hemos definido morfológicamente la arquitectura radicular en los estadios iniciales de plántulas de tomate. Para ello, hemos seleccionado seis rasgos morfológicos presentes en la raíz principal y en las raíces laterales, así como cuatro rasgos adicionales asociados a la formación de raíces adventicias inducidas en respuesta a herida. Hemos generado ocho ideotipos que engloban las diferentes morfologías radiculares que se han descrito en este trabajo.

- Hemos observado un número significativamente mayor de raíces adventicias en los cultivares comerciales, así como en su ancestro silvestre *Solanum pimpinellifolium*, comparados con el resto de genotipos estudiados. También se determinó que la tasa de crecimiento de las raíces adventicias fue mayor en dichos cultivares.

- Hemos realizado una búsqueda de mutantes de tomate afectados en el crecimiento temprano mediante el estudio de 9367 plántulas derivadas de 395 líneas M_3 de una colección de semillas de Micro-Tom mutagenizadas con metanosulfonato de etilo. 946 plántulas en 252 líneas M_3 presentaron fenotipo mutante claramente distinguible del fenotipo mostrado por su ancestro silvestre.

- En 14 de las líneas M_3 estudiadas se observó al menos un individuo con alguna alteración del fenotipo en la raíz principal y/o en las raíces

laterales. En 11 de las líneas, estas alteraciones estaban presentes en diferentes individuos, mientras que en tres de ellas se observaron individuos con fenotipo mutante en ambos tipos radiculares. De estas tres últimas, las líneas P13C12 y P15A4 presentaban reducida la longitud de la raíz principal y el número de raíces laterales, mientras que la línea P16E10 presentaba una longitud corta de raíz principal pero un mayor número de raíces laterales.

- Hemos identificado 17 líneas M_3 con individuos afectados en la formación y desarrollo temprano de raíces adventicias inducidas en respuesta a herida. En otras 23 líneas M_3 se observaron individuos con alteraciones en la raíz principal y en las adventicias. Además, en seis de las líneas estudiadas las alteraciones se encontraron en las raíces laterales y las adventicias. Únicamente anotamos dos líneas M_3 en las que se observaron alteraciones del fenotipo en los tres tipos radiculares estudiados (raíz principal, raíces laterales y raíces adventicias).

- En nuestro sistema experimental, los primordios de las raíces adventicias se forman *de novo* en los hipocótilos de plántulas de Micro-Tom después de la escisión del sistema radicular principal. La iniciación de las raíces adventicias está regulada espacial y temporalmente por las divisiones estereotipadas de algunas células del cambium distal, que se ubican en las regiones que flanquean a los haces vasculares.

- Hemos observado un gradiente interno de respuesta a auxinas en el hipocótilo de Micro-Tom pocas horas después de la escisión del sistema radicular, que alcanza sus niveles máximos en una posición definida de la región basal del hipocótilo, justo por encima de la herida.

- En nuestro sistema experimental de explantos jóvenes de Micro-Tom, las auxinas que inducen la formación de raíces adventicias se transportan mayoritariamente desde los cotiledones, mientras que el meristemo

apical del tallo y las hojas en desarrollo son a su vez fuente y sumidero de auxinas.

- Hemos observado una relación directa entre la cantidad de tejidos productores de auxinas y el tamaño del dominio formativo de raíces adventicias, que contribuye directamente a la capacidad de enraizamiento de los explantos.

- Utilizando una combinación de enfoques fisiológicos y genéticos, hemos proporcionado evidencias adicionales acerca de la relevancia del transporte de las auxinas en la regulación de la formación de las raíces adventicias inducidas por herida en los explantos jóvenes de Micro-Tom.

- Nuestros resultados con explantos de hipocótilo de Micro-Tom de diferentes longitudes proporcionan un marco conceptual para el estudio de la formación de órganos *de novo* en esta especie, ya que estos explantos desarrollaron raíces y brotes adventicios tras la escisión simultánea del sistema radicular principal y de la región apical situada por encima de los cotiledones.

- Encontramos diferencias notables en la emergencia de raíces adventicias con respecto a la posición de los explantos a lo largo del eje apical-basal del hipocótilo, independientemente de la longitud de éstos. El tamaño de la región formativa de las raíces adventicias en la región basal del hipocótilo se mantuvo constante en todos los casos, lo que sugiere su estricta regulación.

4.2 Proyección futura

En la actualidad se dispone de una amplia colección de mutantes hormonales en fondo Micro-Tom y durante esta Tesis doctoral he llevado a cabo un estudio sistemático del sistema radicular en los estadios iniciales del crecimiento de algunos de ellos, encontrando mutantes muy interesantes afectados en la ruta de diferentes hormonas como las auxinas o el etileno y algunas rutas directa o indirectamente relacionadas con ellas como el caso de las antocianinas que han aportado resultados muy interesantes. En este sentido sería muy interesante seguir explorando la arquitectura radicular en la colección de mutantes hormonales con el fin de encontrar nuevos reguladores hormonales que actúen durante el proceso de formación y desarrollo de las raíces adventicias en esta especie.

De todos los fenotipos mutantes observados en las líneas mutagenizadas con MSE en fondo Micro-Tom, hemos seleccionado aquellos que afectan a la estructura de las raíces adventicias. En concreto, hemos encontrado cinco líneas (P12F10, P14F11, P14G10, P15G12 y P16H11) portadoras de presuntas mutaciones causantes de un aumento en el número de raíces adventicias. Dichas mutaciones podrían estar afectando a genes que actúan como reguladores negativos de la formación de las raíces adventicias. Una vez confirmados los fenotipos en la siguiente generación, se podría realizar un estudio de regiones candidatas a través de la secuenciación de grupos de individuos silvestres y mutantes. Posteriormente, gracias a técnicas de edición de genes como CRISPR/Cas9, se podrían obtener mutantes de pérdida de función para cada uno de los genes presentes en las regiones candidatas, lo que nos permitiría confirmar la mutación responsable del fenotipo observado.

Para conocer más en detalle el papel de las auxinas en la formación de las raíces adventicias sería interesante determinar tanto la región concreta de los explantos en la que se acumulan las auxinas como el tiempo que tarda en producirse dicha acumulación, ya que, para que las células del cambium

ubicadas en el borde de los haces vasculares comiencen a dividirse hasta formar un primordio radicular *de novo,* es necesario que se sobrepase un umbral de concentración de auxinas determinado. Para tal fin, podría hacerse uso de líneas marcadoras de la respuesta a auxina como, por ejemplo, *DR5pro::GFP*, la cual permite la observación de un máximo de auxinas en la célula con ayuda de un microscopio de fluorescencia de hoja de luz.

Por otro lado, también resultaría de interés conocer si existe interacción alguna entre las auxinas y otras moléculas y/o rutas hormonales implicadas en el proceso de formación de las raíces adventicias. Para ello podría estudiarse el fenotipo radicular de mutantes de auxinas en medios suplementados con otras hormonas y viceversa.

REFERENCIAS

5. REFERENCIAS

Abas, L., Benjamins, R., Malenica, N., Paciorek, T. T., Wiřniewska, J., Moulinier-Anzola, J. C., Sieberer, T., Friml, J., & Luschnig, C. (2006). Intracellular trafficking and proteolysis of the Arabidopsis auxin-efflux facilitator PIN2 are involved in root gravitropism. *Nature Cell Biology*, *8*(3), 249–256. https://doi.org/10.1038/NCB1369

Abbo, S., Pinhasi van-Oss, R., Gopher, A., Saranga, Y., Ofner, I., & Peleg, Z. (2014). Plant domestication versus crop evolution: a conceptual framework for cereals and grain legumes. *Trends in Plant Science*, *19*(6), 351–360. https://doi.org/10.1016/J.TPLANTS.2013.12.002

Anfang, M., & Shani, E. (2021). Transport mechanisms of plant hormones. *Current Opinion in Plant Biology*, *63*, 102055. https://doi.org/10.1016/j.pbi.2021.102055

Atkinson, J. A., Rasmussen, A., Traini, R., Voß, U., Sturrock, C., Mooney, S. J., Wells, D. M., & Bennett, M. J. (2014). Focus Issue on Roots: Branching Out in Roots: Uncovering Form, Function, and Regulation. *Plant Physiology*, *166*(2), 538. https://doi.org/10.1104/PP.114.245423

Bai, Y., & Lindhout, P. (2007). Domestication and Breeding of Tomatoes: What have We Gained and What Can We Gain in the Future? *Annals of Botany*, *100*(5), 1085–1094. https://doi.org/10.1093/aob/mcm150

Banda, J., Bellande, K., von Wangenheim, D., Goh, T., Guyomarc'h, S., Laplaze, L., & Bennett, M. J. (2019). Lateral Root Formation in Arabidopsis: A Well-Ordered LRexit. *Trends in Plant Science*, *24*(9), 826–839. https://doi.org/10.1016/J.TPLANTS.2019.06.015

Barboza-Barquero, L., Nagel, K. A., Jansen, M., Klasen, J. R., Kastenholz, B., Braun, S., Bleise, B., Brehm, T., Koornneef, M., & Fiorani, F. (2015). Phenotype of Arabidopsis thaliana semi-dwarfs with deep roots and high growth rates under water-limiting conditions is independent of the GA5 loss-of-function alleles. *Annals of Botany*, *116*(3), 321–331. https://doi.org/10.1093/AOB/MCV099

Beeckman, T., Przemeck, G. K. H., Stamatiou, G., Lau, R., Terryn, N., de Rycke, R., Inzé, D., & Berleth, T. (2002). Genetic Complexity of Cellulose Synthase A Gene Function in Arabidopsis Embryogenesis. *Plant Physiology*, *130*(4), 1883. https://doi.org/10.1104/PP.102.010603

Beemster, G. T. S., & Baskin, T. I. (1998). Analysis of cell division and elongation underlying the developmental acceleration of root growth in Arabidopsis thaliana. *Plant Physiology*, *116*(4), 1515–1526. https://doi.org/10.1104/PP.116.4.1515

Bellini, C., Pacurar, D. I., & Perrone, I. (2014). Adventitious Roots and Lateral Roots: Similarities and Differences. *Annu. Rev. Plant Biol*, *65*, 639–666. https://doi.org/10.1146/annurev-arplant-050213-035645

Blanca, J., Esteras, C., Ziarsolo, P., Pérez, D., FernÃndez-Pedrosa, V., Collado, C., RodrÃguez de Pablos, R., Ballester, A., Roig, C., Cañizares, J., & Picó, B. (2012). Transcriptome sequencing for SNP discovery across Cucumis melo. *BMC Genomics*, *13*(1). https://doi.org/10.1186/1471-2164-13-280

Blanca, J., Montero-Pau, J., Sauvage, C., Bauchet, G., Illa, E., Díez, M. J., Francis, D., Causse, M., van der Knaap, E., & Cañizares, J. (2015). Genomic variation in tomato, from wild ancestors to contemporary breeding accessions. *BMC Genomics*, *16*(1), 257. https://doi.org/10.1186/s12864-015-1444-1

Blanca, J., Sanchez-Matarredona, D., Ziarsolo, P., Montero-Pau, J., Knaap, E. van der, Díez, M. J., & Cañizares, J. (2021). Haplotype analyses reveal novel insights into tomato history and domestication including long-distance migrations and latitudinal adaptations. *BioRxiv*, 2021.06.18.448912. https://doi.org/10.1101/2021.06.18.448912

Brinker, M., van Zyl, L., Liu, W., Craig, D., Sederoff, R. R., Clapham, D. H., & von Arnold, S. (2004). Microarray analyses of gene expression during adventitious root development in Pinus contorta. *Plant Physiology*, *135*(3), 1526–1539. https://doi.org/10.1104/pp.103.032235

Caldwell, K. S., Langridge, P., & Powell, W. (2004). Comparative Sequence Analysis of the Region Harboring the Hardness Locus in Barley and Its Colinear Region in Rice. *Plant Physiology*, *136*(2), 3177–3190. https://doi.org/10.1104/PP.104.044081

Campos, M. L., Carvalho, R. F., Benedito, V. A., & Peres, L. E. P. (2010). Small and remarkable: The Micro-Tom model system as a tool to discover novel hormonal functions and interactions. *Plant Signaling & Behavior*, *5*(3), 267–270. https://doi.org/10.4161/PSB.5.3.10622

Carvalho, R. F., Campos, M. L., Pino, L. E., Crestana, S. L., Zsögön, A., Lima, J. E., Benedito, V. A., & Peres, L. E. (2011). Convergence of developmental mutants into a single tomato model system: “Micro-Tom” as an effective toolkit for plant development research. *Plant Methods*, 7, 18. https://doi.org/10.1186/1746-4811-7-18

Cheng, Y., Dai, X., & Zhao, Y. (2006). Auxin biosynthesis by the YUCCA flavin monooxygenases controls the formation of floral organs and vascular tissues in Arabidopsis. *Genes & Development*, *20*(13), 1790. https://doi.org/10.1101/GAD.1415106

Darwin, S. C., Knapp, S., & Peralta, I. E. (2003). Taxonomy of tomatoes in the galápagos islands: Native and introduced species of solarium section lycopersicon (solanaceae). *Systematics and Biodiversity*, *1*(1), 29–53. https://doi.org/10.1017/S1477200003001026

Dawood, T., Rieu, I., Wolters-Arts, M., Derksen, E. B., Mariani, C., & Visser, E. J. W. (2014). Rapid flooding-induced adventitious root development from preformed primordia in Solanum dulcamara. *AoB PLANTS*, *6*. https://doi.org/10.1093/AOBPLA/PLT058

de Klerk, G. J., van der Krieken, W., & de Jong, J. C. (1999). The formation of adventitious roots: New concepts, new possibilities. *In Vitro Cellular and Developmental Biology - Plant*, *35*(3), 189–199. https://doi.org/10.1007/S11627-999-0076-Z

della Rovere, F., Fattorini, L., D'Angeli, S., Veloccia, A., Falasca, G., & Altamura, M. M. (2013). Auxin and cytokinin control formation of the quiescent centre in the adventitious root apex of arabidopsis. *Annals of Botany*, *112*(7), 1395–1407. https://doi.org/10.1093/aob/mct215

Díez, M. J., & Nuez, F. (2008). Tomato. *Vegetables II*, 249–323. https://doi.org/10.1007/978-0-387-74110-9_7

Dolan, L., Janmaat, K., Willemsen, V., Linstead, P., Poethig, S., Roberts, K., & Scheres, B. (1993). Cellular organisation of the Arabidopsis thaliana root. *Development*, *119*(1), 71–84. https://doi.org/10.1242/DEV.119.1.71

Druege, U., Franken, P., & Hajirezaei, M. R. (2016). Plant hormone homeostasis, signaling, and function during adventitious root formation in cuttings. *Frontiers in Plant Science*, *7:* 381. https://doi.org/10.3389/FPLS.2016.00381

Druege, U., Hilo, A., Pérez-Pérez, J. M., Klopotek, Y., Acosta, M., Shahinnia, F., Zerche, S., Franken, P., & Hajirezaei, M. R. (2019). Molecular and physiological control of adventitious rooting in cuttings: phytohormone action meets resource allocation. *Annals of Botany*, *123*(6), 929–949. https://doi.org/10.1093/AOB/MCY234

Du, Y., & Scheres, B. (2018). Lateral root formation and the multiple roles of auxin. *Journal of Experimental Botany*, *69*(2), 155–167. https://doi.org/10.1093/JXB/ERX223

Emmanuel, E., & Levy, A. A. (2002). Tomato mutants as tools for functional genomics. *Current Opinion in Plant Biology*, *5*(2), 112–117. https://doi.org/10.1016/S1369-5266(02)00237-6

Eshed, Y., & Zamir, D. (1995). An Introgression Line Population of *Lycopersicon pennellii* in the Cultivated Tomato Enables the Identification and Fine Mapping of Yield-Associated QTL. *Genetics*, 141.3.1147. https://academic.oup.com/genetics/article/141/3/1147/6013534

Feller, C., Bleiholder, H., Buhr, L., Hack, H., He, M., Klose, R., Meier, U., Stau/, R., van den Boom, T., & Weber, E. (1995). Phanologische Entwicklungsstadien von Gemusepflanzen II. Fruchtgemuse und Hulsenfruchte Codierung und Beschreibung nach der erweiterten BBCH-Skala-rnit Abbildungen Phenological growth stages of vegetable crops II. Fruit vegetables and pulses. In *Nachrichtenbl. Deut. Pflanzenschutzd* (Vol. 47, Issue 9).

Foolad, M. R. (2007). Genome mapping and molecular breeding of tomato. *International Journal of Plant Genomics*, *2007*. https://doi.org/10.1155/2007/64358

Fridman, Y., & Savaldi-Goldstein, S. (2013). Brassinosteroids in growth control: how, when and where. *Plant Science : An International Journal of Experimental Plant Biology*, *209*, 24–31. https://doi.org/10.1016/J.PLANTSCI.2013.04.002

Gady, A. L. F., Hermans, F. W. K., van de Wal, M. H. B. J., van Loo, E. N., Visser, R. G. F., & Bachem, C. W. B. (2009). Implementation of two high through-put techniques in a novel application: Detecting point mutations in large EMS mutated plant populations. *Plant Methods*, *5*(1). https://doi.org/10.1186/1746-4811-5-13

Garcia, V., Bres, C., Just, D., Fernandez, L., Tai, F. W. J., Mauxion, J. P., le Paslier, M. C., Bérard, A., Brunel, D., Aoki, K., Alseekh, S., Fernie, A. R., Fraser, P. D., & Rothan, C. (2016). Rapid identification of causal mutations in tomato EMS populations via mapping-by-sequencing. *Nature Protocols*, *11*(12), 2401–2418. https://doi.org/10.1038/NPROT.2016.143

Geisler, M., Bailly, A., & Ivanchenko, M. (2016). Master and servant: Regulation of auxin transporters by FKBPs and cyclophilins. *Plant Science*, *245*, 1–10. https://doi.org/10.1016/j.plantsci.2015.12.004

Geiss, G., Gutierrez, L., & Bellini, C. (2009). Adventitious Root Formation: New Insights and Perspectives. *Root Development*, *37*, 127–156. https://doi.org/10.1002/9781444310023.CH5

Gonin, M., Bergougnoux, V., Nguyen, T. D., Gantet, P., & Champion, A. (2019). What Makes Adventitious Roots? *Plants,* *8*(7), 240. https://doi.org/10.3390/PLANTS8070240

Greene, E. A., Codomo, C. A., Taylor, N. E., Henikoff, J. G., Till, B. J., Reynolds, S. H., Enns, L. C., Burtner, C., Johnson, J. E., Odden, A. R., Comai, L., & Henikoff, S. (2003). Spectrum of chemically induced mutations from a large-scale reverse-genetic screen in Arabidopsis. *Genetics*, *164*(2), 731–740. https://doi.org/10.1093/GENETICS/164.2.731

Grubbs, F. E. (1969). Procedures for Detecting Outlying Observations in Samples. *American Society for Quality, 11*(1), 1–21.

Guan, L., Tayengwa, R., Cheng, Z. M., Peer, W. A., Murphy, A. S., & Zhao, M. (2019). Auxin regulates adventitious root formation in tomato cuttings. *BMC Plant Biology*, *19*(1), 1–16. https://doi.org/10.1186/S12870-019-2002-9/FIGURES/7

Gutierrez, L., Mongelard, G., Floková, K., Păcurar, D. I., Novák, O., Staswick, P., Kowalczyk, M., Păcurar, M., Demailly, H., Geiss, G., & Bellini, C. (2012). Auxin controls Arabidopsis adventitious root initiation by regulating jasmonic acid homeostasis. *Plant Cell*, *24*(6), 2515–2527. https://doi.org/10.1105/tpc.112.099119

Harrison, E., Burbidge, A., Okyere, J. P., Thompson, A. J., & Taylor, I. B. (2011). Identification of the tomato ABA-deficient mutant sitiens as a member of the ABA-aldehyde oxidase gene family using genetic and genomic analysis. *Plant Growth Regulation*, *64*(3), 301–309. https://doi.org/10.1007/s10725-010-9550-1

Herder, G. den, van Isterdael, G., Beeckman, T., & de Smet, I. (2010). The roots of a new green revolution. *Trends in Plant Science*, *15*(11), 600–607. https://doi.org/10.1016/J.TPLANTS.2010.08.009

Hirakawa, H., Shirasawa, K., Ohyama, A., Fukuoka, H., Aoki, K., Rothan, C., Sato, S., Isobe, S., & Tabata, S. (2013). Genome-wide SNP genotyping to infer the effects on gene

functions in tomato. *DNA Research*, *20*(3), 221–233. https://doi.org/10.1093/dnares/dst005

Hodge, A., Berta, G., Doussan, C., Merchan, F., Crespi, M., Hodge, A., Berta, G., Doussan, C., Merchan, F., & Crespi, M. (2009). Plant root growth, architecture and function. *Plant and Soil*, *321*(1), 153–187. https://doi.org/10.1007/S11104-009-9929-9

Holmes, P., Djordjevic, M. A., & Imin, N. (2010). Global gene expression analysis of in vitro root formation in Medicago truncatula. *Functional Plant Biology*, *37*(12), 1117–1131. https://doi.org/10.1071/FP10159

Hošek, P., Kubeš, M., Laňková, M., Dobrev, P. I., Klíma, P., Kohoutová, M., Petrášek, J., Hoyerová, K., Jiřina, M., & Zažímalová, E. (2012). Auxin transport at cellular level: new insights supported by mathematical modelling. *Journal of Experimental Botany*, *63*(10), 3815. https://doi.org/10.1093/JXB/ERS074

Ivanchenko, M. G., Zhu, J., Wang, B., Medvecká, E., Du, Y., Azzarello, E., Mancuso, S., Megraw, M., Filichkin, S., Dubrovsky, J. G., Friml, J., & Geisler, M. (2015). The cyclophilin A DIAGEOTROPICA gene affects auxin transport in both root and shoot to control lateral root formation. *Development*, *142*(4), 712–721. https://doi.org/10.1242/DEV.113225

Jung, J. K. H., & McCouch, S. (2013). Getting to the roots of it: Genetic and hormonal control of root architecture. *Frontiers in Plant Science*, *4*, 186. https://doi.org/10.3389/FPLS.2013.00186/ABSTRACT

Just, D., Garcia, V., Fernandez, L., Bres, C., Mauxion, J. P., Petit, J., Jorly, J., Assali, J., Bournonville, C., Ferrand, C., Baldet, P., Lemaire-Chamley, M., Mori, K., Okabe, Y., Ariizumi, T., Asamizu, E., Ezura, H., & Rothan, C. (2013). Micro-Tom mutants for functional analysis of target genes and discovery of new alleles in tomato. In *Plant Biotechnology*, 30(3), 225–231. https://doi.org/10.5511/plantbiotechnology.13.0622a

Kareem, A., Radhakrishnan, D., Sondhi, Y., Aiyaz, M., Roy, M. v., Sugimoto, K., & Prasad, K. (2016). De novo assembly of plant body plan: a step ahead of Deadpool. *Regeneration*, *3*(4), 182–197. https://doi.org/10.1002/REG2.68

Karlova, R., Chapman, N., David, K., Angenent, G. C., Seymour, G. B., & de Maagd, R. A. (2014). Transcriptional control of fleshy fruit development and ripening. *Journal of Experimental Botany,* 65(16) 4527–4541. https://doi.org/10.1093/jxb/eru316

Kato, Y., Abe, J., Kamoshita, A., & Yamagishi, J. (2006). Genotypic variation in root growth angle in rice (*Oryza sativa L*.) and its association with deep root development in upland fields with different water regimes. *Plant and Soil*, *287*(1–2), 117–129. https://doi.org/10.1007/S11104-006-9008-4

Kell, D. B. (2011). Breeding crop plants with deep roots: their role in sustainable carbon, nutrient and water sequestration. *Annals of Botany*, *108*(3), 407–418. https://doi.org/10.1093/AOB/MCR175

Khan, S., & Stone, J. M. (2007). *Arabidopsis thaliana* GH3.9 in Auxin and Jasmonate Cross Talk. *Plant Signaling & Behavior*, *2*(6), 483. https://doi.org/10.4161/PSB.2.6.4498

Kim, H. J., Lynch, J. P., & Brown, K. M. (2008). Ethylene insensitivity impedes a subset of responses to phosphorus deficiency in tomato and petunia. *Plant, Cell & Environment*, *31*(12), 1744–1755. https://doi.org/10.1111/J.1365-3040.2008.01886.X

Kim, J. Y., Kim, S. K., Jung, J., Jeong, M. J., & Ryu, C. M. (2018). Exploring the sound-modulated delay in tomato ripening through expression analysis of coding and non-coding RNAs. *Annals of Botany*, *122*(7), 1231–1244. https://doi.org/10.1093/aob/mcy134

Knapp, S., Bohs, L., Nee, M., & Spooner, D. M. (2004). Solanaceae - A model for linking genomics with biodiversity. *Comparative and Functional Genomics*, *5*(3), 285–291. https://doi.org/10.1002/cfg.393

Kohlen, W., Charnikhova, T., Lammers, M., Pollina, T., Tóth, P., Haider, I., Pozo, M. J., de Maagd, R. A., Ruyter-Spira, C., Bouwmeester, H. J., & López-Ráez, J. A. (2012). The tomato CAROTENOID CLEAVAGE DIOXYGENASE8 (SlCCD8) regulates rhizosphere signaling, plant architecture and affects reproductive development through strigolactone biosynthesis. *The New Phytologist*, *196*(2), 535–547. https://doi.org/10.1111/J.1469-8137.2012.04265.X

Lakehal, A., & Bellini, C. (2019). Control of adventitious root formation: insights into synergistic and antagonistic hormonal interactions. *Physiologia Plantarum*, *165*(1), 90–100. https://doi.org/10.1111/ppl.12823

Laňková, M., Smith, R. S., Pešek, B., Kubeš, M., Zažímalová, E., Petrášek, J., & Hoyerová, K. (2010). Auxin influx inhibitors 1-NOA, 2-NOA, and CHPAA interfere with membrane dynamics in tobacco cells. *Journal of Experimental Botany*, *61*(13), 3589. https://doi.org/10.1093/JXB/ERQ172

Lavenus, J., Goh, T., Roberts, I., Guyomarc'h, S., Lucas, M., de Smet, I., Fukaki, H., Beeckman, T., Bennett, M., & Laplaze, L. (2013). Lateral root development in Arabidopsis: fifty shades of auxin. *Trends in Plant Science*, *18*(8), 450–458. https://doi.org/10.1016/J.TPLANTS.2013.04.006

Lee, H. W., Cho, C., Pandey, S. K., Park, Y., Kim, M. J., & Kim, J. (2019). LBD16 and LBD18 acting downstream of ARF7 and ARF19 are involved in adventitious root formation in Arabidopsis. *BMC Plant Biology*, *19*(1), 1–11. https://doi.org/10.1186/S12870-019-1659-4/FIGURES/7

Li, S. W. (2021). Molecular Bases for the Regulation of Adventitious Root Generation in Plants. *Frontiers in Plant Science*, *12*, 1–19. https://doi.org/10.3389/fpls.2021.614072

Li, S. W., Xue, L., Xu, S., Feng, H., & An, L. (2009). Mediators, genes and signaling in adventitious rooting. *Botanical Review*, *75*(2), 230–247. https://doi.org/10.1007/s12229-009-9029-9

Li, Y., Wang, H., Zhang, Y., & Martin, C. (2018). Can the world's favorite fruit, tomato, provide an effective biosynthetic chassis for high-value metabolites? *Plant Cell*

Reports, *37*(10), 1443–1450. https://doi.org/10.1007/S00299-018-2283-8/FIGURES/2

Liu, J., Rowe, J., & Lindsey, K. (2014). Hormonal crosstalk for root development: a combined experimental and modeling perspective. *Frontiers in Plant Science*, *5*, 116. https://doi.org/10.3389/FPLS.2014.00116

Loudet, O., Gaudon, V., Trubuil, A., & Daniel-Vedele, F. (2005). Quantitative trait loci controlling root growth and architecture in *Arabidopsis thaliana* confirmed by heterogeneous inbred family. *TAG. Theoretical and Applied Genetics. Theoretische Und Angewandte Genetik*, *110*(4), 742–753. https://doi.org/10.1007/S00122-004-1900-9

Luo, J. (2015). Metabolite-based genome-wide association studies in plants. In *Current Opinion in Plant Biology*, 24, 31–38. https://doi.org/10.1016/j.pbi.2015.01.006

Lynch, J. P. (2007). Roots of the Second Green Revolution. *Australian Journal of Botany*, *55*(5), 493–512. https://doi.org/10.1071/BT06118

Lynch, J. P., & Brown, K. M. (2012). New roots for agriculture: exploiting the root phenome. *Philosophical Transactions of the Royal Society B: Biological Sciences*, *367*(1595), 1598–1604. https://doi.org/10.1098/RSTB.2011.0243

Maharjan, P. M., Dilkes, B. P., Fujioka, S., Pěnčík, A., Ljung, K., Burow, M., Halkier, B. A., & Choe, S. (2014). Arabidopsis gulliver1/SUPERROOT2-7 identifies a metabolic basis for auxin and brassinosteroid synergy. *The Plant Journal : For Cell and Molecular Biology*, *80*(5), 797–808. https://doi.org/10.1111/TPJ.12678

Maloney, G. S., DiNapoli, K. T., & Muday, G. K. (2014). The anthocyanin reduced tomato mutant demonstrates the role of flavonols in tomato lateral root and root hair development. *Plant Physiology*, *166*(2), 614–631. https://doi.org/10.1104/PP.114.240507

Mano, Y., & Nemoto, K. (2012). The pathway of auxin biosynthesis in plants. *Journal of Experimental Botany*, *63*(8), 2853–2872. https://doi.org/10.1093/JXB/ERS091

Manschadi, A. M., Christopher, J., Devoil, P., & Hammer, G. L. (2006). The role of root architectural traits in adaptation of wheat to water-limited environments. *Functional Plant Biology*, *33*(9), 823–837. https://doi.org/10.1071/FP06055

Martí, E., Gisbert, C., Bishop, G. J., Dixon, M. S., & García-Martínez, J. L. (2006). Genetic and physiological characterization of tomato cv. Micro-Tom. *Journal of Experimental Botany*, *57*(9), 2037–2047. https://doi.org/10.1093/jxb/erj154

Martín-Pizarro, C., & Posé, D. (2018). Genome Editing as a Tool for Fruit Ripening Manipulation. *Frontiers in Plant Science*, *9*. https://doi.org/10.3389/FPLS.2018.01415

Mashiguchi, K., Tanaka, K., Sakai, T., Sugawara, S., Kawaide, H., Natsume, M., Hanada, A., Yaeno, T., Shirasu, K., Yao, H., McSteen, P., Zhao, Y., Hayashi, K. I., Kamiya, Y., & Kasahara, H. (2011). The main auxin biosynthesis pathway in Arabidopsis. *Proceedings of the National Academy of Sciences of the United States of America*, *108*(45), 18512–18517. https://doi.org/10.1073/PNAS.1108434108

Mauriat, M., Petterle, A., Bellini, C., & Moritz, T. (2014). Gibberellins inhibit adventitious rooting in hybrid aspen and Arabidopsis by affecting auxin transport. *The Plant Journal : For Cell and Molecular Biology*, *78*(3), 372–384. https://doi.org/10.1111/TPJ.12478

Mayer, U., Ruiz, R. A. T., Berleth, T., Miseéra, S., & Jürgens, G. (1991). Mutations affecting body organization in the Arabidopsis embryo. *Nature 1991 353:6343*, *353*(6343), 402–407. https://doi.org/10.1038/353402a0

McAdam, S. A. M., Brodribb, T. J., & Ross, J. J. (2016). Shoot-derived abscisic acid promotes root growth. *Plant, Cell & Environment*, *39*(3), 652–659. https://doi.org/10.1111/PCE.12669

Meinke, D. W. (2013). A survey of dominant mutations in *Arabidopsis thaliana*. *Trends in Plant Science*, *18*(2), 84–91. https://doi.org/10.1016/J.TPLANTS.2012.08.006

Meinke, D. W. (2020). Genome-wide identification of EMBRYO-DEFECTIVE (EMB) genes required for growth and development in Arabidopsis. *The New Phytologist*, *226*(2), 306–325. https://doi.org/10.1111/NPH.16071

Meissner, R., Jacobson, Y., Melamed, S., Levyatuv, S., Shalev, G., Ashri, A., Elkind, Y., & Levy, A. (1997). A new model system for tomato genetics. *The Plant Journal*, *12*(6), 1465–1472. https://doi.org/10.1046/J.1365-313X.1997.12061465.X

Menda, N., Semel, Y., Peled, D., Eshed, Y., & Zamir, D. (2004). In silico screening of a saturated mutation library of tomato. *The Plant Journal : For Cell and Molecular Biology*, *38*(5), 861–872. https://doi.org/10.1111/J.1365-313X.2004.02088.X

Mhimdi, M., & Pérez-Pérez, J. M. (2020). Understanding of Adventitious Root Formation: What Can We Learn From Comparative Genetics? *Frontiers in Plant Science*, *11*, 1541. https://doi.org/10.3389/FPLS.2020.582020/BIBTEX

Minoia, S., Petrozza, A., D'onofrio, O., Piron, F., Mosca, G., Sozio, G., Cellini, F., Bendahmane, A., & Carriero, F. (2010). *A new mutant genetic resource for tomato crop improvement by TILLING technology*. *BMC Research Notes*, 3,69. http://www.biomedcentral.com/1756-0500/3/69

Miyazawa, Y., Yamazaki, T., Moriwaki, T., & Takahashi, H. (2011). Root Tropism. Its Mechanism and Possible Functions in Drought Avoidance. *Advances in Botanical Research*, *57*, 349–375. https://doi.org/10.1016/B978-0-12-387692-8.00010-2

Moreno-Risueno, M. A., van Norman, J. M., Moreno, A., Zhang, J., Ahnert, S. E., & Benfey, P. N. (2010). Oscillating gene expression determines competence for periodic Arabidopsis root branching. *Science*, *329*(5997), 1306–1311. https://doi.org/10.1126/SCIENCE.1191937

Motte, H., Vanneste, S., & Beeckman, T. (2019). Molecular and Environmental Regulation of Root Development. *Annual Review of Plant Biology*, 70, 465-488. h*ttps://Doi.Org/10.1146/Annurev-Arplant-050718-100423*, *70*, 465–488.

Mravec, J., Skůpa, P., Bailly, A., Hoyerová, K., Křeček, P., Bielach, A., Petrášek, J., Zhang, J., Gaykova, V., Stierhof, Y. D., Dobrev, P. I., Schwarzerová, K., Rolčík, J., Seifertová, D., Luschnig, C., Benková, E., Zažímalová, E., Geisler, M., & Friml, J. (2009).

Subcellular homeostasis of phytohormone auxin is mediated by the ER-localized PIN5 transporter. *Nature*, *459*(7250), 1136–1140. https://doi.org/10.1038/NATURE08066

Mubarok, S., Okabe, Y., Fukuda, N., Ariizumi, T., & Ezura, H. (2015). Potential Use of a Weak Ethylene Receptor Mutant, Sletr1-2, as Breeding Material To Extend Fruit Shelf Life of Tomato. *Journal of Agricultural and Food Chemistry*, *63*(36), 7995–8007. https://doi.org/10.1021/ACS.JAFC.5B02742

Musseau, C., Just, D., Jorly, J., Gévaudant, F., Moing, A., Chevalier, C., Lemaire-Chamley, M., Rothan, C., & Fernandez, L. (2017). Identification of two new mechanisms that regulate fruit growth by cell expansion in tomato. *Frontiers in Plant Science*, *8*. https://doi.org/10.3389/fpls.2017.00988

Nakazato, T., Warren, D. L., & Moyle, L. C. (2010). Ecological and geographic modes of species divergence in wild tomatoes. *American journal of Botany,* 97(4), 680-693. https://doi.org/10.3732/ajb.0900216

Negi, S., Ivanchenko, M. G., & Muday, G. K. (2008). Ethylene regulates lateral root formation and auxin transport in *Arabidopsis thaliana*. *The Plant Journal: For Cell and Molecular Biology*, *55*(2), 175–187. https://doi.org/10.1111/J.1365-313X.2008.03495.X

Negi, S., Sukumar, P., Liu, X., Cohen, J. D., & Muday, G. K. (2010). Genetic dissection of the role of ethylene in regulating auxin-dependent lateral and adventitious root formation in tomato. *The Plant Journal*, *61*(1), 3–15. https://doi.org/10.1111/J.1365-313X.2009.04027.X

Oh, K. C., Ivanchenko, M. G., White, T. J., & Lomax, T. L. (2006). The diageotropica gene of tomato encodes a cyclophilin: a novel player in auxin signaling. *Planta*, *224*(1), 133–144. https://doi.org/10.1007/S00425-005-0202-Z

Pacurar, D. I., Perrone, I., & Bellini, C. (2014). Auxin is a central player in the hormone cross-talks that control adventitious rooting. *Physiologia Plantarum*, *151*(1), 83–96. https://doi.org/10.1111/PPL.12171

Peralta, I. E., & Spooner, D. M. (2006). History, origin and early cultivation of tomato (solanaceae). In *Genetic Improvement of Solanaceous Crops Volume 2: Tomato* (pp. 1–24). https://doi.org/10.1201/b10744-2

Peralta, I. E., Spooner, D. M., & Knapp, S. (2008). Taxonomy of wild tomatoes and their relatives (Solanum sect. Lycopersicoides, sect. Juglandifolia, sect. Lycopersicon; Solanaceae). *Systematic Botany Monographs*, *84*.

Pérez-Martín, F., Yuste-Lisbona, F. J., Pineda, B., Angarita-Díaz, M. P., García-Sogo, B., Antón, T., Sánchez, S., Giménez, E., Atarés, A., Fernández-Lozano, A., Ortíz-Atienza, A., García-Alcázar, M., Castañeda, L., Fonseca, R., Capel, C., Goergen, G., Sánchez, J., Quispe, J. L., Capel, J., … Lozano, R. (2017). A collection of enhancer trap insertional mutants for functional genomics in tomato. *Plant Biotechnology Journal*, *15*(11), 1439–1452. https://doi.org/10.1111/PBI.12728

Petit, J., Bres, C., Just, D., Garcia, V., Mauxion, J.-P., Marion, D., Bakan, B., Joubès, J., Domergue, F., & Rothan, C. (2014). Analyses of Tomato Fruit Brightness Mutants Uncover Both Cutin-Deficient and Cutin-Abundant Mutants and a New Hypomorphic Allele of GDSL Lipase. *Plant Physiology, 164(2), 888-906.* https://doi.org/10.1104/pp.113.232645

Petricka, J. J., Winter, C. M., & Benfey, P. N. (2012). Control of Arabidopsis Root Development. *Annual Review of Plant Biology*, *63*, 563. https://doi.org/10.1146/ANNUREV-ARPLANT-042811-105501

Pnueli, L., Gutfinger, T., Hareven, D., Ben-Naim, O., Ron, N., Adir, N., & Lifschitz, E. (2001). Tomato SP-Interacting Proteins Define a Conserved Signaling System That Regulates Shoot Architecture and Flowering. *The Plant Cell*, *13*(12), 2687–2702. https://doi.org/10.1105/tpc.010293

Powell, A. L. T., Nguyen, C. v., Hill, T., Cheng, K. L. L., Figueroa-Balderas, R., Aktas, H., Ashrafi, H., Pons, C., Fernández-Muñoz, R., Vicente, A., Lopez-Baltazar, J., Barry, C. S., Liu, Y., Chetelat, R., Granell, A., van Deynze, A., Giovannoni, J. J., & Bennett, A. B. (2012). Uniform ripening encodes a Golden 2-like transcription factor regulating tomato fruit chloroplast development. *Science*, *336*(6089), 1711–1715. https://doi.org/10.1126/SCIENCE.1222218

Rakusová, H., Abbas, M., Han, H., Song, S., Lè Ne, H., Robert, S., Rí, J., & Correspondence, F. (2016). Termination of Shoot Gravitropic Responses by Auxin Feedback on PIN3 Polarity. *Current Biology*, *26*, 3026–3032. https://doi.org/10.1016/j.cub.2016.08.067

Rakusová, H., Gallego-Bartolomé, J., Vanstraelen, M., Robert, H. S., Alabadí, D., Blázquez, M. A., Benková, E., & Friml, J. (2011). Polarization of PIN3-dependent auxin transport for hypocotyl gravitropic response in Arabidopsis thaliana. *The Plant Journal: For Cell and Molecular Biology*, *67*(5), 817–826. https://doi.org/10.1111/J.1365-313X.2011.04636.X

Ramirez-Carvajal, G. A., & Davis, J. M. (2010). Cutting to the base identifying: Regulators of adventitious rooting. *Plant Signaling and Behavior*, *5*(3), 281–283. https://doi.org/10.4161/psb.5.3.10705

Razifard, H., Ramos, A., della Valle, A. L., Bodary, C., Goetz, E., Manser, E. J., Li, X., Zhang, L., Visa, S., Tieman, D., van der Knaap, E., & Caicedo, A. L. (2020). Genomic Evidence for Complex Domestication History of the Cultivated Tomato in Latin America. *Molecular Biology and Evolution*, *37*(4), 1118–1132. https://doi.org/10.1093/MOLBEV/MSZ297

Ron, M., Dorrity, M. W., de Lucas, M., Toal, T., Ivan Hernandez, R., Little, S. A., Maloof, J. N., Kliebenstein, D. J., & Brady, S. M. (2013). Identification of novel loci regulating interspecific variation in root morphology and cellular development in tomato. *Plant Physiology*, *162*(2), 755–768. https://doi.org/10.1104/pp.113.217802

Rosquete, M. R., von Wangenheim, D., Marhavý, P., Barbez, E., Stelzer, E. H. K., Benková, E., Maizel, A., & Kleine-Vehn, J. (2013). An Auxin Transport Mechanism Restricts

Positive Orthogravitropism in Lateral Roots. *Current Biology*, *23*(9), 817–822. https://doi.org/10.1016/J.CUB.2013.03.064

Rothan, C., Bres, C., Garcia, V., & Just, D. (2016). Tomato Resources for Functional Genomics. *The tomato genome,* 75–94. https://doi.org/10.1007/978-3-662-53389-5_5

Rothan, C., Diouf, I., & Causse, M. (2019). Trait discovery and editing in tomato. *The Plant Journal*, *97*(1), 73–90. https://doi.org/10.1111/TPJ.14152

Saito, T., Ariizumi, T., Okabe, Y., Asamizu, E., Hiwasa-Tanase, K., Fukuda, N., Mizoguchi, T., Yamazaki, Y., Aoki, K., & Ezura, H. (2011). TOMATOMA: A novel tomato mutant database distributing micro-tom mutant collections. *Plant and Cell Physiology*, *52*(2), 283–296. https://doi.org/10.1093/pcp/pcr004

Saito, T., Asamizu, E., Mizoguchi, T., Fukuda, N., Matsukura, C., & Ezura, H. (2009). Mutant Resources for the Miniature Tomato (*Solanum lycopersicum* L.) "Micro-Tom." *Journal of the Japanese Society for Horticultural Science,* 78(1), 6-13. https://doi.org/10.2503/jjshs1.78.6

Sato, S., Tabata, S., Hirakawa, H., Asamizu, E., Shirasawa, K., Isobe, S., Kaneko, T., Nakamura, Y., Shibata, D., Aoki, K., Egholm, M., Knight, J., Bogden, R., Li, C., Shuang, Y., Xu, X., Pan, S., Cheng, S., Liu, X., … Gianese, G. (2012). The tomato genome sequence provides insights into fleshy fruit evolution. *Nature*, *485*(7400), 635–641. https://doi.org/10.1038/NATURE11119

Scheres, B., Wolkenfelt, H., Willemsen, V., Terlouw, M., Lawson, E., Dean, C., & Weisbeek, P. (1994). Embryonic origin of the Arabidopsis primary root and root meristem initials. *Development*, *120*(9), 2475–2487. https://doi.org/10.2/JQUERY.MIN.JS

Scott, J. W., & Harbaugh, B. K. (1989). Micro-Tom: A Miniature Dwarf Tomato. *Florida Agricultural Experiment Station.* 370.

Sengupta, D., & Reddy, A. R. (2018). Simplifying the root dynamics: from complex hormone–environment interactions to specific root architectural modulation. *Plant Growth Regulation*, *85*(3), 337–349. https://doi.org/10.1007/S10725-018-0397-1

Shani, E., Ben-Gera, H., Shleizer-Burko, S., Burko, Y., Weiss, D., & Ori, N. (2010). Cytokinin regulates compound leaf development in tomato. *Plant Cell*, *22*(10), 3206–3217. https://doi.org/10.1105/tpc.110.078253

Sharma, M., Singh, D., Saksena, H. B., Sharma, M., Tiwari, A., Awasthi, P., Botta, H. K., Shukla, B. N., & Laxmi, A. (2021). Understanding the Intricate Web of Phytohormone Signalling in Modulating Root System Architecture. *International Journal of Molecular Sciences 2021, Vol. 22, Page 5508*, *22*(11), 5508. https://doi.org/10.3390/IJMS22115508

Shi, L., Shi, T., Broadley, M. R., White, P. J., Long, Y., Meng, J., Xu, F., & Hammond, J. P. (2013). High-throughput root phenotyping screens identify genetic loci associated with root architectural traits in *Brassica napus* under contrasting phosphate

availabilities. *Annals of Botany*, *112*(2), 381–389. https://doi.org/10.1093/AOB/MCS245

Shu, W., Zhou, H., Jiang, C., Zhao, S., Wang, L., Li, Q., Yang, Z., Groover, A., & Lu, M. Z. (2019). The auxin receptor TIR1 homolog (PagFBL 1) regulates adventitious rooting through interactions with Aux/IAA28 in Populus. *Plant Biotechnology Journal*, *17*(2), 338. https://doi.org/10.1111/PBI.12980

Slade, A. J., Fuerstenberg, S. I., Loeffler, D., Steine, M. N., & Facciotti, D. (2005). A reverse genetic, nontransgenic approach to wheat crop improvement by TILLING. *Nature Biotechnology 2004 23:1*, *23*(1), 75–81. https://doi.org/10.1038/nbt1043

Song, W., Wang, B., Hauck, A. L., Dong, X., Li, J., & Lai, J. (2016). Genetic dissection of maize seedling root system architecture traits using an ultra-high density bin-map and a recombinant inbred line population. *Journal of Integrative Plant Biology*, *58*(3), 266–279. https://doi.org/10.1111/JIPB.12452

Song, Y., Chen, D., Lu, K., Sun, Z., & Zeng, R. (2015). Enhanced tomato disease resistance primed by arbuscular mycorrhizal fungus. *Frontiers in Plant Science*, *6*, 786. https://doi.org/10.3389/FPLS.2015.00786/BIBTEX

Sorin, C., Negroni, L., Balliau, T., Corti, H., Jacquemot, M. P., Davanture, M., Sandberg, G., Zivy, M., & Bellini, C. (2006). Proteomic analysis of different mutant genotypes of Arabidopsis led to the identification of 11 proteins correlating with adventitious root development. *Plant Physiology*, *140*(1), 349–364. https://doi.org/10.1104/pp.105.067868

Soyk, S., Lemmon, Z. H., Oved, M., Fisher, J., Liberatore, K. L., Park, S. J., Goren, A., Jiang, K., Ramos, A., van der Knaap, E., van Eck, J., Zamir, D., Eshed, Y., & Lippman, Z. B. (2017). Bypassing Negative Epistasis on Yield in Tomato Imposed by a Domestication Gene. *Cell*, *169*(6), 1142-1155.e12. https://doi.org/10.1016/J.CELL.2017.04.032

Steffens, B., & Rasmussen, A. (2016). The physiology of adventitious roots. *Plant Physiology*, *170*(2), 603–617. https://doi.org/10.1104/pp.15.01360

Su, S. H., Gibbs, N. M., Jancewicz, A. L., & Masson, P. H. (2017). Molecular Mechanisms of Root Gravitropism. *Current Biology : CB*, *27*(17), R964–R972. https://doi.org/10.1016/J.CUB.2017.07.015

Sukumar, P., Maloney, G. S., & Muday, G. K. (2013). Localized induction of the ATP-binding cassette B19 auxin transporter enhances adventitious root formation in Arabidopsis. *Plant Physiology*, *162*(3), 1392–1405. https://doi.org/10.1104/PP.113.217174

Sun, H. J., Uchii, S., Watanabe, S., & Ezura, H. (2006). A highly efficient transformation protocol for Micro-Tom, a model cultivar for tomato functional genomics. *Plant & Cell Physiology*, *47*(3), 426–431. https://doi.org/10.1093/PCP/PCI251

Sun, H., Tao, J., Hou, M., Huang, S., Chen, S., Liang, Z., Xie, T., Wei, Y., Xie, X., Yoneyama, K., Xu, G., & Zhang, Y. (2015). A strigolactone signal is required for adventitious root

formation in rice. *Annals of Botany*, *115*(7), 1155–1162. https://doi.org/10.1093/aob/mcv052

Suresh, B. V., Roy, R., Sahu, K., Misra, G., & Chattopadhyay, D. (2014). Tomato Genomic Resources Database: An Integrated Repository of Useful Tomato Genomic Information for Basic and Applied Research. *PLOS ONE*, *9*(1), e86387. https://doi.org/10.1371/JOURNAL.PONE.0086387

Swarup, R., Péret, B., & Geisler, M. (2012). AUX/LAX family of auxin influx carriers-an overview. *Frontiers in plant science,* 3, 225. https://doi.org/10.3389/fpls.2012.00225

Teale, W., & Palme, K. (2018). Naphthylphthalamic acid and the mechanism of polar auxin transport. *Journal of Experimental Botany*, *69*(2), 303–312. https://doi.org/10.1093/JXB/ERX323

Tieman, D., Zhu, G., Resende, M. F. R., Lin, T., Nguyen, C., Bies, D., Rambla, J. L., Beltran, K. S. O., Taylor, M., Zhang, B., Ikeda, H., Liu, Z., Fisher, J., Zemach, I., Monforte, A., Zamir, D., Granell, A., Kirst, M., Huang, S., & Klee, H. (2017). A chemical genetic roadmap to improved tomato flavor. *Science*, *355*(6323), 391–394. https://doi.org/10.1126/SCIENCE.AAL1556

Till, B. J., Cooper, J., Tai, T. H., Colowit, P., Greene, E. A., Henikoff, S., & Comai, L. (2007). Discovery of chemically induced mutations in rice by TILLING. *BMC Plant Biology*, *7*. https://doi.org/10.1186/1471-2229-7-19

Till, B. J., Reynolds, S. H., Weil, C., Springer, N., Burtner, C., Young, K., Bowers, E., Codomo, C. A., Enns, L. C., Odden, A. R., Greene, E. A., Comai, L., & Henikoff, S. (2004). Discovery of induced point mutations in maize genes by TILLING. *BMC Plant Biology*, *4*(1), 1–8. https://doi.org/10.1186/1471-2229-4-12/FIGURES/2

Tötzke, C., Kardjilov, N., Lenoir, N., Manke, I., Oswald, S. E., & Tengattini, A. (2019). What comes NeXT? – High-Speed Neutron Tomography at ILL. *Optics Express*, *27*(20), 28640. https://doi.org/10.1364/oe.27.028640

Vidoz, M. L., Loreti, E., Mensuali, A., Alpi, A., & Perata, P. (2010). Hormonal interplay during adventitious root formation in flooded tomato plants. *The Plant Journal: For Cell and Molecular Biology*, *63*(4), 551–562. https://doi.org/10.1111/J.1365-313X.2010.04262.X

Warnock, S. J. (1991). Natural Habitats of Lycopersicon Species. *HortScience*, *26*(5), 466–471. https://doi.org/10.21273/hortsci.26.5.466

Waters, M. T., Gutjahr, C., Bennett, T., & Nelson, D. C. (2017). Strigolactone Signaling and Evolution. *Annual review of Plant* Biology, 28(68), 291-322. https://doi.org/10.1146/annurev-arplant-042916

Xiao, Z., Zhang, Y., Liu, M., Zhan, C., Yang, X., Nvsvrot, T., Yan, Z., & Wang, N. (2020). Coexpression analysis of a large-scale transcriptome identified a calmodulin-like protein regulating the development of adventitious roots in poplar. *Tree Physiology*, *40*(10), 1405–1419. https://doi.org/10.1093/TREEPHYS/TPAA078

Zhang, H., Han, W., de Smet, I., Talboys, P., Loya, R., Hassan, A., Rong, H., Jürgens, G., Paul Knox, J., & Wang, M. H. (2010). ABA promotes quiescence of the quiescent centre and suppresses stem cell differentiation in the Arabidopsis primary root meristem. *The Plant Journal: For Cell and Molecular Biology*, *64*(5), 764–774. https://doi.org/10.1111/J.1365-313X.2010.04367.X

Zhang, J., Chen, R., Xiao, J., Qian, C., Wang, T., Li, H., Ouyang, B., & Ye, Z. (2007). A single-base deletion mutation in SlIAA9 gene causes tomato (*Solanum lycopersicum*) entire mutant. *Journal of Plant Research*, *120*(6), 671–678. https://doi.org/10.1007/S10265-007-0109-9

Zhao, J., Sauvage, C., Zhao, J., Bitton, F., Bauchet, G., Liu, D., Huang, S., Tieman, D. M., Klee, H. J., & Causse, M. (2019). Meta-analysis of genome-wide association studies provides insights into genetic control of tomato flavor. *Nature Communications*, *10*(1). https://doi.org/10.1038/S41467-019-09462-W

Zheng, H., Pan, X., Deng, Y., Wu, H., Liu, P., & Li, X. (2016). AtOPR3 specifically inhibits primary root growth in Arabidopsis under phosphate deficiency. *Scientific Reports*, *6*. https://doi.org/10.1038/SREP24778

Zhu, G., Wang, S., Huang, Z., Zhang, S., Liao, Q., Zhang, C., Lin, T., Qin, M., Peng, M., Yang, C., Cao, X., Han, X., Wang, X., van der Knaap, E., Zhang, Z., Cui, X., Klee, H., Fernie, A. R., Luo, J., & Huang, S. (2018). Rewiring of the Fruit Metabolome in Tomato Breeding. *Cell*, *172*(1–2), 249-261.e12. https://doi.org/10.1016/j.cell.2017.12.019.

ANEXOS

COMPENDIO DE PUBLICACIONES

International Journal of
Molecular Sciences

MDPI

Article

Morphological Characterization of Root System Architecture in Diverse Tomato Genotypes during Early Growth

Aurora Alaguero-Cordovilla [1], Francisco Javier Gran-Gómez [1], Sergio Tormos-Moltó [1,2] and José Manuel Pérez-Pérez [1,*]

[1] Instituto de Bioingeniería, Universidad Miguel Hernández, 03202 Elche, Spain; aalaguero@umh.es (A.A.-C.); francisco.gran@goumh.umh.es (F.J.G.-G.); sertormol75@gmail.com (S.T.-M.)
[2] OQOTECH Process Validation System, 03801 Alcoy, Spain
* Correspondence: jmperez@umh.es; Tel.: +34-96-665-8958

Received: 13 November 2018; Accepted: 3 December 2018; Published: 5 December 2018

Abstract: Plant roots exploit morphological plasticity to adapt and respond to different soil environments. We characterized the root system architecture of nine wild tomato species and four cultivated tomato (*Solanum lycopersicum* L.) varieties during early growth in a controlled environment. Additionally, the root system architecture of six near-isogenic lines from the tomato 'Micro-Tom'mutant collection was also studied. These lines were affected in key genes of ethylene, abscisic acid, and anthocyanin pathways. We found extensive differences between the studied lines for a number of meaningful morphological traits, such as lateral root distribution, lateral root length or adventitious root development, which might represent adaptations to local soil conditions during speciation and subsequent domestication. Taken together, our results provide a general quantitative framework for comparing root system architecture in tomato seedlings and other related species.

Keywords: lateral root development; adventitious root development; plant phenomics; root growth analysis; root system architecture

1. Introduction

The root system is essential for plant growth because of its basic functions in the selective absorption of water and nutrients, as a mechanical support and storage organ, as a selective barrier against pathogens, and in the modulation of some stress responses [1,2]. However, our knowledge about the genetic mechanisms that modulate root system architecture (RSA) in species of agronomic interest is, with some exceptions, very limited [3–5]. Cultivated tomato (*Solanum lycopersicum* L.) is an important vegetable grown worldwide [6]. Tomato crops are particularly sensitive to drought, have poor nitrogen and phosphorus use efficiency and consequently require intensive irrigation and fertilization to maintain high yield and fruit quality [7,8]. Manipulation of RSA traits may improve water and nutrient capture under normal and extreme climate conditions [9,10]. The cultivated tomato is phylogenetically related to another 13 species of wild tomatoes, all of which are native to South America and show considerable morphological and ecological diversity [11]. Compared with the large genetic variability found in wild tomato species, the genetic diversity of the thousands of cultivated tomato varieties is very limited due to their recent domestication from a small number of individuals [12,13].

A detailed characterization of root development during early growth in two related tomato species, *S. pennellii* and *S. lycopersicum* 'M82', has been performed previously, which provided significant differences in a large range of root traits with developmental significance [14].

Additionally, a quantitative analysis of cellular and morphological root phenotypes in a population of 76 homozygous introgression lines between these two species featured numerous quantitative trait loci that influence a diversity of root traits [14]. Further analysis of this population can facilitate the eventual identification of genes that regulate some key RSA attributes, such as root length. Conversely, few studies have employed a genetic approach to examine the role of specific factors on tomato RSA. Previous studies identified an essential role for the *DIAGEOTROPICA* (*DGT*) gene in the development of lateral roots (LRs) in tomato [15]. *DGT* encodes a cyclophilin protein that negatively regulates PIN-FORMED auxin efflux transporters by affecting their plasma membrane localization; hence, the *dgt* mutant lacked the auxin maxima relevant to the priming and specification of LR founder cells and was consequently impaired in LR organogenesis [16]. In another study, the regulation of tomato RSA by flavonols was revealed by the analysis of the *anthocyanin reduced* (*are*) mutant, which has been suggested to have a defect in the gene encoding the enzyme FLAVONOID 3-HYDROXYLASE [17]. Auxin transport enhancement, alterations in auxin-induced gene expression and reduced LR initiation in these mutants are consistent with flavonols, reducing auxin transport through the wild-type roots and driving the accumulation of auxin at sites of LR primordia formation [17].

To characterize the phenotypic space of RSA in tomato, we studied several morphological traits during early growth in 19 tomato genotypes selected from a representative sample of wild tomato species, commercial cultivars and monogenic mutants. One the one hand, differential RSA traits among commercial tomato cultivars and related wild tomato species might represent adaptations to local soil conditions that could have been positively selected during domestication or, alternatively, that these traits were genetically linked to the yield-associated traits selected during domestication. On the other hand, the characterization of early RSA traits in a number of developmental mutants of the same genetic background will allow us to understand the hormonal crosstalk contributing to the local activation of growth in postembryonic root meristems. Our results will provide a theoretical framework to initiate the genetic characterization of RSA in tomato seedlings during early growth.

2. Results and Discussion

We established a precise in vitro experimental setup (Figure S1) to explore the RSA of different tomato genotypes (Table 1) during their early growth. Based on the recent phylogeny of wild tomato species (section *Lycopersicon*) [11–13], we selected nine tomato relatives and four reference commercial cultivars for our studies. To search for novel RSA regulators, we also investigated some of the developmental mutants that were introgressed previously by other authors into a unique background, the 'Micro-Tom' cultivar [18], that facilitates comparative studies and double mutant analysis.

2.1. Germination and Early Root Growth

The studied genotypes showed a quick germination as most seeds germinated between 24 and 72 h on wet chamber incubation. *S. chmielewskii*, *S. arcanum* and *S. cheesmaniae* displayed a slight delay in germination, which otherwise did not result in a reduced germination percentage at sowing time (Figure S1). The primary roots (PRs) of 'Moneymaker' and 'Ailsa Craig' grew at higher ratesthan those of 'Craigella' and 'Micro-Tom' during the first three days of growth on plates (Figure 1a,b). Regarding the wild tomato species analyzed, *S. chmielewskii* displayed the lowest PR growth rate (Figure 1a,b). Some of the studied mutants, such as *anthocyanin absent* (*aa*), also showed a delay in germination compared to their counterparts in the 'Micro-Tom' background (Figure S1), indicating a putative role of the *AA* gene in root emergence. Additionally, the *bushy* mutants displayed shorter PR lengths (5.53 ± 2.61 mm; n = 18) compared to their counterparts in the 'Micro-Tom' background (11.93 ± 3.51 mm; n = 20; Figure 1a and Figure S1), which is already affected by cell expansion due to recessive mutations leading to brassinosteroid deficiency [19].

Table 1. Tomato genotypes used in this study.

1. Wild Tomato Species						
Species Name 'Cultivar'	**Accession**	**Collection Site**	**Latitude**	**Longitude**	**Altitude**	**Other Comments**
S. corneliomulleri	LA1274	Lima (Perú)	11°27′36″	76°54′0″	1440 m	Fruits from 6 plants
S. peruvianum	LA1336	Arequipa (Perú)				
S. chilense	LA1932	Arequipa (Perú)	15°25′0″	74°42′0″	1100 m	Fruits from 15 plants, stress tolerant
S. huaylasense	LA1983	Ancash (Perú)	8°4121″	77°58′20″	940 m	Fruits from 1 plant, very dry spot
S. chmielewskii	LA2663	Cusco (Perú)	13°41′44″	74°59′39″	2500 m	Fruits form 6–7 plants
S. arcanum	LA2157	Cajamarca (Perú)	6°30′21″	78°48′32″	1600 m	Fruits from 2 plants
S. galapagense	LA1044	Galapagos Islands (Ecuador)	0°17′4″	90°32′54″	<100 m	
S. cheesmaniae	LA1037	Galapagos Islands (Ecuador)	0°25′21″	91°7′0″	800 m	From bottom of volcano crater
S. pimpinelifollium	LA1587	La Libertat (Perú)	7°20′0″	79°35′0″	<100 m	Fruits from 20 plants. Grown on river sand

2. Commercial Tomato Cultivars	
'Cultivar name'	**Accession**
'Ailsa Craig'	LA2838A
'Craigella'	LA3247
'Moneymaker'	LA2706
'Micro-Tom'	LA4480

3. 'Micro-Tom' developmental mutants				
Mutant	**Phenotype**	**Gene Product**	**Gene Function**	**References**
anthocyanin absent (*aa*)	Anthocyanin deficient	SlGSTAA	Anthocyanin transport	[18,20]
anthocyaninless (*a*)	Low anthocyanin levels	F3′5′H	Anthocyanin biosynthesis	[18,21]
bushy (*bu*)	Short internodes	Unknown		[18]
lutescent (*l*)	Premature senescence	Unknown		[18]
Never ripe (*Nr*)	Low ethylene responses	SlETR3	Ethylene receptor	[18,22]
sitiens (*sit*)	ABA deficient	ABA aldehyde oxidase	ABA biosynthesis	[18,23]

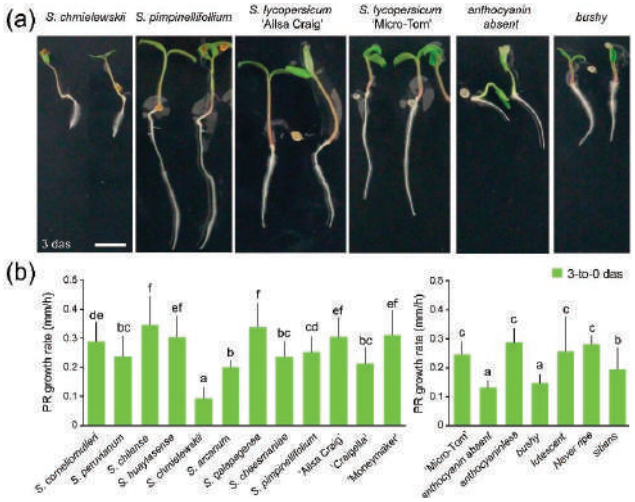

Figure 1. Early growth variation of selected tomato genotypes. (**a**) Seedlings of tomato genotypes differing in early root growth. Scale bar: 10 mm. (**b**) Growth rate (mm/h) of PRs in wild tomato species and commercial tomato cultivars (left), as well as in developmental mutants in the 'Micro-Tom' genetic background (right). Average ± SD values are shown. Different letters indicate significant differences (LSD; p-value < 0.01) over genotypes; das: days after sowing.

Our studies on different tomato genotypes and wild relatives indicated that observed differences during early growth were caused by a combination of (i) differences in their germination time caused by delays in PR protrusion and (ii) growth rate differences of the emerged PRs. In most wild tomato relatives, both PR emergence and PR growth rates were reduced compared to commercial tomato cultivars and their ancestor *S. pimpinellifolium*. Despite the close phylogenetic relationship between *S. chmielewskii* and *S. arcanum* [11,12], both species differed significantly in PR growth rates (Figure 1b), which may indicate adaptation to local soil conditions. The uneven germination of wild tomato species provides an adaptive advantage to rapidly changing environmental conditions (i.e., soil moisture), allowing higher seedling survival; however, uniform germination and rapid seedling growth are prerequisites for crop species [24] that might have been positively selected during tomato domestication [25]. We also found striking differences in early growth rates between commercial cultivars 'Moneymaker' and 'Craigella' that deserve further investigation.

2.2. Lateral Root (LR) Capacity Assay

Previous studies in maize reported significant variations in key RSA parameters, such as LR density, LR length and LR growth angle, between different genotypes [26,27]. Additionally, extensive variations in these parameters have been observed across environments [28–31]. Hence, the dynamic modulation of RSA through time by defined genotype × environment interactions determines root plasticity responses and allows plants to efficiently adapt to environmental constraints [10,30,32].

To characterize RSA during early growth in tomato (see Materials and Methods), we measured several traits (Table S1) in the newly emerged LRs three days after root tip excision (dae), which is known to promote rapid growth of already-specified and dormant LR primordia in Arabidopsis [33]. The number of newly emerged LRs was positively and significantly correlated with PR length at root tip excision in wild tomato relatives and commercial cultivars (Figure S2), which was consistentwith the results found in other species [34–36]. *S. pimpinellifolium* showed the highest number of LRs, *S. peruvianum* displayed non-significant differences in the number of LRs compared to commercial cultivars, and the other wild tomato relatives showed lower LR numbers (Figure 2a,b and Figure S3).

LRs were not evenly distributed along the PR length, with the lowest frequencies found in the distal end of the PR in most genotypes (Figure S4); in *S. arcanum* and *S. galapagense,* however, LRs were found with lower frequencies in the proximal region of the PR close to the hypocotyl base (Figure 2c). The average distances between LRs were significantly different among the studied genotypes (Figure 2d). *S. peruvianum*, *S. chmielewskii* and 'Craigella' displayed the smallest averagedistances between adjacent LRs; in contrast, the LR average distances in *S. chilense* and *S. arcanum* werealmost doubled (Figure 2d).

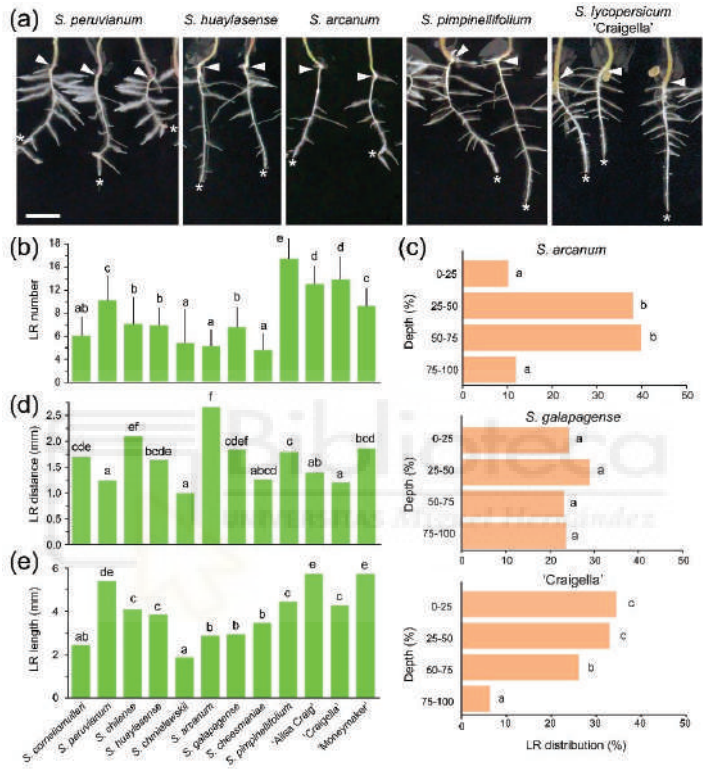

Figure 2. LR development in wild tomato species and commercial tomato cultivars after root tip excision. (**a**) Representative images of the entire root system of selected genotypes at 3 days after root tip excision. The arrowhead points to the root-hypocotyl junction, and the asterisk indicates the tip of the PR. Scale bar: 10 mm. (**b**) Number of LRs. Average ± SD values are shown. (**c**) Average percentages of LR distribution along the length (i.e., depth) of the PR. (**d**) Distance between consecutive LRs and (**e**) LR length; median values are shown. Different letters indicate significant differences (LSD; *p*-value < 0.01) over genotypes (b,d,e) or regarding PR depth domains (c).

LRs display growth tropisms in response to gravity, light, touch and moisture gradients that contribute to enhancing plant growth by increasing nutrient capture from the soil [37]. Although LR distribution in Arabidopsis has been linked to the waving growth pattern of the PR through asymmetric auxin accumulation [38], the LRs in tomato did not show a preference to growing on the outside edge of the PR (Figure S3). For most genotypes, ~60% of the LRs emerged in alternating directions along the PR length, and approximately 20–30% of the LRs emerged from the same edge of the PR in clusters of two to three LRs (Figure S2). In *S. peruvianum*, *S. huaylasense* and *S. pimpinellifolium,*there was a substantial proportion of seedlings (~50%) with clusters of four or more LRs that emerged on the same side of the PR. In monocot plants, such as rice and wheat, a strong correlation between the

root growth angle and drought tolerance has been observed where steeper growth angles increased water capture [39,40]. In our tomato population, the average LR growth angle was 113.9 ± 17.5° (n = 1429), with extreme values found for *S. arcanum* and 'Moneymaker' with 106.4 ± 10.3° (n = 69) and 123.5 ± 20.5° (n = 102), respectively (Figure S2). Drought tolerant rice cultivars bearing functional alleles of *DEEPER ROOTING 1* (*DRO1*) develop LRs with steeper growth angles, reaching deeper into the soil, which maintained high yield performance under water deficit regimes [41]. As *DRO1*-related genes also influence RSA in dicot plants, such as Arabidopsis and plum [42], it is plausible that the observed differences in LR growth angle between tomato genotypes might be explained by natural variation in the DRO1 pathway as well.

In dicot plants, such as Arabidopsis and tomato, the formation of LRs occurs from a subset of pericycle cells that are periodically primed at the so-called oscillation zone of the PR [38,43]. In these species, LRs emerge on a basipetal pattern: LR outgrowth is initiated in a more proximal region of the PR, and hence, the older LRs are longer than the newly emerged LRs [44,45]. LR lengths in our experimental dataset approach a gamma distribution (Figure S5), which might reflect the temporal delay between the early steps of LR initiation and subsequent LR outgrowth after meristem activation. We found significant differences in the distribution of LR length between wild tomato species and commercial cultivars (Figure S5). Most commercial cultivars and *S. peruvianum* displayed longer LRs (Figure 2e), while the LRs in *S. corneliomulleri*, *S. chmielewskii*, *S. arcanum* and *S. galapagense* were much shorter (Figure 2e). The RSA, which is defined by the length of the PR and the distribution, density, length and growth angle of the LRs, determines the soil volume that is explored by a single plant. Additionally, the high degree of plasticity of the root systems allows postembryonic alterations to occur in response to local environmental cues, such as nutrient deficiencies in the soil [30,31,46]. Indeed, a strong shift from PR growth to LR growth is observed in response to phosphate deficiency, which leads to a shorter PR with a high number of longer LRs [30,47,48]. We found substantial variation of early RSA parameters in a small selection of wild tomato species and commercial cultivars, which might represent local adaptation to soil conditions during speciation and that could have been selected during tomato domestication.

Most of the developmental mutants studied in this work displayed altered RSA after root tip excision compared with their counterparts in the 'Micro-Tom' background (Figure 3 and Figure S6). In contrast to 'Micro-Tom', we found a non-significant correlation between LR number and PR length in *lutescent* and *sitiens* (*sit*) mutants (Figure 3b), which also displayed a reduced number of LRs after root tip excision (Figure 3c), indicating that these mutants were affected in LR specification (i.e., prepatterning) and/or LR initiation. Other mutants with significantly lower numbers of LRs than 'Micro-Tom' were *aa*, *bushy* and *Never ripe* (*Nr*) (Figure 3c). By comparing the spatial distribution of LRs along the main root in the studied mutants (Figure S4), we found that most LRs in *aa* and *sit* mutants emerged in the PR region nearest the hypocotyl (Figure 3d), which indicated a substantial delay in LR initiation from the distal region of the PR or a failure to initiate new LRs after root tip excision in these mutants. Interestingly, LR density, estimated as the average distance between two consecutive LRs, was similar in all the studied mutants (Figure 3e). Accumulating evidence suggests that abscisic acid (ABA) plays an important role in stress-regulated root growth suppression [49]. Additionally, studies with ABA-deficient mutants indicate that ABA promotes stem cell maintenance in the root meristem [50]. Consistent with the latter, the ABA-deficient *sit* mutant, which is blocked in the conversion of ABA-aldehyde to ABA [23], displayed a reduced root system during early growth, indicating a requirement of ABA in LR initiation.

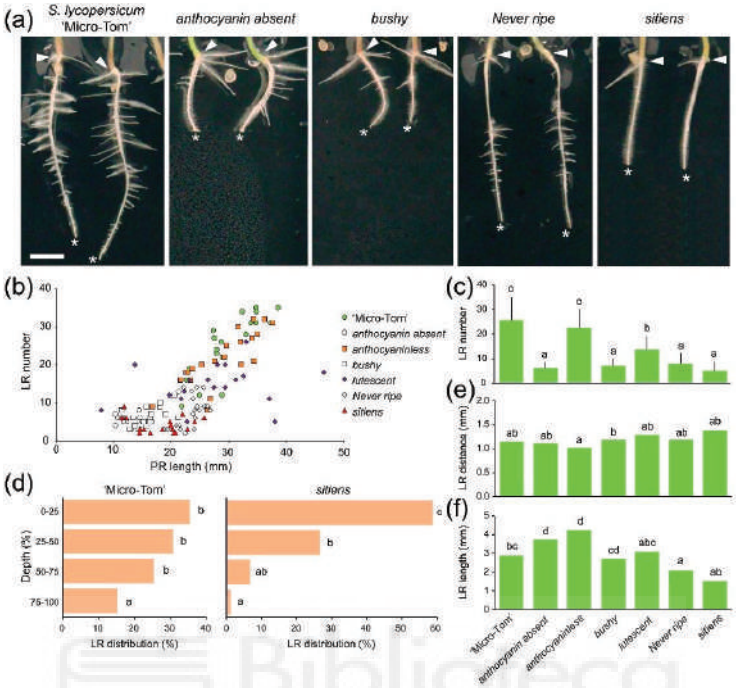

Figure 3. LR development in developmental mutants after root tip excision. (**a**) Representative images of the entire root system of selected genotypes 3 dae. The arrowhead points to the root-hypocotyl junction, and the asterisk indicates the distal tip of the PR. Scale bar: 10 mm. (**b**) Scatter plot of the LR number according to PR length. (**c**) Number of LRs. Average ± SD values are shown. (**d**) Average percentages of LR distribution along the length (i.e., depth) of the PR. (**e**) Distance between consecutive LRs and (**f**) LR length; median values are shown. Different letters indicate significant differences (LSD; p-value < 0.01) over genotypes (c,e,f) or regarding PR depth (d).

The LR lengths were significantly shorter in *Nr* mutants (2.59 ± 1.59 mm; n = 107) compared to 'Micro-Tom' (3.62 ± 2.39 mm; n = 306), while the anthocyanin-defective mutants studied, *aa* and *anthocyaninless* (*a*), displayed significantly longer LRs (Figure 3f). Among the studied mutants,*Nr* displayed more LR emerging on the same side of the PR than 'Micro-Tom', as well as steeper LR growth angles (Figure S2).

We studied RSA during the early growth of two mutants with reduced levels of anthocyanins. A previous study identified positive roles for anthocyanins in LR formation in tomato, likely through their direct regulation of polar auxin transport and the levels of reactive oxygen species [17]. The *a* mutant bears a frameshift mutation in a gene encoding the flavonoid 3′,5′-hydroxylase involved in the conversion of dihydrokaempferol to dihydromyricetin [21]. Recently, the deletion of a gene encoding a putative glutathione S-transferase (*SlGSTAA*) has been proposed as the causal mutation in the *aa* allele [20]. Interestingly, the strongest phenotype observed for RSA in anthocyanin-deficient mutants during early growth corresponded to the *aa* mutant. SlGSTAA is homologous to Arabidopsis TRANSPARENT TESTA19, which functions as a carrier to transport and sequester anthocyanins into the vacuole [51]. Another mutant with reduced anthocyanin levels also displayed altered RSA [17] similar to that found in the *aa* mutants, and the mild phenotype shown in RSA during early growth for the *a* mutant might be due to the different steps where the anthocyanin function is affected in each of these mutants.

2.3. Adventitious Root (AR) Formation in the Hypocotyl after Wounding

ARs are postembryonic roots that are formed from non-root tissues, such as leaves and stems, naturally or in response to altered environments [52,53]; these structures may also be induced by mechanical damage or during vegetative propagation of stem cuttings [54,55]. To test the ability of the different tomato genotypes to produce ARs after wounding, we excised the whole root system 6 days after sowing (das; Figure S1), which induced AR formation at the hypocotyl base above the wounding site shortly afterwards (Figure 4a and Figure S7). We followed AR initiation by scoring the presence of newly emerged AR primordia at the hypocotyl (see Materials and Methods). We found a significant delay in AR initiation in *S. cheesmaniae* and *S. chilense* compared to that in other studied wild tomato species and commercial cultivars; the emergence rate of consecutive ARs also varied, although not significantly, among most of the studied genotypes (Figure S8). We found striking differences in the number of ARs produced by the studied genotypes at 6 and 10 days after induction (dai), irrespective of their hypocotyl length (Figure 4b). Interestingly, the four studied commercial cultivars produced more ARs (7.0 ± 1.6 ARs at 10 dai; n = 102) than the other wild tomato species (Figure 4c), including the direct ancestor of cultivated tomato, *S. pimpinellifolium* (3.3 ± 1.2 ARs at 10 dai; n = 21), suggesting that enhanced AR formation could have been positively selected during domestication or, alternatively, that this trait was genetically linked to the other yield-associated traits selected during *S. lycopersicum* domestication [56]. AR growth rates were significantly higher in commercial cultivars, *S. chmielewskii*, *S. galapagense* and *S. pimpinellifolium*, than in the other studied genotypes (Figure 4d). In contrast, we found no differences in the growth rates of the first, second and third ARs during the first 12 h for the studied genotypes (Figure 4d), suggesting that ARs grow autonomously from the hypocotyl after emergence or that the hypocotyl-derived signal fueling AR growth was not limiting. Differences in AR length were observed between the wild tomato species and commercial cultivars studied at 6 dai (Figure 4e), but these differences were normalized at later stages (Figure S8), indicating a genotype-dependent dynamic regulation of the AR growth rate. Concerning the growth angle of ARs, *S. arcanum* and 'Moneymaker' also presented extreme values, with 110.8 ± 8.2° (n = 29) and 131.4 ± 24.1° (n = 33), respectively (Figure S8), which were very similar to the growth angles found for their LRs (see above).

When compared to other commercial cultivars, some traits of the AR system in 'Micro-Tom', such as AR initiation, AR growth rate, AR growth angle and total AR length, were not significantly different among the studied genotypes (Figure 4 and Figures S7–S9). The number of ARs, however, was significantly reduced in the 'Micro-Tom' cultivar (3.2 ± 0.8 ARs at 10 dai; n = 25), which was correlated with its smaller hypocotyl length (Figure 4b–c). Regarding the studied mutants in the 'Micro-Tom' background, the *Nr* mutants showed some delay in AR initiation and in the emergence rate of consecutive ARs, while the *aa* and *sit* mutants displayed a significant reduction in AR initiation (Figures S7 and S8). Consistent with these results, ARs were longer in *aa* and *sit* mutants than in *Nr* mutants (Figure 4E and Figures S8 and S9). Ethylene and ABA have a complicated interaction in many developmental processes [57]. In Arabidopsis and tomato, ethylene caused a reduction in PR elongation and inhibited the initiation and elongation of LRs [58,59]. Interestingly, the results found in tomato suggested a positive role for ethylene in the regulation of ARs through the modulation of auxin transport [60,61]. In addition, submerged tomato roots triggered ethylene synthesis, which is required for flooding-induced auxin accumulation in the hypocotyl and thus AR formation [61]. Our results are consistent with *Nr* being affected in both the local activation of LR growth after root tip excision and AR initiation in the hypocotyl after whole root excision, which directly indicates a role for ethylene in wound-induced postembryonic root formation. In a recent study, transcriptome analysis during flood-induced AR formation in *Solanum dulcamara* uncovered a tissue-specific crosstalk between ethylene and ABA levels [62]. According to this model, the flooding-dependent ethylene response pathway that activates AR formation controls two downstream processes: the suppression of ABA signaling and the enhancement of auxin signaling [62]. The observed AR phenotypes in *Nr* and

sit mutants suggest the function of a similar pathway during wound-induced AR formation, which will require further investigation.

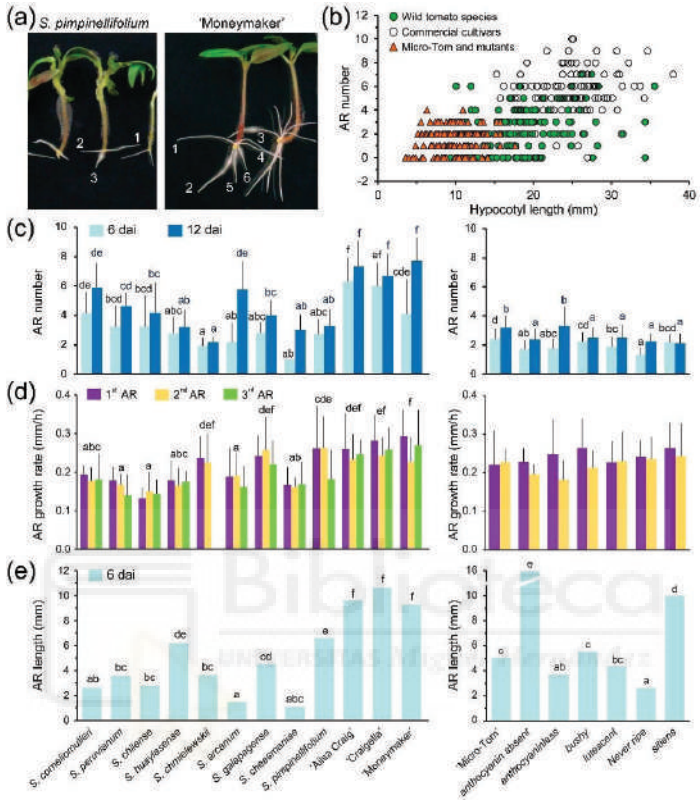

Figure 4. Variation of some AR traits in the studied genotypes after whole root excision. (**a**) Representative images of the AR system of selected genotypes at 10 dai. The numbers indicate the order of emergence of consecutive ARs. (**b**) Scatter plot of AR number according to hypocotyl length at 6 dai. (**c**) Number of Ars at 6 and 10 dai. Average ± SD values are shown. (**d**) AR growth rate of the first, second and third ARs during the first 12 h post-emergence. (**e**) Median values of AR length. Different letters indicate significant differences (LSD; p-value < 0.01) over genotypes (c–e).

2.4. Capturing Quantitative Variation of Early RSA in Tomato

To generate a parametrized space that captured variation in early RSA for the studied genotypes, we performed a heatmap representation with some of the parameters measured (Figure 5a).The studied commercial cultivars shared similar RSA traits and were clustered together and with its direct ancestor, *S. pimpinellifolium*. Although *S. chmielewskii*, *S. galapagense* and *S. cheesmaniae* clustered together, these plants displayed contrasting differences in some of the studied traits, such as PR growth rate and AR growth rate, indicating that these two traits might be independently controlled. Interestingly, some of the mutants in the 'Micro-Tom' background displayed specific alterations insome of the studied traits, such as LR and AR length (*aa*), which are likely controlled by the same genetic pathway. To further define the morphological space for early RSA in tomato, we chose six relevant RSA traits, PR growth, LR number, LR distance, LR distribution, LR length and LR growth angle, as well as four additional traits associated with the wound-induced AR system, number, length, growth angle and growth rate. For each of these traits, we defined three distinct states, named A,

B and C, representing the first quartile, the second plus the third quartile and the fourth quartile of measured data values, respectively. The studied genotypes were grouped according to these traits and states (Table S2), and representative diagrams of the early RSA ideotypes found in our study were drawn (Figure 5b).

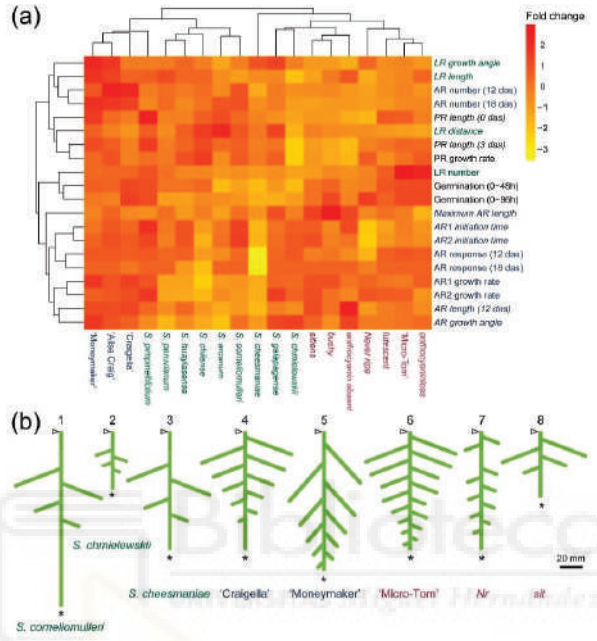

Figure 5. Morphological characteristics of early RSA in tomato. (**a**) Heat map representation of wild tomato species (green), commercial tomato cultivars (blue) and 'Micro-Tom' developmental mutants (red). Some of the morphological parameters analyzed (black, germination and early root growth; green, LR capacity assay; blue, wound-induced AR formation) are shown in the right column. The data from the parameters indicated in italics were transformed before the analysis (see Materials and Methods). The color code in the histogram ranges from yellow (lowest values) to red (highest values). (**b**) EarlyRSA ideotypes found in the studied tomato genotypes. The arrowhead points to the root-hypocotyl junction, and the asterisk indicates the tip of the PR. Representative genotypes for each ideotype are indicated.

Plant roots exploit morphological plasticity to adapt and respond to different soil environments and therefore help to improve resource use efficiency and to maintain productivity during limited nutrient and water availability [9,63]. Genotypic variation for RSA traits has been reported for many crops [64–66], and thus represents a suitable toolbox for targeted breeding. In our study, we identified a number of meaningful traits in tomato RSA (such as LR distribution in the soil depth, LR length or AR number) that displayed significant variation in a reduced number of commercial cultivars and related wild species. We plan to extend our root phenotyping studies to additional wild tomato accessions and commercial cultivars and to test their performance in response to some nutrient (phosphate and nitrate) deficiencies as well as simulated drought. Recently, a number of noninvasive methods for imaging plant roots on natural substrates have been developed [67,68], but their use is restricted due to high infrastructure cost or the availability of specific expertise. A low-cost high-throughput system for tomato root phenotyping has been developed in our lab, allowing automated image capture and implementation of software tools for root tracing and data analysis. To identify the genetic determinants of some of the differences found in RSA in tomato, we are studying

a recombinant inbred line population derived from the cross *Solanum lycopersicum* 'Moneymaker' × *Solanum pimpinellifolium* [69]. The characterization of early RSA traits in the developmental mutants studied here indicated crosstalk between ethylene and abscisic acid signals for the local activation of growth in postembryonic root meristems. Additionally, several mutant collections on the 'Micro-Tom' background are available [70–73], which will allow screening for novel regulators of RSA in tomato and the rapid identification of the causal mutations by using a mapping-by-sequencing approach [74]. Our results provide a theoretical framework to initiate the genetic characterization of early RSA in tomato.

3. Materials and Methods

3.1. Plant Material and Growth Conditions

Seeds of wild tomato species and cultivated tomato (*Solanum lycopersicum* L.) varieties (Table 1) were obtained from the C.M. Rick Tomato Genetics Resource Center (TGRC; http://tgrc.ucdavis.edu/). The tomato cultivar 'Micro-Tom' and the near-isogenic lines (NILs) used in this study (Table 1) were obtained from the tomato mutant collection [18] maintained at the Escola Superior de Agricultura "Luiz de Queiroz", Universidade de São Paulo, Brazil (http://www.esalq.usp.br/tomato/). Seeds of cultivated tomato cultivars and 'Micro-Tom' mutants were harvested between March and July 2017 from healthy plants grown in a gothic arch greenhouse at 38°16′43″ N, 0°41′15″ W, and 96 m altitude (Elche, Spain).

The seeds were surface-sterilized in 2% weight/volume sodium hypochlorite for 10 min, rinsed thoroughly with sterile distilled water (4 times) and cold-stored for 2 days. The sterilized seeds were transferred to wet chambers at 28 °C in a dark growth cabinet for 96 h. Germination was monitored daily on a sample of approximately 50 seeds per genotype. After 72 h on the wet chambers, germinated seedlings with a radicle >2 mm were transferred to 120 mm-square Petri dishes (0 days after sowing; das) containing 75 mL of sterile half-Murashige and Skoog basal salt medium (Duchefa, The Netherlands), 20 g L^{-1} sucrose (Duchefa), 2.5 g L^{-1} Gelrite (Duchefa), 0.5 g L^{-1} 2-(N-morpholino) ethanesulfonic acid (MES; Duchefa) and 2 mL L^{-1} Gamborg B5 vitamin solution (Duchefa), pH 5.8. Seven germinated seedlings were placed on each Petri dish, and three to five dishes per genotype were maintained in nearly vertical positions in a growth cabinet during 16 h light (average photosynthetic photon flux density of 50 µmol m^{-2} s^{-1}) at 26 ± 1 °C and 8 h darkness at 23 ± 1 °C. In the lateral root (LR) capacity assay [33], 3–4 mm of the root tip was excised at 3 das, and the seedlings were grown for another 3 days (Figure S1); newly emerged LRs were then counted under a dissecting microscope. The formation of hypocotyl-derived adventitious roots (ARs) was induced at 6 das by removing the entire root system of each plant 1-2 mm above the hypocotyl-root junction with a sharp scalpel; ARs were periodically counted between 12 and 18 das (6 and 12 days after AR induction [dai], respectively). Primary root (PR), LR and AR pictures were taken using a Sony Cyber-shot DSC-H3 camera (Sony Corporation, Tokyo, Japan) at a resolution of 3264×2448 pixels and saved as an RGB color image in the jpeg format.

To measure AR initiation time, AR growth rate and AR growth angle, 4 dai (10 das) seedlings were transferred to new nearly vertically oriented plates, and serial images were taken every 3 h using a Canon EOS1100D camera (Canon Inc., Tokyo, Japan) with a Canon EF-S 17–55 mm f/3.5–5.6 lens at a resolution of 4272 × 2848 pixels and saved as an RGB color image in the jpeg format.

3.2. Image Analysis

PR length was estimated by the "Measure" tool after drawing a segmented line along the main root using Fiji [75]. For the measurement of most RSA traits (Table S1), we used the EZ-Rhizo software as described elsewhere [76]. Briefly, all roots from a single image were semi-automated processed and skeletonized and then manually corrected for reconnecting any discontinuities in the root path and/or for separating overlapping roots. All measured RSA parameters in a text file were exported to an Excel

datasheet (Table S3). AR initiation and AR response were estimated by visually screening time-series images for the emergence of AR at the hypocotyl base in each seedling. The maximum AR length was measured in the AR system of seedlings 10 dai (18 das) by using a ruler.

3.3. Statistical Analyses

Descriptive statistics (average, standard deviation [SD], median, maximum and minimum) were calculated by using the StatGraphics Centurion XV software (StatPoint Technologies, Inc. Warrenton, VA, USA) and SPSS 21.0.0 (SPSS Inc., Chicago, IL, USA) programs. Data outliers were identified based on aberrant SD values and excluded for posterior analyses as described elsewhere [77]. One-sample Kolmogorov–Smirnov tests were performed to analyze the goodness-of-fit between the distribution of the data and a theoretical distribution (normal, gamma, log-logistic, or Weibull). Correlations were studied using Pearson product-moment correlation coefficient (Pearson's r). Non-normal data values were transformed before the ANOVA by using $\sqrt{x}$ (length, distance), $\log_2 x$ (growth angle) or $\frac{1}{x}$ (initiation time). Average ± SD values were represented, except in cases that did not exhibit a normal distribution and for which the median was used instead. We performed multiple testing analyses using the ANOVA F-test or Fisher's least significant difference (LSD) methods (p-value < 0.01). Nonparametric tests were used when necessary.

3.4. Heat Map Representation

Standardized datasets obtained from the analysis of early RSA were processed using the pheatmap package of R version 3.3.2 (http://www.r-project.org/). Euclidean distance matrixes between morphological parameters (rows) and genotypes (columns) were calculated to build the dendrograms.

Supplementary Materials: Supplementary materials can be found at http://www.mdpi.com/1422-0067/19/12/3888/s1.

Author Contributions: Conceptualization, J.M.P.-P.; methodology, J.M.P.-P. and A.A.-C.; formal analysis, A.A.-C.; investigation, A.A.-C. and F.J.G.-G.; resources, S.T.-M.; data curation, A.A.-C.; writing—original draft preparation, J.M.P.-P.; writing—review and editing, J.M.P.-P. and A.A.-C.; and supervision, project administration and funding acquisition, J.M.P.-P.

Funding: This research was funded by the Ministerio de Economía, Industria y Competitividad (MINECO) of Spain (grants no. AGL2012-33610 and BIO2015-64255-R) and the European Regional Development Fund (ERDF) of the European Commission.

Acknowledgments: We would like to thank Lázaro Eustáquio Pereira Peres (Universidade de São Paulo, Brazil) for providing the seeds for the studied mutants from the 'Micro-Tom' collection and Sergio Ibáñez (Universidad Miguel Hernández, Spain) for help with heatmap drawing.

Conflicts of Interest: The authors declare no conflict of interest.

References

1. Petricka, J.J.; Winter, C.M.; Benfey, P.N. Control of *Arabidopsis* root development. *Annu. Rev. Plant Biol.* **2012**, *63*, 563–590. [CrossRef] [PubMed]
2. Atkinson, J.A.; Rasmussen, A.; Traini, R.; Voss, U.; Sturrock, C.; Mooney, S.J.; Wells, D.M.; Bennett, M.J. Branching out in roots: Uncovering form, function, and regulation. *Plant Physiol.* **2014**, *166*, 538–550. [CrossRef]
3. Coudert, Y.; Périn, C.; Courtois, B.; Khong, N.G.; Gantet, P. Genetic control of root development in rice, the model cereal. *Trends Plant Sci.* **2010**, *15*, 219–226. [CrossRef] [PubMed]
4. Orman-Ligeza, B.; Parizot, B.; Gantet, P.P.; Beeckman, T.; Bennett, M.J.; Draye, X. Post-embryonic root organogenesis in cereals: Branching out from model plants. *Trends Plant Sci.* **2013**, *18*, 459–467. [CrossRef] [PubMed]
5. Hochholdinger, F.; Yu, P.; Marcon, C. Genetic control of root system development in maize. *Trends Plant Sci.* **2018**, *23*, 79–88. [CrossRef] [PubMed]
6. Food and Agriculture Organization of the United Nations (FAO). Available online: http://www.fao.org/land-water/databases-and-software/crop-information/tomato/en/ (accessed on 6 November 2018).

7. Patanè, C.; Tringali, S.; Sortino, O. Effects of deficit irrigation on biomass, yield, water productivity and fruit quality of processing tomato under semi-arid Mediterranean climate conditions. *Sci. Hortic.* **2011**, *129*, 590–596. [CrossRef]
8. Wang, X.; Xing, Y. Evaluation of the effects of irrigation and fertilization on tomato fruit yield and quality: A principal component analysis. *Sci. Rep.* **2017**, *7*, 350. [CrossRef] [PubMed]
9. Lynch, J.P.; Chimungu, J.G.; Brown, K.M. Root anatomical phenes associated with water acquisition from drying soil: Targets for crop improvement. *J. Exp. Bot.* **2014**, *65*, 6155–6166. [CrossRef] [PubMed]
10. Koevoets, I.T.; Venema, J.H.; Elzenga, J.T.M.; Testerink, C. Roots withstanding their environment: Exploiting root system architecture responses to abiotic stress to improve crop tolerance. *Front. Plant Sci.* **2016**, *7*, 1335. [CrossRef] [PubMed]
11. Peralta, I.E.; Spooner, D.M.; Knapp, S. Taxonomy of wild tomatoes and their relatives (*Solanum* Sect. *Lycopersicoides*, Sect. *Juglandifolia*, Sect. *Lycopersicon*; Solanaceae). *Syst. Bot. Monogr.* **2008**, *84*, 1–186. [CrossRef]
12. Aflitos, S.; Schijlen, E.; de Jong, H.; De Rider, D.; Smit, S.; Finkers, R.; Wang, J.; Zhang, G.; Li, N.; Mao, L.; et al. Exploring genetic variation in the tomato (*Solanum* section *Lycopersicon*) clade by whole-genome sequencing. *Plant J.* **2014**, *80*, 136–148. [CrossRef] [PubMed]
13. Blanca, J.; Montero-Pau, J.; Sauvage, C.; Bauchet, G.; Illa, E.; Diez, M.J.; Francis, D.; Causse, M.; van der Knaap, E.; Cañizares, J. Genomic variation in tomato, from wild ancestors to contemporary breeding accessions. *BMC Genom.* **2015**, *16*, 257. [CrossRef]
14. Ron, M.; Dorrity, M.W.; de Lucas, M.; Toal, T.; Hernandez, R.I.; Little, S.A.; Maloof, J.N.; Kiebenstein, D.J.; Brady, S.M. Identification of novel loci regulating interspecific variation in root morphology and cellular development in tomato. *Plant Physiol.* **2013**, *162*, 755–768. [CrossRef] [PubMed]
15. Ivanchenko, M.G.; Coffeen, W.C.; Lomax, T.L.; Dubrovsky, J.G. Mutations in the *Diageotropica* (*Dgt*) gene uncouple patterned cell division during lateral root initiation from proliferative cell division in the pericycle. *Plant J.* **2006**, *46*, 436–447. [CrossRef] [PubMed]
16. Ivanchenko, M.G.; Zhu, J.; Wang, B.; Medvecká, E.; Du, Y.; Azzarello, E.; Mancuso, S.; Megraw, M.; Filichkin, S.; Dubrovsky, J.G.; et al. The cyclophilin A *DIAGEOTROPICA* gene affects auxin transport in both root and shoot to control lateral root formation. *Development* **2015**, *142*, 712–721. [CrossRef]
17. Maloney, G.S.; DiNapoli, K.T.; Muday, G.K. The anthocyanin reduced tomato mutant demonstrates the role of flavonols in tomato lateral root and root hair development. *Plant Physiol.* **2014**, *166*, 614–631. [CrossRef]
18. Carvalho, R.F.; Campos, M.L.; Pino, L.E.; Crestana, S.L.; Zsögön, A.; Lima, J.E.; Benedito, V.A.; Peres, L.E. Convergence of developmental mutants into a single tomato model system: "Micro-Tom" as an effective toolkit for plant development research. *Plant Methods* **2011**, *7*, 18. [CrossRef]
19. Martí, E.; Gisbert, C.; Bishop, G.J.; Dixon, M.S.; García-Martínez, J.L. Genetic and physiological characterization of tomato cv. Micro-Tom. *J. Exp. Bot.* **2006**, *57*, 2037–2047. [CrossRef]
20. Zhang, L.; Huang, Z.; Wang, X.; Gao, J.; Guo, Y.; Du, Y.; Hu, H. Fine mapping and molecular marker development of anthocyanin absent, a seedling morphological marker for the selection of male sterile 10 in tomato. *Mol. Breed.* **2016**, *36*, 107. [CrossRef]
21. De Jong, W.S.; Eannetta, N.T.; De Jong, D.M.; Bodis, M. Candidate gene analysis of anthocyanin pigmentation loci in the *Solanaceae*. *Theor. Appl. Genet.* **2004**, *108*, 423–432. [CrossRef]
22. Wilkinson, J.Q.; Lanahan, M.B.; Yen, H.C.; Giovannoni, J.J.; Klee, H.J. An ethylene-inducible component of signal transduction encoded by *Never-ripe*. *Science* **1995**, *270*, 1807–1809. [CrossRef] [PubMed]
23. Harrison, E.; Burbidge, A.; Okyere, J.P.; Thompson, A.J.; Taylor, I.B. Identification of the tomato ABA-deficient mutant *sitiens* as a member of the ABA-aldehyde oxidase gene family using genetic and genomic analysis. *Plant Growth Regul.* **2011**, *64*, 301–309. [CrossRef]
24. Abbo, S.; Pinhasi van-Oss, R.; Gopher, A.; Saranga, Y.; Ofner, I.; Peleg, Z. Plant domestication versus crop evolution: A conceptual framework for cereals and grain legumes. *Trends Plant Sci.* **2014**, *19*, 351–360. [CrossRef]
25. Bai, Y.; Lindhout, P. Domestication and breeding of tomatoes: What have we gained and what can we gain in the future? *Ann. Bot.* **2007**, *100*, 1085–1094. [CrossRef]
26. Postma, J.A.; Dathe, A.; Lynch, J.P. The optimal lateral root branching density for maize depends on nitrogen and phosphorus availability. *Plant Physiol.* **2014**, *166*, 590–602. [CrossRef]

27. Zhan, A.; Lynch, J.P. Reduced frequency of lateral root branching improves N capture from low-N soils in maize. *J. Exp. Bot.* **2015**, *66*, 2055–2065. [CrossRef]
28. Osmont, K.S.; Sibout, R.; Hardtke, C.S. Hidden branches: Developments in root system architecture. *Annu. Rev. Plant Biol.* **2007**, *58*, 93–113. [CrossRef] [PubMed]
29. Trachsel, S.; Kaeppler, S.M.; Brown, K.M.; Lynch, J.P. Shovelomics: High throughput phenotyping of maize (*Zea mays* L.) root architecture in the field. *Plant Soil* **2011**, *341*, 75–87. [CrossRef]
30. Gruber, B.D.; Giehl, R.F.H.; Friedel, S.; von Wirén, N. Plasticity of the Arabidopsis root system under nutrient deficiencies. *Plant Physiol.* **2013**, *163*, 161–179. [CrossRef]
31. Giehl, R.F.H.; Gruber, B.D.; von Wirén, N. It's time to make changes: Modulation of root system architecture by nutrient signals. *J. Exp. Bot.* **2014**, *65*, 769–778. [CrossRef]
32. Rellán-Álvarez, R.; Lobet, G.; Dinneny, J.R. Environmental control of root system biology. *Annu. Rev. Plant Biol.* **2016**, *67*, 619–642. [CrossRef] [PubMed]
33. Van Norman, J.M.; Zhang, J.; Cazzonelli, C.I.; Pogson, B.J.; Harrison, P.J.; Bugg, T.D.H.; Chan, K.X.; Thompson, A.J.; Benfey, P.N. Periodic root branching in *Arabidopsis* requires synthesis of an uncharacterized carotenoid derivative. *Proc. Natl. Acad. Sci. USA* **2014**, *111*, E1300–E1309. [CrossRef] [PubMed]
34. Loudet, O.; Gaudon, V.; Trubuil, A.; Daniel-Vedele, F. Quantitative trait loci controlling root growth and architecture in *Arabidopsis thaliana* confirmed by heterogeneous inbred family. *Theor. Appl. Genet.* **2005**, *110*, 742–753. [CrossRef] [PubMed]
35. Shi, L.; Shi, T.; Broadley, M.R.; White, P.J.; Long, Y.; Meng, J.; Xu, F.; Hammond, J.P. High-throughput root phenotyping screens identify genetic loci associated with root architectural traits in *Brassica napus* under contrasting phosphate availabilities. *Ann. Bot.* **2013**, *112*, 381–389. [CrossRef] [PubMed]
36. Song, W.; Wang, B.; Hauck, A.L.; Dong, X.; Li, J.; Lai, J. Genetic dissection of maize seedling root system architecture traits using an ultra-high density bin-map and a recombinant inbred line population. *J. Integr. Plant Biol.* **2016**, *58*, 266–279. [CrossRef] [PubMed]
37. Miyazawa, Y.; Yamazaki, T.; Moriwaki, T.; Takahashi, H. Root tropism: Its mechanism and possible functions in drought avoidance. *Adv. Bot. Res.* **2011**, *57*, 349–375. [CrossRef]
38. Van Norman, J.M.; Xuan, W.; Beeckman, T.; Benfey, P.N.; Poething, S.; Roberts, K.; Scheres, B. To branch or not to branch: The role of pre-patterning in lateral root formation. *Development* **2013**, *140*, 4301–4310. [CrossRef] [PubMed]
39. Kato, Y.; Abe, J.; Kamoshita, A.; Yamagishi, J. Genotypic variation in root growth angle in rice (*Oryza sativa* L.) and its association with deep root development in upland fields with different water regimes. *Plant Soil* **2006**, *287*, 117–129. [CrossRef]
40. Manschadi, A.M.; Christopher, J.; deVoil, P.; Hammer, G.L. The role of root architectural traits in adaptation of wheat to water-limited environments. *Funct. Plant Biol.* **2006**, *33*, 823–837. [CrossRef]
41. Uga, Y.; Sugimoto, K.; Ogawa, S.; Rane, J.; Ishitani, M.; Hara, N.; Kitomi, Y.; Inukai, Y.; Ono, K.; Kanno, N.; et al. Control of root system architecture by *DEEPER ROOTING 1* increases rice yield under drought conditions. *Nat. Genet.* **2013**, *45*, 1097–1102. [CrossRef] [PubMed]
42. Guseman, J.M.; Webb, K.; Srinivasan, C.; Dardick, C. *DRO1* influences root system architecture in Arabidopsis and Prunus species. *Plant J.* **2017**, *89*, 1093–1105. [CrossRef] [PubMed]
43. Du, Y.; Scheres, B. Lateral root formation and the multiple roles of auxin. *J. Exp. Bot.* **2018**, *69*, 155–167. [CrossRef] [PubMed]
44. Dubrovsky, J.G.; Gambetta, G.A.; Hernández-Barrera, A.; Shishkova, S.; González, I. Lateral root initiation in *Arabidopsis*: Developmental window, spatial patterning, density and predictability. *Ann. Bot.* **2006**, *97*, 903–915. [CrossRef] [PubMed]
45. Péret, B.; De Rybel, B.; Casimiro, I.; Benková, E.; Swarup, R.; Laplaze, L.; Beeckman, T.; Bennett, M.J. *Arabidopsis* lateral root development: An emerging story. *Trends Plant Sci.* **2009**, *14*, 399–408. [CrossRef] [PubMed]
46. Giehl, R.F.H.; von Wirén, N. Root nutrient foraging. *Plant Physiol.* **2014**, *166*, 509–517. [CrossRef] [PubMed]
47. López-Bucio, J.; Hernández-Abreu, E.; Sánchez-Calderón, L.; Nieto-Jacobo, M.F.; Simpson, J.; Herrera-Estrella, L. Phosphate availability alters architecture and causes changes in hormone sensitivity in the Arabidopsis root system. *Plant Physiol.* **2002**, *129*, 244–256. [CrossRef] [PubMed]

48. Pérez-Torres, C.A.; López-Bucio, J.; Cruz-Ramírez, A.; Ibarra-Laclette, E.; Dharmasiri, S.; Estelle, M.; Herrera-Estrella, L. Phosphate availability alters lateral root development in *Arabidopsis* by modulating auxin sensitivity via a mechanism involving the TIR1 auxin receptor. *Plant Cell* **2008**, *20*, 3258–3272. [CrossRef]
49. Ding, Z.; De Smet, I. Localised ABA signalling mediates root growth plasticity. *Trends Plant Sci.* **2013**, *18*, 533–535. [CrossRef]
50. Zhang, H.; Han, W.; De Smet, I.; Talboys, P.; Loya, R.; Hassan, A.; Rong, H.; Jürgens, G.; Paul Knox, J.; Wang, M.H. ABA promotes quiescence of the quiescent centre and suppresses stem cell differentiation in the Arabidopsis primary root meristem. *Plant J.* **2010**, *64*, 764–774. [CrossRef]
51. Sun, Y.; Li, H.; Huang, J.R. *Arabidopsis* TT19 functions as a carrier to transport anthocyanin from the cytosol to tonoplasts. *Mol. Plant* **2012**, *5*, 387–400. [CrossRef]
52. Bellini, C.; Pacurar, D.I.; Perrone, I. Adventitious roots and lateral roots: Similarities and differences. *Annu. Rev. Plant Biol.* **2014**, *65*, 639–666. [CrossRef] [PubMed]
53. Steffens, B.; Rasmussen, A. The physiology of adventitious roots. *Plant Physiol.* **2016**, *170*, 603–617. [CrossRef] [PubMed]
54. da Costa, C.T.; de Almeida, M.R.; Ruedell, C.M.; Schwambach, J.; Maraschin, F.S.; Fett-Neto, A.G. When stress and development go hand in hand: Main hormonal controls of adventitious rooting in cuttings. *Front. Plant Sci.* **2013**, *4*, 133. [CrossRef] [PubMed]
55. Druege, U.; Franken, P.; Hajirezaei, M.R. Plant hormone homeostasis, signaling, and function during adventitious root formation in cuttings. *Front. Plant Sci.* **2016**, *7*, 381. [CrossRef] [PubMed]
56. Soyk, S.; Lemmon, Z.H.; Oved, M.; Fisher, J.; Liberatore, K.L.; Park, S.J.; Goren, A.; Jiang, K.; Ramos, A.; van der Knaap, E.; et al. Bypassing negative epistasis on yield in tomato imposed by a domestication gene. *Cell* **2017**, *169*, 1142–1155. [CrossRef] [PubMed]
57. Van de Poel, B.; Smet, D.; Van Der Straeten, D. Ethylene and hormonal cross talk in vegetative growth and development. *Plant Physiol.* **2015**, *169*, 61–72. [CrossRef] [PubMed]
58. Negi, S.; Ivanchenko, M.G.; Muday, G.K. Ethylene regulates lateral root formation and auxin transport in *Arabidopsis thaliana*. *Plant J.* **2008**, *55*, 175–187. [CrossRef]
59. Negi, S.; Sukumar, P.; Liu, X.; Cohen, J.D.; Muday, G.K. Genetic dissection of the role of ethylene in regulating auxin-dependent lateral and adventitious root formation in tomato. *Plant J.* **2010**, *61*, 3–15. [CrossRef]
60. Kim, H.J.; Lynch, J.P.; Brown, K.M. Ethylene insensitivity impedes a subset of responses to phosphorus deficiency in tomato and petunia. *Plant Cell Environ.* **2008**, *31*, 1744–1755. [CrossRef]
61. Vidoz, M.L.; Loreti, E.; Mensuali, A.; Alpi, A.; Perata, P. Hormonal interplay during adventitious root formation in flooded tomato plants. *Plant J.* **2010**, *63*, 551–562. [CrossRef]
62. Dawood, T.; Yang, X.; Visser, E.J.W.; Te Beek, T.A.; Kensche, P.R.; Cristescu, S.M.; Lee, S.; Floková, K.; Nguyen, D.; Mariani, C.; et al. A co-opted hormonal cascade activates dormant adventitious root primordia upon flooding in *Solanum dulcamara*. *Plant Physiol.* **2016**, *170*, 2351–2364. [CrossRef] [PubMed]
63. Lynch, J.P.; Wojciechowski, T. Opportunities and challenges in the subsoil: Pathways to deeper rooted crops. *J. Exp. Bot.* **2015**, *66*, 2199–2210. [CrossRef] [PubMed]
64. Henry, A.; Cal, A.J.; Batoto, T.C.; Torres, R.O.; Serraj, R. Root attributes affecting water uptake of rice (*Oryza sativa*) under drought. *J. Exp. Bot.* **2012**, *63*, 4751–4763. [CrossRef] [PubMed]
65. Burton, A.L.; Brown, K.M.; Lynch, J.P. Phenotypic diversity of root anatomical and architectural traits in *Zea* species. *Crop Sci.* **2013**, *53*, 1042–1055. [CrossRef]
66. Lynch, J.P. Steep, cheap and deep: An ideotype to optimize water and N acquisition by maize root systems. *Ann. Bot.* **2013**, *112*, 347–357. [CrossRef] [PubMed]
67. Thomas, C.L.; Graham, N.S.; Hayden, R.; Meacham, M.C.; Neugebauer, K.; Nightingale, M.; Dupuy, L.X.; Hammond, J.P.; White, P.J.; Broadley, M.R. High-throughput phenotyping (HTP) identifies seedling root traits linked to variation in seed yield and nutrient capture in field-grown oilseed rape (*Brassica napus* L.). *Ann. Bot.* **2016**, *118*, 655–665. [CrossRef] [PubMed]
68. Pflugfelder, D.; Metzner, R.; van Dusschoten, D.; Reichel, R.; Jahnke, S.; Koller, R. Non-invasive imaging of plant roots in different soils using magnetic resonance imaging (MRI). *Plant Methods* **2017**, *13*, 102. [CrossRef]
69. Rambla, J.L.; Medina, A.; Fernández-del-Carmen, A.; Barrantes, W.; Grandillo, S.; Cammareri, M.; López-Casado, G.; Rodrigo, G.; Alonso, A.; García-Martínez, S.; et al. Identification, introgression, and validation of fruit volatile QTLs from a red-fruited wild tomato species. *J. Exp. Bot.* **2016**, *68*, 429–442. [CrossRef]

70. Okabe, Y.; Ariizumi, T.; Ezura, H. Updating the Micro-Tom TILLING platform. *Breed. Sci.* **2013**, *63*, 42–48. [CrossRef]
71. Kudo, T.; Kobayashi, M.; Terashima, S.; Katayama, M.; Ozaki, S.; Kanno, M.; Saito, M.; Yokoyama, K.; Ohyanagi, H.; Aoki, K.; et al. TOMATOMICS: A web database for integrated omics information in tomato. *Plant Cell Physiol.* **2017**, *58*, e8. [CrossRef]
72. Shikata, M.; Ezura, H. Micro-Tom tomato as an alternative plant model system: Mutant collection and efficient transformation. *Methods Mol. Biol.* **2016**, *16*, 47–55. [CrossRef]
73. Shikata, M.; Hoshikawa, K.; Ariizumi, T.; Fukuda, N.; Yamazaki, Y.; Ezura, H. TOMATOMA update: Phenotypic and metabolite information in the Micro-Tom mutant resource. *Plant Cell Physiol.* **2016**, *57*, e11. [CrossRef] [PubMed]
74. Garcia, V.; Bres, C.; Just, D.; Fernandez, L.; Tai, F.W.; Mauxion, J.P.; Le Paslier, M.C.; Bèrard, A.; Brunel, D.; Aoki, K.; et al. Rapid identification of causal mutations in tomato EMS populations via mapping-by-sequencing. *Nat. Protoc.* **2016**, *11*, 2401–2418. [CrossRef] [PubMed]
75. Schindelin, J.; Arganda-Carreras, I.; Frise, E.; Kaynig, V.; Logair, M.; Pietzsch, T.; Preibisch, S.; Rueden, C.; Saalfeld, S.; Schmid, B.; et al. Fiji: An open-source platform for biological-image analysis. *Nat. Methods* **2012**, *9*, 676–682. [CrossRef] [PubMed]
76. Armengaud, P.; Zambaux, K.; Hills, A.; Sulpice, R.; Pattison, R.J.; Blatt, M.R.; Amtmann, A. EZ-Rhizo: Integrated software for the fast and accurate measurement of root system architecture. *Plant J.* **2009**, *57*, 945–956. [CrossRef] [PubMed]
77. Aguinis, H.; Gottfredson, R.K.; Joo, H. Best-practice recommendations for defining, identifying, and handling outliers. *Organ. Res. Methods* **2013**, *16*, 270–301. [CrossRef]

Figure S1

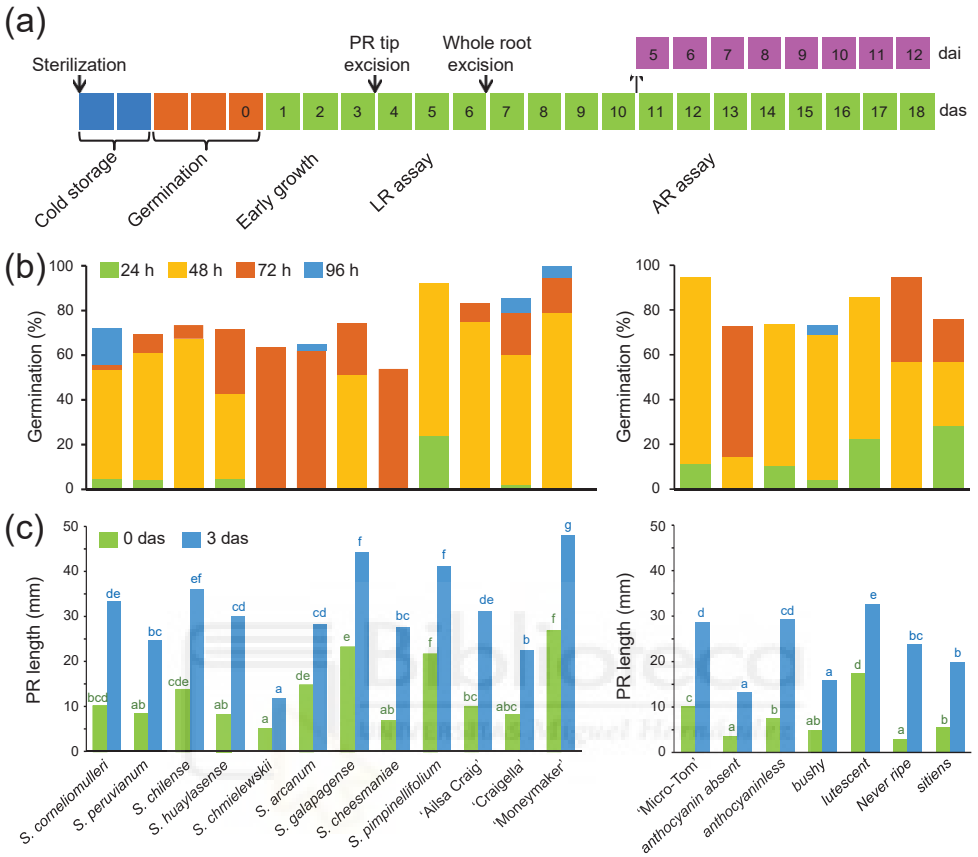

Figure S1. Early growth variation of selected tomato genotypes. (**a**) Experimental design for the evaluation of early RSA in tomato. Seeds were cold stored for 2 days and germinated for 3 days in a humid chamber (24 h darkness at 28ºC) before being transferred to half-Murashige and Skoog plates in a growth chamber (16 h light 26±1°C and 8 h darkness 23±1°C). The PR tips were excised 3 days after sowing (3 das) to induce LR formation, which were scored 6 das. Subsequently, the whole root was excised to induce AR formation from the hypocotyl that were scored at 6 and 12 days after AR induction (dai), corresponding to 12 and 18 das. In parallel, at 10 das, the seedlings were transferred to new plates to measure AR initiation and AR growth rates. (**b**) The germination percentages of wild tomato species, commercial tomato cultivars, and developmental mutants in the 'Micro-Tom' background between 1 and 4 days. (**c**) Lengths of PR at 0 and 3 days. Average ± SD values are shown. Different letters indicate significant differences (LSD; p-value<0.01) over genotypes.

Figure S2

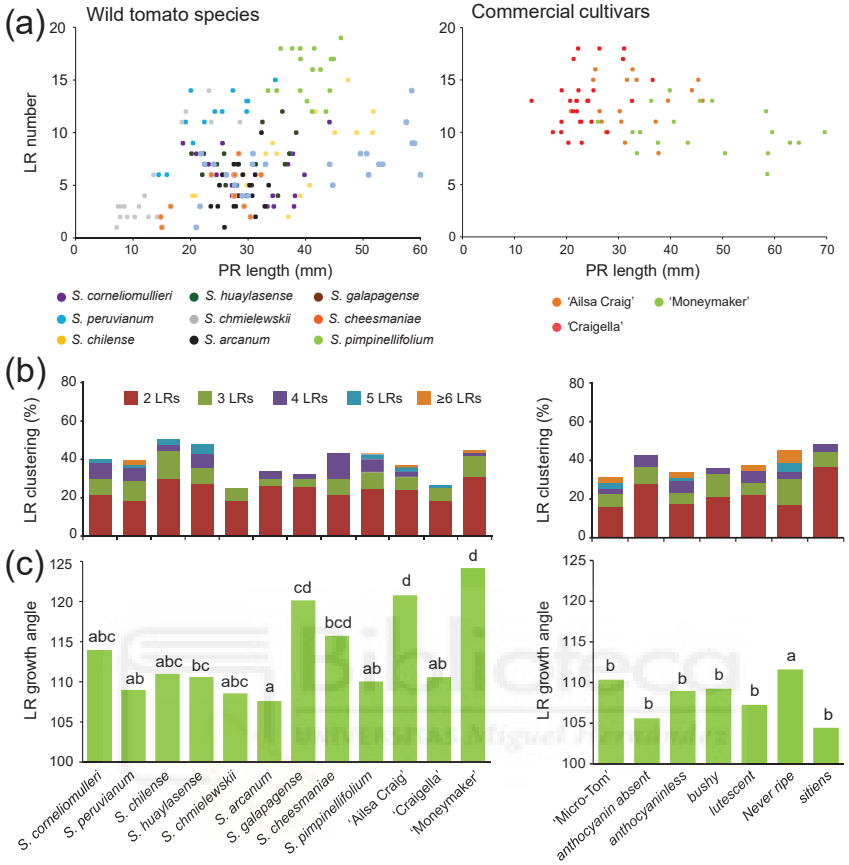

Figure S2. Variation of some LR traits in the studied genotypes. (**a**) Scatter plots of LR number according to PR length in wild tomato species and commercial tomato cultivars. (**b**) Percentage of consecutive LRs arising on the same side of the PR. Clusters from 2 to ≥6 LRs with the same growth direction are indicated. (**c**) Median values of the LR growth vector. Different letters indicate significant differences (LSD; p-value<0.01) over genotypes.

Figure S3

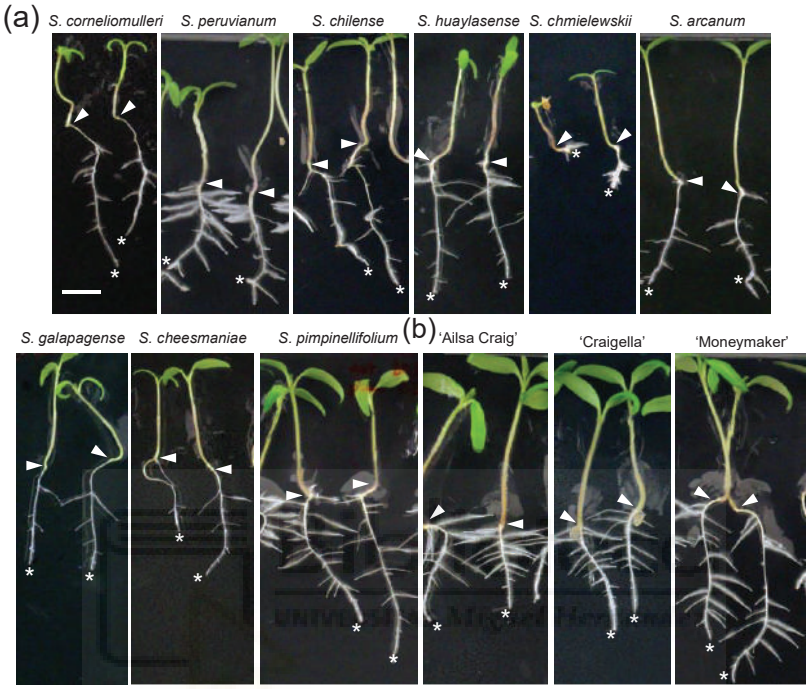

Figure S3. RSA after root tip excision in (**a**) wild tomato species and (**b**) commercial tomato cultivars. Arrowheads point to the root-hypocotyl junction, and the asterisks indicate the distal end of the PR after excision. Scale bar: 10 mm.

Figure S4

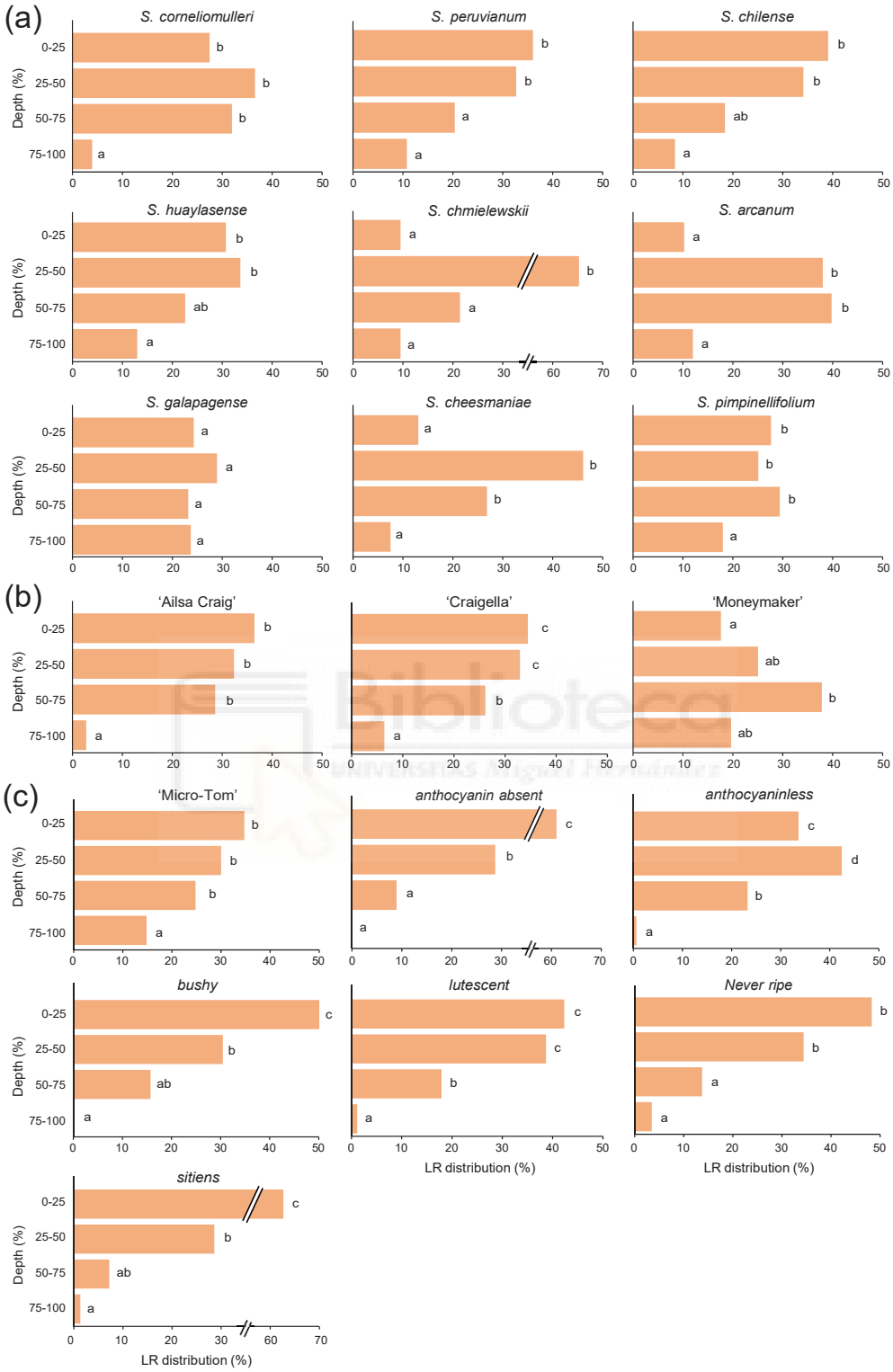

Figure S4. LR distribution in the studied genotypes. (**a-c**) Average percentages of LR distribution along the length of the PR in (**a**) wild tomato species, (**b**) commercial tomato cultivars, and (**c**) developmental mutants in the 'Micro-Tom' genetic background. Different letters indicate significant differences (LSD; p-value<0.01) with regard to PR length (i.e., root depth).

Figure S5

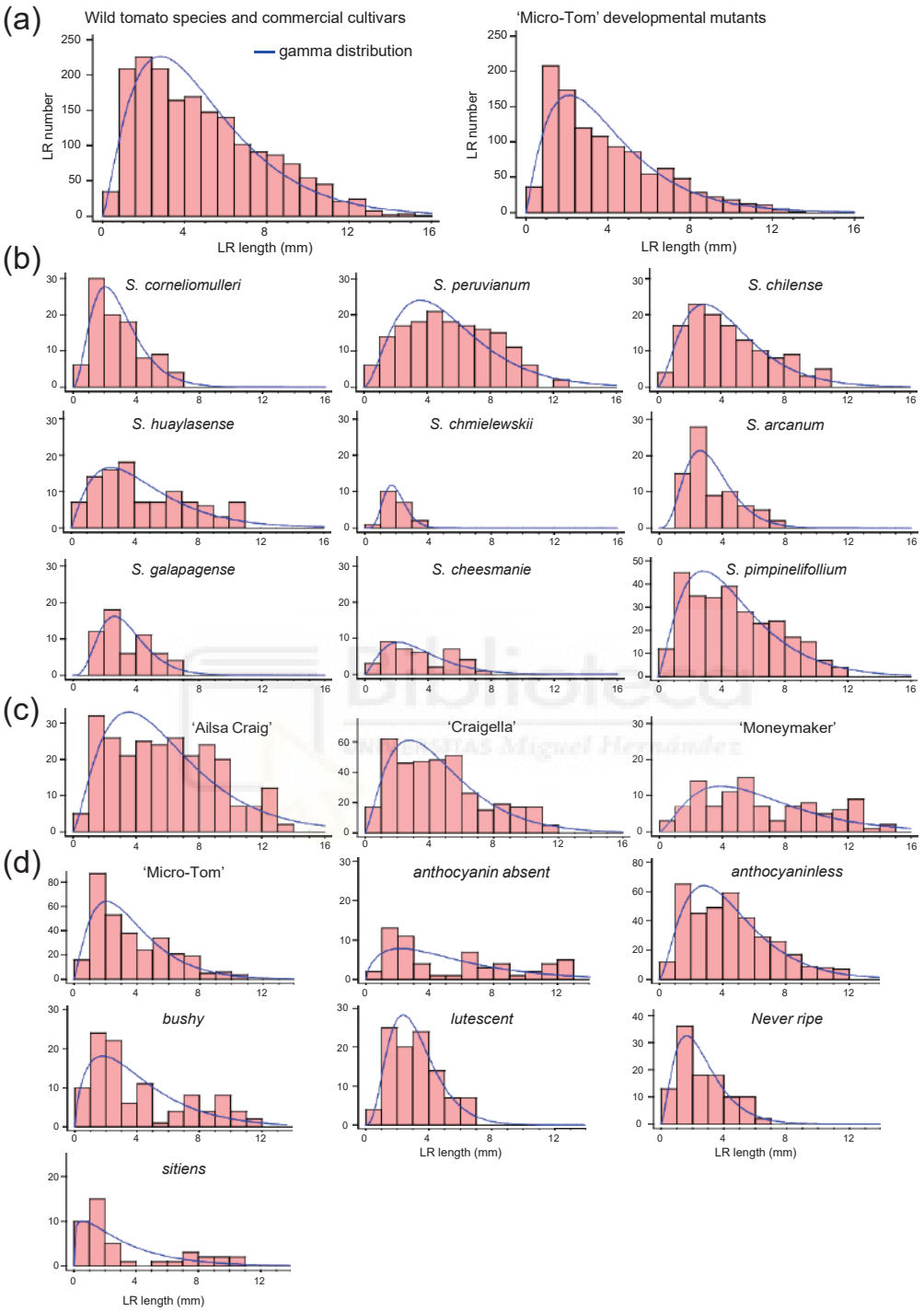

Figure S5. LR length distribution in the studied genotypes. (**a**) Histograms for LR length in wild tomato species and commercial tomato cultivars (left), as well as in 'Micro-Tom' developmental mutants (right), with an overlay of the theoretical gamma distribution. (**b-d**) Histograms for LR length in (**b**) wild tomato species, (**c**) commercial tomato cultivars, and (**d**) 'Micro-Tom' developmental mutants.

Figure S6

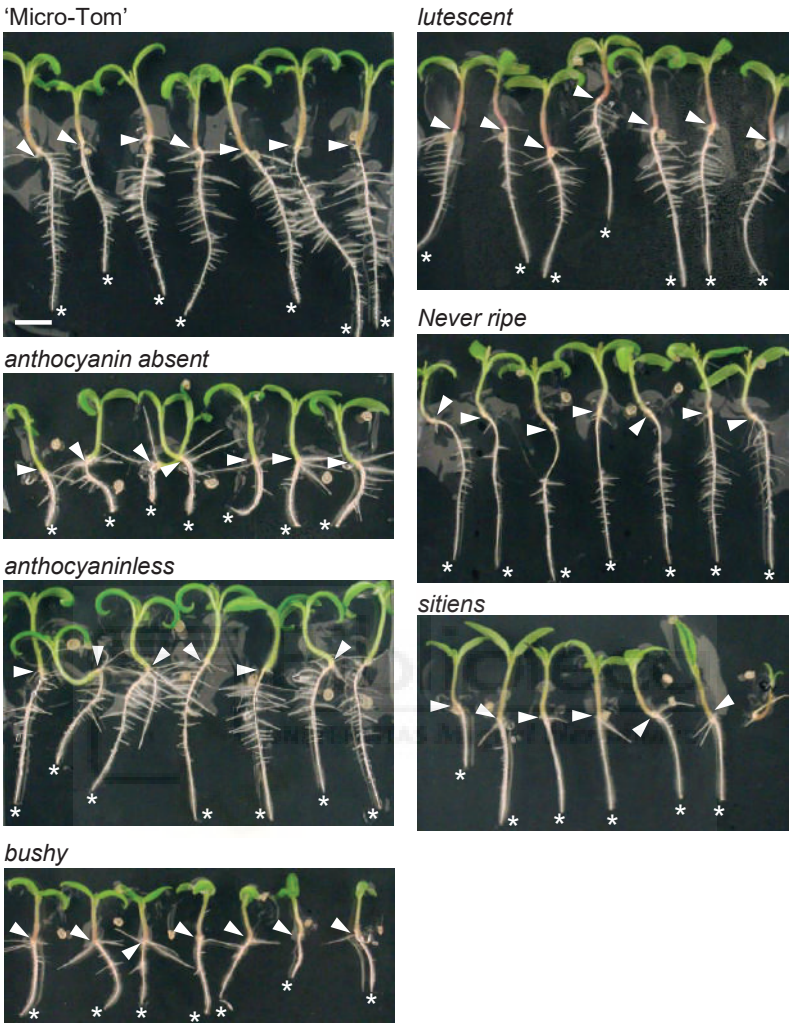

Figure S6. RSA after PR tip excision in 'Micro-Tom' developmental mutants. Arrowheads point to the root-hypocotyl junction, and the asterisks indicate the distal end of the PR after excision. Scale bar: 10 mm.

Figure S7

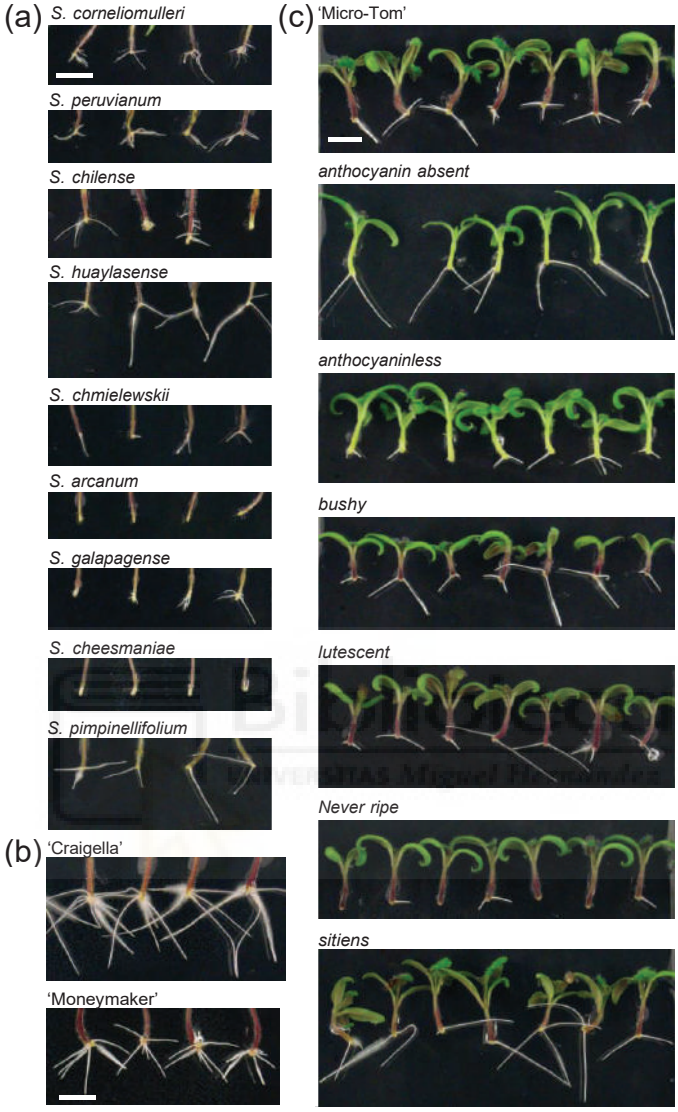

Figure S7. ARs in the hypocotyl after whole root excision of selected tomato genotypes. (**a**) Wild tomato species, (**b**) some commercial tomato cultivars, and (**c**) 'Micro-Tom' developmental mutants. Scale bars: 10 mm.

Figure S8

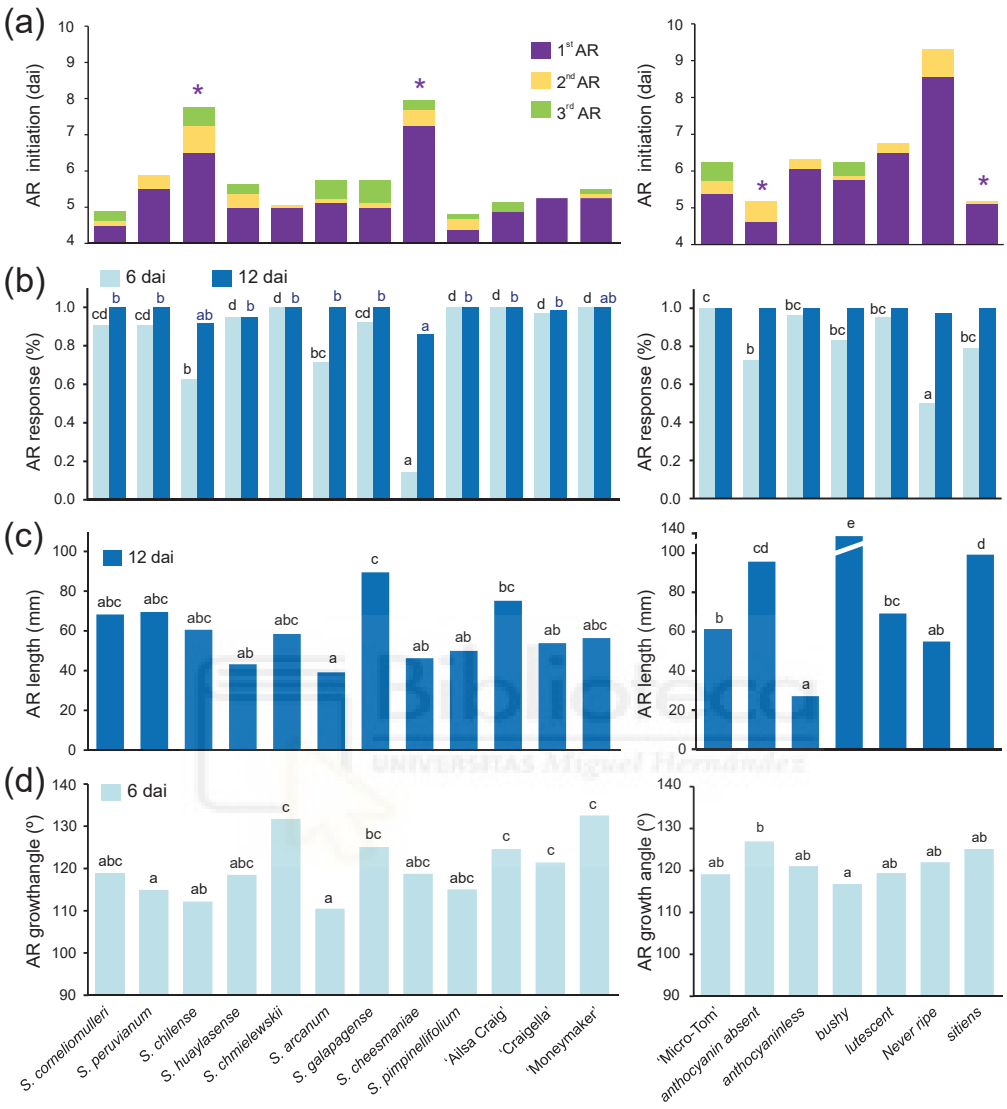

Figure S8. Variation of some AR traits after whole root excision. (**a**) Average initiation time of consecutive ARs (first, second and third); dai: days after AR induction. (**b**) AR response estimated as the percentage of hypocotyl explants showing emergence of ARs at the indicated times. Asterisks indicate significant differences (LSD; p-value<0.01) over genotypes. (**c-d**) Median values of (**c**) AR length and (**d**) AR growth angle. Different letters indicate significant differences (LSD; p-value<0.01) over genotypes (**c**, **d**).

Figure S9

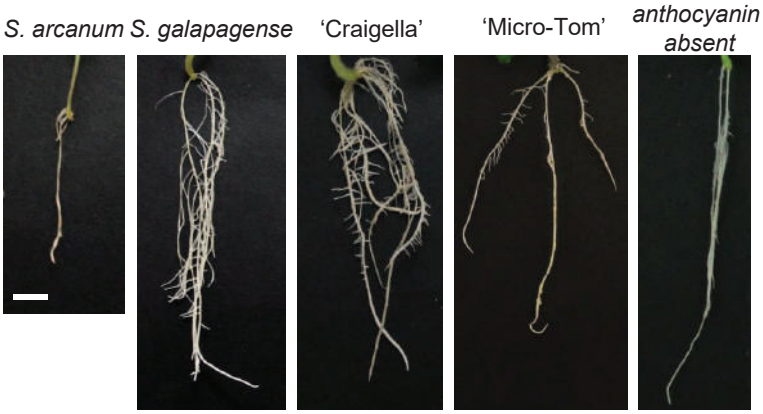

Figure S9. ARs in the hypocotyl after whole root excision of selected tomato genotypes. Scale bar: 10 mm.

Table 1. RSA traits measured in this study.

Studied trait	Description	Measured
Germination (%)	Percentage of seeds with emerged radicle (>2 mm)	Between 1 and 4 days after cold storage
Primary root (PR) length (mm)	Average length of PR after sowing	0 days after sowing (das), 3 das
PR growth rate (mm/h)	Average increase of PR length between 3 and 0 das	-
Lateral root (LR) number	Average number of lateral roots	3 days after root tip excision (6 das)
LR distribution (%)	Average proportion of LRs along quartiles of PR length (i.e. depth)	6 das
LR distance (mm)	Median distance of two consecutive LRs	6 das
LR length (mm)	Median length of LRs	6 das
LR clustering (%)	Average percentage of consecutive LRs with the same growth direction	6 das
LR growth angle (º)	Average angle of LR growth vector as regards its PR growth vector	6 das
Adventitious root (AR) number	Average number of ARs	6 and 12 days after whole root excision (12 and 18 das)
AR growth rate (mm/h)	Average increase of AR length during the first 12 h after AR emergence	-
AR initiation time (h)	Average time from whole root excision until AR emergence	-
AR response (%)	Percentage of hypocotyls with emerged ARs	12 and 18 das
AR length (mm)	Median length of ARs	12 das
AR growth angle (º)	Average angle of AR growth vector as regards its hypocotyl growth vector	12 das
Maximum AR length (mm)	Maximum length of ARs	18 das

Technical Perspectives

A quick protocol for the identification and characterization of early growth mutants in tomato

Aurora Alaguero-Cordovilla[1], Francisco Javier Gran-Gómez[1], Paula Jadczak[1,2], Mariem Mhimdi[1], Sergio Ibáñez[1], Cécile Bres[3], Daniel Just[3], Christophe Rothan[3], José Manuel Pérez-Pérez[1,*]

[1] Instituto de Bioingeniería, Universidad Miguel Hernández, 03202 Elche, Alicante, Spain
(A.A.-C., aalaguero@umh.es; M.M, mmhimdi@umh.es; S.I., s.ibanez@umh.es; J.M.P.-P., jmperez@umh.es)
[2] Present address: Department of Genetics, Plant Breeding and Biotechnology, West Pomeranian University of Technology, 71270 Szczecin, Poland (paula.jadczak@zut.edu.pl)
[3] INRAE and University of Bordeaux, UMR 1332 Biologie du Fruit et Pathologie, F-33140, Villenave d'Ornon, France (C.B., cecile.bres@inrae.fr; D.J., daniel.just@inrae.fr; C.R., christophe.rothan@inrae.fr)

Corresponding author: José Manuel Pérez-Pérez (jmperez@umh.es)

Published in:

Alaguero-Cordovilla A, Gran-Gómez FJ, Jadczak P, Mhimdi M, Ibáñez S, Bres C, Just D, Rothan C, Pérez-Pérez JM. A quick protocol for the identification and characterization of early growth mutants in tomato. Plant Sci. 2020 Dec;301:110673. doi: 10.1016/j.plantsci.2020.110673. Epub 2020 Sep 14. PMID: 33218638.

Abstract

Root system architecture (RSA) manipulation may improve water and nutrient capture by plants under normal and extreme climate conditions. With the aim of initiating the genetic dissection of RSA in tomato, we established a defined ontology that allowed the curated annotation of the observed phenotypes on 12 traits at four consecutive growth stages. In addition, we established a quick approach for the molecular identification of the mutations associated with the trait-of-interest by using a whole-genome sequencing approach that does not require the building of an additional mapping population. As a proof-of-concept, we screened 4,543 seedlings from 300 tomato M_3 lines (*Solanum lycopersicum* L. cv. Micro-Tom) generated by chemical mutagenesis with ethyl methanesulfonate. We studied the growth and early development of both the root system (primary and lateral roots) and the aerial part of the seedlings as well as the wound-induced adventitious roots emerging from the hypocotyl. We identified 659 individuals (belonging to 203 M_3 lines) whose early seedling and RSA phenotypes differed from those of their reference background. We confirmed the genetic segregation of the mutant phenotypes affecting primary root length, seedling viability and early RSA in 31 M_4 families derived from 15 M_3 lines selected in our screen. Finally, we identified a missense mutation in the *SlCESA3* gene causing a seedling-lethal phenotype with short roots. Our results validated the experimental approach used for the identification of tomato mutants during early growth, which will allow the molecular identification of the genes involved.

Keywords

Solanum lycopersicum; Micro-Tom; EMS mutagenesis; root system architecture (RSA); plant phenotyping; whole-genome sequencing

Abbreviations

AR: adventitious root

CESA: cellulose synthase A

emb: *embryo-defective* (*emb*)

EMS: ethyl methanesulfonate

LR: lateral root

LSD: least significant difference

MT: Micro-Tom

PR: primary root

RSA: root system architecture

SD: standard deviation

SNP: single nucleotide polymorphism

WT: wild type

1. Introduction

In addition to its primary importance as a vegetable crop, cultivated tomato (*Solanum lycopersicum* L.) is used as a model plant for *Solanaceae* genomics (Rothan et al., 2016) and fleshy fruit development (Quinet et al., 2019). Tomato seedlings have poor nitrogen and phosphorus use efficiency and are particularly sensitive to drought; therefore, they require intensive irrigation and fertilization to maintain high yields and fruit quality (Wang and Xing, 2017). Despite the importance of the root system architecture (RSA) in optimal nutrient and water uptake (Kellermeier et al., 2014; Robbins and Dinneny, 2015), our knowledge about the genetic mechanisms that modulate RSA in tomato is limited (Ivanchenko et al., 2015; Toal et al., 2018; Rothan et al., 2019; Cheng et al., 2020). On the other hand, several genes controlling major checkpoints of root development in monocot crops, such as maize (Hochholdinger et al., 2018) and rice (Meng et al., 2019), have been recently characterized from detailed analyses of their mutant phenotypes. The maize mutant *rootless with undetectable meristems1* is defective in lateral root (LR) initiation, and the affected gene encodes a canonical Aux/IAA protein that acts as a transcriptional repressor of downstream targets by interacting with ZmARF25 and ZmARF34 (von Behrens et al., 2011). Furthermore, transcriptome profiling revealed root type-specific transcriptomic reprogramming of pericycle cells in response to local high nitrate stimulation in this species (Yu et al., 2016), which might account for their high developmental RSA plasticity in response to changing soil conditions.

Due to its small size and short life cycle, the Micro-Tom (MT) cultivar was previously proposed as a model for functional genomics in tomato (Emmanuel and Levy, 2002). Since then, a wealth of genetic resources have been developed for this cultivar (Kobayashi et al., 2014; Shikata and Ezura, 2016). Among those, the TOMATOMA mutant database (https://tomatoma.nbrp.jp/) contains visible phenotypic data for 10,793 M_2 mutagenized lines generated by ethyl methanesulfonate (EMS) mutagenesis or γ-ray irradiation (Saito et al., 2011; Shikata et al., 2016). The large size of the available MT mutant population increases the chance of isolating allelic variants in selected genes by TILLING (Okabe et al., 2013). Following this approach, several point mutations have been identified in three genes of the L-ascorbic acid biosynthesis pathway, and the corresponding loss-of-function mutants displayed a strong reduction in leaf ascorbate content (Baldet et al., 2013). As with many other tomato cultivars, MT contains

some distinctive mutations: its dwarf and determinate behavior is caused by recessive alleles of the *DWARF* and *SELF-PRUNING* genes, respectively (Martí et al. 2006; Campos et al., 2010). Because these mutations are recessive and the greenhouse-type tomato variety Moneymaker is one of the MT progenitors (Scott and Harbaugh, 1989), the results obtained from MT research can be easily transferred to commercial cultivars by crossing. For example, a weak ethylene receptor allele identified in the MT background line was applied to extend the fruit shelf life of hybrid commercial tomato cultivars (Mubarok et al., 2015). This application supports the potential of MT to become "the mouse model of plant genetics" (Rick, 1991).

The tomato mutant collection used in this work was an EMS mutant population generated in the miniature cultivar MT at INRA Bordeaux (Just et al., 2013; Garcia et al., 2016). The collection comprises ca. 3,500 highly mutagenized mutant families that have been thoroughly phenotyped for approximately 150 plant and fruit traits stored in a web-searchable database. However, this database does not include any information about their root phenotypes (Petit et al., 2014; Musseau et al., 2017). The identification of the causal mutations that underlie particular phenotypes in this collection has been recently facilitated by a whole-genome sequencing-based mapping approach (Garcia et al., 2016). The high mutation frequencies reported in this population (up to 1 mutation per 130 Kb) facilitate saturation mutagenesis; hence, large allelic series for a given gene of interest can be obtained by studying a limited number of mutant lines (Just et al., 2013) (see above). Systematic annotation of mutant phenotypes has been carefully performed in the plant model *Arabidopsis thaliana* by recording the phenotypic descriptions in Plant Ontology and Phenotypic Quality Ontology terms (Akiyama et al., 2014). With the aim of initiating the genetic dissection of root development in tomato, we screened a highly mutagenized MT collection to search for mutants affected in several developmental traits during early growth, focusing on specific RSA phenotypes. We established a controlled vocabulary for the curated annotation of the observed phenotypes. We developed a quick procedure for the molecular identification of causal mutations through a whole-genome sequencing approach. The experimental layout developed here will allow the identification of some of the genetic determinants involved in root development during early growth in tomato through mutant analyses.

2. Materials and methods

2.1. Plant materials and growth conditions

We studied M_3 seeds obtained by selfing 395 M_2 lines (Supplementary Table S1) from a highly mutagenized EMS mutant collection described previously (Just et al., 2013; Petit et al., 2014). For scarification, ~30 seeds per M_3 line were treated with 10% sulfuric acid for 3 min and rinsed thoroughly with sterile water (3 times). Next, seeds were surface-sterilized in 3% (w/v) sodium hypochlorite for 10 min, rinsed with sterile water (4 times), and transferred to wet chambers on a 28°C–dark growth cabinet. Germinated seedlings at 96 h (radicle > 4 mm length) were transferred to 120 mm-square Petri dishes (0 days after sowing) containing 75 mL of sterile half-Murashige and Skoog basal salt medium (Duchefa, The Netherlands), 5 g L^{-1} plant agar (Duchefa), 0.5 g L^{-1} 2-(N-morpholino) ethanesulfonic acid (Duchefa) and 2 mL L^{-1} Gamborg B5 vitamin solution (Duchefa), pH 5.8. Six or seven germinated seedlings were placed on each Petri dish, and three to four dishes per genotype were kept in near-vertical positions in a growth cabinet under 16 h light (average photosynthetic photon flux density of 50 μmol m^{-2} s^{-1}) at 26±1°C and 8 h darkness at 23±1°C (Supplementary Figure S1). For the lateral root (LR) capacity assay (Van Norman et al., 2014), 3–4 mm of the root tip was excised after 3 days, and the seedlings were grown for another 5 days (Figure 1A). The formation of adventitious roots (ARs) was then induced by removing the whole root system 2–3 mm above the hypocotyl-root junction with a sharp scalpel after 8 days, and the shoot explants were transferred to sterile 500 mL glass bottles with 75 mL of the plant culture medium.

2.2. Phenotype annotation and microphotography

To describe the observed mutant phenotypes (Figure 1B), we established a controlled vocabulary based on Plant Ontology, Phenotypic Quality Ontology and Environment Ontology terms (Cooper and Jaiswal, 2016; Cooper et al., 2018). We gathered visual information from each seedling for 12 phenotypic traits in several plant structures (i.e., germinated seedlings, primary roots [PR], LRs, shoots and ARs) at four consecutive phenological growth stages (Feller et al., 1995) during the 26 days after seed imbibition (Tables 1 and Supplementary Table S2). LRs and ARs were scored at 8 and 22 days after sowing, respectively (5 and 14 days after LR

and AR induction, respectively). Photographs of the PR, LRs and ARs were taken at the indicated times (Figure 1) using a Sony Cyber-shot DSC-H3 camera (Sony Corporation, Tokyo, Japan) at a resolution of 3,264×2,448 pixels, and the images were saved as RGB color images in the jpeg format.

Chi-square analyses were used to test the goodness-of-fit (p-value<0.05) to expected ratios for the monogenic inheritance of the mutant phenotype in individual M_3 lines (Supplementary Table S3); when two different mutant phenotypes were observed in the same line, we confirmed the independent segregation of the mutant alleles by the chi-square test. Considering a 10% chance of type II error in monogenic inheritance, we did not take into account those lines with fewer than eight WT-like seedlings studied and that did not segregate for the observed mutant phenotypes (Supplementary Table S1).

2.3. Mutant confirmation and whole-genome sequencing

In M_3 lines for which monogenic inheritance for the studied mutations could not be ruled out (Supplementary Table S4), four to six wild-type (WT) siblings were transferred to pots and allowed to self-pollinate in the greenhouse to collect and store M_4 seed families in our seed bank (Figure 1C). Between two and four M_4 families derived from WT-like M_3 plants in the selected lines (16 M_3 lines) were used for segregation studies (Table 2) using the experimental layout described above.

Between 10-24 M_4 WT-like plants from WT-like non-segregating M_3 families and 10-24 M_4 mutant plants from presumably heterozygous-segregating M_3 families were collected to prepare WT-like and mutant bulks, respectively, and were stored at −80°C (Figure 1C). In the case of P14A1, we gathered tissue samples from 20 WT-like and 11 mutant M_4 seedlings from two different M_3 families (P14A1#15 and P14A1#2, respectively). DNA extraction was performed by using the NucleoSpin Plant II commercial kit (Macherey-Nagel Inc. USA) according to the manufacturer's instructions. DNA integrity was evaluated by agarose gel electrophoresis and spectrophotometric methods prior to whole-genome sequencing. Libraries were constructed and sequenced at the Beijing Genomics Institute (BGI, China) using the BGISEQ-500 platform, which is based on novel DNA Nanoball sequencing technology (Zhu et al., 2018). The 150 bp-long paired-end reads that were generated were used for bioinformatics analyses after adapter cleansing and quality checks. To optimize whole-genome coverage, we reconstructed the MT genome sequence file by using the FastaAlternateReferenceMaker tool from the

Genome Analysis Toolkit (McKenna et al., 2010), which implemented polymorphism data from the MT genome into the Heinz 1706-BC reference genome SL3.0 (https://solgenomics.net/). Reads were then mapped to this modified reference genome using HISAT2 (Kim et al., 2019), including some parameters that limited the number of polymorphisms per read to a maximum of two. Matrix manipulation was carried out with SAMtools (Li et al., 2009) and Picard Tools (http://broadinstitute.github.io/picard/). The polymorphic positions between the WT-like and mutant bulk alignments were extracted with Genome Analysis Toolkit and later filtered to exclusively preserve SNPs. The SNPs mostly consisted of G/C to A/T transitions, as expected for EMS mutations (Shirasawa et al., 2016), with coverage ranging from 10x to 100x. To graphically identify the candidate regions, we used the ratio parameter described elsewhere (Wachsman et al., 2017), which consists of the difference between the reference allelic frequency in the WT-like bulk and the reference allelic frequency in the mutant bulk. Graphic representation smoothing was achieved by applying the moving average method with a window width of five genomic coordinates (Beissinger et al., 2015).

We confirmed the presence of single nucleotide polymorphism (SNP) candidate nº7 in ten WT-like seedlings derived from P14A1 #15 and P14A1 #2, as well as in 5 seedling-lethal plantlets derived from P14A1 #2, by using the primer pairs SlCESA3-F (TACTGTATGCCCAAGAGACCC) and SlCESA3-R (ACTTGACTTTTGGAACTTGTGG) for PCR amplification, followed by PCR product purification and Sanger sequencing using the SlCESA3-F primer. The presence of the SNP candidate nº3 was also evaluated in the same seedlings by using the primer pairs Solyc01g073770-F (ACCCCAATTCACTCAGATTCAC) and Solyc01g073770-R (CTCTTCCTTCGCTACATCAGC). Solyc01g073770-F was used for Sanger sequencing. The 3D structure analysis of the CESA protein was carried out with the program PyMOL (DeLano Scientific LLC, 2006) available at http://www.pymol.org.

2.4. Chemical inhibition of cellulose biosynthesis

MT seedlings were sterilized as described in section 2.1 and placed in 90 mm-diameter Petri dishes containing 40 mL sterile plant culture medium supplemented with 0 nM (mock), 10 nM or 40 nM isoxaben (Merck, USA) and incubated in a 28°C-dark growth cabinet for three days. Then, half of the Petri dishes were transferred to standard growing conditions, while the other half ones remained in darkness. After three days, photographs were

taken using the Sony Cyber-shot DSC-H3 camera (Sony Corporation, Tokyo, Japan). PR length was measured and analyzed from the image files with ImageJ (Schneider et al., 2012).

2.5. Statistical analysis

Descriptive statistics (average, standard deviation [SD], median, etc.) were calculated using GraphPad Prism version 8.3.1 for Windows (GraphPad Software, La Jolla California USA). Data outliers were identified based on aberrant SD values and excluded for posterior analyses (Aguinis et al., 2013). Average values ± SDs are shown in the graphs, except in cases that did not exhibit a normal distribution and for which the median was used instead. We performed multiple testing analyses using the Fisher's least significant difference (LSD) method (p-value<0.01). Nonparametric tests were used when necessary.

3. Results

3.1. Early seedling and root architecture mutant phenotype screening

Following the scheme shown in Figure 1, we searched for mutant phenotypes during early growth in 9,367 M_3 seedlings derived from 395 M_3 lines. Overall, we found lower germination rates in the studied M_3 lines (53.4±21.5%) than in the MT background line (87.9±15.2%; Supplementary Figure S2). We discarded 95 M_3 lines (24.1% of M_3 lines; indicated in bold in Supplementary Table S1) whose low germination rates led to a reduced number of seedlings ($n<8$), which made the identification of recessive mutant seedlings difficult. Therefore, we studied the early seedling and rooting phenotypes in 4,543 seedlings from 300 M_3 lines. We manually annotated the phenotypic differences in the early RSA and seedling growth of the MT background line in 946 seedlings from 252 M_3 lines (20.8% of the studied seedlings and 84.0% of the studied M_3 lines; Supplementary Tables S2 and S3).

3.2. Mutants defective in embryo development and early shoot growth

We found 235 seedlings with seedling-lethal phenotypes (5.2% of studied seedlings and 24.8% of annotated mutants) that were similar to the *embryo-defective* (*emb*) mutants of *Arabidopsis thaliana* (Meinke, 2019). The observed seedling-lethal phenotypes segregated as a recessive trait in 87 of the studied M_3 lines (29.0%; Tables S3 and S4). These results are in agreement with the high mutation rates previously reported in this population (Garcia et al., 2016). Only in P11H6 was the phenotypic segregation of the observed seedling-lethal phenotype likely due to a dominant effect of the causal mutation. Twenty-one of these lines segregated as seedlings that were unable to elongate the radicle and stopped growing at stage 005 (shown as [0] on Supplementary Tables S3 and S4). The other seedlings survived through stage 005 but showed striking alterations in the development of their apical-basal axis and were named Emb-1 to Emb-4 (shown as [1] to [4] on Supplementary Tables S3 and S4) depending on the missing developmental structure (Figure 2A). We found 25 lines segregating for putative recessive mutations that caused the Emb-1 phenotype, which is characterized by the absence/disruption of the apical region of the embryo (i.e., the cotyledons and the shoot apical meristem; Figures 2A, 2B); these resembled the *gurke* mutants of Arabidopsis (Mayer et al., 1991). Four and three lines were in turn found to segregate for Emb-2 and Emb-4 phenotypes (Figures 2A, 2B and Supplementary Table S3), which were reminiscent of the *monopteros* and *gnom* mutants, respectively (Mayer et al., 1991). Interestingly, we found 34 M_3 lines that segregated for more than one Emb-like phenotype within the same line (Figure 2C), indicating a complex disturbance of embryo development in these lines. However, these results are a clear underestimation of all the seedling-lethal phenotypes segregating in the MT EMS-mutagenized population; many seeds were unable to germinate (Supplementary Figure S2), and we did not study their embryo phenotypes in detail.

We found 91 seedlings from 49 M_3 lines (2.0% of studied seedlings and 9.6% of annotated mutants) with some variation in their shoot phenotype compared to that of the MT background line (Supplementary Table S4). We clearly distinguished between seedlings with “delayed growth” or “dwarf” phenotypes, the latter being characterized by reduced size in all tissues compared with those of their WT siblings. Thirty-three seedlings from 13 M_3 lines were defined as “dwarf” and likely contain recessive mutations that mostly affect cell growth (Figure 3D and Supplementary Table S4), as eight of these lines also caused PR growth defects in the same plants (see next

section). On the other hand, 22 seedlings from 11 M_3 lines annotated as "delayed shoot growth" did not affect root growth. Three other lines, P12A2, P14C10 and P15H6, segregated for albino plants. Additionally, we found that seven out of 20 M_3 lines segregated for individuals with three cotyledons, but no other phenotypic RSA alterations were observed in these seedlings (Supplementary Tables S3 and S4).

3.3. Early seedling root growth mutants

PR morphologies were studied at 3 days, and the mutant phenotypes found were visually assigned to six categories according to PR length, root hair distribution, or root gravitropism alterations. We found 465 seedlings in 160 M_3 lines with some alteration in PR morphology, most of which displayed shorter PRs or with a premature differentiation of the PR (427 seedlings and 145 M_3 lines; 9.4% of studied seedlings and 45.1% of annotated mutant seedlings; Figure 3A and Supplementary Table S3). Only in three of the lines (P11H11, P12A12 and P15A1) did the short-root phenotype segregate as a dominant trait, while the phenotype of the P11G10 line was likely fixed from the previous generation (Supplementary Tables S3 and S4). Ten lines were characterized by the presence of several seedlings with significantly (p-value<0.01) longer PRs (57.9±15.1 mm; n=25 seedlings) than their WT-like siblings (27.7±12.4 mm; n=100 seedlings; Figure 3A). We identified five seedlings in two M_3 lines, P15G2 and P16A11, and four in the P15A6 line, with higher and lower root hair densities, respectively (Figure 3B and Supplementary Table S3). We found six seedlings in three M_3 lines (P11G11, P12A4 and P13D11) with agravitropic root responses, as their PR growth was not oriented towards the gravity vector (Figure 3C). In all these lines, the agravitropic mutant phenotypes were likely caused by recessive mutations (Supplementary Table S4).

We studied LR architecture at 5 days after surgical excision of the PR tip (see Materials and Methods), which induced the emergence of LR primordia derived from already-specified LR founder cells (Moreno-Risueno et al., 2010; Du and Scheres, 2018). We found 141 seedlings in 43 M_3 lines with altered LR numbers (3.1% of studied seedlings and 14.9% of annotated mutants). Thirty-two lines displayed segregation for a decreased amount of LRs (3.4±1.8; n=73 seedlings) compared with their WT siblings (12.4±5.4; n=376 seedlings), which were likely caused by recessive mutations (Figure 3D and Supplementary Table S3). Thirty-six seedlings from 12 lines were unable to produce any LRs after root tip excision,

suggesting that their causal mutations might affect the positive regulators of LR formation. On the other hand, 34 seedlings from 11 M_3 lines displayed an increased number of LRs (35.4±7.3) compared to their WT-like siblings (p-value<0.01; Figure 3D and Supplementary Table S3), and their mutations might affect negative regulators of LR growth.

Sixteen of the studied M_3 lines were annotated to segregate for seedling phenotypes affecting several PR and LR attributes (Supplementary Table S4). In 11 of them, different seedlings displayed either PR length or LR number mutant phenotypes, suggesting that different mutations independently affected those two phenotypic traits. The other three lines contained seedlings with pleiotropic phenotypes regarding PR length and LR number. On the one hand, the segregating mutations in P13C12 and P15A4 reduced both PR length and LR number, whereas the segregating mutation in P16E10 reduced PR length, but the number of LRs increased (Supplementary Table S4).

3.4. Mutants affected in wound-induced AR formation

ARs arising from the hypocotyl were studied after the removal of the whole root system at 8 days (see Materials and Methods). We identified 105 seedlings from 48 M_3 lines with some alterations in wound-induced AR formation (2.3% of studied seedlings and 11.1% of annotated mutants; Figure 4A and Supplementary Table S3) in proportions that were consistent with recessive inheritance of the mutant phenotypes in most cases (47 M_3 lines; Supplementary Table S4). Thirty-six M_3 lines included some seedlings with a significant reduction in AR number (1.6±1.3; n=35 seedlings in 13 M_3 lines) compared with their WT-like siblings (6.9±3.0; n=135 seedlings; Figure 4B) or did not produce any AR under our experimental conditions (n=46 seedlings in 23 M_3 lines). Twenty-four individuals from 11 M_3 lines displayed a significant increase in AR number (14.3±5.6; Figure 4B) compared to their WT-like siblings (5.7±3.0; n=127 seedlings; p-value<0.001).

We found a substantial overlap (64.5%) in the M_3 lines of seedlings with wound-induced AR mutant phenotypes and those with PR and LR mutant phenotypes (Figure 4C). However, most of these lines segregated for the observed mutant phenotypes in different seedlings, suggesting that different mutations altered the PR, LR and AR traits independently (Supplementary Table S4). Only in P13D11 and P14C12 did we find several seedlings displaying reductions in both PR length and wound-induced ARs (Supplementary Table S4). Intriguingly, the mutation present

in P13D11 also altered PR gravitropism. Our results suggested that the causal mutations in these lines would affect the shared pathways required for postembryonic root development. On the other hand, we found 17 M_3 lines segregating for seedlings with altered numbers of wound-induced ARs with no pleiotropic effects on other RSA traits (Figure 4C and Supplementary Table S4). Among these, segregating mutations in P12F10, P14F11, P14G10, P15G12 and P16H11 caused an increased number of ARs only and might have affected some of the negative regulators required for the early stages of wound-induced AR formation; these mutations deserve further investigation.

3.5. Confirmation of tomato mutants affected in early growth

We estimated the number of mutations and their inheritance patterns in the studied M_3 lines that affected early seedling and RSA traits (Supplementary Table S4). The number of mutations found resembled a Poisson distribution with λ=1.65 (Figure 4D). To confirm the genetic basis of the observed mutant phenotypes, we selected 14 M_3 seed batches that segregated for mutants with shorter PRs and one that segregated for longer PRs. We studied the phenotypic segregation for the annotated mutants in 27 M_4 families obtained by selfing several M_3 plants that displayed a WT-like phenotype from each of these lines (71.0%; Supplementary Table S5). We assessed the recessive inheritance of the shorter PR phenotype in 11 of the 18 M_4 families (61.1%) derived from P11H8, P12A1, P12A6, P12C12, P12D2 and P12G2 (Table 2 and Figure 5A).

In addition, we found that the P11H4, P14A1, P14A9, P14A12, P14B4 and P14C12 lines segregated for two independent mutations, one affecting PR length and the other affecting seedling lethality; that all three M_4 families from P16F4 segregated for seedlings with longer PRs; and that two families in this line segregated for a seedling-lethal phenotype (Table 2). The results found in P11H4, P14A1, P14B4, P14C12 and P16F4 are in agreement with the hypothesis that the two mutations segregate independently, as they might be located on different chromosomes. However, we were not able to confirm the genetic basis of the shorter PR phenotype from P12A7 due to the lack of mutants in the three M_4 families derived from this line (Table 2 and Supplementary Table S5).

We studied five other M_4 families derived from P14D10 and P14D2, segregating in the M_3 for seedlings with a decreased number of LRs or ARs, respectively. We found nine seedlings with a significantly reduced number

of ARs (1.5±0.9) in two M_4 P14D2 families as compared with those of their WT siblings (4.8±1.3; n=52; p-value<0.01; Table 2 and Figure 5B).

3.6. Molecular identification of a gene required for embryo development and early root growth

In our phenotypic screen, we found a significant number of seedlings from M_3 seed batches that displayed seedling-lethal phenotypes. We further confirmed in M_4 the recessive inheritance of some of these seedling-lethal phenotypes in four lines derived from P14 (A1, A9, B4, and C12), P11H4 and P16F4 (Table 2 and Supplementary Table S5). In the studied lines, the seedling-lethal phenotypes segregated in a proportion compatible with single recessive mutations in eight of the M_4 families studied (40.0%, Table 2). The M_3 mutants segregating in P14A1 exhibited a characteristic seedling-lethal phenotype of defective (or very short) PR growth, cotyledon expansion defects and the absence (or severe delay) of the shoot apex (Figure 6A). SNP calling between mutant and WT genomic sequences allowed us to identify (and to discard) non-causal mutations in the genetic background of the P14A1 line, as well as several SNPs between mutant and WT-like bulks (Supplementary Table S6). We focused on 24 SNPs (G/C to A/T transitions) located in the long arm of chromosome 1 (Figure 6B) with ratio values ~1, indicating high mutant allelic frequencies in the mutant bulk (n=11 mutant seedlings), while the ratio values in the WT-like bulk (n=20 WT-like seedlings derived from non-segregating M_3 families for the studied mutant phenotype ; see Materials and Methods) were close to zero. SNP candidate nº3 (Supplementary Table S6) is responsible for an arginine-to-glutamic acid mutation at the 27th residue of Solyc01g073770, a protein similar to At5g19900, whose function is unknown. Another of the studied SNPs (candidate nº7) affected the coding region of the cellulose synthase A (CESA) catalytic subunit encoded by Solyc01g087210 (Figure 6B and Supplementary Table S6). To identify the causal mutation, we sequenced the region including these SNPs in several WT-like and mutant seedlings from the #2 and #15 M_4 families (see Materials and Methods). Plants displaying the mutant phenotype were homozygous for the mutated allele containing the SNP candidate nº7 in homozygosity (Figure 6C), while segregated for the SNP candidate nº 3. Based on the PROVEAN analysis tool (http://provean.jcvi.org/seq_submit.php), the Arg-toGlu^{27} mutation was considered neutral for the Solyc01g073770 protein, while the Leu-to-Phe^{869} mutation in the CESA protein was deleterious. These results suggest that the missense mutation in Solyc01g087210, which causes a leucine-to-

phenylalanine substitution at the conserved position 869 of the fifth transmembrane domain of the CESA protein (Figure 6D), might affect the stability of the transmembrane domain of the protein (Figure 6E) and therefore its function.

To further analyze the consequences of cellulose synthase inactivation on early growth of tomato seedlings, we studied the effect of the chemical inhibition of its activity by isoxaben, a well-known inhibitor of cellulose synthesis that interferes with the correct insertion of cellulose synthase A into the plasma membrane (Tateno et al., 2016). Germinated MT seedlings in the presence of isoxaben (both 10 and 40 nM) resembled the seedling-lethal phenotype observed in the P14A1 M_3 and M_4 lines studied (Figure 6F). PR growth was severely impaired in the isoxaben-treated MT seedlings, even at the lowest concentration used, causing a >80% PR length reduction when compared to that in the non-treated MT seedlings (Figure 6G). Taken together, our results suggest that the missense mutation found in Solyc01g087210 disrupts SlCES3A activity and may be responsible for the observed seedling-lethal phenotype in P14A1.

4. Discussion

A systematic observation of mutant phenotypes caused by loss-of-function alleles is required to elucidate gene function through forward genetic analysis. In *Arabidopsis thaliana* (Arabidopsis), several large-scale phenotypic analyses have generated huge phenotypic data sets, most of which are publicly available (Ajjawi et al., 2010; Lloyd and Meinke, 2012; Myouga et al., 2013; Akiyama et al., 2014; Wilson-Sánchez et al., 2014; Meinke, 2019). Tomato (*Solanum lycopersicum* L.) was proposed as an alternative model for the study of particular traits not found in Arabidopsis, such as fleshy fruit and compound leaf development (Rothan et al., 2016). However, reliable comparative studies of mutations affecting genes in the same pathway are lacking in this species due to large differences in the genetic backgrounds of the different cultivars studied (Carvalho et al., 2011). In an attempt to initiate the genetic dissection of RSA in tomato, we developed an appropriate experimental framework for the identification of tomato mutants affected in 12 phenotypic traits at four consecutive phenological growth stages. Forward genetic approaches provide access to species-specific gene functions, which will contribute to the better understanding of the studied traits. In this work, a subset (n=300 M_3 lines) of a highly chemically mutagenized mutant collection in the miniature

determinate cultivar MT was screened for early seedling and root mutant phenotypes (20 traits). We observed that 37% of the studied M_3 lines segregated for several mutant traits in different plants, such as seedling lethality or PR growth, which is indicative of the large number of homozygous mutations present in the EMS-mutagenized collection studied (Garcia et al., 2016).

To facilitate the subsequent identification of the causal mutation through whole-genome sequencing, we developed a procedure of preparing the mutant bulks by combining the mutant seedlings collected from the segregating M_4 families and preparing the WT bulks by combining the WT-like seedlings collected from the non-segregating M_4 families. As a proof-of-concept, we identified the mutation associated with the seedling-lethal phenotype of the P14A1 line. Mutants defective in embryo development were commonly found in mutagenized Arabidopsis collections, with the frequency of mutant seeds in heterozygous siliques ranging from 5% to 50% (Meinke, 2019). To date, more than 2,200 mutants affecting 510 *EMB* genes (1.8% of all coding genes) have been identified in Arabidopsis, most of which encode chloroplast-localized proteins, proteins involved in RNA binding and modification, or multiple components of essential protein complexes (Meinke, 2019). Following a method for bulk sequencing previously used in rice (Fekih et al., 2013) that does not require the building of a new mapping population, we were able to identify a missense mutation in the coding region of Solyc01g087210 in the seedling-lethal mutants of the P14A1 line. This mutation changed a conserved leucine-to-phenylalanine residue in the fifth transmembrane domain of the protein, which might affect its stability. Solyc01g087210 encodes the catalytic subunit of cellulose synthase A, CESA3, which forms a large plasma membrane-localized cellulose-synthesizing complex with CESA1 and CESA6 required for primary cell wall biosynthesis in Arabidopsis (Carroll et al., 2012). Null mutations of *CESA1* in Arabidopsis, also named *RADIALLY SWOLLEN1*, produce extreme defects in the primary cell wall and cell shape, which lead to a seedling-lethal phenotype (Beeckman et al., 2002) that is indistinguishable from the tomato seedling-lethal mutant found in P14A1 (this work). The Arabidopsis CESA3 is coexpressed with CESA1, and null *cesa3* alleles are lethal to male gametophytes (Persson et al., 2007). Interestingly, a missense semidominant mutation affecting the conserved proline-578 residue of CESA3 in Arabidopsis also caused a characteristic seedling-lethal phenotype (Daras et al., 2009) that is indistinguishable from that described above in P14A1. In addition, a forward genetic screen in Arabidopsis identified a missense mutation in the sixth transmembrane

domain of CESA1 (Ala-to-Val^{903}) that increased cellulose synthase movement in the plasma membrane and produced structurally aberrant cellulose microfibrils (Harris et al., 2012). We were able to mimic the seedling-lethal phenotype of P14A1 by incubating WT tomato seeds on isoxaben, a known inhibitor of the cellulose synthase activity (Burn et al., 2002; Pysh et al., 2012). Taken together, we propose that the missense mutation identified in P14A1 (Leu-to-Phe^{869}) affects the activity of the cellulose-synthesizing complex in tomato, which is essential for primary cell wall biosynthesis.

The most frequent mutant phenotypes found in our phenotypic screen affected PR growth, with a high prevalence of seedlings with shorter roots than the WT (in 47.0% of the studied lines). PR growth depends on the production of new cells in the meristem and their subsequent expansion in the elongation zone of the root (Petricka et al., 2012). In Arabidopsis, many recessive mutations result in shorter root lengths than in the WT. On the one hand, mutations in the brassinosteroid pathway led to a significant reduction in shoot as well as root size and are considered dwarf mutants (Fridman and Savaldi-Goldstein, 2013). On the other hand, mutations in the gibberellin pathway mostly affected shoot growth (and as such are considered semidwarfs) and might confer a selective advantage under specific environmental conditions, such as drought (Barboza-Barquero et al., 2015). We found seedlings with dwarf (shoot and root) phenotypes segregating as a single recessive trait in 13 M_3 lines; in six of these lines, other seedlings displayed decreased PR lengths, suggesting that additional mutations specifically affecting PR growth could also be segregating. We found three lines where the short-root phenotype segregated as a dominant trait; these seedlings also displayed a characteristic pleiotropic phenotype consisting of a twisted hypocotyl and delayed shoot growth. Because the number of dominant mutations with a short-root phenotype in Arabidopsis is limited (Meinke, 2013) and most of them directly affect the auxin pathway (i.e., *YUCCA*, *SHORT HYPOCOTYL2* and *CRANE*), a candidate gene approach will facilitate the identification of causal mutations in these tomato lines. We are conducting allelism tests between some of the short-root tomato mutants that we identified to initiate the bulk of allelic mutant seedlings required for the whole-genome sequencing approach described here.

We found seedlings with agravitropic root and/or shoot growth in four M_3 lines (P11G11, P12A4, P12H3 and P16H8). We will confirm the recessive inheritance of this phenotype in M_4 families, while crosses among the agravitropic mutants from different lines will allow us to determine the number of genes affected in these mutants. Several genetic loci have been

identified as being involved in root gravitropism in Arabidopsis (Su et al., 2017), a process that is directly dependent on the intracellular auxin gradient in the elongation zone of the root established by dynamic PIN-FORMED polarity establishment at the cell membrane (Abas et al., 2006; Rosquete et al., 2013). The *diageotropica* tomato mutant, affected by polar auxin efflux within the root, displays reduced gravitropic responses (Oh et al., 2006; Ivanchenko et al., 2015). On the other hand, in the *polycotyledon* mutant, with enhanced polar auxin transport, a higher root gravitropic curvature was observed compared with that in the WT (Al-Hammadi et al., 2003). Whole-genome sequencing will allow us to identify the genes altered in the agravitropic tomato mutants found in our screen.

Interestingly, we found seedlings with significantly longer PR lengths segregating in a recessive manner in ten M_3 lines; their mutations might affect the negative regulators of root growth. A number of recessive mutants in Arabidopsis with longer roots revealed an interesting crosstalk between jasmonic acid and auxin (Khan and Stone, 2007; Zheng et al., 2016). As deeper roots may be advantageous for water capture from the subsoil in dry environments, increasing our knowledge of the molecular pathways involved in such processes in tomato is of utmost importance for increasing yield in adverse environments.

Both LRs and ARs are essential for increasing the surface area of root systems to explore heterogeneous soil environments in different species (Atkinson et al., 2014; Banda et al., 2019). *De novo* root formation can be divided into several developmental stages, and a number of different mutants have been identified as being affected in specific LR stages (Banda et al., 2019). We found 11 M_3 tomato lines with a significant increase in LR number. The *anthocyanin-reduced* tomato mutant, which is defective in the gene encoding FLAVONOID 3-HYDROXYLASE, the first step in flavonol synthesis, developed 50% fewer LRs than the wild type (Maloney et al., 2014). Conversely, the *anthocyanin without* tomato mutant, with increased flavonol levels, displayed a significant increase in the number of LRs compared with the WT (Maloney et al., 2014). Additional experiments suggested that flavonols reduce auxin flux through WT roots, enhancing the accumulation of auxin at sites of LR formation (Maloney et al., 2014). A time-series analysis of LR formation, as well as a study of the effect of exogenously applied auxin and/or flavonols, in the MT mutants identified here will help us to define the developmental pathway affected in these mutants and would surely help with candidate gene assignment after whole-genome sequencing.

5. Conclusions

We aimed to develop a standardized experimental procedure for root trait screening in young tomato seedlings using a thoroughly characterized EMS-mutagenized collection on the MT background (Just et al., 2013). We were able to identify and confirm a number of recessive mutations that affect several RSA traits, such as PR length, LR number and AR initiation. We established a whole-genome sequencing approach by using WT-like and mutant bulks from non-segregating and segregating M_3 families that allowed us to identify a missense mutation in *SlCESA3* that was associated with a seedling-lethal phenotype with very short roots. Further work will allow us and others to identify some of the key molecular players involved in RSA in tomato, which will help us to increase our understanding of RSA plasticity in response to environmental conditions.

Author contributions

Conceptualization, J.M.P.-P.; methodology, A.A.-C., F.G.-G., P.J. and J.M.P.-P.; investigation, A.A.-C., F.G.-G., P.J., M.M., C.B. and S.I.; resources, D.J., C.B. and C.R.; data curation, A.A.-C. and J.M.P.-P.; writing—original draft preparation, A.A.-C. and J.M.P.-P.; writing—review and editing, C.R. and J.M.P.-P.; supervision, J.M.P.-P.; project administration, J.M.P.-P.; funding acquisition, J.M.P.-P. All authors have read and agreed to the published version of the manuscript.

Declaration of Competing Interest

The authors declare that there are no conflicts of interest.

Acknowledgements

We thank María José Ñíguez for her expert technical assistance and David Esteve-Bruna for help during the setup of the whole-genome sequencing approach.

Funding

This research was funded by the Ministerio de Ciencia e Investigación of Spain (grant numbers BIO2015-64255-R and RTI2018-096505-B-I00) the Conselleria d'Educació, Cultura i Sport of the Generalitat Valenciana (grant numbers IDIFEDER/2018/016 and PROMETEO/2019/117), and the European Regional Development Fund of the European Commission. SI and MM are research fellows of the Generalitat Valenciana (grant numbers ACIF/2018/220 and GRISOLIAP/2019/098).

Appendix. Supplementary data

The following is Supplementary data to this article:
Supplementary Figure S1. Air temperature and relative humidity during the phenotype screening
Supplementary Figure S2. Germination percentage for the studied lines
Supplementary Table S1. Tomato EMS lines studied
Supplementary Table S2. Ontology annotations
Supplementary Table S3. Individual data values of the studied M_3 lines
Supplementary Table S4. Segregation studies of the studied M_3 lines
Supplementary Table S5. Individual data values of the studied M_4 lines
Supplementary Table S6. Candidate SNPs of P14A1 in chromosome 1

References

Abas L, Benjamins R, Malenica N, Paciorek TT, Wiřniewska J, Moulinier-Anzola JC, Sieberer T, Friml J, Luschnig C (2006) Intracellular trafficking and proteolysis of the Arabidopsis auxin-efflux facilitator PIN2 are involved in root gravitropism. Nat Cell Biol **8**: 249–256

Aguinis H, Gottfredson RK, Joo H (2013) Best-Practice Recommendations for Defining, Identifying, and Handling Outliers. Organ Res Methods **16**: 270–301

Ajjawi I, Lu Y, Savage LJ, Bell SM, Last RL (2010) Large-scale reverse genetics in Arabidopsis: Case studies from the Chloroplast 2010 project. Plant Physiol **152**: 529–540

Akiyama K, Kurotani A, Iida K, Kuromori T, Shinozaki K, Sakurai T (2014) RARGE II: An Integrated Phenotype Database of Arabidopsis Mutant Traits Using a Controlled Vocabulary. Plant Cell Physiol **55**: e4–e4

Al-Hammadi ASA, Sreelakshmi Y, Negi S, Siddiqi I, Sharma R (2003) The polycotyledon mutant of tomato shows enhanced polar auxin transport. Plant Physiol **133**: 113–125

Atkinson JA, Rasmussen A, Traini R, Voß U, Sturrock C, Mooney SJ, Wells DM, Bennett MJ (2014) Branching out in roots: uncovering form, function, and regulation. Plant Physiol **166**: 538–50

Baldet P, Bres C, Okabe Y, Mauxion J-P, Just D, Bournonville C, Ferrand C, Mori K, Ezura H, Rothan C (2013) Investigating the role of vitamin C in tomato through TILLING identification of ascorbate-deficient tomato mutants. Plant Biotechnol **30**: 309–314

Banda J, Bellande K, von Wangenheim D, Goh T, Guyomarc'h S, Laplaze L, Bennett MJ (2019) Lateral Root Formation in Arabidopsis: A Well-Ordered LRexit. Trends Plant Sci **24**: 826–839

Barboza-Barquero L, Nagel KA, Jansen M, Klasen JR, Kastenholz B, Braun S, Bleise B, Brehm T, Koornneef M, Fiorani F (2015) Phenotype of *Arabidopsis thaliana* semi-dwarfs with deep roots and high growth rates under water-limiting conditions is independent of the *GA5* loss-of-function alleles. Ann Bot **116**: 321–331

Beeckman T, Przemeck GKH, Stamatiou G, Lau R, Terryn N, De Rycke R, Inzé D, Berleth T (2002) Genetic complexity of cellulose synthase A gene function in arabidopsis embryogenesis. Plant Physiol **130**: 1883–1893

von Behrens I, Komatsu M, Zhang Y, Berendzen KW, Niu X, Sakai H, Taramino G, Hochholdinger F (2011) Rootless with undetectable meristem 1 encodes a monocot-specific AUX/IAA protein that controls embryonic seminal and post-embryonic lateral root initiation in maize. Plant J **66**: 341–353

Beissinger TM, Rosa GJ, Kaeppler SM, Gianola D, De Leon N (2015) Defining window-boundaries for genomic analyses using smoothing spline techniques. Genet Sel Evol. doi: 10.1186/s12711-015-0105-9

Burn JE, Hocart CH, Birch RJ, Cork AC, Williamson RE (2002) Functional analysis of the cellulose synthase genes CesA1, CesA2, and CesA3 in Arabidopsis. Plant Physiol **129**: 797–807

Campos ML, Carvalho RF, Benedito VA, Peres LEP (2010) The micro-tom model system as a tool to discover novel hormonal functions and interactions. Plant Signal Behav **5**: 267–270

Carroll A, Mansoori N, Li S, Lei L, Vernhettes S, Visser RGF, Somerville C, Gu Y, Trindade LM (2012) Complexes with mixed primary and secondary cellulose synthases are functional in Arabidopsis plants. Plant Physiol **160**: 726–737

Carvalho RF, Campos ML, Pino LE, Crestana SL, Zsögön A, Lima JE, Benedito VA, Peres LE (2011) Convergence of developmental mutants into a single tomato model system: "Micro-Tom" as an effective toolkit for plant development research. Plant Methods **7**: 18

Cheng W, Yin S, Tu Y, Mei H, Wang Y, Yang Y (2020) SlCAND1, encoding cullin-associated Nedd8-dissociated protein 1, regulates plant height, flowering time, seed germination, and root architecture in tomato. Plant Mol Biol. doi: 10.1007/s11103-020-00963-7

Cooper L, Jaiswal P (2016) The plant ontology: A tool for plant genomics. Methods Mol. Biol. Humana Press Inc., pp 89–114

Cooper L, Meier A, Laporte M-A, Elser JL, Mungall C, Sinn BT, Cavaliere D, Carbon S, Dunn NA, Smith B, et al (2018) The Planteome database: an integrated resource for reference ontologies, plant genomics and phenomics. Nucleic Acids Res **46**: D1168–D1180

Daras G, Rigas S, Penning B, Milioni D, McCann MC, Carpita NC, Fasseas C, Hatzopoulos P (2009) The thanatos mutation in Arabidopsis thaliana cellulose synthase 3 (AtCesA3) has a dominant-negative effect on cellulose synthesis and plant growth. New Phytol **184**: 114–126

Du Y, Scheres B (2018) Lateral root formation and the multiple roles of auxin. J Exp Bot **69**: 155–167

Emmanuel E, Levy AA (2002) Tomato mutants as tools for functional genomics. Curr Opin Plant Biol **5**: 112–117

Fekih R, Takagi H, Tamiru M, Abe A, Natsume S, Yaegashi H, Sharma S, Sharma S, Kanzaki H, Matsumura H, et al (2013) MutMap+: Genetic Mapping and Mutant Identification without Crossing in Rice. PLoS One **8**: e68529

Feller C, Bleiholder H, Buhr L, Hack H, Hess M, Klose R, Meier U, Stauss R, Van den Boom T, Weber E (1995) Phänologische entwicklungsstadien von

gemüsepflanzen: II. Fruchtgemüse und hülsenfrüchte. Nachrichtenbl Deut Pflanzenschutzd **47**: 217–232

Fridman Y, Savaldi-Goldstein S (2013) Brassinosteroids in growth control: How, when and where. Plant Sci **209**: 24–31

Garcia V, Bres C, Just D, Fernandez L, Tai FWJ, Mauxion JP, Le Paslier MC, Bérard A, Brunel D, Aoki K, et al (2016) Rapid identification of causal mutations in tomato EMS populations via mapping-by-sequencing. Nat Protoc **11**: 2401–2418

Harris DM, Corbin K, Wang T, Gutierrez R, Bertolo AL, Petti C, Smilgies DM, Estevez JM, Bonetta D, Urbanowicz BR, et al (2012) Cellulose microfibril crystallinity is reduced by mutating C-terminal transmembrane region residues CESA1 A903V and CESA3 T942I of cellulose synthase. Proc Natl Acad Sci U S A **109**: 4098–4103

Hochholdinger F, Yu P, Marcon C (2018) Genetic Control of Root System Development in Maize. Trends Plant Sci **23**: 79–88

Ivanchenko MG, Zhu J, Wang B, Medvecká E, Du Y, Azzarello E, Mancuso S, Megraw M, Filichkin S, Dubrovsky JG, et al (2015) The cyclophilin a DIAGEOTROPICA gene affects auxin transport in both root and shoot to control lateral root formation. Dev **142**: 712–721

Just D, Garcia V, Fernandez L, Bres C, Mauxion J-P, Petit J, Jorly J, Assali J, C^|^eacute, Bournonville L, et al (2013) Micro-Tom mutants for functional analysis of target genes and discovery of new alleles in tomato. Plant Biotechnol **30**: 225–231

Kellermeier F, Armengaud P, Seditas TJ, Danku J, Salt DE, Amtmann A (2014) Analysis of the root system architecture of Arabidopsis provides a quantitative readout of crosstalk between nutritional signals. Plant Cell **26**: 1480–1496

Khan S, Stone J (2007) *Arabidopsis thaliana* GH3.9 in Auxin and Jasmonate Cross Talk. Plant Signal Behav **2**: 483–485

Kim D, Paggi JM, Park C, Bennett C, Salzberg SL (2019) Graph-based genome alignment and genotyping with HISAT2 and HISAT-genotype. Nat Biotechnol **37**: 907–915

Kobayashi M, Nagasaki H, Garcia V, Just D, Bres C, Mauxion JP, Le Paslier MC, Brunel D, Suda K, Minakuchi Y, et al (2014) Genome-wide analysis of intraspecific dna polymorphism in “micro-tom”, a model cultivar of

tomato (solanum lycopersicum). Plant Cell Physiol **55**: 445–454

Li H, Handsaker B, Wysoker A, Fennell T, Ruan J, Homer N, Marth G, Abecasis G, Durbin R (2009) The Sequence Alignment/Map format and SAMtools. Bioinformatics **25**: 2078–2079

Lloyd J, Meinke D (2012) A comprehensive dataset of genes with a loss-of-function mutant phenotype in Arabidopsis. Plant Physiol **158**: 1115–1129

Maloney GS, DiNapoli KT, Muday GK (2014) The anthocyanin reduced tomato mutant demonstrates the role of flavonols in tomato lateral root and root hair development. Plant Physiol **166**: 614–31

Martí E, Gisbert C, Bishop GJ, Dixon MS, García-Martínez JL Genetic and physiological characterization of tomato cv. Micro-Tom. doi: 10.1093/jxb/erj154

Mayer U, Ruiz RAT, Berleth T, Miseéra S, Jürgens G (1991) Mutations affecting body organization in the Arabidopsis embryo. Nature **353**: 402–407

McKenna A, Hanna M, Banks E, Sivachenko A, Cibulskis K, Kernytsky A, Garimella K, Altshuler D, Gabriel S, Daly M, et al (2010) The genome analysis toolkit: A MapReduce framework for analyzing next-generation DNA sequencing data. Genome Res **20**: 1297–1303

Meinke DW (2019) Genome-wide identification of *<scp>EMBRYO</scp>* - *<scp>DEFECTIVE</scp>* (*<scp>EMB</scp>*) genes required for growth and development in Arabidopsis. New Phytol nph.16071

Meinke DW (2013) A survey of dominant mutations in Arabidopsis thaliana. Trends Plant Sci **18**: 84–91

Meng F, Xiang D, Zhu J, Li Y, Mao C (2019) Molecular Mechanisms of Root Development in Rice. Rice. doi: 10.1186/s12284-018-0262-x

Moreno-Risueno MA, Van Norman JM, Moreno A, Zhang J, Ahnert SE, Benfey PN (2010) Oscillating Gene Expression Determines Competence for Periodic Arabidopsis Root Branching. Science (80-) **329**: 1306–1311

Mubarok S, Okabe Y, Fukuda N, Ariizumi T, Ezura H (2015) Potential Use of a Weak Ethylene Receptor Mutant, Sletr1-2, as Breeding Material To Extend Fruit Shelf Life of Tomato. J Agric Food Chem **63**: 7995–8007

Musseau C, Just D, Jorly J, Gévaudant F, Moing A, Chevalier C, Lemaire-Chamley M, Rothan C, Fernandez L (2017) Identification of two new mechanisms that regulate fruit growth by cell expansion in tomato. Front

Plant Sci. doi: 10.3389/fpls.2017.00988

Myouga F, Akiyama K, Tomonaga Y, Kato A, Sato Y, Kobayashi M, Nagata N, Sakurai T, Shinozaki K (2013) The chloroplast function database II: A comprehensive collection of homozygous mutants and their phenotypic/genotypic traits for nuclear-encoded chloroplast proteins. Plant Cell Physiol. doi: 10.1093/pcp/pcs171

Van Norman JM, Zhang J, Cazzonelli CI, Pogson BJ, Harrison PJ, Bugg TDH, Chan KX, Thompson AJ, Benfey PN (2014) Periodic root branching in Arabidopsis requires synthesis of an uncharacterized carotenoid derivative. Proc Natl Acad Sci U S A **111**: E1300-9

Oh K, Ivanchenko MG, White TJ, Lomax TL (2006) The diageotropica gene of tomato encodes a cyclophilin: a novel player in auxin signaling. Planta **224**: 133–144

Okabe Y, Ariizumi T, Ezura H (2013) Updating the Micro-Tom TILLING platform. Breed Sci **63**: 42–48

Persson S, Paredez A, Carroll A, Palsdottir H, Doblin M, Poindexter P, Khitrov N, Auer M, Somerville CR (2007) Genetic evidence for three unique components in primary cell-wall cellulose synthase complexes in Arabidopsis. Proc Natl Acad Sci U S A **104**: 15566–15571

Petit J, Bres C, Just D, Garcia V, Mauxion JP, Marion D, Bakan B, Joubès J, Domergue F, Rothan C (2014) Analyses of tomato fruit brightness mutants uncover both cutin-deficient and cutin-abundant mutants and a new hypomorphic allele of GDSL Lipase. Plant Physiol **164**: 888–906

Petricka JJ, Winter CM, Benfey PN (2012) Control of Arabidopsis Root Development . Annu Rev Plant Biol **63**: 563–590

Pysh L, Alexander N, Swatzyna L, Harbert R (2012) Four alleles of AtCESA3 form an allelic series with respect to root phenotype in Arabidopsis thaliana. Physiol Plant **144**: 369–381

Quinet M, Angosto T, Yuste-Lisbona FJ, Blanchard-Gros R, Bigot S, Martinez JP, Lutts S (2019) Tomato Fruit Development and Metabolism. Front Plant Sci. doi: 10.3389/fpls.2019.01554

Rick CM (1991) Tomato paste: a concentrated review of genetic highlights from the beginnings to the advent of molecular genetics. Genetics 128:

Robbins NE, Dinneny JR (2015) The divining root: Moisture-driven responses of roots at the micro- and macro-scale. J Exp Bot **66**: 2145–2154

Rosquete MR, von Wangenheim D, Marhavý P, Barbez E, Stelzer EHK, Benková E, Maizel A, Kleine-Vehn J (2013) An auxin transport mechanism restricts positive orthogravitropism in lateral roots. Curr Biol **23**: 817–22

Rothan C, Bres C, Garcia V, Just D (2016) Tomato Resources for Functional Genomics. pp 75–94

Rothan C, Diouf I, Causse M (2019) Trait discovery and editing in tomato. Plant J **97**: 73–90

Saito T, Ariizumi T, Okabe Y, Asamizu E, Hiwasa-Tanase K, Fukuda N, Mizoguchi T, Yamazaki Y, Aoki K, Ezura H (2011) TOMATOMA: A novel tomato mutant database distributing micro-tom mutant collections. Plant Cell Physiol **52**: 283–296

Schneider CA, Rasband WS, Eliceiri KW (2012) NIH Image to ImageJ: 25 years of image analysis. Nat Methods **9**: 671–675

Scott J, Harbaugh B. (1989) Micro-Tom : A Miniature Dwarf Tomato. Agricultural Experiment Station Institute of Food and Agricultural Sciences University of Florida, Gainesville FL

Shikata M, Ezura H (2016) Micro-Tom Tomato as an Alternative Plant Model System: Mutant Collection and Efficient Transformation. Humana Press, New York, NY, pp 47–55

Shikata M, Hoshikawa K, Ariizumi T, Fukuda N, Yamazaki Y, Ezura H (2016) TOMATOMA Update: Phenotypic and Metabolite Information in the Micro-Tom Mutant Resource. Plant Cell Physiol **57**: e11–e11

Shirasawa K, Hirakawa H, Nunome T, Tabata S, Isobe S (2016) Genome-wide survey of artificial mutations induced by ethyl methanesulfonate and gamma rays in tomato. Plant Biotechnol J **14**: 51–60

Su S-H, Gibbs NM, Jancewicz AL, Masson PH (2017) Molecular Mechanisms of Root Gravitropism. Curr Biol **27**: R964–R972

Tateno M, Brabham C, DeBolt S (2016) Cellulose Biosynthesis Inhibitors - A Multifunctional Toolbox. J Exp Bot **67**: 533–542

Toal TW, Ron M, Gibson D, Kajala K, Splitt B, Johnson LS, Miller ND, Slovak R, Gaudinier A, Patel R, et al (2018) Regulation of root angle and gravitropism. G3 Genes, Genomes, Genet **8**: 3841–3855

Wachsman G, Modliszewski JL, Valdes M, Benfey PN (2017) A simple pipeline for mapping point mutations. Plant Physiol **174**: 1307–1313

Wang X, Xing Y (2017) Evaluation of the effects of irrigation and fertilization on tomato fruit yield and quality: A principal component analysis. Sci Rep. doi: 10.1038/s41598-017-00373-8

Wilson-Sánchez D, Rubio-Díaz S, Muñoz-Viana R, Pérez-Pérez JM, Jover-Gil S, Ponce MR, Micol JL (2014) Leaf phenomics: a systematic reverse genetic screen for Arabidopsis leaf mutants. Plant J.

Yu P, Baldauf JA, Lithio A, Marcon C, Nettleton D, Li C, Hochholdinger F (2016) Root type-specific reprogramming of maize pericycle transcriptomes by local high nitrate results in disparate lateral root branching patterns. Plant Physiol **170**: 1783–1798

Zheng H, Pan X, Deng Y, Wu H, Liu P, Li X (2016) AtOPR3 specifically inhibits primary root growth in Arabidopsis under phosphate deficiency. Sci Rep. doi: 10.1038/srep24778

Zhu F-Y, Chen M-X, Ye N-H, Qiao W-M, Gao B, Law W-K, Tian Y, Zhang D, Zhang D, Liu T-Y, et al (2018) Comparative performance of the BGISEQ-500 and Illumina HiSeq4000 sequencing platforms for transcriptome analysis in plants. Plant Methods **14**: 69

Figures

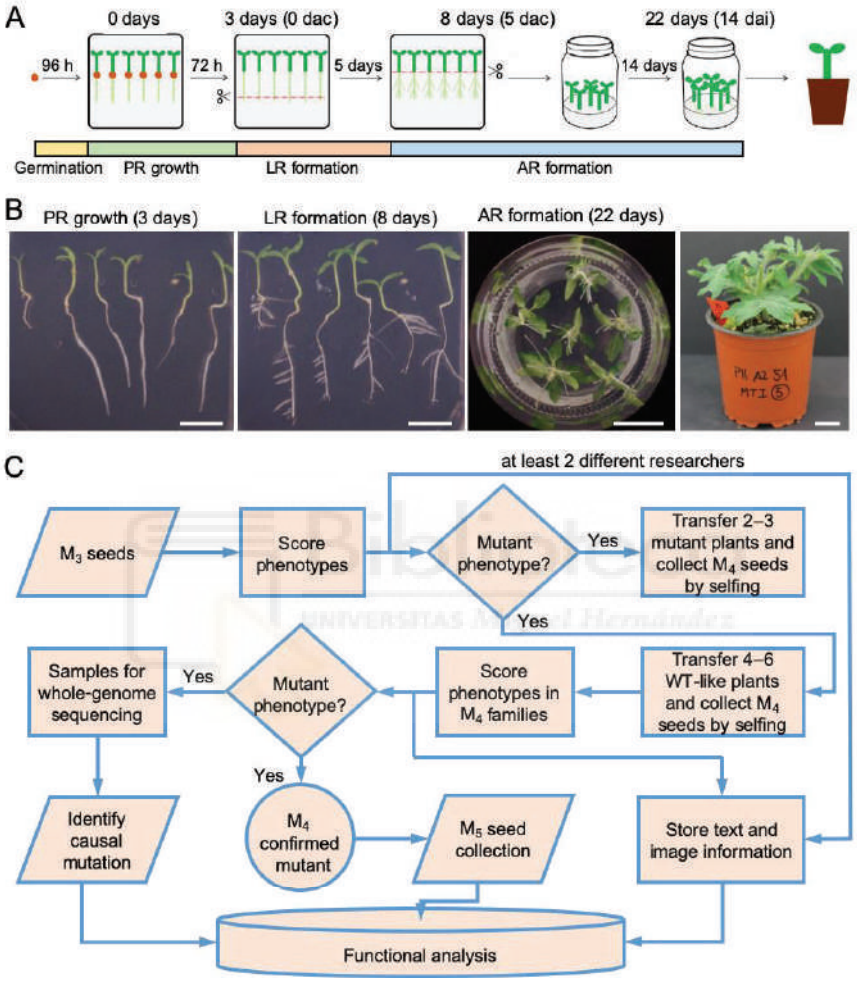

Figure 1. Design of the early seedling and RSA mutant screening in tomato. (A) Experimental layout used in this work. (B) Representative images of the studied phenological growth stages. Scale bars: 20 mm. (C) Workflow chart of our mutant screening. AR: adventitious root, dac: days after root tip cutting, dai: days after AR induction, LR: lateral root, PR: primary root, WT: wild type.

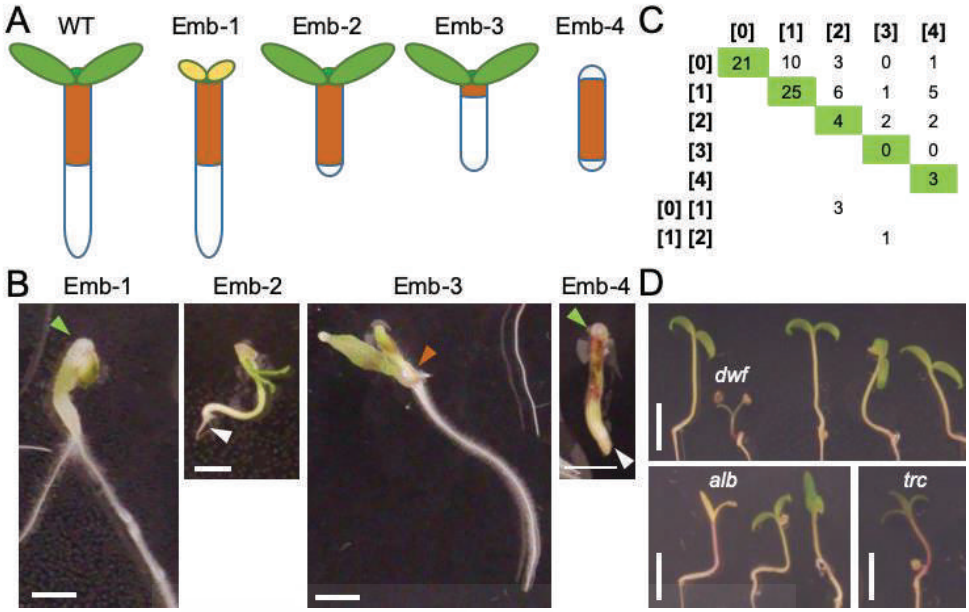

Figure 2. Tomato mutants with defective embryo development. (A) Schematic diagram of WT and Emb phenotypes found in our study. Emb-1 and Emb-2 mutants display apical or basal patterning defects, respectively. Emb-3 mutants lack the central domain of the embryo (i.e., the hypocotyl), while Emb-4 mutants resemble the Arabidopsis *gnom* mutants, with only the central domain present. (B) Representative images of the observed Emb phenotypes in tomato. Arrowheads indicate missing embryo structures (green: apical, brown: central, white: basal). (C) Number of M_3 lines segregating for the observed Emb phenotypes; [0] represents seedlings that stopped growth at stage 005 (Feller et al., 1995). (D) Representative images of some segregating shoot phenotypes, such as dwarf (*dwf*), albino (*alb*) or tricotyledon seedlings (*trc*). Scale bars: 5 mm.

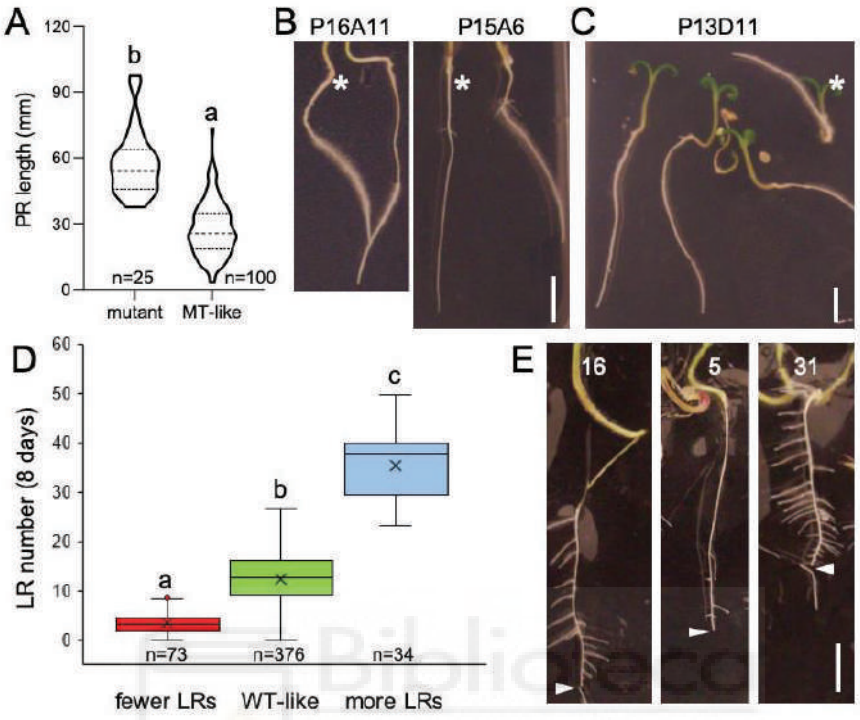

Figure 3. Rooting phenotypes studied during early growth in tomato. (A) Violin plot of PR lengths in putative mutants with increased values compared with those of their WT-like siblings. Dashed and dotted lines indicate median and quartiles, respectively. Letters indicate significant differences between groups (p-value<0.001). (B) Representative images of segregating root hair phenotypes (indicated by asterisks), such as an increased amount of root hairs in P16A11 and a decreased amount of root hairs in P15A6. (C) Agravitropic root phenotype segregating in the P13D11 line. (D) Boxplots of the LR number in putative mutants with decreased or increased values compared with those of their WT-like siblings. The average and median are shown. Letters indicate significant differences between groups (p-value<0.001). (E) Representative images of seedlings with average (left), reduced (middle) and increased (right) numbers of LRs. Scale bars: 10 mm.

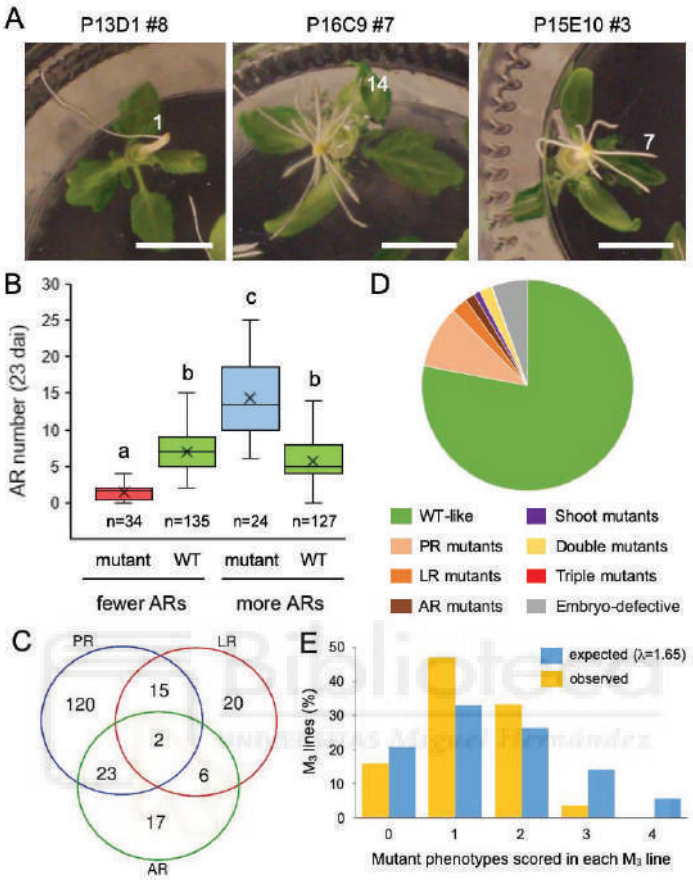

Figure 4. Wound-induced AR phenotypes. (A) Representative images of rooted hypocotyls of some mutants with reduced (P13D1 #8) or increased (P16C9 #7) AR numbers compared with the Micro-Tom background line (represented by P15E10 #3). Scale bar: 10 mm. (B) Boxplots of AR numbers in putative mutants with reduced or increased values compared with their WT-like siblings. The average and median are shown. Letters indicate significant differences between groups (p-value<0.001). (C) Venn diagram of the studied M_3 lines with annotated phenotypes for PR, LRs and ARs. (D) Percentage of early seedling and root mutant phenotypes studied. (E) Distribution of annotated mutations in the studied M_3 lines (orange) and Poisson distribution estimate for λ=1.65 (blue).

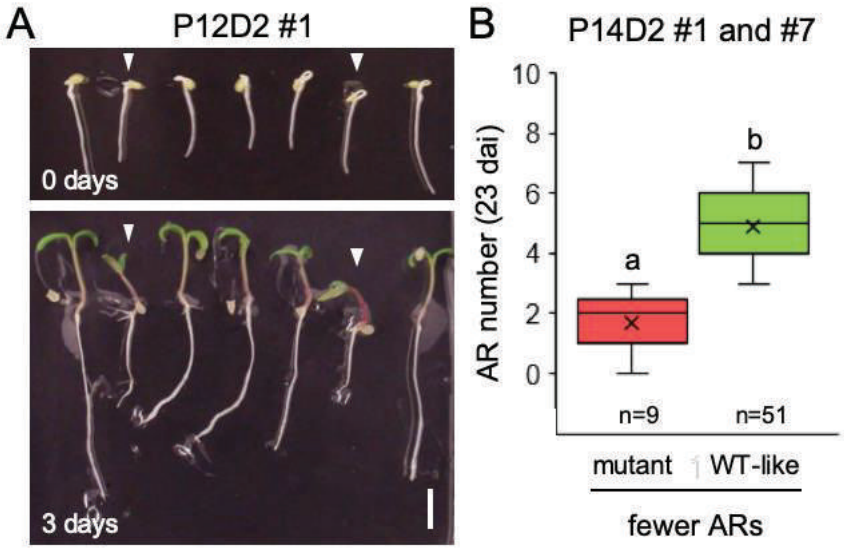

Figure 5. Genetic confirmation of early seedling and RSA tomato mutants. (A) Representative images of seedlings from an M_4 family segregating for plants with short-root and dwarf phenotypes; Scale bar: 10 mm. (B) Boxplots of AR numbers in two M_4 families from P14D2 segregating for mutants with decreased AR numbers. The average and median are shown. Letters indicate significant differences between groups (p-value<0.001).

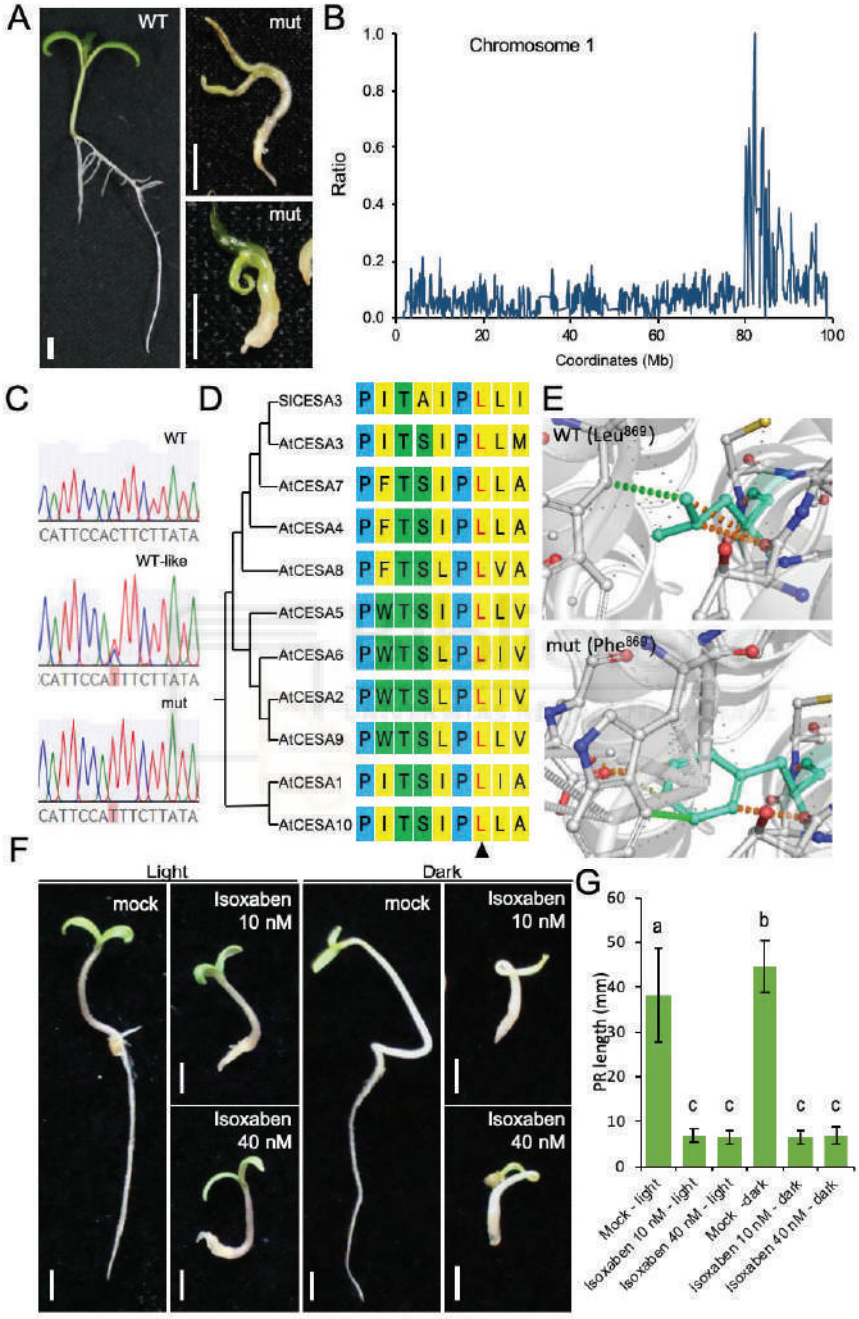
A
WT
mut
mut
B
Chromosome 1
Ratio
1.0
0.8
0.6
0.4
0.2
0.0
0
20
40
60
80
100
Coordinates (Mb)
C
WT
CATTCCACTTCTTATA
WT-like
CATTCCATTTCTTATA
mut
CATTCCATTTCTTATA
D
SlCESA3 P I T A I P L L I
AtCESA3 P I T S I P L L M
AtCESA7 P F T S I P L L A
AtCESA4 P F T S I P L L A
AtCESA8 P F T S L P L V A
AtCESA5 P W T S I P L L V
AtCESA6 P W T S L P L I V
AtCESA2 P W T S L P L I V
AtCESA9 P W T S L P L L V
AtCESA1 P I T S I P L I A
AtCESA10 P I T S I P L L A
E
WT (Leu869)
mut (Phe869)
F
Light
Dark
mock
Isoxaben 10 nM
Isoxaben 40 nM
mock
Isoxaben 10 nM
Isoxaben 40 nM
G
PR length (mm)
60
50
40
30
20
10
0
a
b
c
c
c
c
c
Mock - light
Isoxaben 10 nM - light
Isoxaben 40 nM - light
Mock - dark
Isoxaben 10 nM - dark
Isoxaben 40 nM - dark

Figure 6. Molecular confirmation of early seedling and RSA tomato mutants. (A) Representative images of seedlings from the P14A1#2 M4 family segregating for plants with the studied seedling-lethal phenotype. Scale bars: 10 mm. (B) Genomic region of chromosome 1 associated with the studied mutant phenotype. The plot represents the allelic ratio for the studied SNPs along the chromosome using the average smoothing method. (C) Sanger electropherogram showing genotype-phenotype correlation for SNP candidate nº7. (D) Solyc01g087210 (SlCESA3) and Arabidopsis CESA-family proteins (AtCESA) show strong amino acid conservation near the mutation site (black arrowhead). (E) Intramolecular interactions of Leu^{869} (WT) and Phe^{869} (mut) residues. Green and orange dashed lines represent hydrophobic contacts and hydrogen bonds, respectively; gray dashed lines represent aromatic interactions. (F) Representative images of isoxaben- and mock-treated seedlings under light (16/8) and dark conditions. (G) PR length of isoxaben- and mock-treated seedlings under light (16/8) and dark conditions. Scale bars: 50 mm.

Table 1. Early seedling and root mutant phenotypes studied.

Structure	Trait	Value	Description	Days
Germinated seedling	Development	Do not germinate	Radicle is not visible after 96 h at 28° C in darkness	0
		Delayed germination	A ≤4 mm radicle is visible after 96 h at 28° C in darkness	0
		Do germinate	A >4 mm radicle is visible after 96 h at 28° C in darkness	0
PR	Development	Absent	A functional PR is not observed in the seedling	3
		Present	A functional PR is observed in the seedling	3
		Embryonic lethality	Seedlings that were unable to complete organogenesis after germination	3
	Length	Decreased length	PR length is ≥25% lower from that of the average of the siblings	3
		Normal length	PR length is not different from that of the average of the siblings	3
		Increased length	PR length is ≥25% higher from that of the average of the siblings	3
	Gravitropism	Positive gravitropism	PR growths towards gravity vector	3
		Agravitropic	PR growths away gravity vector	3
	Root hair number	Decreased amount	Root hair number is ≥25% lower from that of the average of the siblings	3
		Normal amount	Root hair number is not different from that of the average of the siblings	3
		Increased amount	Root hair number is ≥25% higher from that of the average of the siblings	3
LRs	Development	Absent	Functional LRs are not observed within the PR	8
		Present	Functional LRs are observed within the PR	8
	Number	Decreased amount	LR number is ≥25% lower from that of the average of the siblings	8

		Normal amount	LR number is not different from that of the average of the siblings	8
		Increased amount	LR number is ≥25% higher from that of the average of the siblings	8
Shoot	Development	Dwarf	Shoot development is ≥25% lower from that of the average of the siblings	8
		Delayed growth	Shoot development is delayed as regards that of the average of the siblings	8
		Normal size	Shoot development is not different from that of the average of the siblings	8
	Color	Albino	Absent shoot pigmentation due to lack of chlorophyll	8
	Cotyledons	Decreased amount	Cotyledons number is lower from that of the average of the siblings	8
		Normal amount	Cotyledons number is not different from that of the average of the siblings	8
		Increased amount	Cotyledons number is higher from that of the average of the siblings	8
ARs	Development	Absent	Functional ARs are not observed at the lower hypocotyl	23
		Present	Functional ARs are observed at the lower hypocotyl	23
	Number	Decreased amount	AR number is ≥25% lower from that of the average of the siblings	23
		Normal amount	AR number is not different from that of the average of the siblings	23
		Increased amount	AR number is ≥25% higher from that of the average of the siblings	23

Table 2. Confirmation of early root mutants in M4 families.

M_3 line	M_3 mutant phenotypes (*m1*; *m2*)	M_4 family	WT	*m1*	*m2*	*m1m2*	χ^2 (segregation); hypothesis[1]
P11H4	shorter PR; seedling lethal	P1#2 WT-like	14				*4.667* (3:1)
		P1#3 WT-like	13	4	2		2.146 (9:3:4); recessive epistasis (*m2*>*m1*)
		P2#3 *m1*		14		4	0.074 (3:1); *m1* homozygous, segregates for *m2*
P11H8	shorter PR	P2#3 WT-like	15	2			1.588 (3:1); segregates for a recessive mutation (*m1*)
		P2#6 WT-like	17	2			2.123 (3:1); segregates for a recessive mutation (*m1*)
		P2#8 WT-like	16				*5.333* (3:1)
P12A1	shorter PR	P1#3 WT-like	18	3			1.286 (3:1); segregates for a recessive mutation (*m1*)
		P1#7 MT-like	18				*6.000* (3:1)
P12A6	shorter PR	P1#1 WT-like	19				*6.333* (3:1)
		P1#2 WT-like	10	7			2.373 (3:1); segregates for a recessive mutation (*m1*)
P12A7	shorter PR	P1#1 WT-like	19				*6.333* (3:1)
		P1#2 WT-like	20				*6.667* (3:1)
		P1#3 WT-like	19				*6.333* (3:1)
P12C12	shorter PR	P1#7 WT-like	15	5			0.000 (3:1); segregates for a recessive mutation (*m1*)
		P1#8 WT-like	14	3			0.490 (3:1); segregates for a recessive mutation (*m1*)
P12D2	shorter PR	P1#1 WT-like	13	3			0.333 (3:1); segregates for a recessive mutation (*m1*)
		P1#3 WT-like	14				*4.667* (3:1)
		P2#1 WT-like	17	4			0.397 (3:1); segregates for a recessive mutation (*m1*)
P12G2	shorter PR	#3 WT-like	14	8			1.515 (3:1); 0.488 (9:7); dominant epistasis
		#5 WT-like	13	9			2.970 (3:1); 0.072 (9:7)
		#6 WT-like	16	8			0.889 (3:1); 1.058 (9:7)
P14A1	shorter PR; seedling lethal	#2 WT-like	17	3	4		2.074 (9:3:4); recessive epistasis (*m2*>*m1*)
		#15 WT-like	21	3			2.000 (3:1); segregates for a recessive mutation (*m1*)
P14A9	shorter PR; seedling lethal	#1 WT-like	21	3	5		3.138 (9:3:4); recessive epistasis (*m2*>*m1*)
		#9 WT-like	24				*8.000* (3:1)
P14A12	shorter PR; seedling lethal	#3 WT-like	21	3			2.000 (3:1); segregates for a recessive mutation (*m1*)
		#4 WT-like	22				*7.333* (3:1)

		#7 WT-like	12	2		0.857 (3:1); segregates for a recessive mutation (*m1*)
P14B4	shorter PR; seedling lethal	#1 WT-like	17	5		0.061 (3:1); segregates for a recessive mutation (*m1*)
		#2 WT-like	20	3	4	3.486 (9:3:4); recessive epistasis (*m2>m1*)
		#3 WT-like	19	6		0.013 (3:1); segregates for a recessive mutation (*m1*)
P14C12	shorter PR; seedling lethal	#4 WT-like	14	7	8	0.854 (9:3:4); recessive epistasis (*m2>m1*)
		#5 WT-like	26	4		2.178 (3:1); segregates for a recessive mutation (*m1*)
P14D2	decreased AR number; seedling lethal	#1 WT-like	25	4		1.943 (3:1); segregates for a recessive mutation (*m1*)
		#7 WT-like	25	5		1.111 (3:1); segregates for a recessive mutation (*m1*)
P14D10	shorter PR; decreased LR number	#4 WT-like	17	3	4	1.463 (9:3:3:1); two unlinked recessive mutations
		#6 WT-like	13		5	0.074 (3:1); segregates for a recessive mutation (*m2*)
		#8 WT-like	19	5		0.222 (3:1); segregates for a recessive mutation (*m1*)
P16F4	longer PR; seedling lethal	#2 WT-like	15	7	8	0.578 (9:3:4); recessive epistasis (*m2>m1*)
		#4 WT-like	26	4		1.943 (3:1); segregates for a recessive mutation (*m1*)
		#5 WT-like	23	4	3	5.393 (9:3:4); recessive epistasis (*m2>m1*)

[1] The χ^2 values in italics indicate that the observed data do not fit the expected segregation of the mutant phenotype to the proposed hypothesis (p-value<0.05).

Supplementary figures and tables

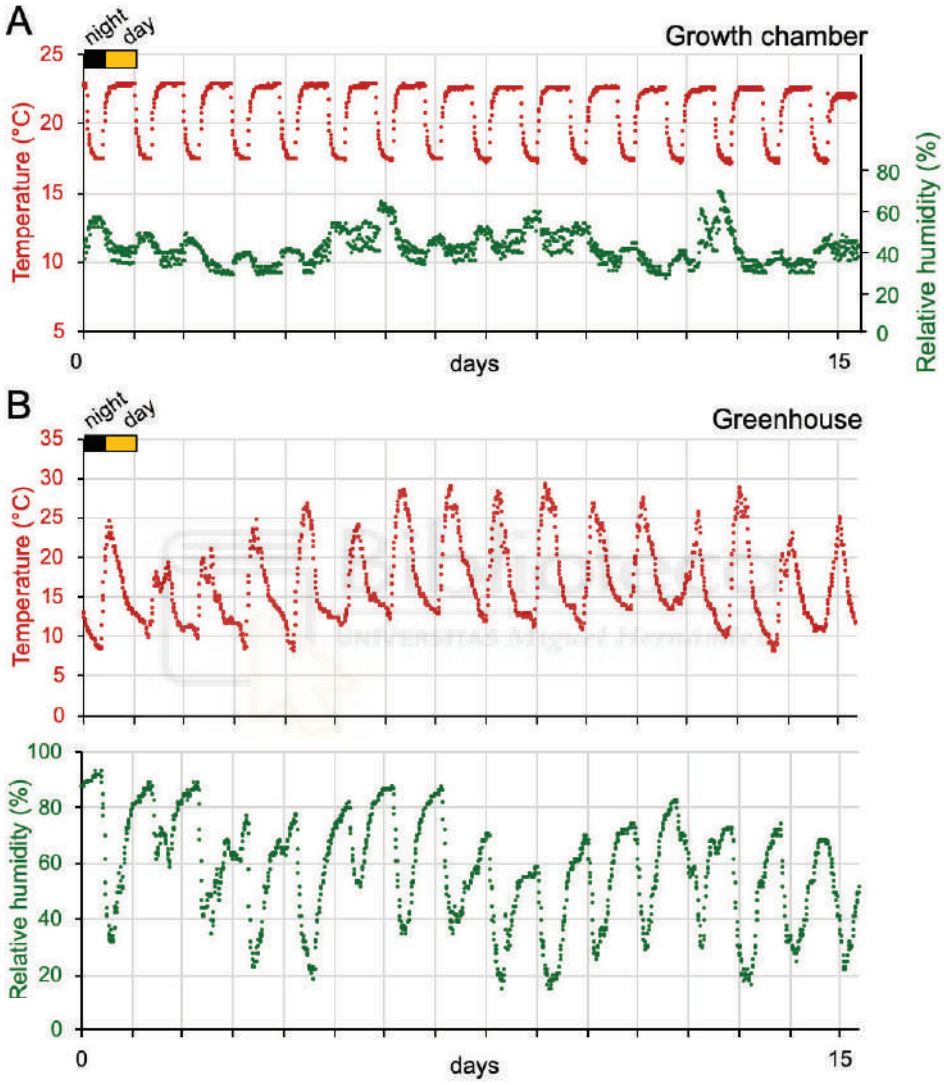

Supplementary Figure S1. Air temperature and relative humidity during the phenotype screening. (A) Growth chamber conditions. (B) Greenhouse conditions. A representative 15-days window is shown. Data points were taken every 15 min.

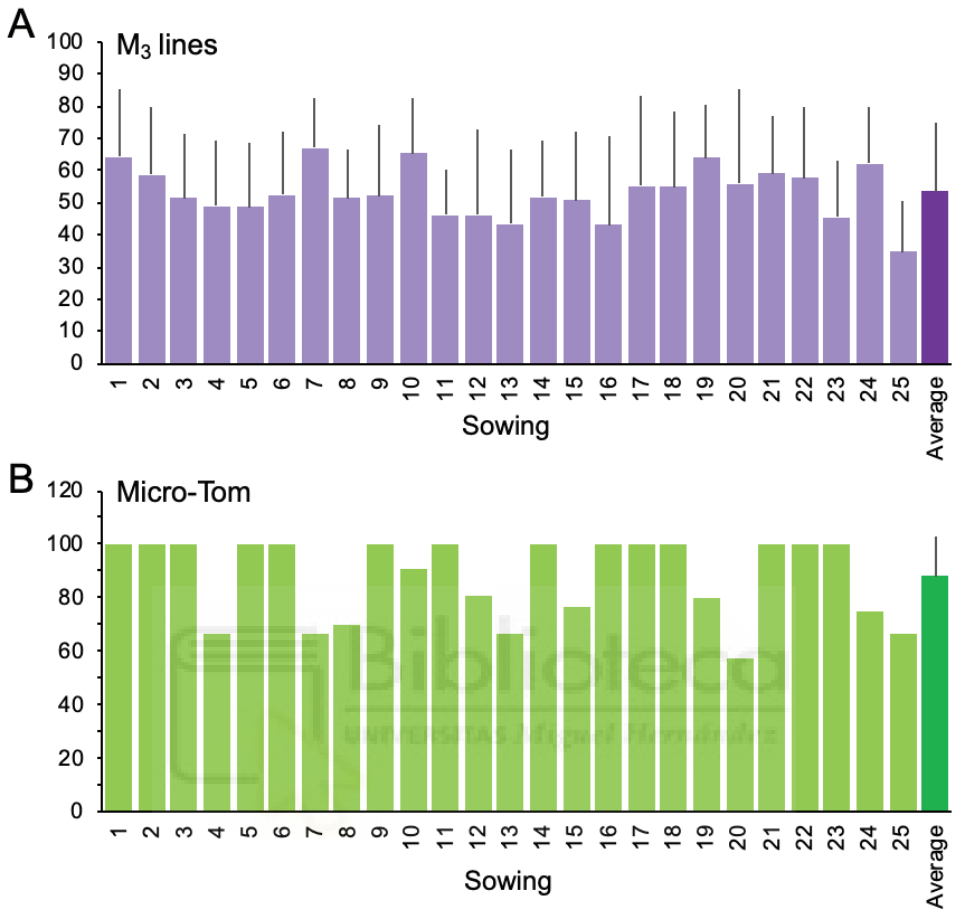

Supplementary Figure S2. Germination percentage for the studied lines. (A) M_3 lines. (B) Micro-Tom background used as a reference.

Supplementary Table S1. Tomato EMS lines studied in this work.

Sowing	Identification code [1]	n
01	P11G6, P11G7, P11G8, P11G9, P11G10, P11G11, P11G12, P11H1, P11H2, P11H3, P11H4, P11H5, P11H6, P11H7, P11H8, P11H9, **P11H10**, P11H11, P11H12	1
02	P12A1, P12A2, **P12A3**, P12A4, P12A5, P12A6, P12A7, P12A8, P12A9, P12A10, P12A11, P12A12, P12B1, P12B2, **P12B3**, P12B4, **P12B5**, P12B6, P12B7, P12B8	2
03	P12B9, P12B10, P12B11, P12B12, **P12C1**, P12C2, P12C3, P12C4, P12C5, P12C6, P12C7, P12C8, **P12C9**, P12C10, P12C11, P12C12, **P12D1**, P12D2, **P12D3**, P12D4	2
04	P13C12, P13D1, P13D2**, P13D3**, **P13D4**, P13D5, P13D6, P13D9, **P13D10**, P13D11, **P13D12**, P12E1, P12E2, **P12E3**, **P12E4**, P12E5, **P12E6**, P12E7, P12E8, **P12E9**	2
05	**P12E10**, **P12E11**, P12E12, P12F1, **P12F2**, P12F3, P12F4, **P12F5**, P12F6, **P12F7**, **P12F8**, P12F9, P12F10, **P12F11**, P12F12, **P12H1**, **P12H2**, P12H3, P12H4, P12H5	2
06	P12H6, P12H7, P12H8, **P12H9**, **P12H10**, P12H11, P12H12, P12G1, P12G2, **P12G3**, P12G4, **P12G6**, P12G7, P12G8, P12G9, **P12G10**, P12G11, P12G12	1
07	P14A1, P14A2, P14A3, **P14A4**, P14A5, P14A6, P14A7, P14A8, P14A9, P14A10, P14A11, P14A12, P14B1, P14B2, P14B3, P14B4	1
08	P14B5, **P14B6**, P14B7, **P14B8**, P14B10, P14B11, P14B12, P14C1, P14C2, P14C3, P14C4, P14C5, P14C6, P14C7, P14C8, P14C9	1
09	P14C10, P14C11, P14C12, **P14D1**, P14D2, **P14D3**, P14D4, P14D5, P14D6, P14D7, P14D8, P14D9, P14D10, P14D11	1
10	P14D12, P14E1, P14E2, P14E3, P14E4, P14E5, P14E6, P14E7, P14E8, P14E9, P14E10, P14E12, P14F1, P14F2, P14F3, P14F4, P14F5	1
11	P14F6, P14F7, P14F8, P14F9, P14F10, P14F11, P14F12, P14G1, P14G2, P14G3, P14G4, **P14G5**, P14G6, P14G8, **P14G9**, P14G10, P14G11	1
12	P14G12, P14H1, **P14H2**, **P14H3**, P14H4, P14H5, **P14H6**, P14H7, P14H8, P14H9, P14H10, P14H11, **P14H12**, P15A1, **P15A2**, P15A3, P14A4	1
13	P15A10, P15A11, **P15A12**, **P15B1**, **P15B2**, P15B3, P15B4, P15B5, **P15B6**, P15B7, P15B8, P15B9, P15B10, **P15B11**	1
14	P15B12, P15C1, **P15C2**, **P15C3**, **P15C4**, P15C5, **P15C6**, P15C7, P15C8, P15C9, P15C10, P15C11, P15C12, P15D1	1
15	P15D2, P15D3, **P15D4**, **P15D5**, P15D6, P15D7, P15D8, P15D9, **P15D10**, **P15D11**, P15D12, P15E1, P15E2, P15E3	1
16	P15E4, **P15E6**, P15E7, **P15E8**, **P15E9**, P15E10, P15E11, P15E12, **P15F1**, P15F2, P15F3, **P15F4**, **P15F5**, P15F6	1
17	P15F7, P15F8, P15F9, **P15F10**, **P15F11**, P15F12, P15G1, P15G2, P15G3, P15G4, P15G5, P15G6, **P15G7**, P15G8	1
18	P15G9, P15G10, **P15G11**, P15G12, **P15H1**, P15H2, P15H3, **P15H4**, **P15H5**, P15H6, P15H7, P15H8, P15H9, P15H10	1
19	**P15H11**, P16A1, P16A2, **P16A3**, P16A5, P16A6, **P16A7**, P16A8, P16A9, P16A10, P16A11, P16A12, P16B1, P16B3	1
20	P16B4, **P16B5**, P16B6, P16B7, P16B8, P16B9, P16B10, P16B11, **P16B12**, **P16C1**, **P16C2**, **P16C3**, P16C4, P16C5	1

	21	P16C6, P16C7, P16C8, P16C9, **P16C10**, P16C11, P16C12, P16D1, **P16D2**, P16D3, P16D4, P16D5, P16D6, P16D7	1
130	22	P16D8, P16D9, **P16D10**, P16D11, **P16D12**, P16E1, **P16E2**, **P16E3**, P16E4, P16E5, P16E6, **P16E7**, P16E8, P16E9	1
	23	P16E10, P16E11, P16E12, **P16F1**, **P16F2**, P16F3, P16F4, P16F7, **P16F8**, P16F9, **P16F10**, **P16F11**, P16F12, **P16G1**	1
	24	P16G3, P16G4, P16G5, P16G6, P16G7, P16G8, P16G9, P16G10, **P16G11**, **P16G12**, P16H1, P16H2, P16H3, P16H4	1
	25	P15A5, P15A6, P15A7, P15A8, P15A9, **P16H5**, **P16H6**, P16H7, P16H8, **P16H9**, P16H10, P16H11, **P16H12**	1

[1] M_3 lines with less than eight germinated seedlings (in bold) were not further studied (n = 95).

An Auxin-Mediated Regulatory Framework for Wound-Induced Adventitious Root Formation in Tomato Shoot Explants

Aurora Alaguero-Cordovilla, Instituto de Bioingeniería, Universidad Miguel Hernández, 03202 Elche, Spain, aalaguero@umh.es

Ana Belén Sánchez-García, Instituto de Bioingeniería, Universidad Miguel Hernández, 03202 Elche, Spain, ana.sanchezg@umh.es

Sergio Ibáñez, Instituto de Bioingeniería, Universidad Miguel Hernández, 03202 Elche, Spain, sibaez94@gmail.com

Alfonso Albacete, Instituto Murciano de Investigación y Desarrollo Agrario y Alimentario (IMIDA), 30150 La Alberca, Spain, alfonsoa.albacete@carm.es

Antonio Cano, Departamento de Biología Vegetal, Universidad de Murcia, 30100 Murcia, Spain, aclario@um.es

Manuel Acosta, Departamento de Biología Vegetal, Universidad de Murcia, 30100 Murcia, Spain, macosta@um.es

José Manuel Pérez-Pérez, Instituto de Bioingeniería, Universidad Miguel Hernández, 03202 Elche, Spain, jmperez@umh.es

Corresponding author: José Manuel Pérez-Pérez (jmperez@umh.es)

Running Head: Wound-induced AR formation in 'Micro-Tom'

Word count breakdown: Abstract, 184; Introduction, 769; Materials and Methods, 1824; Results, 4000; Discussion, 2031; References, 2744; Fig. Legends, 1330.

Figures: 9 **Supporting Information**: 5

ABSTRACT

Adventitious roots (ARs) are produced from non-root tissues in response to different environmental signals, such as abiotic stresses, or after wounding, in a complex developmental process that requires hormonal crosstalk. Here, we characterized AR formation in young seedlings of *Solanum lycopersicum* cv. 'Micro-Tom' after whole root excision by means of physiological, genetic and molecular approaches. We found that a regulated basipetal auxin transport from the shoot and local auxin biosynthesis triggered by wounding are both required for the re-establishment of internal auxin gradients within the vasculature. This promotes cell proliferation at the distal cambium near the wound in well-defined positions of the basal hypocotyl and during a narrow developmental window. In addition, a pre-established pattern of differential auxin responses along the apical-basal axis of the hypocotyl and an as of yet unknown cell-autonomous inhibitory pathway contribute to the temporal and spatial patterning of the newly formed ARs on isolated hypocotyl explants. Our work provides an experimental outline for the dissection of wound-induced AR formation in tomato, a species that is suitable for molecular identification of gene regulatory networks via forward and reverse genetics approaches.

KEYWORDS

Solanum lycopersicum, cell reprogramming, auxin biosynthesis, polar auxin transport, *de novo* root formation, auxin response, hormone regulation, mechanical damage, adventitious rooting, tissue regeneration.

INTRODUCTION

Adventitious roots (ARs) develop post-embryonically from non-root tissues, such as stems and leaves, usually in response to challenging environmental conditions; they may also be induced by mechanical damage or during *in vitro* tissue culture (Bellini *et al.*, 2014; Druege *et al.*, 2019; Gonin *et al.*, 2019). During normal development though, many plant species develop ARs to perform specialized functions, such as increasing soil foraging and water absorption (Mhimdi and Pérez-Pérez, 2020). AR formation involves several developmental stages (de Klerk *et al*., 1999), and the key regulatory events occurring during the induction phase result in the molecular reprogramming of some vascular-associated cells (Lakehal and Bellini, 2019). In Arabidopsis leaf explants, wounding induces jasmonic acid (JA) production that indirectly upregulates auxin biosynthesis in the whole leaf (Chen *et al.*, 2016; Zhang *et al.*, 2019). Auxin is then actively transported to the wounded site where it promotes the fate change from regeneration-competent cells to root founder cells in the vasculature through *WUSCHEL-RELATED HOMEOBOX 11* (*WOX11*) expression (Liu *et al.*, 2014). In turn, WOX11 (and the partially redundant WOX12) along with other auxin responsive factors, upregulate the expression of *WOX5* and *LATERAL ORGAN BOUNDARIES DOMAIN 16* (*LBD16*), which trigger the development of the AR primordia (Hu and Xu 2016).

The rooting of stem cuttings is a common vegetative propagation practice in many ornamental plants. Petunia (*Petunia* × *hybrida*) has been proposed as an adequate experimental system to analyze the relationship between plant hormones and excision-induced AR formation in stem cuttings (Druege *et al.*, 2016; Druege and Franken, 2019). Upon excision, wounding triggers the early accumulation of JA and ethylene in the stem base, while subsequent accumulation of the active auxin, indole-3-acetic acid (IAA), in the basal end of the cutting is dependent on the pre-established polar auxin transport from

the shoot (Ahkami *et al.*, 2013; 2014; Druege *et al.*, 2014; Lischweski *et al.*, 2015). Additional studies in this species have contributed to the understanding of the effects of the nutritional status of whole cuttings on AR formation (Ahkami *et al.*, 2009; Klopotek *et al.*, 2016), as well as the specialized functions of specific nutrients, such as nitrogen (Zerche *et al.*, 2016; Yang *et al.*, 2019) and iron (Hilo *et al.*, 2017). However, the lack of functional genomics tools complicates the identification of the molecular players involved in AR initiation in these and other non-model crops.

Among the Solanaceae, cultivated tomato (*Solanum lycopersicum* L.) has been used as a model species for research in genetics, fruit development and biotic and abiotic stress resistance (Rothan *et al.*, 2016, 2019). Soil flooding induces AR formation in tomato hypocotyls via crosstalk between ethylene signaling and polar auxin transport regulation (Negi *et al.*, 2010; Vidoz *et al.*, 2010). The AR overproducing phenotype of the *aerial roots* (*aer*) tomato mutant seems strictly linked to an altered distribution of active auxin along the stem because of auxin transport deregulation, but the causal mutation is still unknown (Mignolli *et al.*, 2017). The key role of polar auxin transport during adventitious rooting was established in *Arabidopsis thaliana* early through physiological studies (Ludwig-Müller *et al.*, 2005), and was later confirmed by the study of mutants affected in efflux carrier proteins of the ATP-binding cassette (ABC) and PIN-FORMED (PIN) families (Della Rovere *et al.*, 2013; Sukumar *et al.*, 2013). In these and other studies, the wound-induced signal subsequently modulated auxin content by affecting the expression of auxin biosynthesis and polar auxin transport genes, thereby stimulating AR induction (Huang *et al*., 2020). However, a systematic analysis of the factors that regulate wound-induced AR formation in tomato is missing. Due to its small size and short life cycle, the ‘Micro-Tom’ cultivar has been proposed as a model for functional genomics in this species (Emmanuel and Levy, 2002). Since then, a wealth of genetic resources has been developed for this tomato cultivar (Kobayashi *et al.*, 2014; Shikata *et*

al., 2016). Therefore, we chose the 'Micro-Tom' cultivar to investigate the relative contribution of polar auxin transport from the shoot and of local auxin biosynthesis during wound-induced AR formation. Our results showed that wound-induced AR formation in 'Micro-Tom' hypocotyls occurred *de novo* through auxin-mediated activation of specialized cambial cells. We provide strong evidence that both regulated polar auxin transport from the shoot and local auxin biosynthesis near the wounded site cooperatively contribute to the build-up of endogenous auxin response gradients in a stereotyped pattern that, in turn, negatively regulates some Aux/IAA genes, such as *ENTIRE* (also known as *SlIAA9*). We also found that local auxin biosynthesis could partially overcome the requirement for shoot-derived auxin during AR formation; hence, a functional root system could be obtained from a hypocotyl explant.

MATERIALS AND METHODS

Plant material and growth conditions

Seeds of cultivated tomato (*Solanum lycopersicum* L.) lines (Supplementary Table S1) were obtained from the C.M. Rick Tomato Genetics Resource Center (http://tgrc.ucdavis.edu/). The tomato cultivar 'Micro-Tom', the *DR5::GUS* line and the near-isogenic lines (NILs) used in this study have been described previously (Supplementary Table S1). Seeds were surface-sterilized in 2% (w/v) NaClO for 10 min and rinsed thoroughly with sterile distilled water (four times). Seeds were then transferred to wet chambers at 28 °C in a dark growth cabinet for 96 h. Germinated seedlings with primary roots > 4 mm (0 days after sowing) were transferred to 65 × 120 mm (diameter × height) glass jars containing 75 mL of sterile one-half-Murashige and Skoog basal salt medium (Duchefa Biochemie, The Netherlands), 20 g L^{-1} sucrose (Duchefa Biochemie), 2.5 g L^{-1} Gelrite (Duchefa Biochemie), 0.5 g L^{-1} 2-(N-morpholino) ethanesulfonic acid (Duchefa Biochemie), and 2 mL L^{-1} Gamborg B5 vitamin solution (Duchefa Biochemie), at pH 5.8. Glass jars were transferred to a growth cabinet during 16 h light (average photosynthetic photon flux density of 50 µmol m^{-2} s^{-1}) at 26 ± 1 °C, and 8 h darkness at 23 ± 1 °C. The formation of ARs was then induced by removing with a sharp scalpel the whole root system 2–3 mm above the hypocotyl-root junction of young tomato seedlings at the 100–101 growth stages (fully expanded cotyledons and first leaf ~0.5 cm; Feller *et al.*, 1995) [0 days after whole root excision; 0 dae]. The shoot explants were transferred to new glass jars with 75 mL of the standard growing medium (SGM) described above. Each jar contained six or seven seedlings of the same genotype and/or treatment. All experiments were performed in duplicate with a minimum of six biological replicates.

Macroscopic studies of wound-induced AR formation

Shoot explants or hypocotyl explants (obtained by sectioning shoot explants just below the cotyledons) were incubated for 21 days in SGM glass jars supplemented with 0.25 µM 1-naphthalene acetic acid (NAA, Duchefa Biochemie). In another experiment, a 10-µL 0.5% (w/v) agarose drop with 0.25 µM NAA was applied directly to the distal (apical) end of the hypocotyl explants. To evaluate the effect of the chemical inhibition of polar auxin transport, we performed three experiments using shoot explants (Feller's stages 100–101). In the first experiment, the explants were incubated for 21 days in SGM glass jars supplemented with either 40 µM 2-naphthoxyacetic acid (2-NOA; Sigma-Aldrich, St. Louis, MO, USA; Lanková *et al*., 2010), or 40 µM N-1-naphthylphthalamic acid (NPA; Sigma-Aldrich; Vidoz *et al.*, 2010). In the second experiment, a lanolin ring containing mock, 40 µM 2-NOA or 40 µM NPA was applied directly below the cotyledons of the explants. In the third experiment, a 10-µL 0.5% (w/v) agarose drop with 40 µM NPA was applied directly to the cotyledons. For gravitropism studies, shoot explants or hypocotyl explants grown on SGM were transferred to the growth chamber and reoriented relative to gravity by 0° or 180° for measuring several AR traits, as described below. Hypocotyl explants were excised into two or three fragments. These explants were then transferred to vertically oriented glass jars with 75 mL of SGM supplemented with 0 (mock) or 0.01 µM NAA, as well as with 50 µM yucasin DF (YDF) for auxin biosynthesis inhibition (Tsugafune *et al*., 2017).

In all these cases, ARs arising from the hypocotyl were visually scored and periodically annotated during 21 dae. AR emergence was estimated based on the day before the annotation of the first AR. Maximum AR length, hypocotyl length and maximum shoot length were measured at 21 dae, unless otherwise indicated; the length of the hypocotyl with emerged ARs was also measured. To study wound-induced AR formation in older tomato seedlings, explants

from the hypocotyl, the first node or the apex were obtained from 16-day-old seedlings (Feller's stages 102−103).

Phytohormone extraction and analysis

Three biological replicates, each consisting of hypocotyl thin sections (~5 mm long) of several shoot explants, were collected from apical and basal ends of the shoot explants at 0, 1 and 3 dae. The shoot apical distal ends (including the meristem and the emerging leaves) and the cotyledons were also harvested at 3 dae. Phytohormones were extracted from frozen tissues and analyzed according to Großkinsky *et al.* (2014) and Villacorta-Martín *et al.* (2015). Auxin metabolites were identified according to their exact molecular masses and retention times as determined from total ion chromatograms generated by U-HPLC-HRMS (Accela-Exactive, ThermoFisher Scientific, Waltham, MA, USA) analysis.

Light and laser confocal scanning microscopy

Five-millimeter basal sections from shoot explants were obtained at different time points during adventitious rooting. Samples were fixed in a paraformaldehyde/Triton solution (1.85% volume/volume formaldehyde, 45% ethanol, 5% acetic acid, and 1% Triton X-100) for 3 days at 4 °C. The fixed tissue was rinsed three times in 0.1 M sodium phosphate buffer (pH 7.2) before dehydration in a graded ethanol series (50%, 70%, 90%, and 96% ethanol, 30 min each). Dehydrated samples were then embedded in Technovit 7100 resin (Heraeus Kulzer GmbH, Germany) according to the manufacturer's instructions with slight modifications, as follows. Samples were immersed in the pre-infiltration solution (50% resin and 50% ethanol) for 2.5 h. The stem cutting samples remained for 4 h in the infiltration solution under a light vacuum at 25 °C and polymerized for 20 h at 4 °C. Thin sections

of 7 μm thickness were cut using a tungsten microtome knife (MICROM International GmbH, Germany) on an HS 350 S rotary microtome (MICROM International GmbH). Sections were stained either with 0.05% weight/volume (w/v) toluidine blue (Sigma-Aldrich) or 0.05% w/v ruthenium red (Sigma-Aldrich) in water and mounted in Eukitt (Chem-Lab NV, Belgium). Samples were observed using a bright-field Motic BA210 microscope (Motic Spain, Spain) and selected images were captured with a built-in Moticam 580INT documentation station (Motic Spain) and processed with GIMP 2.10.12 (GIMP Development Team, http://www.gimp.org). For GUS staining, whole hypocotyl sections from shoot explants at 0, 1 and 3 dae were incubated at 37 °C for 24 h in multiwell plates in the presence of the GUS staining solution and processed as described by Bustillo-Avendaño *et al*. (2018).

For laser scanning confocal microscopy (LCSM), a razor blade was used to make cuts of ~400 μm thickness on a Petri dish containing ice-cold 0.1 M sodium phosphate buffer (pH 7.2), and then the cuts were fixed with 4% w/v paraformaldehyde, which was dissolved in 0.1 M sodium phosphate buffer (pH 7.2). The fixed tissue was rinsed three times with 0.1 M sodium phosphate buffer and immersed in ClearSee solution (Kurihara *et al.*, 2015). Before LCSM visualization, cleared samples were stained with 0.5% w/v calcofluor white on ClearSee solution for 2 h and then rinsed three times with ClearSee solution. Excitation of calcofluor white was achieved by using the 405 nm wavelength diode, while the fluorescence emission was collected between 425 and 475 nm. Images of the vascular bundles were taken at different regions of the Z-position of the sample and cambium cells were counted on each bundle.

Immunolocalization of IAA

The basal region of shoot explants was manually sectioned with a razor blade and immediately fixed in freshly prepared 3% 1-ethyl-3-(dimethylaminopropyl)-carbodiimide hydrochloride (EDAC) (Sigma-Aldrich) in 1× PBS containing 0.1% Triton X-100 (PBS-T) for 1 h on ice. The sample sections were post-fixed for 1–2 h in 4% paraformaldehyde in PBS-T and washed three times in PBS-T for 5 min. The sample sections were then dehydrated and rehydrated with 30%, 50%, 70%, 100%, 70%, 50%, and 30% methanol in PBS-T (5 min each step) and incubated with 2% cellulase Onozuka R-10 (Duchefa Biochemie) for 30 min at 25 °C. After washing as above, sections were incubated overnight at 4 °C with a 1:100 dilution of the anti-IAA-C-monoclonal antibody (A0855; Sigma-Aldrich) in PBS-T. The sections were then rinsed three times for 10 min with PBS-T. Samples were incubated with 1:200 dilution of Alexa Fluor 647-conjugated donkey anti-mouse IgG (ThermoFisher Scientific) antibody for 2 h at 25 °C. The prepared samples were observed with LCSM as described elsewhere (Bustillo-Avendaño *et al*., 2018).

RNA isolation and first-strand cDNA synthesis

Total RNA from ~100 mg of powdered tomato hypocotyls from 3–6 seedlings at 0, 1 and 4 days after whole root excision was extracted in triplicate using the Spectrum Plant Total RNA Kit (Sigma-Aldrich). Contaminating genomic DNA was removed via incubation for 20 min at 37 °C with 4 units of DNase I (Thermo Fisher Scientific, Waltham, MA, USA). After DNase I inactivation at 70 °C for 15 min, RNA was used directly for downstream applications. First strand cDNA was synthesized with 1 µg of purified RNA using SuperScript IV Reverse Transcriptase (Thermo Fisher

Scientific), along with Oligo(dT)18 primers. The resulting cDNA was diluted by adding 40 µL of sterile distilled water, reaching a final volume of 60 µL.

Gene expression analysis by real-time quantitative PCR

Primers amplified 93–324 base pairs of the cDNA sequences (Supplementary Table S2). To avoid amplifying genomic DNA, forward and reverse primers were designed to bound to different exons and to hybridize across consecutive exons. For real-time quantitative PCR, 14 µL reactions were prepared with 7 µL of SsoAdvanced Universal SYBR Green Supermix (Bio-Rad, Hercules, CA; USA), 4 µM of specific primer pairs (5 µM each), 1 µL of cDNA, and 2 µL of DNase-free water. PCR amplifications were carried out in 96-well optical reaction plates on a Step One Plus Real-Time PCR System (Thermo Fisher Scientific). Three biological and two technical replicates were performed for each gene. The thermal cycling program started with a step of 10 s at 95 °C, followed by 40 cycles (15 s at 95 °C and 60 s at 60 °C), and the melt curve (from 60 to 95 °C, with increments of 0.3 °C every 5 s). The dissociation kinetics of the amplified products confirmed their specificity. Primer validation was performed by the absolute quantification method (Lu *et al.*, 2012) using a standard curve that comprised equal amounts from each cDNA sample. Gene expression analyses were carried out using the $2^{-\Delta\Delta Ct}$ method (Livak and Schmittgen, 2001). The housekeeping *SlACTIN2* (Solyc03g078400) gene was chosen to ensure reproducibility (Dekkers *et al.*, 2012; Expósito-Rodríguez *et al.*, 2008). For each gene, the mean fold-change values relative to the basal part of 'Micro-Tom' hypocotyls at 0 dae were used for graphical representation.

Statistical analyses

Descriptive statistics (e.g., average, standard deviation [SD], median, maximum, and minimum) were calculated using StatGraphics Centurion XV software (StatPoint Technologies, Inc. Warrenton, VA, USA) and SPSS 21.0.0 (SPSS Inc., Chicago, IL, USA). Data outliers were identified based on the Grubbs' test and excluded for posterior analyses as described elsewhere (Grubbs, 1969). One-sample Kolmogorov–Smirnov tests were performed to analyze the goodness-of-fit between the distribution of the data and a theoretical normal distribution. We performed multiple testing analyses using the ANOVA F-test or Fisher's least significant difference (LSD) methods (p-value < 0.01, unless otherwise indicated). Non-parametric tests (Student t, Mann-Whitney or Kolmogorov-Smirnov) were used when necessary (i.e., AR emergence and AR number).

RESULTS

Environmental dependence of wound-induced AR formation in tomato shoot explants

When whole-root excised shoot explants of the 'Micro-Tom' cultivar were grown under different light regimes, ARs emerged significantly earlier (p-value=0.000) in continuous light than in the 16/8 h light/dark photoperiod or in continuous darkness, but rooting capacity at 14 dae was higher under standard 16/8 h light/dark conditions (Supplementary Fig. S1A). We found significant differences (p-value=0.000) in the rooting capacity of shoot explants at 10 days after whole-root excision (10 dae), with the highest values obtained in standard 16/8 h light/dark conditions (Supplementary Fig. S1B, C). We did not find significant differences (p-value=0.123) in any of the studied parameters with regard to the gelling agent concentration

(Supplementary Fig. S1D-F), and a slight decrease in AR emergence and rooting capacity at 14 dae without sucrose (Supplementary Fig. S1G-I). Hence, we selected 16/8 h light/dark, 2% sucrose and 0.25% w/v Gelrite as the standard conditions to study wound-induced AR formation in 'Micro-Tom' shoot explants.

Cellular changes in the distal cambium anticipate the initiation of wound-induced Ars

To understand the cellular events leading to wound-induced AR formation in 'Micro-Tom' shoot explants, we studied transverse sections of the basal region of the hypocotyl between 0 and 4 dae (Fig. 1). Before wounding (0 dae), the hypocotyl contained four vascular bundles, which were orthogonally arranged (Fig. 1A, 0 dae). Each vascular bundle was radially composed of external phloem tissue, several layers (3–5) of isodiametric cambial cells and internal xylem vessels (Fig. 1A, 0 dae). Despite the clear discontinuity of the xylem, phloem tissues and cambial cells were also observed between the vascular bundles (Fig. 1A, 0 dae). AR primordia within the hypocotyl were visualized by *DR5::GUS* marker expression (Welander *et al.*, 2014). We found one preformed AR primordia in the most basal region of the 'Micro-Tom' shoot explants before whole root excision, and this number significantly increased afterwards (Fig. 1B, C). Interestingly, the newly formed AR primordia were regularly spaced along the apical-basal axis of the hypocotyl within a narrow region and at a certain distance from the wounded tissue (Fig. 1C, 3 dae). The earliest morphological event related to AR initiation [i.e., initiation phase (de Klerk *et al*., 1999)] occurred at 2 dae, when small clusters of dividing cells located at the edge of the vascular bundles were observed (Fig. 1A, 2 dae). These cells seemed to originate from the cambial rows facing towards the phloem (i.e., distal cambium). Even at these early stages, we confirmed that these presumptive AR initiation foci

expressed the auxin-responsive *DR5::GUS* marker at higher levels in the distal tip of the primordium (Fig. 1D, 2 dae), when some root-like internal anatomy was observed, such as the lateral root cap and the vascular initials (Fig. 1A, dotted section in 2 dae). These AR primordia eventually grew over the bundle sheath cells (Fig. 1D, 3 dae) and through the cortex [i.e., expression phase (de Klerk *et al*., 1999)], with an organized internal structure that fully resembled a mature root meristem, which later emerged through the epidermis (Fig. 1A, 4 dae). At this point, the internal vasculature of the ARs was connected to the xylem vessels of the hypocotyl bundles, and the continuity of the cambium was maintained through the pericycle cells of the emerging ARs (Fig. 1A, 4 dae).

Auxin is required for AR induction in the hypocotyl upon wounding

Auxin, which is routinely used to induce ARs in stem cuttings when applied exogenously (Druege *et al.*, 2019), is a well-known endogenous player of AR formation in several species (Pacurar *et al.*, 2014), including the 'Micro-Tom' tomato cultivar (Guan *et al.*, 2019). We detected endogenous IAA in some vascular cells near the xylem in the basal region of the explant at 2 dae by immunolocalization (Fig. 1E, white arrow). We measured the concentration of IAA in both the apical and basal regions of the shoot explants during AR formation by HPLC-MS (Fig. 1F). IAA levels were similarly partitioned between the apical- and basal-half of the hypocotyl before wounding (Fig. 1G, 0 dae). Between 1 and 2 dae, IAA levels were much higher in the basal-half of the hypocotyl than in its apical region (Fig. 1G), which is indicative of the generation of an internal auxin gradient within the hypocotyl after whole root excision. Interestingly, at 4 dae, and consistent with the expression phase of AR formation (see above), the internal auxin levels were similar in the apical-derived and basal-derived regions of the hypocotyl (Fig. 1G).

To confirm the functional relevance of the endogenous IAA gradient observed in the basal region of the hypocotyl at 1 dae, we studied the expression of two Aux/IAA genes, *SlIAA11* and *SlIAA12* (Supplementary Fig. S2A, D), which are known to be upregulated by auxin in tomato (Audran-Delalande *et al.*, 2012). *SlIAA11* and *SlIAA12* genes were differentially upregulated in the basal region of the hypocotyl at 1 dae (p-value=0.000; Fig.1H), mirroring the high IAA levels (Fig. 1G) and *DR5::GUS* expression in this region at 1 dae (Fig. 1C). In Arabidopsis leaf explants, wounding indirectly upregulates several *YUCCA* (*YUC*) genes involved in IAA biosynthesis in the whole mesophyll, which then enhances rooting by increasing auxin levels near the wounding via polar auxin transport (Chen *et al.*, 2016). Hence, we studied the expression of some auxin biosynthesis genes, such as *SlTAR2a* and *SlYUC2/6* (Supplementary Fig. S2B, C, E, F), in shoot explants during rooting, and we found a slight increase (p-value=0.000) in *SlYUC2/6* expression at 1 dae as compared to their steady-state levels at 0 dae (Fig. 1I).

To determine the relevance of the endogenous auxin source for AR formation, we studied hypocotyl explants obtained by sectioning shoot explants just below the cotyledons. These hypocotyl explants lacked the IAA supply from the shoot apex and showed a significant delay (p-value=0.015) in AR emergence (8.3 ± 5.7 dae) in comparison with shoot explants with an intact auxin source (Fig. 2A). As a result, the rooting capacity at 14 dae was much lower (p-value=0.000) in hypocotyl explants than that in shoot explants (Fig. 2B). We observed that incubation of the explants with 0.25 μM NAA (NAA_m) induced abundant tissue over proliferation (i.e., callus-like growth) at the basal end of the explants, even in the absence of the shoot apex (Fig. 2C, D). Therefore, AR emergence was severely delayed (~3 dae) by NAA_m treatment in shoot and hypocotyl explants (Fig. 2A). The NAA_m treatment significantly increased (p-value=0.024) rooting capacity in shoot explants at 14 dae by about 3-fold (Fig. 2B, C), but the emerging ARs were significantly

shorter (p-value=0.000; Fig. 2E). The basal region of the hypocotyl that produced ARs (hereinafter referred to as the AR formative region) enlarged upward by the NAA_m treatment in both cases (Fig. 2F). To discard local inhibitory effects caused by high NAA concentration at the basal end of the explants, we directly applied 0.25 µM NAA on the distal end of the hypocotyl explants (NAA_d), which might then be actively transported to the proximal region near the wound (Hošek *et al.*, 2012). Accordingly, the AR emergence delay caused by the excision of the shoot apex was fully rescued by the non-cell-autonomous NAA_d treatment (Fig. 2A) and their rooting capacity was also enhanced with respect to that of the hypocotyl explants without NAA (Fig. 2B, C).

Auxin transport inhibition primarily affects wound-induced AR formation

Our results suggest that auxin from the distal shoot is required for AR formation in the proximal (basal) hypocotyl region near the wound. To evaluate the role of basipetal auxin transport through the wounded hypocotyl, we applied 2-NOA or NPA, which respectively inhibit auxin influx (Lanková *et al.*, 2010) or auxin efflux (Teale and Palme, 2018). AR emergence was completely blocked in shoot explants treated with NPA in the medium (NPA_m) and there was a significant delay (p-value=0.000) in AR emergence in samples treated with 2-NOA_m (12.3 ± 3.0 dae) with respect to the mock-treated samples (4.8 ± 0.7 dae; Fig. 3A). Shoot explants treated with 2-NOA (2-NOA_m) displayed profuse tissue proliferation (i.e., callus-like growth; Fig. 3B, C) in their basal region, with numerous AR primordia that were unable to grow (Fig. 3C, E). Remarkably, 2-NOA_m-treated shoot explants mirrored the NAA (0.25 µM) effect observed previously, with the only difference being an increased AR number on the latter (Fig. 2C). Furthermore, there was

no sign of tissue proliferation on the hypocotyl of NPA_m-treated shoot explants, and their shoot growth was also severely delayed (Fig. 3C).

To evaluate whether the local inhibition of auxin transport affected wound-induced AR formation, we applied a lanolin collar of 2-NOA (2-NOA_c) or NPA (NPA_c) just below the cotyledons. We found that 2-NOA_c or NPA_c produced a mild but statistically significant delay (p-value=0.013) in AR initiation as compared with the control treatment (Fig. 3A). Therefore, the rooting capacity was significantly reduced (p-value=0.003) with regard to the control treatment, and these differences were higher in the NPA_c-treated samples (Fig. 3D). In turn, the ARs produced from the NPA_c-treated shoot explants were shorter than in $mock_c$- or 2-NOA_c-treated ones at 21 dae (Fig. 3E). Interestingly, the length of the AR formative region was slightly increased in 2-$NOA_{c,\ m}$-treated shoot explants (Fig. 3F). We next evaluated wound-induced AR formation in the *diageotropica* mutant, which was defective on a cyclophilin protein putatively required for auxin efflux regulation (Oh *et al.*, 2006; Ivanchenko *et al.*, 2015). AR emergence was delayed in the *diageotropica* shoot explants with regard to its 'Micro-Tom' background, which also showed reduced rooting capacity at 14 dae (Fig. 3G), mirroring the mild effects caused by inhibiting polar auxin transport through the hypocotyl with local NPA application (NPA_c; see above).

Wound-induced AR initiation is independent of gravitropism

Shoot or hypocotyl explants in vertically oriented jars or reoriented by 180° relative to the gravity vector (Fig. 4A) showed non-significant differences (p-value=0.748) in their wound-induced AR emergence (Fig. 4B) or in their rooting capacity at 14 dae (Fig. 4C). In addition, we did not find significant differences in AR lengths (p-value=0.075) among the four conditions tested (Fig. 4D). In Arabidopsis, auxin accumulates at the lower side of hypocotyls during gravity stimulation, ultimately leading to

asymmetric growth and organ bending (Su *et al.*, 2017). We did not observe bending of 'Micro-Tom' hypocotyls (measured below the cotyledons) but we found bending against the gravity vector of the newly produced shoots (Fig. 4E). The angle of emerging ARs relative to the hypocotyl was similar in the four experiments, although the growing roots later reoriented their growth towards the gravity vector (Fig. 4E). Intriguingly, we found that although vertically oriented shoot explants hardly produced additional ARs from 14 dae onwards, the shoot explants that were reoriented by 180° produced ~1.5-fold more ARs at 21 dae. This increase in AR numbers in reoriented shoot explants might be caused by the AR formative region expanding upward (Fig. 4F).

Endogenous IAA produced both in the shoot and the cotyledons are required for wound-induced AR emergence

In stem cuttings of different species, the auxin produced in mature leaves accumulates in the stem region above the wound and triggers AR formation within the vasculature (Druege *et al*., 2019). In 'Micro-Tom' shoot explants, both the shoot apex and the cotyledons might act as a direct source for the auxin required for wound-induced AR formation. Hence, we performed a series of experiments to address this hypothesis (Fig. 5A). Hypocotyl explants showed a significant delay (p-value=0.000) in AR emergence (7.8 ± 3.7 dae; Fig. 5B) as compared to that of shoot explants that included both the shoot apex and the cotyledons (4.6 ± 0.5 dae; Fig. 5B). We did not find significant differences in AR emergence between explants with deletions of either the shoot apex, or the shoot apex and one cotyledon, or both cotyledons but retaining the shoot apex (Fig. 5A-B), suggesting that the auxin signal required for wound-induced AR emergence was produced both in the cotyledons and in the shoot apex.

We observed striking differences in the rooting capacity for the assayed conditions. On the one hand, we did not find significant differences (p-value=0.172) in rooting capacity at 14 dae between shoot, 1-cotyledon, and 1-leaf explants (Fig. 5C). The 2-cotyledon explants (without the shoot apex) produced a significant increase (p-value=0.004) in rooting capacity at 14 dae (Fig. 5C, D), with ~1.5 more ARs at 21 dae on average than whole shoot explants containing both cotyledons and the shoot apex. However, hypocotyl explants showed a significant decrease (p-value=0.000) in their rooting capacity (1.7 ± 0.6 ARs at 14 dae; Fig. 5C, D). These results suggested that the cotyledons were the major source of auxin required for wound-induced AR emergence and that the shoot apex acted both as a source and a sink for auxin. To confirm this hypothesis, we locally applied the auxin efflux inhibitor NPA on cotyledons (referred to as shoot NPA_{cot} explants), which resulted in a significant reduction (p-value=0.000) in the rooting capacity of the shoot explants at 14 dae (2.0 ± 0.6 ARs at 14 dae; Fig. 5C, D), mirroring the results found on the hypocotyl explants (see above). We measured the endogenous levels of the active auxin (IAA) and of the inactive form of IAA conjugated to aspartic acid (IAA-Asp) in the shoot apex and the cotyledons of shoot explants at 3 dae, confirming a higher ratio of IAA to IAA-Asp in the cotyledons than in the shoot apex (Fig. 5E).

Intriguingly, AR emergence was not significantly altered (p-value=0.471) in the shoot NPA_{cot} explants, suggesting that auxin from the shoot apex was sufficient to trigger AR initiation. Following the differences in AR emergence described earlier, the shortest AR length was observed in hypocotyl explants (Fig. 5F). In addition, the size of the AR formative region in the basal hypocotyl was a direct read-out of endogenous auxin levels, as this domain was significantly expanded (p-value=0.00) upwards in explants without the shoot apex (Fig. 5G).

A pre-established auxin response gradient within the hypocotyl supports wound-induced AR development

Our results thus far suggested that auxin levels within the hypocotyl were dynamically established by basipetal auxin transport from the shoot apex and cotyledons. However, in the absence of this endogenous auxin source, the hypocotyl explants were able to develop a few ARs, which might have been non-cell autonomously induced by the residual auxin within the explant or by an unknown cell-autonomous signal. We dissected the hypocotyl explants in three fragments (apical, central, and basal) of similar lengths (2.6 ± 0.7 mm; Fig. 6A). The central explants displayed an intermediate AR emergence response (6.8 ± 5.8 dae) compared to those of the apical-derived explants or of the basal-derived explants (Fig. 6B, solid lines). Consistent with these results, we found significant differences (p-value=0.000) in the rooting capacity of the explants according to their initial position along the apical-basal axis of the hypocotyl, with the highest rooting capacity observed in the basal-derived explants (3.4 ± 0.8 ARs at 14 dae; Fig. 6C, D). Indeed, the differences found in AR lengths at 21 dae between the different explants (Fig. 6E) might be explained by the earliest AR emergence observed in the basal-derived explants. The size of the AR formative region was slightly expanded upwards (p-value=0.056) according to the explant position along the apical-basal axis (Fig. 6F). The observed differences in AR formation might be caused by differences in endogenous auxin levels or in auxin responses of the explants along the apical-basal axis. Next, we assayed the sensitivity of the different hypocotyl regions to the exogenously applied synthetic auxin NAA. Exogenously applied NAA induced callus-like growth in the proximal (basal) end of the explants at similar levels, regardless of their position within the intact hypocotyl (Fig. 6G). AR emergence was significantly enhanced (p-value=0.002) by NAA only in the apical-derived explants (Fig. 6B, dotted

lines). However, NAA application did not significantly increase the rooting capacity of the explants (Fig. 6C).

To discard the possibility that the observed differences in explants along the apical-basal axis were mirroring the circulating IAA levels at the time of excision, we studied AR formation in explants obtained from sectioning hypocotyls in two fragments of different lengths (Fig. 7A). AR emergence was significantly delayed (p-value=0.000) in all three apical-derived explants (11.6 ± 6.2 dae; Fig. 7B, apical) as compared with those of the basal-derived explants (2.0 ± 0.9 dae; Fig. 7B, basal), which occurred irrespective of their length in all cases (p-value=0.982). Interestingly, incubation of apical-derived explants with NAA almost fully complemented their AR emergence delay (5.0 ± 0.7 dae; Fig. 7B, apical), while it slightly delayed the AR emergence of the basal-derived explants (2.8 ± 0.8 dae; Fig. 7B, basal). However, rooting capacity at 14 dae was only significantly higher in the basal-derived explants (p-value=0.000) irrespective of their length (p-value=0.117; Fig. 7C). Callus-like tissue formation at the proximal (basal) end of the explants in response to NAA incubation depended on their apical-basal polarity with respect to the intact hypocotyls (see above). Indeed, only the apical-derived explants containing a large portion of the hypocotyl (C3_DBC) displayed higher levels of callus-like formation in response to exogenously applied NAA (p-value=0.000; Fig. 7D). Additionally, NAA-treatment increased callus-like formation in all basal-derived explants (i.e., containing the A region of the hypocotyl; Fig. 7D). These results support the hypothesis of an endogenous pre-established auxin response gradient within the hypocotyl before wounding, with higher auxin responses at the proximal (basal) end of the hypocotyl that determine wound-induced AR formation in response to endogenous auxin levels.

To assess whether auxin biosynthesis was locally activated by the wounding signal prior to AR formation in these explants, we studied the expression of several auxin biosynthesis genes in the apical (D, B) and basal

(C, A) regions of the C2_DC and C2_BA explants (Fig. 7A). We found that *SlTAR2a* and *SlTAR2b* expression was significantly enhanced (p-value=0.000) in the basal region of the explants at 2 dae (Fig. 7E). In addition, *SlYUC2/6* expression was slightly induced at the basal region of the explants both before wounding and at 2 dae (Fig. 7E). We then evaluated the functionality of the endogenous auxin response gradient of the explants by studying Aux/IAA gene expression. *SlIAA11* and *SlIAA12* expression at 2 dae was significantly increased (p-value=0.000) in the basal region with respect to that of the basal region (Fig. 7F), mirroring the observed increase in auxin biosynthesis gene expression after wounding. Interestingly, while no expression gradient along the apical-basal axis was observed for these genes at 0 dae, a higher expression of *SlIAA11* and *SlIAA12* was found in the basal (C, A) region of the explants with respect to that of the apical (D, B) region (Fig. 7F). These results suggested that, in 'Micro-Tom' hypocotyl explants, wounding acts locally to enhance auxin levels through the specific upregulation of *SlTAR2* genes in the tissues near the wound, and that the newly synthesized IAA is rapidly transported towards the most-basal region of the explants to activate specific target genes required for AR initiation. We then treated hypocotyl C2_DB and C2_BA explants with 50 µM yucasin DF (YDF) that specifically inhibits YUC activity and hence IAA biosynthesis (Tsugafune *et al.*, 2017). YDF did not affect AR emergence (Fig. 7G) but rooting capacity at 14 dae was significantly reduced (p-value=0.016) compared with the control treatment, mainly in the C2_BA explants (Fig. 7H). In addition, wound-induced ARs were much shorter in YDF-treated explants at 21 dae (Fig. 7I). We also found that the size of the AR formative region was reduced by YDF (Fig. 7J), and confirmed that the YDF treatment specifically reduced AR formation (Fig 9A). Taken together, these results confirmed that, in 'Micro-Tom' hypocotyl explants, wounding regulates the formation of *de novo* auxin gradients near the basal region of the explants that are required for AR formation.

A functional auxin gradient in the basal region of the hypocotyl drives wound-induced AR formation in tomato shoot explants

To gain additional insight into the relevance of the endogenous auxin response to wound-induced AR formation in tomato shoot explants, we studied the *entire* mutant, which is defective in the Aux/IAA auxin repressor SlIAA9 (Zhang *et al.*, 2007). We used a NIL of the *entire* mutant on the 'Micro-Tom' background with the characteristic simple leaf phenotype for our studies (Fig. 8A). AR emergence in the *entire* mutant was not significantly different (p-value=0.065) from that of the 'Micro-Tom' genetic background (Fig. 8B). However, the rooting capacity at 14 dae was significantly higher (p-value=0.000) in the *entire* mutant compared to that of the wild type (Fig. 8C), with a net difference of approximately 4 more ARs in *entire* at 21 dae than in 'Micro-Tom' (Fig. 8B), which nevertheless were of similar lengths in both genotypes (Fig. 8D). Interestingly, the AR formative region in the *entire* mutant was significantly expanded upward (p-value=0.000) as compared to that of the 'Micro-Tom' background (Fig. 8E and 9B). Different from that found for the C2_DC and C2_BA hypocotyl explants (see the previous section), we only observed minor changes in auxin biosynthesis gene expression along the apical-basal axis of 'Micro-Tom' shoot explants between 0 and 1 dae (Fig. 8F). However, we found that the *entire* mutant presented higher expression of the auxin biosynthesis genes *SlTAR2b* and *SlYUC2/6* in the basal region of the shoot explants at 1 dae when compared to 'Micro-Tom' (Fig. 8F), suggesting upregulation of auxin biosynthesis genes in the *entire* shoot explants after wounding. Besides, the rooting capacities at 14 dae of *entire* hypocotyl explants of different regions (C2_DC, C2_BA) were slightly higher (p-value=0.032) than those of the wild type (Fig. 8G).

In the *entire* hypocotyls, the ARs originated from the same vascular region as those in the 'Micro-Tom' background (Fig. 8H, I). However, we observed a significant increase (p-value=0.000) in the number of rows of cambial cells in the *entire* mutant at 1 dae (Fig. 8J), which, together with the enhanced auxin biosynthesis after wounding, would contribute to the higher rooting capacities observed in the shoot explants and hypocotyl explants of the *entire* mutant.

We wondered whether the wound-induced AR formation observed in the hypocotyl could also be elicited on higher nodes of young tomato seedlings. Hence, we studied wound-induced AR formation in three different regions of 16-day-old tomato seedlings (Fig. 9C). A high proportion (~65%) of explants from the first node did not produce any ARs even four weeks after excision, and the explants that had produced ARs were severely delayed in their initiation (Fig. 9C). Therefore, the rooting capacity of the explants from the first node was reduced (Fig. 9D), and their ARs were also shorter (Fig. 9E). We observed profuse tissue proliferation in the basal region of the explants from the first node that did not produce ARs (Fig. 9F, G), resembling hypocotyl explants treated with NAA (Fig. 2C). However, the explants from the shoot apex were mostly unable to produce any response in the basal region near the wound (Fig. 9C). These results confirmed that a developmental gradient along the apical-basal axis of the plant restricts wound-induced AR formation to the most basal tissues in 'Micro-Tom' seedlings.

Variation of wound-induced AR formation in several tomato cultivars

We previously studied several traits of the AR system in whole-root excised shoot explants in different tomato cultivars (Alaguero-Cordovilla *et al.*, 2018). AR emergence was significantly delayed (p-value=0.000) in the 'Micro-Tom' cultivar when compared to that of the other studied cultivars (Supplementary Fig. S3A). Consequently, the rooting capacity was significantly reduced (p-value=0.000) in the 'Micro-Tom' cultivar (4.0 ± 1.3

ARs at 14 dae) as compared to those in ‘Moneymaker’, ‘UC-82’ or ‘Heinz 1706-BG’ (7.7 ± 2.8; Supplementary Fig. S3B). Interestingly, AR formation was restricted to the most basal region of the hypocotyl in ‘UC-82’ while it was expanded upward in ‘Moneymaker’ and ‘Heinz 1706-BG’ (Supplementary Fig. S3C, D), irrespective of their hypocotyl lengths (Supplementary Fig. S3E). Furthermore, despite the differences in AR emergence between the studied cultivars, the length of the AR system at the end of the experiment (18 dae) did not significantly change (p-value=0.462; Supplementary Fig. S3F). These results suggested that genetic variation within the tomato cultivars might contribute to variation in wound-induced AR system attributes and hence deserves further investigation.

DISCUSSION

AR formation is a critical developmental process in cutting propagation within the horticultural industry (Druege *et al.*, 2019). Despite the key role of auxin in this process (Pacurar *et al.*, 2014), our knowledge about the molecular determinants is still incomplete. In Arabidopsis hypocotyls, ARs are initiated from xylem pole pericycle cells (Sukumar *et al.*, 2013) in a process resembling lateral root initiation (Bellini *et al.*, 2014). However, ARs in adult tissues, such as excised leaves, originate from the proliferating lineage of some vascular-associated cells that express the WOX11 transcription factor (Liu *et al.*, 2014; Hu and Xu 2016; Bustillo-Avendaño *et al.*, 2018). In contrast to *Solanum dulcamara*, where preformed AR primordia in the stem emerge in response to flooding (Dawood *et al.*, 2014), we found that wound-induced AR primordia in young ‘Micro-Tom’ hypocotyls were formed *de novo* after whole root excision (Fig. 9H). In our experimental system, AR initiation is temporally and spatially regulated by the stereotyped divisions of the distal cambium located at the edge of the vascular bundles. In the earliest stage, a small cluster of dividing cambial cells expresses the

auxin-responsive *DR5::GUS* marker (stage 1; Bustillo-Avendaño *et al.*, 2018), and in response, the root founder cells (RFCs) are then specified within this cluster (stage 2). In a recent report, Guan *et al.* (2019) localized the expression of the auxin reporter *DR5pro:YFP* in a subset of cambial cells during wound-induced AR formation in 'Micro-Tom' shoot explants, which is consistent with our findings with regards to the exact site of AR initiation. The lack of suitable cell-autonomous markers of cambial stem cell identity (Smetana *et al*., 2019) make detailed lineage analyses during AR formation in 'Micro-Tom' difficult. It has been reported that in petunia stem cuttings, several clusters of meristematic cells develop simultaneously within the same cambial ring in response to the auxin signal (Ahkami *et al*., 2014). In our study, however, consecutive ARs appeared to originate from opposite vascular rings and at a certain distance within the hypocotyl. This intriguing observation might be related to the internal vascular arrangement of the 'Micro-Tom' hypocotyl (vascular bundles arranged in a cross shape instead of the continuous vascular ring observed in petunia stem cuttings) or to an unknown lateral inhibition mechanism that spatially restricts AR initiation in the 'Micro-Tom' hypocotyl.

Day length was among the environmental factors that positively regulated AR initiation in 'Micro-Tom' hypocotyls, and sucrose exerted an additive effect on the rooting capacity of tomato shoot explants (this work). A previous study on tomato shoot explants found that the effect of light on AR formation was not directly related to photoreceptor-dependent light perception (Tyburski and Tretyn, 2004). Hence, the regulatory effect of light on adventitious rooting might result from its interaction with phytohormones, particularly auxin (Sorin *et al.*, 2005; Gutierrez *et al.*, 2009). Alternatively, light may influence AR formation due to its significant role in the synthesis of sugars. Studies on petunia cuttings highlighted the contribution of carbon allocation to AR formation sites in the basal region of the stem under different light regimes (Klopotek *et al*., 2016). Additional experiments using the

'Micro-Tom' model will enhance our understanding of the crosstalk between light, carbohydrate levels, and wound-induced AR formation.

In the current model for AR formation in stem cuttings (Druege *et al*., 2019), a pre-established polar auxin transport from mature leaves produced IAA accumulation in the basal region of the stem just above the wounding site, which triggered the de-differentiation and cell cycle reactivation of the neighboring cambial cells prior to AR initiation. We found that wound-induced AR formation in 'Micro-Tom' shoot explants resembled that of AR formation in stem cuttings. We observed the buildup of an internal IAA response gradient within the tomato hypocotyl shortly after whole root excision that reached its maximum levels at a defined position of the cambium, on a narrow proximal (basal) region of the hypocotyl just above the wound (Fig. 9I). In 'Micro-Tom' shoot explants, auxin is mainly produced in the cotyledons, and the emerging leaves are both a source and a sink for auxin (Fig. 9H). We found a direct correlation between the amount of auxin-producing tissues and the size of the AR-formative domain, which directly contributed to the rooting capacity of the explants (Fig. 9J). Indeed, local application of IAA in the proximal (basal) region of the hypocotyl resulted in the AR formative region significantly expanded upwards and concomitantly increased the number of wound-induced ARs (this work).

Using a combination of physiological and genetic approaches, we provided additional evidence of the key role of basipetal auxin transport in the regulation of wound-induced AR formation in 'Micro-Tom' shoot explants (Guan *et al.*, 2019). First, we demonstrated that actively transported and shoot-derived IAA was required to trigger AR formation in the proximal (basal) hypocotyl region as the AR reduction caused by shoot decapitation could be fully rescued via local auxin application through the apical (distal) region of the explants. Disruption of basipetal auxin transport with 2-NOA and NPA also reduced the initiation of ARs in the basal region of the hypocotyl. In addition, the observation that local inhibition of auxin efflux in

the basal hypocotyl domain blocked AR initiation suggested that transverse auxin flow, likely from the internal vasculature to the distal cambial cells, is also required for the formative divisions during AR initiation (Fig. 9I). Interestingly, the chemical inhibition of the auxin influx carriers AUX1/LAX by 2-NOA allowed the formation of callus-like tissue at the basal hypocotyl (resembling NAA-treated hypocotyl explants), which were severely delayed in AR formation. Indeed, in Arabidopsis hypocotyls, the activity of AUX1 is essential for AR initiation (da Costa *et al.*, 2020), while other LAX members (such as LAX3) are required for AR emergence (Della Rovere *et al.*, 2013; 2015). Consequently, when the new ARs emerged during the expression phase (de Klerk *et al*., 1999), they acted as active sinks for the basipetal auxin transported from the shoot, limiting the auxin overflow effect observed in the most basal region of the hypocotyl at earlier time-points. The tomato *diageotropica* mutant lacks lateral roots due to abnormal polar auxin transport that prevents the buildup of the auxin maxima in the vascular pericycle cells (Ivanchenko *et al.*, 2015). *DIAGEOTROPICA* encodes a cyclophyllin protein with peptidyl-prolyl isomerase activity (Oh *et al.*, 2006) that has been proposed to regulate PIN-mediated IAA efflux (Ivanchenko *et al.*, 2015). As expected from a defect in basipetal auxin transport, we observed a reduction in the rooting capacity in wound-induced shoot explants of *diageotropica* mutants, a phenotype that mirrors our results on the chemical inhibition of polar auxin transport through the hypocotyl in ‘Micro-Tom’ seedlings. We found that gravistimulation enhanced the AR formative region, which might be consistent with a reduced flow of basipetal auxin transport through the hypocotyl, likely though PIN3 repolarization upon gravistimulation, as it occurs in Arabidopsis (Rakusová *et al.*, 2011; 2016). Together, these results indicate that tightly regulated polar auxin transport through the hypocotyl is required to set up the AR formative region during wound-induced AR formation.

We previously determined that the stabilization of the Aux/IAA repressor SOLITARY ROOT (SLR), also named IAA14, in Arabidopsis leaf explants reduced *de novo* root initiation downstream of the IAA28 module that regulates RFC specification (Bustillo-Avendano *et al.*, 2018). The tomato *ENTIRE* gene encodes SlIAA9, a close SLR homolog (Wu *et al.*, 2012), and the *entire* loss-of-function mutant displayed simple leaves instead of compound leaves but normal lateral root development (Zhang *et al.*, 2007). We found that reduced levels of the SlIAA9 repressor enhanced wound-induced AR formation due to the apical expansion of the AR-formative domain. In addition, we found upregulation of two auxin biosynthesis genes in the basal region of the *entire* shoot explants after whole-root excision, which might directly contribute to the high endogenous auxin pool in this mutant. Our results suggest that reduced Aux/IAA levels in *entire* shoot explants lead to enhanced auxin responses that, in turn, lower the threshold for AR initiation at more distally located vascular bundles. Alternatively, the *entire* mutation might cause subtle developmental defects in the hypocotyl, which might alter the cellular interactions required for AR initiation. Downstream of the IAA14 repressor, the AUXIN RESPONSIVE FACTOR7 (ARF7) and ARF19 are required to activate formative divisions of pericycle cells during AR formation in etiolated Arabidopsis hypocotyls upon transfer to light (Lee *et al*., 2019). Several tomato homologs of *ARF7* and *ARF9* genes are expressed during the early stages of fruit development and their inactivation using RNAi renders fruits with thick pericarp due to increased cell expansion (de Jong *et al.*, 2015; 2008). Additional experiments are ongoing to determine whether ARF7 and ARF9 inactivation affects wound-induced AR formation in tomato shoot explants. Since the tomato genome contains 25 Aux/IAA genes (Audran-Delalande *et al.*, 2012) and 22 ARF genes (Zouine *et al*., 2014), multiple Aux/IAA and ARF genes might contribute to wound-induced AR formation and additional studies will be required to elucidate the Aux/IAA-ARF gene regulatory pathway(s) involved

in this process. During wound-induced AR formation in Arabidopsis leaf explants, two parallel pathways downstream of the auxin signal converge on the upregulation of several genes of the LATERAL ORGAN BOUNDARIES DOMAIN (LBD) gene family, such as *LBD16*, *LBD18*, and *LBD29* (Liu *et al.*, 2014; Lee *et al*., 2019). Indeed, we found that two tomato genes encoding LBD16 and LBD29 homologs (Solyc09g066260 and Solyc09g066270) were differentially upregulated in stages 2 and 3 of wound-induced AR formation in 'Micro-Tom' hypocotyl explants suggesting a conserved developmental framework for *de novo* root formation in both species (E. Larriba and J.M. Pérez-Pérez, unpublished).

Our results with 'Micro-Tom' hypocotyl explants of different lengths provide a conceptual framework for the study of *de novo* organ formation in this species, as these explants were able to develop both ARs and adventitious shoots. We found striking differences in AR emergence and rooting capacity with respect to the position of the explants along the apical-basal axis of the hypocotyl, irrespective of the length of the explants used. Hence, an endogenous pre-pattern of auxin responses within the hypocotyl is already established during early development, which limits AR initiation to most basal tissues. Interestingly, the size of the AR formative region remained constant in all cases, suggesting their tight regulation. Our results also suggested that wound-induced AR formation in excised hypocotyl explants was independent of shoot-derived auxin but dependent on a short-range signal produced near the wounded tissue. In Arabidopsis, root meristem regeneration requires multiple auxin biosynthetic sources that are newly specified near the cut site and it has been suggested that regeneration competence relies on the ability to specify new local auxin sources in a precise temporal pattern (Matosevich *et al*., 2020). We found mild upregulation of some auxin biosynthesis genes in the excised hypocotyl explants upon wounding, while the auxin responses were subsequently localized to the most basal region of the explants, suggesting that polar auxin transport might

contribute to the buildup of new auxin maxima in the basal region triggering AR initiation. In our working model for wound-induced AR formation in excised hypocotyl explants, AR initiation is dependent on the extent of local auxin biosynthesis in the wounded tissue and the endogenous auxin response of the explants (Fig. 9J). We demonstrated that both factors varied according to the apical-basal position of the explant on the intact hypocotyl.

During wound-induced AR formation in Arabidopsis leaf explants, wound-induced JA directly induces the expression of *ETHYLENE RESPONSE FACTOR109* (*ERF109*), which functions directly upstream of a key gene in the auxin biosynthesis pathway (Zhang *et al.*, 2019; Ye *et al.*, 2020). In addition, ERF109 activates *ERF115* expression (Zhou *et al.*, 2019), which in turn promotes stem cell renewal and grants regeneration competence after physical damage (Heyman *et al*., 2016). Two recent reports provide additional evidence of a mechanistic model for wound-induced stem cell regeneration that involves the sensing of damaged cells and the activation of local auxin signaling to coordinate downstream transcriptional responses near the wound through ERF115 activity (Canher *et al*., 2020; Hoermayer *et al*., 2020). The tomato genome contains several ERF109 and ERF115 homologs, some of which are differentially upregulated after wounding (E. Larriba and J.M. Pérez-Pérez, unpublished); hence, a similar regulatory network might be involved in the fine-tuning of wound-induced AR formation in excised tomato explants.

ACKNOWLEDGEMENTS

We are grateful to María José Ñíguez-Gómez for her expert technical assistance. We thank Prof. Lázaro E. Peres (Universidade de São Paulo, Brazil) and Prof. Yoshinori Kanayama (Tohoku University, Japan) for providing lines in the 'Micro-Tom' background studied in this work, and Prof. Ken-Ichiro Hayashi (Okayama University of Science, Japan) for providing the yucasin DF auxin biosynthesis inhibitor. We thank several members of the Instituto de Bioingeniería (Universidad Miguel Hernández, Spain) for sharing their equipment. This work was supported by the Ministerio de Ciencia e Innovación of Spain (BIO2015-64255-R and RTI2018-096505-B-I00), the Conselleria d'Educació, Cultura i Esport of the Generalitat Valenciana (IDIFEDER 2018/016 and PROMETEO/2019/117), and the European Regional Development Fund (ERDF) of the European Commission. SI was a research fellow of the Generalitat Valenciana (ACIF/2018/220).

CONFLICT OF INTEREST

The authors declare that they have no competing financial interests as defined by Plant, Cell and Environment, or other interests that might be perceived to influence the results and/or discussion reported in this article.

AUTHOR CONTRIBUTIONS

Conceptualization and Supervision: J.M.P.-P.; Methodology, J.M.P.-P., A.A.-C., A.B.S.-C., S.I., and A.A.; Investigation, A.A.-C., A.B.S.-C., S.I., and A.C.; Formal Analysis: A.A.-C., A.C., and S.I.; Writing – Original Draft Preparation, J.M.P.-P., and A.A.-C.; Writing – Review & Editing, J.M.P.-P.,

A.A., and M.A.; Funding Acquisition, J.M.P.-P.; Resources, J.M.P.-P., A.A., and M.A.

DATA AVAILABILITY STATEMENT

The datasets generated during and/or analysed during the current study are available from the corresponding author on reasonable request.

REFERENCES

Acosta, M., Oliveros-Valenzuela, M. R., Nicolás, C., & Sánchez-Bravo, J. (2009). Rooting of carnation cuttings. *Plant Signaling & Behavior*, **4**, 234–236.

Aguinis, H., Gottfredson, R. K., & Joo, H. (2013). Best-practice recommendations for defining, identifying, and handling outliers. *Organizational Research Methods*, **16**, 270–301.

Agulló-Antón, M. Á., Ferrández-Ayela, A., Fernández-García, N., Nicolás, C., Albacete, A., Pérez-Alfocea, F., Sánchez-Bravo, J., Pérez-Pérez, J. M., & Acosta M. (2014). Early steps of adventitious rooting: morphology, hormonal profiling and carbohydrate turnover in carnation stem cuttings. *Physiologia Plantarum*, **150**, 446–462.

Ahkami, A., Scholz, U., Steuernagel, B., Strickert, M., Haensch, K-T., Druege, U., Reinhardt, D., Nouri, E., von Wirén, N., Franken, P., & Hajirezaei M. R. (2014). Comprehensive transcriptome analysis unravels the existence of crucial genes regulating primary metabolism during adventitious root formation in *Petunia hybrida*. *PLoS ONE*, **9**, e100997.

Ahkami, A. H., Lischewski, S., Haensch, K. T., Porfirova, S., Hofmann, J., Rolletschek, H., Melzer, M., Franken, P., Hause, B., Druege, U., & Hajirezaei, M. R. (2009). Molecular physiology of adventitious root formation in *Petunia hybrida* cuttings: Involvement of wound response and primary metabolism. *New Phytologist*, **181**, 613–625.

Alaguero-Cordovilla, A., Gran-Gómez, F., Tormos-Moltó, S., & Pérez-Pérez, J. M. (2018). Morphological characterization of root system architecture in diverse tomato genotypes during early growth. *International Journal of Molecular Sciences*, **19**, 3888.

Audran-Delalande, C., Bassa, C., Mila, I., Regad, F., Zouine, M., & Bouzayen, M. (2012). Genome-wide identification, functional analysis and expression profiling of the Aux/IAA gene family in tomato. *Plant and Cell Physiology*, **53**, 659–672.

Bellini, C., Pacurar, D.I., & Perrone, I. (2014). Adventitious roots and lateral roots:

similarities and differences. *Annual Review of Plant Biology*, **65**, 639–666.

Bustillo-Avendaño, E., Ibáñez, S., Sanz, O., Barros, J. A. S., Gude, I., Perianez-Rodriguez, J., Micol, J. L., del Pozo, J. C., Moreno-Risueno, M. A., & Pérez-Pérez, J. M. (2018). Regulation of hormonal control, cell reprogramming, and patterning during *de novo* root organogenesis. *Plant Physiology*, **176**, 1709–1727.

Canher, B., Heyman, J., Savina, M., Devendran, A., Eekhout, T., Vercauteren, I., Prinsen, E., Matosevich, R., Xu, J., Mironova, V., & De Veylder, L. (2020). Rocks in the auxin stream: Wound-induced auxin accumulation and ERF115 expression synergistically drive stem cell regeneration. *Proceedings of the National Academy of Sciences*, **117**, 16667–16677.

Cano, A., Sánchez-García, A. B., Albacete, A., González-Bayón, R., Justamante, M. S., Ibáñez, S., Acosta, M., & Pérez-Pérez, J. M. (2018). Enhanced conjugation of auxin by GH3 enzymes leads to poor adventitious rooting in carnation stem cuttings. *Frontiers in Plant Science*, **9**, 566.

Chen, L., Tong, J., Xiao, L., Ruan, Y., Liu, J., Zeng, M., Huang, H., Wang, J. W., & Xu, L. (2016). *YUCCA* -mediated auxin biogenesis is required for cell fate transition occurring during *de novo* root organogenesis in Arabidopsis. *Journal of Experimental Botany*, **67**, 4273–4284.

da Costa, C. T., Offringa, R., & Fett-Neto, A. G. (2020). The role of auxin transporters and receptors in adventitious rooting of *Arabidopsis thaliana* pre-etiolated flooded seedlings. *Plant Science*, **290**, 110294.

Dawood, T., Rieu, I., Wolters-Arts, M., Derksen, E.B., Mariani, C., & Visser, E. J. W. (2014). Rapid flooding-induced adventitious root development from preformed primordia in *Solanum dulcamara*. *AoB Plants*, **6**, plt058.

de Klerk, G. J., van der Krieken, W., & de Jong, J. C. (1999). Review the formation of adventitious roots: New concepts, new possibilities. *In Vitro Cellular & Developmental Biology – Plant*, **35**, 189–199.

Dekkers, B. J. W., Willems, L., Bassel, G. W., van Bolderen-Veldkamp, R. P. M., Ligterink, W., Hilhorst, H. W. M, & Bentsink, L. (2012). Identification of reference genes for RT-qPCR expression analysis in Arabidopsis and tomato

seeds. *Plant & Cell Physiology*, **53**, 28–37.

Della Rovere, F., Fattorini, L., D'Angeli, S., Veloccia, A., Del Duca, S., Cai, G., Falasca, G., & Altamura, M. M. (2015). Arabidopsis SHR and SCR transcription factors and AUX1 auxin influx carrier control the switch between adventitious rooting and xylogenesis in planta and in *in vitro* cultured thin cell layers. *Annals of Botany*, **115**, 617–628.

Della Rovere, F., Fattorini, L., D'Angeli, S., Veloccia, A., Falasca, G., & Altamura, M. M. (2013). Auxin and cytokinin control formation of the quiescent centre in the adventitious root apex of Arabidopsis. *Annals of Botany*, **112**, 1395–1407.

Díaz-Sala, C., Garrido, G., & Sabater, B. (2002). Age-related loss of rooting capability in *Arabidopsis thaliana* and its reversal by peptides containing the Arg-Gly-Asp (RGD) motif. *Physiologia Plantarum*, **114**, 601–607.

Druege, U., Franken, P., & Hajirezaei, M. R. (2016). Plant hormone homeostasis, signaling and function during adventitious root formation in cuttings. *Frontiers in Plant Science*, **7**, 381.

Druege, U., Franken, P., Lischewski, S., Ahkami, A.H., Zerche, S., Hause, B., & Hajirezaei, M. R. (2014). Transcriptomic analysis reveals ethylene as stimulator and auxin as regulator of adventitious root formation in petunia cuttings. *Frontiers in Plant Science*, **5**, 494.

Druege, U., & Franken, P. (2019). Petunia as model for elucidating adventitious root formation and mycorrhizal symbiosis: at the nexus of physiology, genetics, microbiology and horticulture. *Physiologia Plantarum*, **165**, 58–72.

Druege, U., Hilo, A., Pérez-Pérez, J.M., Klopotek, Y., Acosta, M., Shahinnia, F., Zerche, S., Franken, P., & Hajirezaei, M. R. (2019). Molecular and physiological control of adventitious rooting in cuttings: phytohormone action meets resource allocation. *Annals of Botany*, **123**, 929–949.

Emmanuel, E., & Levy, A. A. (2002). Tomato mutants as tools for functional genomics. *Current Opinion in Plant Biology*, **5**, 112–117.

Expósito-Rodríguez, M., Borges, A. A., Borges-Pérez, A., & Pérez, J. A. (2008). Selection of internal control genes for quantitative real-time RT-PCR studies

during tomato development process. *BMC Plant Biology*, **8**, 131.

Feller, C., Bleiholder, H., Buhr, L., Hack, H., Hess, M., Klose, R., Meier, U., Stauss, R., Van den Boom, T, & Weber, E. (1995). Phänologische entwicklungsstadien von gemüsepflanzen: II. Fruchtgemüse und hülsenfrüchte. *Nachrichtenblatt des Deutschen Pflanzenschutzdienstes*, **47**, 217–232.

Fukaki, H., Tameda, S., Masuda, H., & Tasaka, M. (2002). Lateral root formation is blocked by a gain-of-function mutation in the *SOLITARY-ROOT/IAA14* gene of *Arabidopsis*. *The Plant Journal*, **29**, 153–168.

Gonin, M., Bergougnoux, V., Nguyen, T. D., Gantet, P., & Champion, A. (2019). What makes adventitious roots? *Plants*, **8**, 240.

Großkinsky, D. K., Albacete, A., Jammer, A., Krbez, P., van der Graaff, E., Pfeifhofer, H., & Roitsch, T. (2014). A rapid phytohormone and phytoalexin screening method for physiological phenotyping. *Molecular Plant*, **7**, 1053–1056.

Grubbs, F. (1969). Procedures for detecting outlying observations in samples. *Technometrics*, **11**, 1–21.

Guan, L., Tayengwa ,R., Cheng, Z. M., Peer, W. A., Murphy, A. S., & Zhao, M. (2019). Auxin regulates adventitious root formation in tomato cuttings. *BMC Plant Biology*, **19**, 435.

Gutierrez, L., Bussell, J.D., Pacurar, D.I., Schwambach, J., Pacurar, M., & Bellini C. (2009). Phenotypic plasticity of adventitious rooting in Arabidopsis is controlled by complex regulation of AUXIN RESPONSE FACTOR transcripts and microRNA abundance. *The Plant Cell*, **21**, 3119–3132.

Heyman, J., Cools, T., Canher, B., Shavialenka, S., Traas, J., Vercauteren, I., Van den Daele, H., Persiau, G., De Jaeger, G., Sugimoto, K., & De Veylder, L. (2016). The heterodimeric transcription factor complex ERF115-PAT1 grants regeneration competence. *Nature Plants*, **2**, 16165.

Huang, A., Wang, Y., Liu, Y., Wang, G., She, X. (2020). Reactive oxygen species regulate auxin levels to mediate adventitious root induction in Arabidopsis hypocotyl cuttings. *Jounal of Integrative Plant Biology*, **62**, 912–926.

Hilo, A., Shahinnia, F., Druege, U., Franken, P., Melzer, M., Rutten, T., Von Wirén, N., & Hajirezaei, M. R. (2017). A specific role of iron in promoting meristematic cell division during adventitious root formation. *Journal of Experimental Botany*, **68**, 4233–4247.

Hoermayer, L., Montesinos, J. C., Marhava, P., Benková, E., Yoshida, S., & Friml, J. (2020). Wounding-induced changes in cellular pressure and localized auxin signalling spatially coordinate restorative divisions in roots. *Proceedings of the National Academy of Sciences*, 117, 15322–15331.

Hošek, P., Kubeš, M., Laňková, M., Dobrev, P. I., Klíma, P., Kohoutová, M., Petrášek, J., Hoyerová, K., Jiřina, M., & Zažímalová, E. (2012). Auxin transport at cellular level: new insights supported by mathematical modelling. *Journal of Experimental Botany*, **63**, 3815–3827.

Hu X, & Xu L. (2016). Transcription factors WOX11/12 directly activate WOX5/7 to promote root primordia initiation and organogenesis. *Plant Physiology*, **172**, 2363–2373.

Ivanchenko, M. G., Zhu, J., Wang ,B., Medvecká, E., Du, Y., Azzarello, E., Mancuso, S., Megraw, M., Filichkin, S., Dubrovsky, J.G., Friml, J., & Geisler, M. (2015). The cyclophilin a *DIAGEOTROPICA* gene affects auxin transport in both root and shoot to control lateral root formation. *Development*, **142**, 712–721.

Klopotek, Y., Franken, P., Klaering, H. P., Fischer, K., Hause, B., Hajirezaei, M. R., & Druege, U. (2016). A higher sink competitiveness of the rooting zone and invertases are involved in dark stimulation of adventitious root formation in *Petunia hybrida* cuttings. *Plant Science*, **243**, 10–22.

Kobayashi, M., Nagasaki, H., Garcia, V., Just, D., Bres, C., Mauxion, J-P., Le Paslier, M-C., Brunel, D., Suda, K., Minakuchi, Y., Toyoda, A., Fujiyama, A., Toyoshima, H., Suzuki, T., Igarashi, K., Rothan, C., Kaminuma, E., Nakamura, Y., Yano, K., & Aoki, K. (2014). Genome-wide analysis of intraspecific DNA polymorphism in 'Micro-Tom', a model cultivar of tomato (*Solanum lycopersicum*). *Plant and Cell Physiology*, **55**, 445–454.

Kurihara, D., Mizuta, Y., Sato, Y., Higashiyama, T. (2015). ClearSee: a rapid optical

clearing reagent for whole-plant fluorescence imaging. *Development*, **142**, 4168–4179.

Lakehal, A., & Bellini, C. (2019). Control of adventitious root formation: insights into synergistic and antagonistic hormonal interactions. *Physiologia Plantarum*, **165**, 90–100.

Lanková, M., Smith, R. S., Pesek, B., Kubes, M., Zazímalová, E., Petrásek, J., & Hoyerová, K. (2010). Auxin influx inhibitors 1-NOA, 2-NOA, and CHPAA interfere with membrane dynamics in tobacco cells. *Journal of Experimental Botany*, **61**, 3589–3598.

Lee, H. W., Cho, C., Pandey, S. K., Park, Y., Kim, M. J., & Kim, J. (2019). LBD16 and LBD18 acting downstream of ARF7 and ARF19 are involved in adventitious root formation in Arabidopsis. *BMC Plant Biology*, **19**, 46.

Liu, J., Sheng, L., Xu, Y., Li, J., Yang, Z., Huang, H., & Xu, L. (2014). WOX11 and 12 are involved in the first-step cell fate transition during de novo root organogenesis in Arabidopsis. *The Plant Cell*, **26**, 1081–1093.

Livak, K. J., & Schmittgen, T. D. (2001). Analysis of relative gene expression data using real-time quantitative PCR and the $2^{-\Delta\Delta C_T}$ method. *Methods*, **25**, 402–408.

Ludwig-Müller, J., Vertocnik, A., & Town, C. D. (2005). Analysis of indole-3-butyric acid-induced adventitious root formation on Arabidopsis stem segments. *Journal of Experimental Botany*, **56**, 2095–2105.

Lu, Y., Xie, L., & Chen, J. (2012). A novel procedure for absolute real-time quantification of gene expression patterns. *Plant Methods*, **8**, 9.

Matosevich, R., Cohen, I., Gil-Yarom, N., Modrego, A., Friedlander-Shani, L., Verna, C., Scarpella, E., & Efroni, I. (2020). Local auxin biosynthesis is required for root regeneration after wounding. *Nature Plants*, **6**, 1020–1030.

Mignolli, F., Mariotti, L., Picciarelli, P., & Vidoz, M. L. (2017). Differential auxin transport and accumulation in the stem base lead to profuse adventitious root primordia formation in the *aerial roots* (*aer*) mutant of tomato (*Solanum lycopersicum* L.). *Journal of Plant Physiology*, **213**, 55–65.

Negi, S., Sukumar, P., Liu, X., Cohen, J. D., & Muday, G. K. 2010. Genetic

dissection of the role of ethylene in regulating auxin-dependent lateral and adventitious root formation in tomato. *The Plant Journal*, **61**, 3–15.

Oh, K. C., Ivanchenko, M. G., White, T. J., & Lomax, T. L. (2006). The *DIAGEOTROPICA* gene of tomato encodes a cyclophilin: a novel player in auxin signaling. *Planta*, **224**, 133–144.

Pacurar, D.I., Perrone, I., & Bellini, C. (2014). Auxin is a central player in the hormone cross-talks that control adventitious rooting. *Physiologia Plantarum*, **151**, 83–96.

Pařízková, B., Pernisová, M., & Novák, O. (2017). What has been seen cannot be unseen – detecting auxin *in vivo*. *International Journal of Molecular Sciences*, **18**, 2736.

Rakusová, H., Abbas, M., Han, H., Song, S., Robert, H. S., & Friml, J. (2016). Termination of shoot gravitropic responses by auxin feedback on PIN3 polarity. *Current Biology*, **26**, 3026–3032.

Rakusová, H., Gallego-Bartolomé, J., Vanstraelen, M., Robert, H. S., Alabadí, D., Blázquez, M. A., Benková, E., & Friml, J. (2011). Polarization of PIN3-dependent auxin transport for hypocotyl gravitropic response in Arabidopsis thaliana. *The Plant Journal*, **67**, 817–826.

Rothan, C., Bres, C., Garcia, V., & Just, D. (2016). Tomato resources for functional genomics. In: Causse, M., Giovannoni, J., Bouzayen, M., Zouine M. (eds) The Tomato Genome. Compendium of Plant Genomes. Springer, Berlin, Heidelberg.

Rothan, C., Diouf, I., & Causse, M. (2019). Trait discovery and editing in tomato. *The Plant Journal*, **97**, 73–90.

Shikata, M., Hoshikawa, K., Ariizumi, T., Fukuda, N., Yamazaki, Y., & Ezura, H. (2016). TOMATOMA update: phenotypic and metabolite information in the Micro-Tom Mutant resource. *Plant and Cell Physiology*, **57**, e11.

Smetana, O., Mäkilä, R., Lyu, M., Amiryousefi, A., Sánchez-Rodríguez, F., Wu, M. F., Solé-Gil, A., Leal Gavarrón, M., Siligato, R., Miyashima, S., Roszak, P., Blomster, T., Reed, J. W., Broholm, S., & Mähönen, A. P. (2019). High levels of auxin signalling define the stem-cell organizer of the vascular cambium. *Nature*,

565, 485–489.

Sorin, C., Bussell, J. D., Camus, I., Ljung, K., Kowalczyk, M., Geiss, G., McKhann, H., Garcion, C., Vaucheret, H., Sandberg, G., & Bellini, C. (2005). Auxin and light control of adventitious rooting in Arabidopsis require ARGONAUTE1. *The Plant Cell*, **17**, 1343–1359.

Su, S-H., Gibbs, N. M., Jancewicz, A.L., & Masson, P. H. (2017). Molecular mechanisms of root gravitropism. *Current Biology*, **27**, R964–R972.

Sukumar, P., Maloney, G. S., & Muday, G. K. (2013). Localized induction of the ATP-binding cassette B19 auxin transporter enhances adventitious root formation in Arabidopsis. *Plant Physiology*, **162**, 1392–1405.

Teale, W., & Palme, K. (2018). Naphthylphthalamic acid and the mechanism of polar auxin transport. *Journal of Experimental Botany*, **69**, 303–312.

Tsugafune, S., Mashiguchi, K., Fukui, K., Takebayashi, Y., Nishimura, T., Sakai, T., Shimada, Y., Kasahara, H., Koshiba, T., & Hayashi, K. I. (2017). Yucasin DF, a potent and persistent inhibitor of auxin biosynthesis in plants. *Scientific Reports*, **7**, 13992.

Tyburski, J., & Tretyn, A. (2004). The role of light and polar auxin transport in root regeneration from hypocotyls of tomato seedling cuttings. *Plant Growth Regulation*, **42**, 39–48.

Vidoz, M. L., Loreti, E., Mensuali, A., Alpi, A., & Perata, P. (2010). Hormonal interplay during adventitious root formation in flooded tomato plants. *The Plant Journal*, **63**, 551–562.

Villacorta-Martín, C., Sánchez-García, A. B., Villanova, J., Cano, A., van de Rhee, M., de Haan, J., Acosta, M., Passarinho, P., & Pérez-Pérez, J. M. (2015). Gene expression profiling during adventitious root formation in carnation stem cuttings. *BMC Genomics*, **16**, 789.

Welander, M., Geier, T., Smolka, A., Ahlman, A., Fan, J., & Zhu, L.H. (2014). Origin, timing, and gene expression profile of adventitious rooting in Arabidopsis hypocotyls and stems. *American Journal of Botany*, **101**, 255–266.

Wu, J., Peng, Z., Liu, S., He, Y., Cheng, L., Kong, F., Wang, J., & Lu, G. (2012).

Genome-wide analysis of Aux/IAA gene family in Solanaceae species using tomato as a model. *Molecular Genetics and Genomics*, **287**, 295–311.

Yang, H., Klopotek, Y., Hajirezaei, M. R., Zerche, S., Franken, P., & Druege, U. (2019). Role of auxin homeostasis and response in nitrogen limitation and dark stimulation of adventitious root formation in petunia cuttings. *Annals of Botany*, **124**, 1053–1066.

Ye, B-B., Shang, G. D., Pan, Y., Xu, Z. G., Zhou, C. M., Mao, Y. B., Bao, N., Sun, L., Xu, T., & Wang, J. W. (2020). AP2/ERF transcription factors integrate age and wound signals for root regeneration. *The Plant Cell*, **32**, 226–241.

Zerche, S., Haensch, K-T. T., Druege, U., Hajirezaei, M. R. 2016. Nitrogen remobilisation facilitates adventitious root formation on reversible dark-induced carbohydrate depletion in *Petunia hybrida*. *BMC Plant Biology*, **16**, 219.

Zhang, G., Zhao, F., Chen, L., Pan, Y., Sun, L., Bao, N., Zhang, T., Cui, C-X., Qiu, Z., Zhang, Y, Yang, L., & Xu, L. (2019). Jasmonate-mediated wound signalling promotes plant regeneration. *Nature Plants*, **5**, 491–497.

Zhang, J., Chen, R., Xiao, J., Qian, C., Wang, T., Li, H., Ouyang, B., & Ye, Z. (2007). A single-base deletion mutation in *SlIAA9* gene causes tomato (*Solanum lycopersicum*) *entire* mutant. *Journal of Plant Research*, **120**, 671–678.

Zhou, W., Lozano-Torres, J. L., Blilou, I., Zhang, X., Zhai, Q., Smant, G., Li, C., & Scheres, B. (2019). A jasmonate signaling network activates root stem cells and promotes regeneration. *Cell*, **177**, 942–946.

Zouine, M., Fu, Y., Chateigner-Boutin, A. L., Mila, I., Frasse, P., Wang, H., Audran, C., Roustan, J. P., & Bouzayen, M. (2014). Characterization of the tomato ARF gene family uncovers a multi-levels post-transcriptional regulation including alternative splicing. *PLoS ONE*, **9**, e84203.

FIGURES

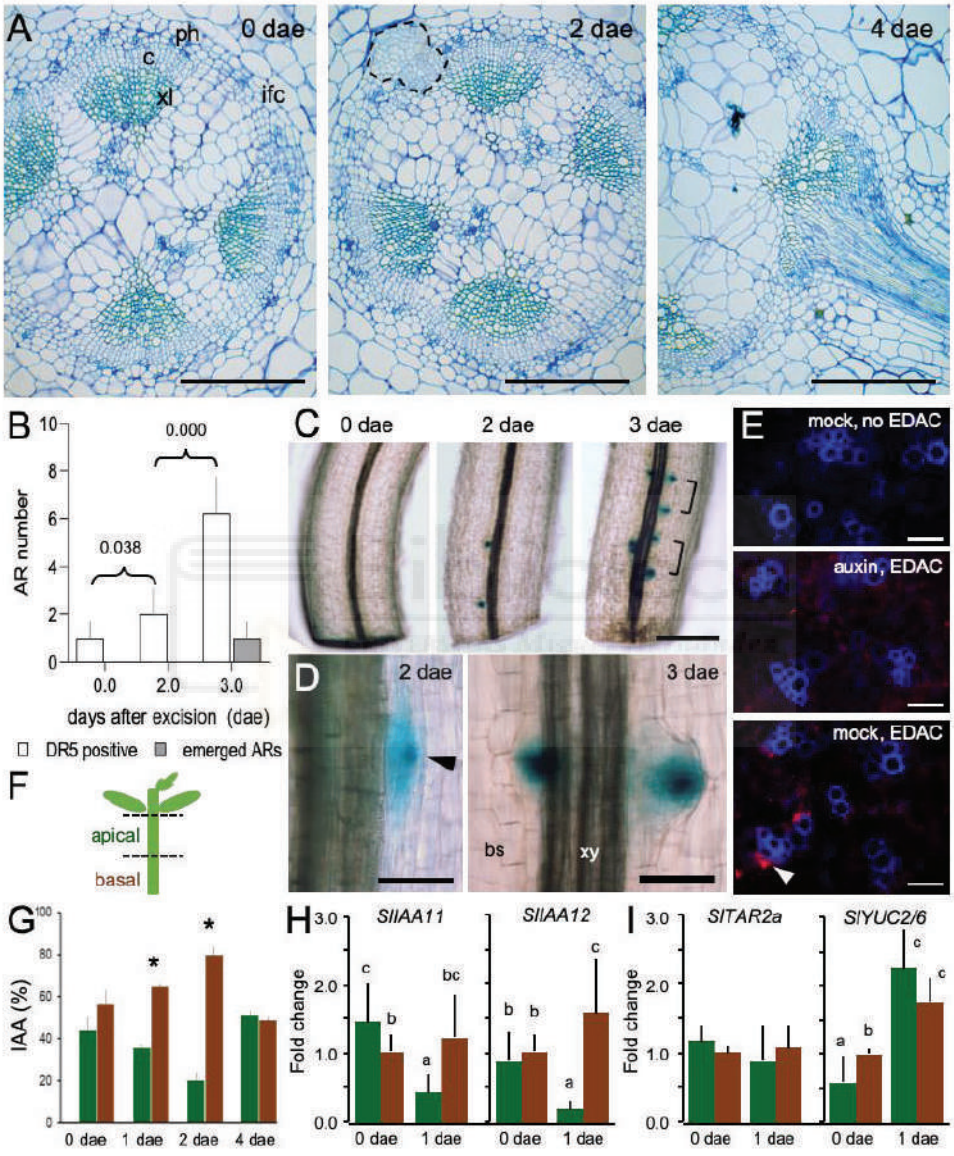

Fig. 1. A functional auxin gradient in the basal region of the hypocotyl correlates with wound-induced AR formation in tomato shoot explants. (A) Representative cross sections of the basal region of the hypocotyl during

AR formation. Dotted lines surround an early AR primordia arising from the cambium next to the vascular bundle; c, cambium; ifc, interfascicular cambium; ph, phloem; xl, xylem. (B) Wound-induced AR number expressing *DR5::GUS* after whole root excision. (C, D) Representative images of GUS expression in the AR primordia of *DR5::GUS* lines. Black lines indicate regular spacing between adjacent AR primordia. (E) Immunolocalization of IAA near the xylem pole (white arrow) of the basal region of the shoot explants at 2 dae. (F) Diagram showing the different regions studied in G-I. (G) Percentage of IAA levels in the different hypocotyl regions during AR formation. (H, I) Relative expression of Aux/IAA-related (H) and auxin biosynthesis (I) genes. Bars indicate normalized expression levels ± SD with regards to the expression at the basal region at 0 dae. Letters/Asterisks indicate significant differences (p-value<0.01) between regions. Scale bars: 200 μM (A, D, E) and 1 mm (C).

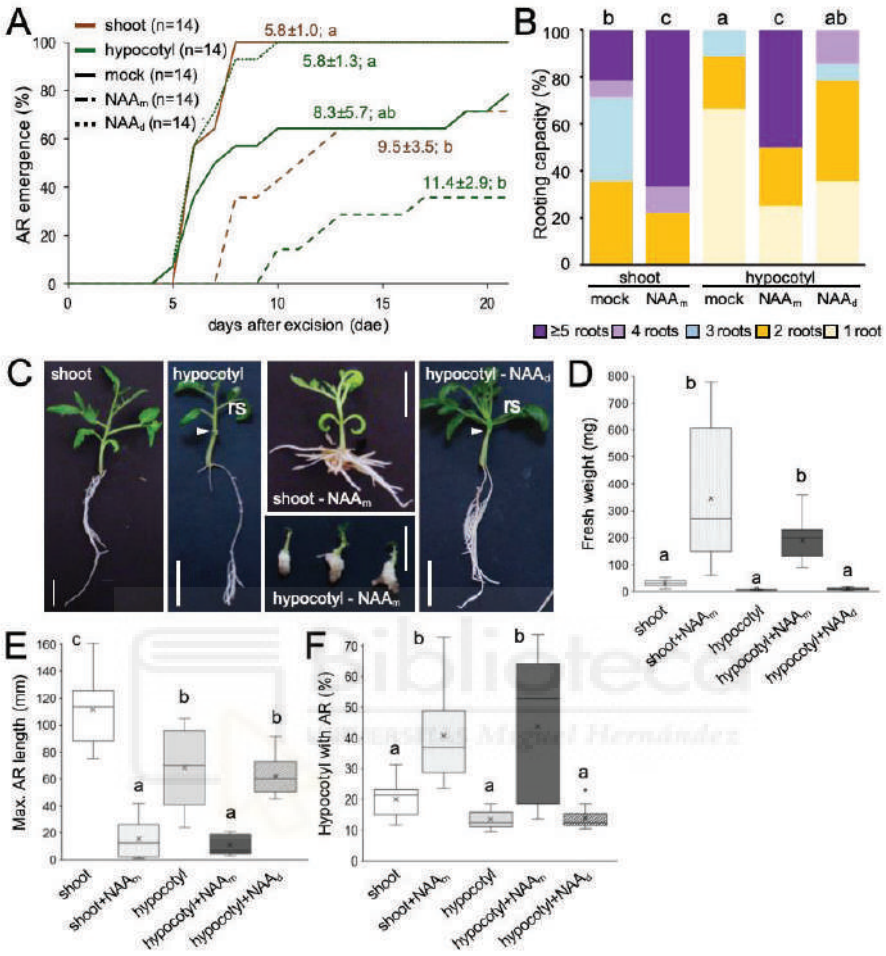

Fig. 2. Auxin effect on wound-induced AR formation in tomato shoot explants. (A) AR emergence of the studied explants. (B) Rooting capacity of 'Micro-Tom' shoot explants at 14 dae. (C) Representative images of rooted shoot explants. Arrow indicate the apical end of the hypocotyl explants; rs: regenerated shoot, NAA_m: NAA added to the SGM; NAA_d: NAA added to the distal end of the hypocotyl explants. (D) Fresh weight of the distal region of the shoot explants with ARs at 21 dae. (E) Maximum length of ARs at 21 dae. (F) Percentage of hypocotyl length with ARs at 21 dae. Letters indicate significant differences (p-value<0.01) between the assayed conditions. Scale bars: 20 mm.

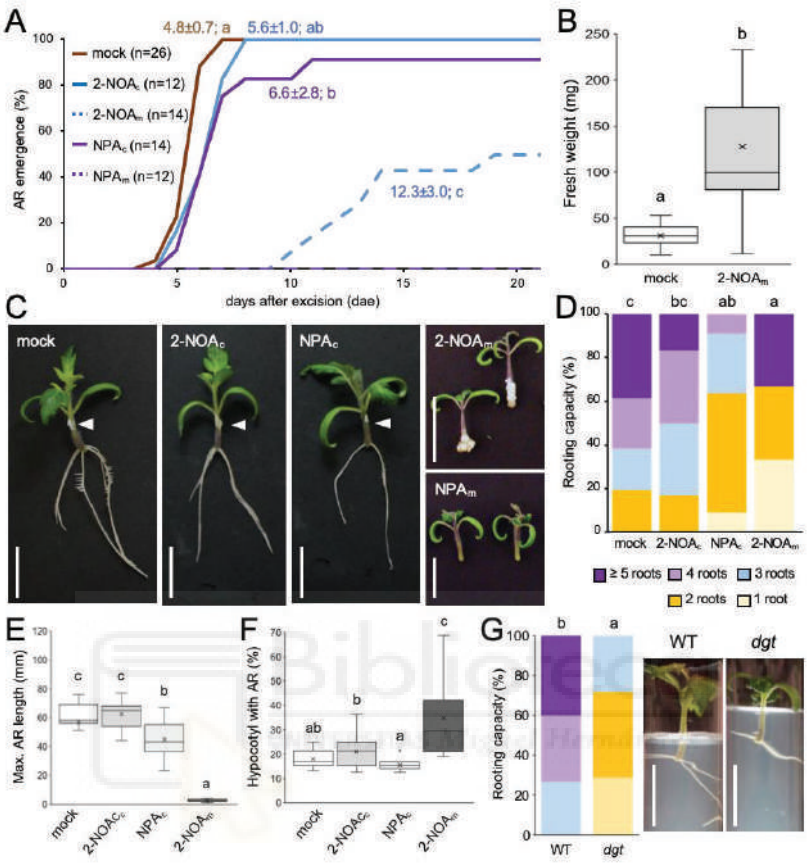

Fig. 3. Polar auxin transport is required for wound-induced AR formation in tomato shoot explants. (A) AR emergence of the studied explants. (B) Fresh weight of the AR formative region of the shoot explants at 21 dae. (C) Representative images of rooted shoot explants at 14 dae. The chemical treatments were applied on a lanolin collar (c; white arrow) or to the medium (m). (D, G left) Rooting capacity of shoot explants at 14 dae. (E) Maximum lengths of ARs at 14 dae. (F) Percentage of hypocotyl length with ARs at 14 dae. (G right) Representative images of rooted shoot explants at 14 dae in *diageotropica* (*dgt*) and 'Micro-Tom' (WT). Letters indicate significant differences (p-value<0.01) between treatments and genotypes. Scale bars: 20 mm.

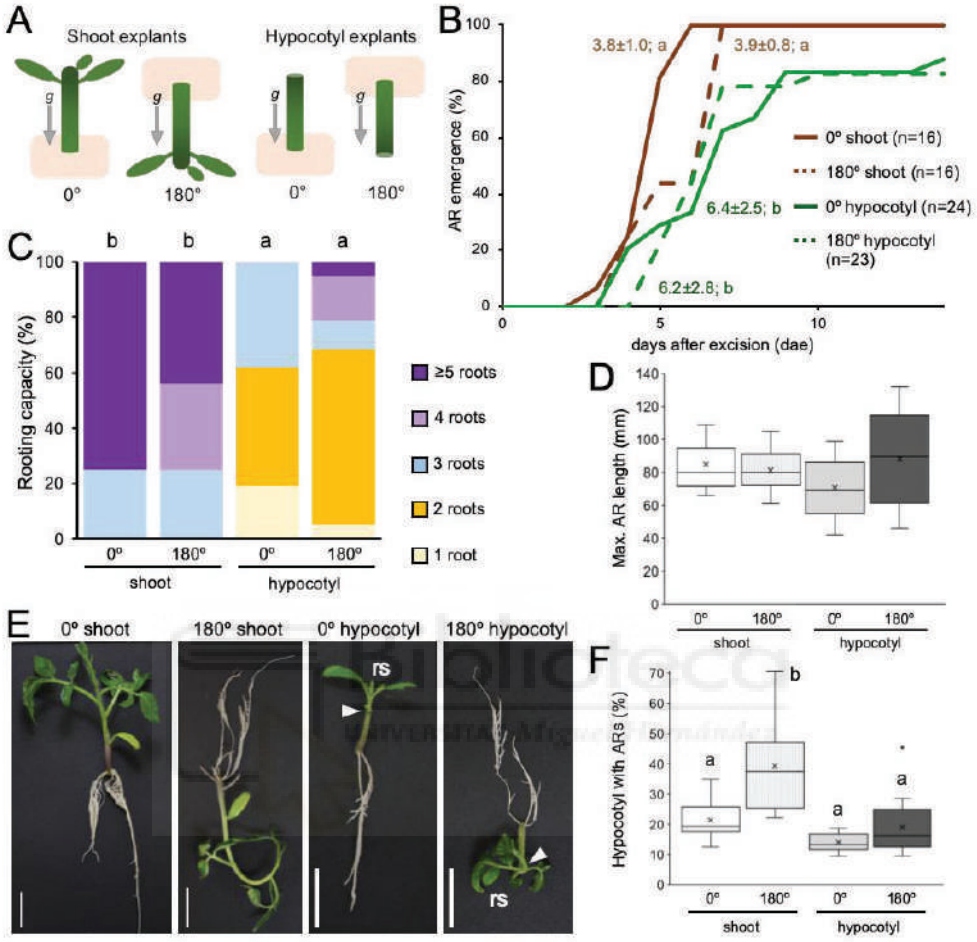

Fig. 4. Wound-induced AR formation in tomato explants is independent of the gravity vector. (A) Shoot or hypocotyl explants were oriented with (0º) or opposite (180º) the gravity vector. (B) AR emergence of the explants in the studied conditions. (C) Rooting capacity of 'Micro-Tom' explants at 14 dae. (D) Maximum lengths of ARs at 21 dae. (E) Representative images of rooted shoot explants at 21 dae. Arrows indicate the apical end of the hypocotyl explants; rs: regenerated shoot. (F) Percentage of hypocotyl lengths with functional ARs at 21 dae. Letters indicate significant differences (p-value<0.01) between treatments. Scale bars: 20 mm.

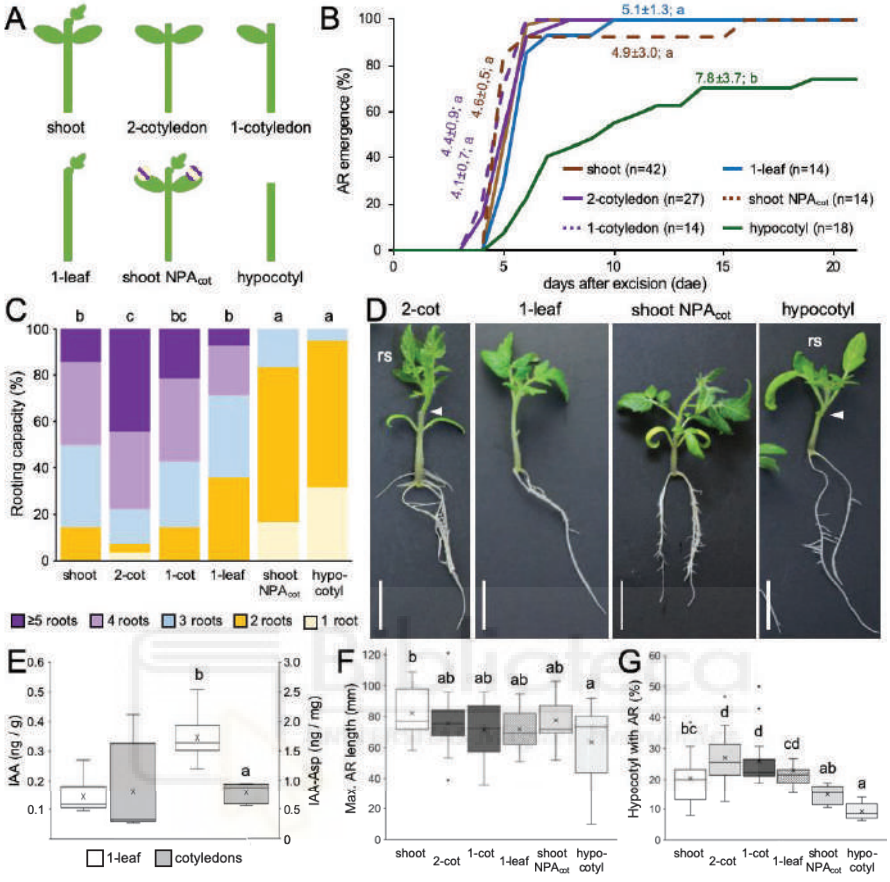

Fig. 5. Source of active auxin required for wound-induced AR formation in tomato hypocotyl explants. (A) Diagram showing the different conditions assayed. (B) AR emergence of the studied explants. (C) Rooting capacity of 'Micro-Tom' shoot explants at 14 dae. (D) Representative images of rooted shoot explants at 21 dae. Arrows indicate the apical end of the hypocotyl explants; rs: regenerated shoot. (E) IAA and IAA-Asp levels in the shoot apex or the cotyledons in shoot explants at 21 dae. (F) Maximum lengths of ARs at 21 dae. (G) Percentage of hypocotyl length with ARs at 21 dae. Letters indicate significant differences (p-value<0.01) between treatments. Scale bars: 20 mm.

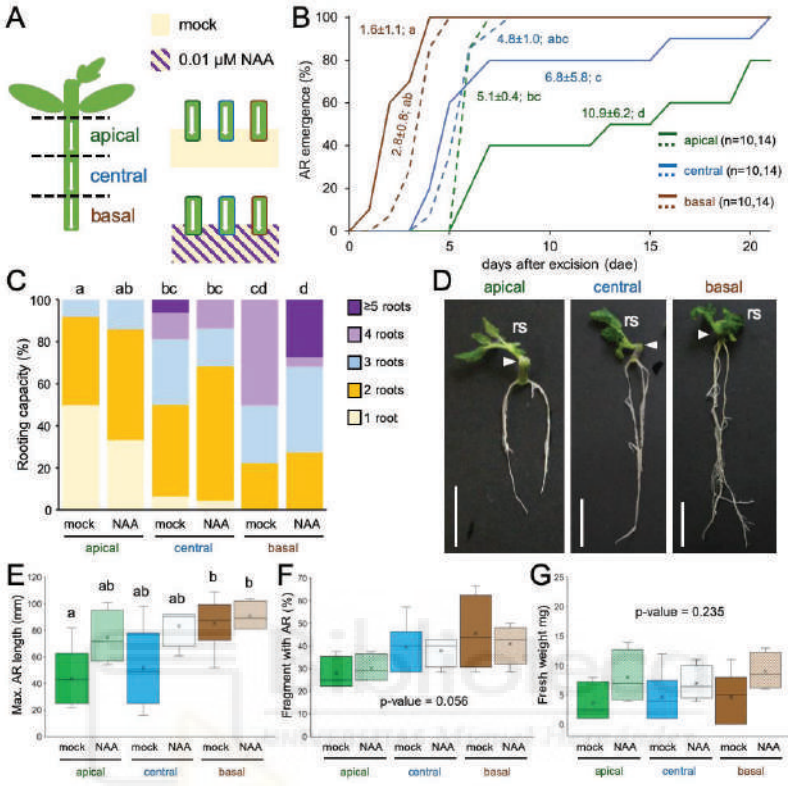

Fig. 6. Apical-basal gradient of auxin signaling within the hypocotyl influences wound-induced AR formation. (A) Diagram showing the different conditions assayed. White arrow indicates the internal tissue polarity. (B) AR emergence of the studied explants. Dotted lines indicate hypocotyl explants incubated with 0.01 µM NAA. (C) Rooting capacity of 'Micro-Tom' shoot explants at 14 dae in the different conditions assayed. (D) Representative images of rooted shoot explants at 21 dae in the studied regions without exogenous auxin treatment. Arrows indicated the apical end of the hypocotyl explants; rs: regenerated shoot. (E) Maximum lengths of ARs at 21 dae. (F) Percentage of hypocotyl length with ARs at 21 dae. (G) Fresh weight of the distal end of the explants with AR formative region. Letters indicate significant differences (p-value<0.01) between the experimental conditions tested. Scale bars: 20 mm.

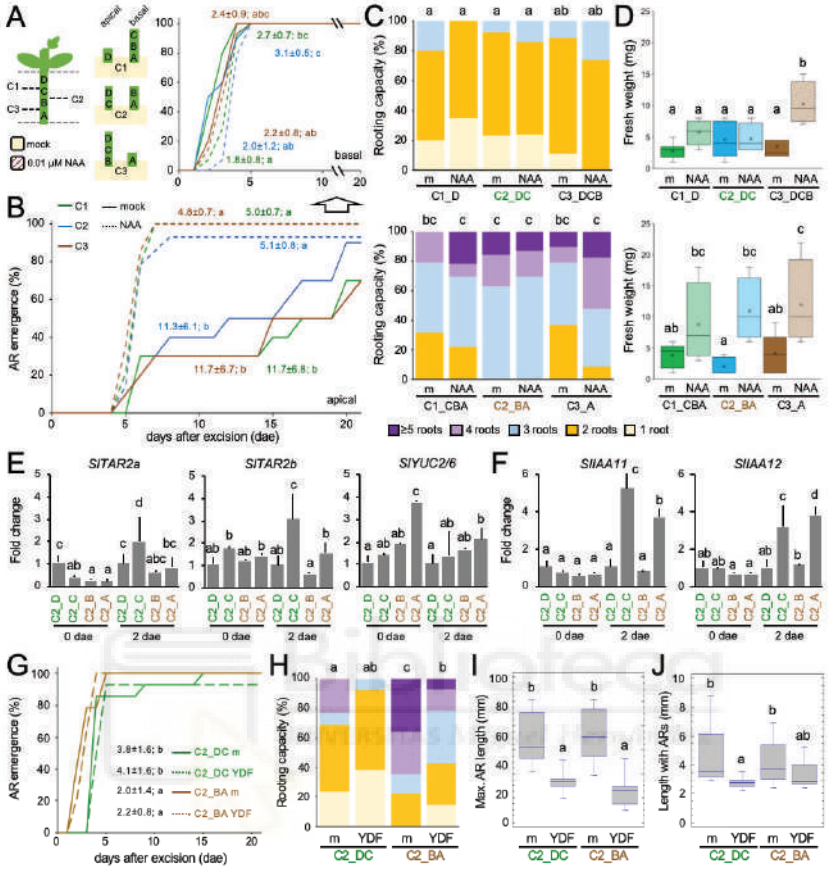

Fig 7. Apical-basal polarity within the hypocotyl regulates wound-induced AR formation. (A) Diagram showing the different conditions assayed. (B, G) AR emergence of the explants in the studied conditions. YDF: 50 µM yucasin DF; m: mock. (C, H) Rooting capacity of 'Micro-Tom' shoot explants at 14 dae. (C) Upper graph: apical; lower graph: basal. (D) Fresh weight of the distal end of the explants with ARs at 21 dae. (E, F) Relative expression of auxin biosynthesis (E) and auxin responsive (F) genes. Bars indicate normalized expression levels ± SD with regards to the apical region of the hypocotyl (C2_A) at a given time. (I) Maximum lengths of ARs at 21 dae. (J) Hypocotyl length with ARs at 21 dae. Letters indicate significant differences (p-value<0.01) between the studied conditions.

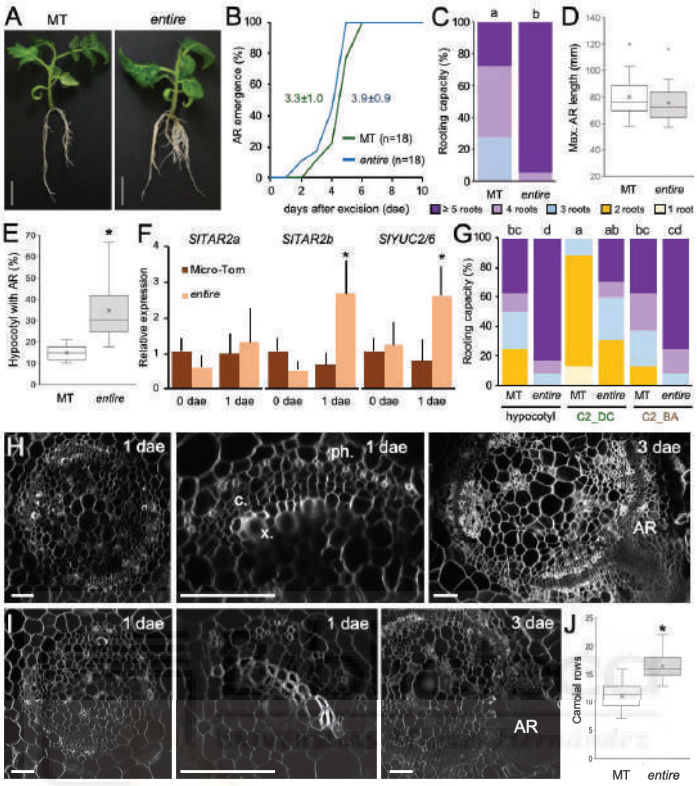

Fig. 8. Auxin response in the basal region of the hypocotyl is required for wound-induced AR formation in tomato shoot explants. (A) Representative images of rooted shoot explants at 21 dae. (B) AR emergence of the studied explants. (C, G) Rooting capacity of wild-type (WT) and *entire* shoot and hypocotyl explants at 14 dae. (D) Maximum lengths of ARs at 21 dae. (E) Percentage of hypocotyl lengths with ARs at 21 dae. (F) Relative expression of auxin biosynthesis genes. Bars indicate normalized expression levels ± SD with regards to the WT expression in the basal region at 0 dae. (H, I) Representative cross sections of shoot explants of *entire* (H) and WT (I) at 1 and 3 dae. (J) Number of cambial rows per vascular bundle in hypocotyl cross sections of WT and *entire* at 1 dae. Letters (C, G) or asterisks (E, F, J) indicate significant differences (p-value<0.01) between genotypes and/or conditions tested. Scale bars: 20 mm (A) and 100 μM (H, I).

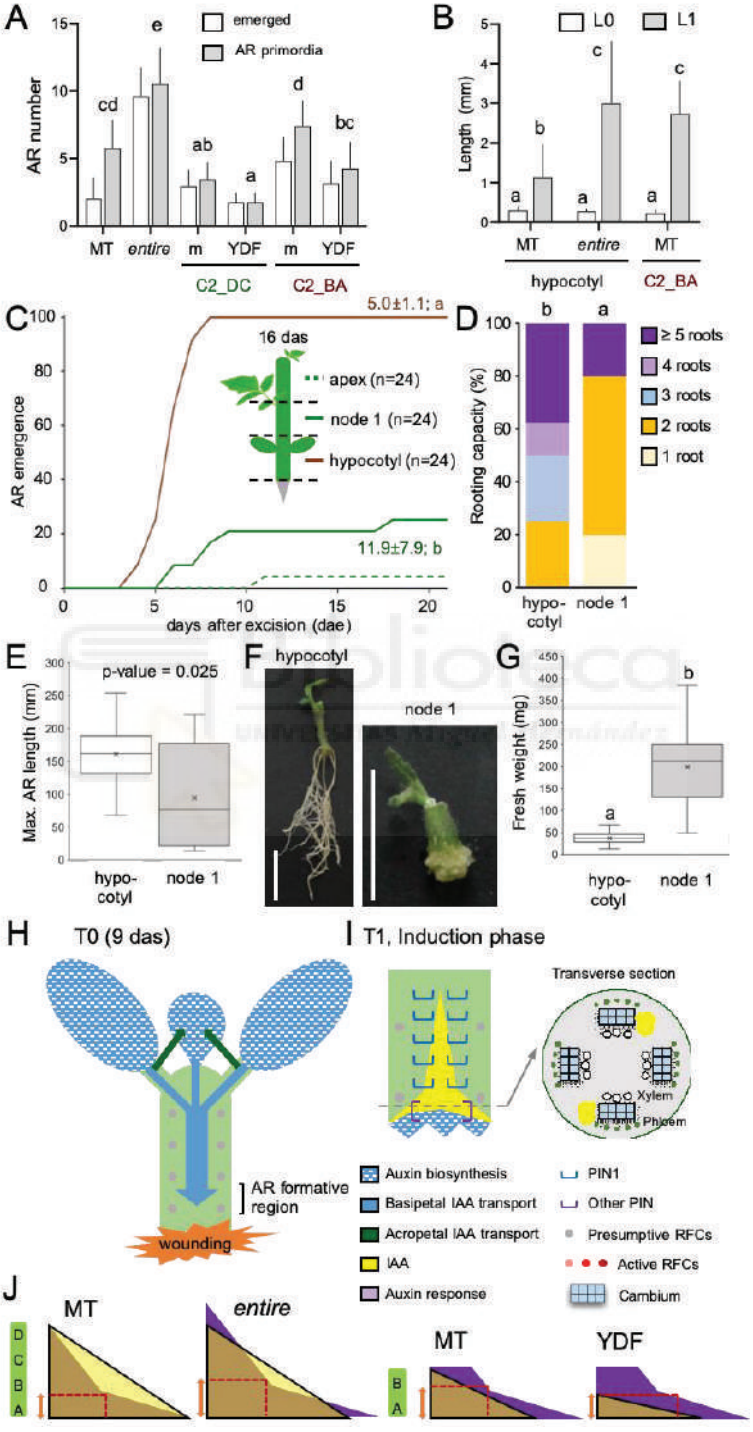
A
AR number
emerged
AR primordia
cd
e
ab
a
d
bc
MT
entire
m
YDF
m
YDF
C2_DC
C2_BA
B
Length (mm)
L0
L1
a
b
a
c
a
c
MT
entire
MT
hypocotyl
C2_BA
C
AR emergence
5.0±1.1; a
16 das
apex (n=24)
node 1 (n=24)
hypocotyl (n=24)
11.9±7.9; b
days after excision (dae)
D
Rooting capacity (%)
b
a
≥ 5 roots
4 roots
3 roots
2 roots
1 root
hypo-cotyl
node 1
E
Max. AR length (mm)
p-value = 0.025
hypo-cotyl
node 1
F
hypocotyl
node 1
G
Fresh weight (mg)
a
b
hypo-cotyl
node 1
H
T0 (9 das)
AR formative region
wounding
I
T1, Induction phase
Transverse section
Xylem
Phloem
Auxin biosynthesis
Basipetal IAA transport
Acropetal IAA transport
IAA
Auxin response
PIN1
Other PIN
Presumptive RFCs
Active RFCs
Cambium
J
MT
entire
D
C
B
A
MT
YDF
B
A

Fig. 9. A developmental gradient of auxin response is required for wound-induced AR formation in tomato. (A) Number of AR primordia in different conditions; m: mock, YDF: 50 μM yucasin DF. (B) Length of the basal region of the hypocotyl with no AR formation (L0) or with AR formation (L1). (C) AR emergence of the studied explants, as indicated in the diagram. (D) Rooting capacity of hypoctyl and node 1 explants at 14 dae. (E) Maximum lengths of ARs. (F) Representative images of explants at 28 dae. Scale bars: 20 mm. (G) Fresh weight of the distal end of the explants at 14 dae. Letters indicate significant differences (p-value<0.01) between the assayed conditions. (H-J) Model of wound-induced AR formation in tomato shoot explants. (H) IAA is produced in some shoot tissues (cotyledons and young leaves) and it is transported through the hypocotyl and into the primary root. Auxin produced in the cotyledons also contributes to the growth of young leaves. Immediately after whole root excision, wound-induced signaling is produced near the wound. RFCs: root founder cells. (I) In the AR formative region, the IAA levels in the vascular bundles increase due to basipetal auxin transport from the shoot and local auxin biosynthesis near the wound. AUX/LAX1 and PIN proteins actively contribute to the buildup of endogenous auxin gradients within the vascular bundles, where they activate RFCs within the cambium. (J) In hypocotyl explants, an internal pre-pattern of auxin sensitivity is already established, likely through regulation of Aux/IAA protein levels. The size of the AR formative region depends on a given threshold of IAA level, which is directly interpreted by the prepatterned auxin-response gradient.

SUPPORTING INFORMATION

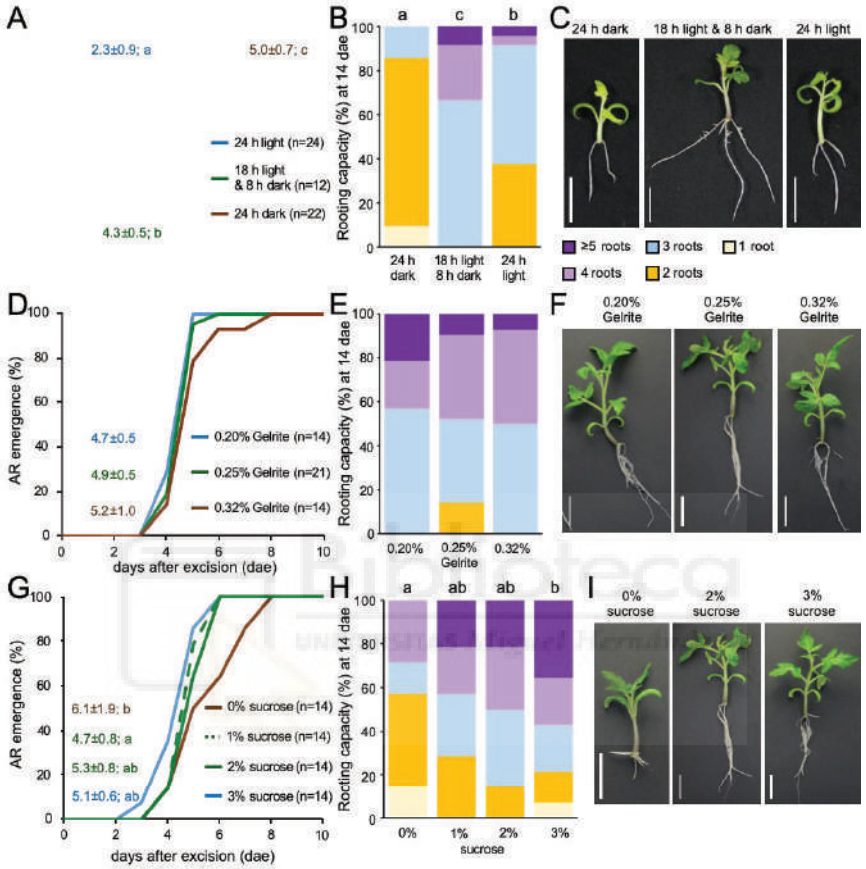

Fig. S1. Environmental dependence of wound-induced AR formation in tomato shoot explants. Effect of light regime (A-C), gelling agent (D-F) or sucrose (G-I) on wound-induced AR formation in tomato shoot explants. (A, D, G) AR emergence of the explants in the studied conditions; numbers indicate average ± SD of days for AR emergence. (B, E, H) Rooting capacity of 'Micro-Tom' shoot explants in the studied conditions. (C, F, I) Representative images of rooted shoot explants in the different conditions assayed. Letters indicate significant differences (p-value<0.01) between treatments. Scale bars: 20 mm.

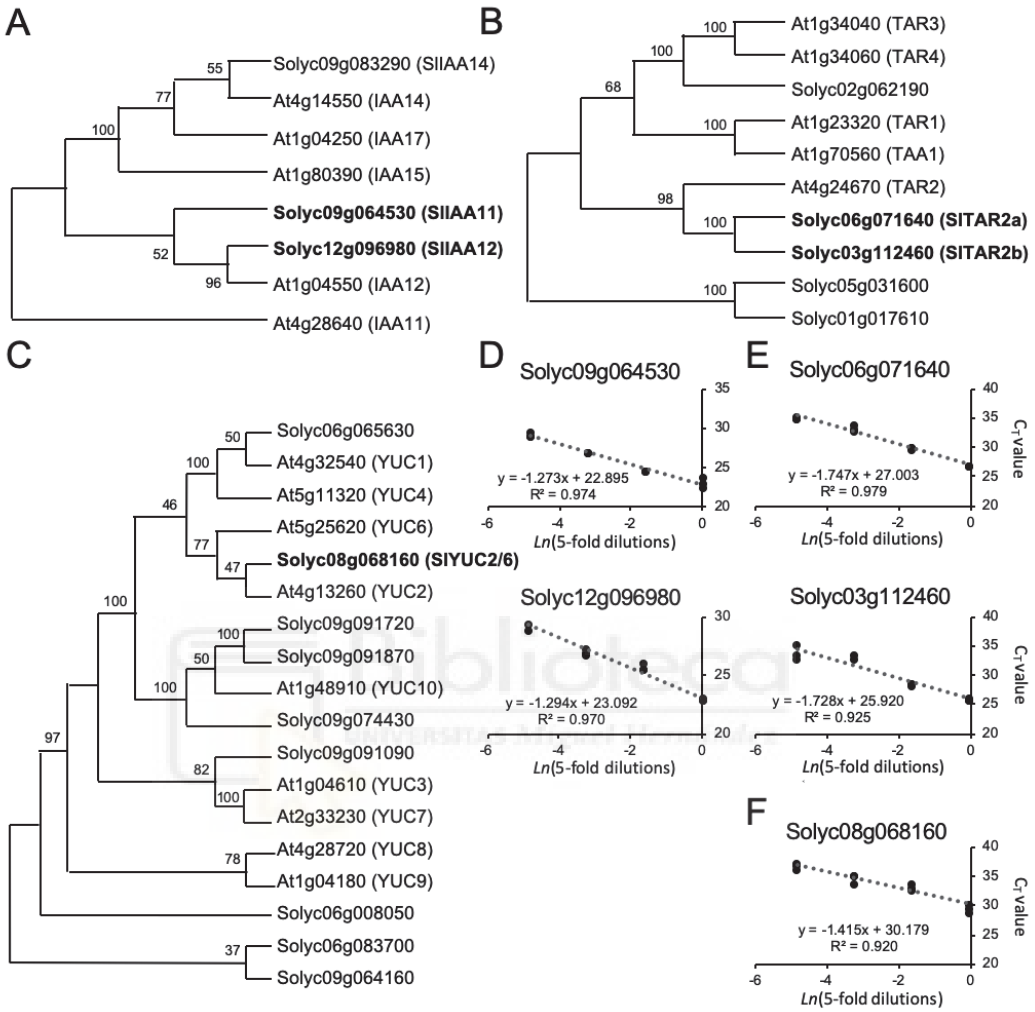

Fig. S2. Phylogenetic analysis of auxin biosynthesis genes in tomato and primer validation for real-time quantitative PCR. (A, B, C) Phylogenetic trees of a subset of Aux/IAA (A), TAA/TAR (B) and YUCCA (C) proteins. The trees were inferred from protein alignments by using the Maximum Likelihood method based on the Le Gascuel (2008) model. (D, E, F) Primer validation was performed for selected Aux/IAA (D), TAA/TAR (E) and YUC (F) genes. Each dot represents the relative expression data for a given sample.

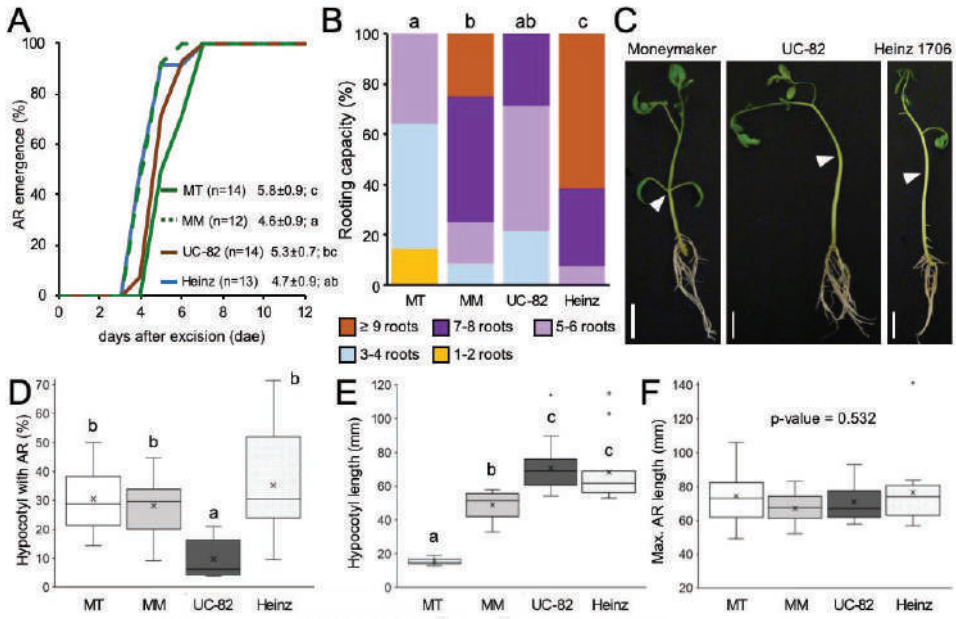

Fig. S3. Wound-induced AR formation in tomato shoot explants is genotype-dependent. (A) AR emergence of the studied explants. (B) Rooting capacity of shoot explants in the studied cultivars at 14 dae. (C) Representative images of rooted shoot explants at 14 dae in the studied cultivars. Arrowheads indicate the position of the cotyledons. (D) Percentage of hypocotyl length with ARs and (E) hypocotyl lengths at 14 dae. Letters indicate significant differences (p-value<0.01) between cultivars and conditions assayed. Scale bars: 20 mm.

Table S1. Tomato genotypes used in this study.

Cultivar / *mutant*	Accession	Genotype	Other comments	References
Micro-Tom (MT)	LA3911	*d*; *ej-2*^{w}; *I*; *Sm*; *sp*; *u*	Determinate growth habit. Dwarf plants. Brassinosteroid deficiency.	1
DR5::GUS		Micro-Tom (MT) background		2
diageotropica (*dgt*)		NIL of *dgt* mutation in a MT background	Altered polar auxin transport. Defect in a cyclophilin biosynthesis gene. Altered LR development.	3, 4, 5
entire (*e*)		NIL of *e* mutation in a MT background	Loss-of-SlIAA9 function. Entire leaves. Enhanced auxin responses.	6
Moneymaker	LA2706	*ej-2*^{w}; *obv*$^{+}$; *sp*$^{+}$*; u*	Indeterminate growth habit.	
UC-82	LA1706	*obv*; *sp; u*	Determinate growth habit.	
Heinz 1706-BG	LA4345	*I*; *sp*, *Ve*	Determinate growth habit.	

1. Martí, E., Gisbert, C., Bishop, G. J., Dixon, M. S. & García-Martínez, J. L. Genetic and physiological characterization of tomato cv. Micro-Tom. J. Exp. Bot. 57, 2037–47 (2006).

2. Nishio, S. et al. Expression analysis of the auxin efflux carrier family in tomato fruit development. Planta 232, 755–764 (2010).

3. Oh, K. C., Ivanchenko, M. G., White, T. J. & Lomax, T. L. The *diageotropica* gene of tomato encodes a cyclophilin: A novel player in auxin signaling. Planta 224, 133–144 (2006).

4. Ivanchenko, M. G. et al. The cyclophilin A *DIAGEOTROPICA* gene affects auxin transport in both root and shoot to control lateral root formation. Dev. 142, 712–721 (2015).

5. Carvalho, R. F. et al. Convergence of developmental mutants into a single tomato model system: 'Micro-Tom' as an effective toolkit for plant development research. Plant Methods 7, 18 (2011).

6. Zhang, J. et al. A single-base deletion mutation in *SlIAA9* gene causes tomato (*Solanum lycopersicum*) *entire* mutant. J. Plant Res. 120, 671–678 (2007).

Table S2. Oligonucleotides used in this study.

Gene	Accession number	Oligonucleotide sequences (5'→3')		Product size (base pairs)
SlTAR2a	Solyc06g071640	CATCAATCTGGACCATGGTG	TAGTCTGAGCATTACCAACTAG	197
SlTAR2b	Solyc03g112460	TTTGCAACACAGCCAGCTTTTG	CCCCGCCTCTTGTCAATATC	97
SlYUC2/6	Solyc08g068160	CCTCGTGGCTAAAGGAAAAAG	CACTGCATAAAGTCCACACTC	101
SlIAA11	Solyc12g096980	CTACAAGTGCCAGTCAGGTTG	GTTCTTTTTCTCCACAATTAGTAG	324
SlIAA12	Solyc09g064530	TGTTCCTTGGGAGATGTTTATTAG	ATGAAAGTTGGAGATGTACCG	93
SlACTIN2	Solyc03g078400	CCAAGCAGCATGAAGATTAAGG	CCTTTGAGATCCACATCTGCTG	115

AGRADECIMIENTOS

7. AGRADECIMIENTOS

En primer lugar, agradecer a mi director de tesis José Manuel Pérez, por darme la oportunidad de realizar la tesis en su laboratorio, con él he aprendido mucho sobre ciencia. Pero sobre todo he aprendido que con esfuerzo y dedicación se consiguen grandes cosas.

A Joan Villanova y Ana Belén Sánchez, Mª Ángeles Fernández, María Salud Justamante, Sergio Ibañez, Virginia Birlanga, Rebeca Bayon, Paula Jadczak, Mariem Mhimdi, Diana Navarro y Mª José Ñiguez por compartir laboratorio y esfuerzo, risas y momentos inolvidables.

A María Salud Justamante, por ser calma en mitad de la tempestad, por darme esa serenidad que a veces me falta y equilibrar la balanza hacia el bien, no hay mejor persona en el mundo. Por su ayuda incondicional y su paciencia conmigo y mi problema con los ordenadores, con el papeleo y con mil cosas más. Eres una compañera espectacular pero sobre todo eres una amiga entre un millón.

A Sergio Ibáñez, mi partner de tesis, de alegrías y tristezas, mi compañero de horas y horas de trabajo duro. Mi hombro en el que llorar, el que sabe mejor que nadie como me he sentido en cada momento de este camino y con el que sigo compartiendo a día de hoy trabajo y despacho. Porque a veces la vida te pone en el camino personas maravillosas a las que te aferras y te niegas a dejar ir, porque esto amigo mío no ha sido una etapa en nuestra vida sino el principio de una amistad para siempre. Eres el siguiente, te quiero nene.

A todos los alumnos de TGF y Máster que han pasado por el laboratorio y de los que tanto he aprendido, espero que su paso por el laboratorio haya despertado en ellos la pasión por la ciencia. En especial a Francisco Javier Gran, por su esfuerzo y dedicación en el trabajo, por su compañerismo y su entera disposición a ayudar siempre con una sonrisa. Espero que la vida te depare solo cosas bonitas.

A Eva María Rodríguez, la tercera pata de mi cama. Nadie se imagina cuanto puede unir compartir una cabina. Sin ti los congresos, las comidas y la vida en general habrían tenido mucho menos interés y aunque no me voy a mudar a Orihuela, aquí tienes una amiga para lo que necesites.

Al Laboratorio de Eduardo Fernández por todo el equipamiento prestado, porque ha habido épocas que pasaba allí todas mis horas y siempre me han tratado genial. En especial a mi Gemi, mi tesis no habría sido lo mismo sin ti, sin nuestras horas de confocal y sin tus ratitas. Gracias por enseñarme con paciencia, por ayudarme siempre que lo he necesitado y por tener esa sonrisa tan grande que te hace tan especial. Eres un sol maripuri.

Al laboratorio de Fitopatología de la Universidad de Alicante por abrirme la puerta de la investigación y meterme el gusanillo de la tesis. En especial a Leticia Asensio que me hizo enamorarme de su asignatura y me llevo al laboratorio y a Nuria Escudero que me hizo amar la ciencia desde el minuto 0, por su forma de trabajar y enseñar, por su forma bonita de ver la vida y de transmitírselo a los demás. Un ejemplo a

seguir en la investigación y la vida.

A Almudena Aranda y Ernesto Zavala por compartir horas y horas de risas en el Fitolab y fuera de él. Porque son ejemplo de trabajo duro, y de que al final la vida te lo compensa. Porque son imprescindibles en mi vida y lo seguirán siendo. Chicos chicos gracias por vuestro apoyo, por vuestros consejos desde el saber y por estar ahí siempre SIEMPRE que lo he necesitado. Ir pensando próximo destino. Os quiero

A Adela Yañez, por abrirme las puertas a una nueva etapa en mi vida, la laboral. Por confiar en mi y asignarme la difícil pero emocionante tarea de poner a funcionar un equipo de personas que han resultado maravillosas. A las chicas COVID, a todas ellas, por trabajar sin descanso y dar lo mejor de cada una. Da gusto encontrar gente con tantas ganas de aprender y trabajar. A toda la gente de Labaqua porque me hicieron sentir en casa siempre, en particular al departamento de microbiología que me animaban a seguir escribiendo y probaban todas mis creaciones culinarias “desestresantes de tesis”. Victoria y Loli por favor no cambiéis nunca, no sabéis la suerte que tiene la gente que comparte tiempo con vosotras.

A María García, mi bebé, la que empezó viniendo a dar follón un rato cada día y se quedo en el COVID y en mi vida. Como una persona tan joven puede ser tan madura. Ha sido increíble enseñarte, conocerte y corregir tu TFM (bueno eso no fue tan divertido..). Juré vengarme con la bibliografía de mi tesis pero no he cumplido. ¡Al final los de la Vega Baja vais a tener algo especial! Gracias al abuelo por suministrarme

alimentos del huerto durante toda la escritura, sin él habría comido muchísimo peor. A Loreto por hacerme la portada de la tesis, gracias por aguantar todos mis “no se” y “no me convence”, al final ha merecido la pena.

A mi familia, aunque ellos no lo sepan son mi vía de escape. Un fin de semana en el Bigotes es todo lo que necesito para recargar pilas y coger fuerzas para todo lo que vendrá. No hay nada más maravilloso que haber crecido compartiendo el tiempo con mis tíos y mis primos y seguir disfrutando de ellos siempre que puedo. A mis TIAS por ser ejemplo de todo lo que una mujer puede ser; fuertes, luchadoras, divertidas, incansables y cariñosas (entre otras cien mil cualidades), sois todo en lo que me quiero convertir. Os quiero.

A Maria del Mar, Quino, Rosa, Quinico y Javier, mi otra familia. Por estar siempre, por acogerme como una más desde el primer día que llegué a vuestra casa. Porque esos arroces de domingo son sanadores para cualquier alma y las risas con vosotros están aseguradas. No sabía que se podía querer tanto a la familia política.

A mis amigos, a todos ellos quiero agradecerles su tiempo, sus risas y sus consejos. En especial a Malaguita y Sory, Bo, y mis ludicofestivos. Porque la vida se ve mucho mejor con una cerveza en la mano y cada vez que nos vemos es como si no hubiera pasado el tiempo.

A mi hermana Espe, porque aunque nos entendemos regular en el fondo ella sabe que siempre tengo razón yo y al final cede. Nunca una melliza dio tanta guerra y comió tanta pizza. Te quiero Espe.

A mi madre, mi luz, mi vida y mi todo. Mama eres el ejemplo perfecto de lucha incansable y de amor incondicional. Has sacrificado mucho para que me formara y me formé, para que fuera fuerte y lo soy y para que fuera independiente y también lo hemos conseguido. Me has escuchado sin entender del todo lo que te decía cuando un experimento me salía mal o si por fin me salía bien, me has animado a seguir cuando quedaba mucho y cuando me quedaba poco. Has aguantado meses sin verme porque no podía dejar experimentos a medias y has tenido preparados mis platos favoritos cuando por fin podía escaparme a Salamanca. Me animaste a empezar este camino, a dar el paso a la empresa y a dejarla cuando no me convencía lo que veía. Siempre has estado para mi y siempre voy a estar para ti. TE QUIERO MAMA.

A Johan, mi media langosta, mi filósofo favorito. Simplemente gracias por estar, por aguantar y por no cansarte de mi y de mi tesis, que es más nuestra que mía. Me has aguantado todos los humores posibles y a veces más de uno al día, me has escuchado cuando te contaba y me has dado espacio cuando no hablaba. Porque has aguantado sentado en una silla mientras se me hacían las mil en el laboratorio en vez de estar por ahí cenando juntos y nunca te has quejado, porque has regado conmigo y te sabes al dedillo cada una de mis presentaciones,

porque tienes enmarcados en casa todos los pósteres que he presentado en los congresos y por mil cosas más: GRACIAS. TE QUIERO BICHI.